Involvement of *pre*-proenkephalin and sigma-1 receptors in nicotine addiction

Sami Kummer

Doctoral Thesis/2019

Thesis directors:

Prof. Dr. Rafael Maldonado López
Dr. Elena Martín-García
Dr. Ana Montero Pastor

Departament de ciències experimentals i de la salut

Universitat Pompeu Fabra Barcelona

Abstract

Tobacco smoking is the leading cause of preventable death worldwide, responsible for more than 7 million deaths per year. Nicotine is the main psychoactive component of tobacco and responsible for its addictive properties. Although smoking cessation produces significant health benefits, around 80% of former smokers relapse within the first month. Nicotine acts on nicotinic acetylcholine receptors, however, nicotine addiction is a complex brain disease that involves the participation of several neurotransmitter systems. In a first approach, we combined sophisticated operant behavioral models with genetic and virus-mediated chemogenetic tools to demonstrate that opioid signaling and corticostriatal glutamatergic signaling critically contribute to the reinforcing properties of nicotine. We further revealed that nicotine self-administration triggers structural plasticity in the nucleus accumbens (NAc) core and shell. Interestingly, structural plasticity was singularly driven by contingent nicotine self-administration, but not non-contingent nicotine administration, concluding that goal-directed behavior and conditioning are necessary to trigger the mechanisms that underly structural plasticity. In a second approach, we demonstrated for the first time the implication of the sigma-1 receptor (Sig-1R), a novel receptor type that is thought to lack its own specific signaling machinery, in the relapse to nicotine-seeking. Acute blockade of Sig-1Rs significantly decreased cue-induced reinstatement of nicotine-seeking by inhibiting neurobiological adaptations in the medial prefrontal cortex and NAc, including Sig-1Rs, glutamatergic, cholinergic and opioid receptors. Together, our study provided new insights about the involvement of opioid, glutamatergic and Sig-1R signaling in nicotine addiction that can help to develop new therapeutic strategies to treat nicotine addiction.

Resúmen

El tabaquismo es la principal causa de muerte evitable en todo el mundo, responsable de más de 7 millones de muertes al año. La nicotina es el principal componente psicoactivo del tabaco y la responsable de sus propiedades adictivas. Aunque dejar de fumar produce importantes beneficios para la salud, alrededor del 80% de los ex fumadores recaen en el primer mes. La nicotina actúa sobre los receptores de acetilcolina nicotínicos, sin embargo, la adicción a la nicotina es una enfermedad cerebral compleja que implica la participación de varios sistemas de neurotransmisores. En un primer enfoque, combinamos sofisticados modelos de comportamiento operante con herramientas genéticas y quimiogenéticas mediadas por virus para demostrar que la señalización de opioides y la señalización glutamatérgica corticostriatal contribuyen de manera crítica a las propiedades de refuerzo de la nicotina. Además, revelamos que la autoadministración de nicotina desencadena la plasticidad estructural en la zona central y la corteza del núcleo accumbens (NAc). Curiosamente, la plasticidad estructural fue impulsada exclusivamente por la autoadministración contingente de nicotina, pero no por la administración no contingente, concluyendo que el comportamiento dirigido a objetivos y el condicionamiento son necesarios para activar los mecanismos que subyacen a la plasticidad estructural. En un segundo enfoque, demostramos por primera vez la implicación del receptor sigma-1 (Sig-1R), un nuevo tipo de receptor que se cree que carece de su propia maquinaria de señalización específica, en la recaída la búsqueda de nicotina. El bloqueo agudo de Sig-1Rs disminuyó significativamente el restablecimiento de la búsqueda de nicotina inducido por estimulos asociados al inhibir las adaptaciones neurobiológicas en la corteza prefrontal medial y el NAc, incluidos los

receptores Sig-1R, glutamatérgicos, colinérgicos y opioides. En conjunto, nuestro estudio proporciona nuevos conocimientos sobre la participación de la señalización opioide, glutamatérgica y Sig-1R en la adicción a la nicotina que pueden ayudar a desarrollar nuevas estrategias terapéuticas para tratar la adicción a la nicotina.

Abbreviations

AC: Adenylate cyclase

ACh: Acetylcholine

AMG: Amygdala

AMPAR: α-amino-3-hydroxy-5-methyl-4-isoxazolepropionic acid receptor

APA: American Psychiatric Association

aVTA: Anterior-lateral ventral tegmental area

BiP: Binding immunoglobulin protein/78 kDa glucose-regulated protein

cAMP: Cyclic adenosine monophosphate

CeA: Central nucleus of the amygdala

BD 1063: 1-[2-(3,4-Dichlorophenyl)ethyl]-4-methylpiperazine dihydrochloride

BNST: Bed nucleus of the stria terminalis

CIN: Cholinergic interneurons neuron

CNO: Clozapine-N-oxide

CPP: Conditioned place preference

CREB: cAMP response element binding protein

CRF: Corticotropin-releasing factor

DA: Dopamine

DAT: Dopamine transporter

DSM: Diagnostic and Statistical Manual

DALY: Disability-adjusted life years

DREAAD: Designer receptor exclusively activated by designer drugs

DOR: δ-opioid receptor

EOS: Endogenous opioid system

ER:	Endoplasmic reticulum
ERK:	Extracellular-signal regulated kinase
FR:	Fixed ratio
Fra-2:	Fos-related antigen 2
FSI:	Fast-spiking interneuron
GABA:	γ-aminobutyric acid
GAD:	glutamic acid decarboxylase
GIRK:	G protein gated inwardly rectifying potassium channel
GluR:	Ionic glutamate receptors
GPCR:	G protein-coupled receptor
HPC:	Hippocampus
ICSS:	Intra-cranial self-stimulation
IL:	Infralimbic cortex
i.p.:	Intraperitoneal
i.v.:	Intravenous
IP_3:	Inositol-1,4,5-triphosphate
KO:	Knock out
KOR:	κ-opioid receptor
LDTg:	Laterodorsal tegmentum
LHb:	Lateral habenula
LTP:	Long-term potentiation
MAPK:	Mitogen-activated protein kinase
MDT:	Mediodorsal thalamus
mGluR:	Metabotropic glutamate receptor
MOR:	μ-opioid receptor
mAChR:	Muscarinic acetylcholine receptor
mPFC:	Medial prefrontal cortex
MSN:	Medium spiny neuron

NAc: Nucleus accumbens

nAChR: Nicotinic acetylcholine receptor

NFκB: nuclear factor kappa-light-chain-enhancer of activated B cells

NFSI: Non- fast-spiking interneuron

NMDAR: N-methyl-D-aspartate receptor

nNOS: Nitric oxide synthase

NUD: Nicotine use disorder

OR: Opioid receptors

PBS: Na_2HPO_4/ NaH_2PO_4/NaCl buffer

PCP: Phencyclidine

PDYN: Pre-prodynorphin

PFA: Paraformaldehyde

PLTS: Persistent and low-threshold spike

PENK: Pre-proenkephalin

PFC: Prefrontal cortex

PKA: Protein kinase A

PKC: Protein kinase C

PL: Prelimbic cortex

PLC: Phospholipase C

POMC: Proopiomelanocortin

PPTg: Pedunculopontine nucleus

PR: Progressive ratio

pVTA: Posterior-medial ventral tegmental area

ROS: Reactive oxygen species

RMTg: Rostromedial tegmentum

SBDL: Steroid binding domain like

s.c.: Subcutaneous

Sig-1R: Sigma-1 receptor

Scr:sP: Scripps Research Institute Sardinian alcohol-preferring rats

SUD: Substance use disorder

TH: Tyrosine hydroxylase

TrkB: Tyrosine kinase receptor B

vAChT: Vesicular acetylcholine transporter

vGLUT: Vesicular glutamate transporter

vHPC: Ventral hippocampus

VP: Ventral pallidum

VTA: Ventral tegmental area

WHO: World health organization

WT: Wildtype

Table of Contents

Introduction

1 Substance use disorder

Substance use disorder (SUD) is a chronic relapsing brain disorder characterized by compulsive drug-seeking and drug-taking, loss of control in limiting drug intake and continuing drug use despite adverse consequences (DSM-5, 2013). The appearance of a negative emotional state and craving when access to the drug of abuse is prevented, and the relapse to drug-seeking and/or -taking even after protracted abstinence which remains the major clinical health concern (Koob *et al.*, 1997; Koob & Le Moal, 2008a; Koob & Volkow, 2016).

1.1 Epidemiology

SUDs are a major public health problem that soaks throughout all social classes of the world's population. Indeed, the World Health Organization (WHO) estimated that more than half (57%, or 3.1 billion people) of the global population, aged 15 years and over, had abstained from drinking alcohol in the previous 12 months. Furthermore, approximately 2.3 billion people are current drinkers (WHO, 2018) which represents an increase of about 15% compared to the WHO report in 2002 (WHO, 2002). In 2016, the harmful use of alcohol resulted in approximately 3 million deaths worldwide (5.3% of all deaths) and 132.6 million disability-adjusted life years (DALYs), 5.1% of all DALYs in that year. Mortality resulting from alcohol consumption is higher than that caused by diseases such as tuberculosis, HIV/AIDS and diabetes.

About 275 million people worldwide, which is roughly 5.6 % of the global population aged 15–64 years (Figure 1), used illicit drugs of abuse, including cannabis, opioids, and psychostimulants, at least once during 2016. Some 31 million people who use drugs suffer from drug use

disorders, meaning that their drug use is harmful to the point where they may need treatment. Roughly 450,000 people died as a result of drug use in 2015, according to the WHO, 167,750 of those deaths were directly associated with drug use disorders (mainly overdoses). The rest were indirectly attributable to drug use and included deaths related to HIV and hepatitis C acquired through unsafe injecting practices. Opioids continued to cause the most harm, accounting for 76 % of deaths where drug use disorders were implicated. The non-medical use of pharmaceutical opioids is of increasing concern for both law enforcement authorities and public health professionals. Different pharmaceutical opioids are misused in different regions. In North America, illicitly sourced fentanyl, and its analogs, with heroin or other drugs, is driving the unprecedented number of overdose deaths.

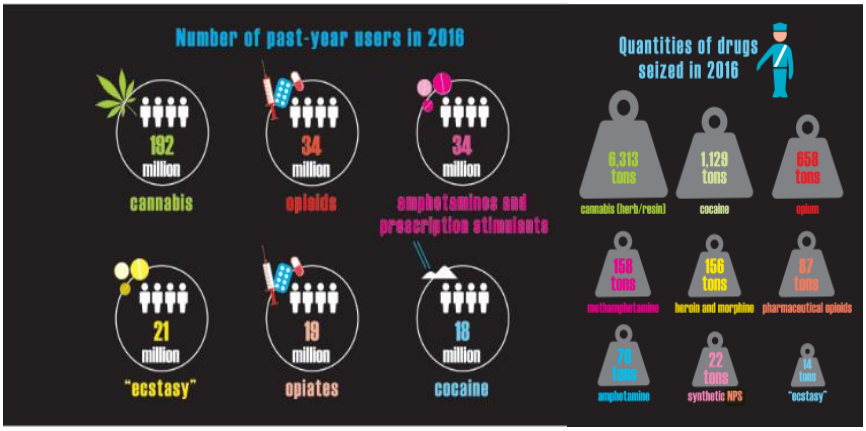

Figure 1. Number of individuals that used illicit drugs and/or abused prescriptions in 2016 (adapted from UNODC, 2018)

1.2 Tobacco smoking: a major health concern

The tobacco epidemic is one of the biggest public health threats the world has ever faced, killing more than 7 million people a year. More than 6 million of those deaths are the result of direct tobacco use while around 890 000 are the result of non-smokers being exposed to second-hand smoke. This mortality is mainly due to lung cancer, coronary heart disease, respiratory and chronic obstructive pulmonary disease, which represent an important impact on health care expenses. Despite public awareness of the harmful effects of tobacco use, it is estimated that 22.5% (32% men, 7% women) of the global adult population are current smokers (Gowing *et al.*, 2015). Around 80% of the 1.1 billion smokers worldwide live in low- and middle-income countries, where the burden of tobacco-related illness and death is heaviest (WHO, 2017).

Tobacco is mainly consumed in the form of cigarettes, conceived as the most effective form to deliver nicotine to the organism. Nicotine is the main psychoactive component of tobacco and responsible for its addictive properties (Grenhoff & Svensson, 1989; West, 1992; Stolerman & Jarvis, 1995). Moreover, tobacco contains more than 4000 toxic components with many been reported as irritating, carcinogenic and toxic contributing to the development of smoking-related diseases. Even though smoking cessation produces significant health benefits and decreases the risk of tobacco-associated diseases within few years after quitting (USHHS, 1990; Doll *et al.*, 2004), around 80% of former smokers relapse within the first month of abstinence with only 3% of them remaining abstinent at six months (Benowitz, 2010). Therefore, it is necessary to provide more efficacious and alternative pharmacotherapies (Schlam & Baker, 2013).

1.3 The nosology of substance use disorders

Although psychoactive substances (including alcohol and nicotine) have been around for nearly as long as recorded history, the scientific classification of SUDs only began in the early 19th century. While this work is focused almost exclusively on the American classification system, it is certainly noteworthy that the nosology of modern psychiatry began with the German classifiers of the late 19th century, especially Emil Kraepelin who believed the chief origin of psychiatric disease to be biological and genetic malfunction, and was identified as the founder of modern scientific psychiatry (Eysenck *et al.*, 1975). Despite Kraepelin's work, SUDs used to be underappreciated as diseases rooted in neuropathology (O'Brien, 2003). Indeed, prior to the third publication of the Diagnostic and Statistical Manual (DSM), SUDs were largely conceptualized as manifestations of underlying primary psychopathologies.

In 1952 appeared the first edition of the DSM that was based upon an expanded nosology created by psychoanalyst William Menninger (author of *'Medical 203'*, 1945). It conceptualized substance use disorders (i.e., drug addiction and alcoholism) as most commonly arising from a primary personality disorder (DSM-I, 1952).

In 1959, not even a decade after the release of the first DSM, major advances in the treatment of mental disorders occurred. Following WHO's recommendations (1951), the American Medical Association (1965) recognized the severity of alcoholism and declared it to be a medical disorder. The DSM-II however, did only minor modifications to change the influence of psychoanalysis and its characteristic descriptions of disorders described in the DSM-I. Yet, it did encourage separate diagnoses for alcoholism and drug addiction: "even when it begins as a symptomatic expression of another disorder" (DSM-II, 1968). Three types of alcoholism

were recognized: (a) episodic excessive drinking; (b) habitual excessive drinking and (c) alcohol addiction. Although withdrawal was emphasized for drug addiction, it was also recognized that dependence could occur without withdrawal. However, medically prescribed drugs were excluded considering that they were taken in proportion "to the medical need" (DSM-II, 1968).

The third edition of the DSM, published in 1980, broke with psychoanalytic tradition by instituting consensus-based diagnoses and diagnostic criteria (Wilson, 1993). It came rapidly into widespread international use by multiple stakeholders and has been termed a revolution or transformation in psychiatry. The American Psychiatric Association (APA) based the criteria, including those for SUDs, on prior work in this field (Jellinek E. M., 1960; Feighner *et al.*, 1972). For the first time, SUDs were seen as autonomous diseases, diagnosed separately, and were set apart from other mental health conditions. Two independent categories of *'substance abuse'* and *'substance dependence'* were adopted. Although these categories were not explicitly explained within the manual, it was suggested that the former was equated with pathological use (e.g., social or occupational consequences, including legal problems) and the latter with physiological dependence (i.e., tolerance or withdrawal) (Spitzer *et al.*, 1980). However, since those criteria lacked a precise explanation, several criticisms arose stating that the distinction between substance abuse and dependence was made only based on the development of physiological tolerance or withdrawal (*'drug-centered model'*). In addition to that criticism, some notable irregularities existed within the DSM-III. Data was lacking in support of the main physiological criterion necessary for a cannabis dependence diagnosis, i.e., "the existence and significance of tolerance with regular heavy use of cannabis are controversial" (DSM-

III, 1980)(p. 176). Furthermore, while cocaine abuse was a recognized diagnosis, cocaine dependence was not included "since only transitory withdrawal symptoms occur after cessation of or reduction in prolonged use" (DSM-III, 1980) (p. 173). Such criticisms and irregularities would form the basis for recommendations to alter these categories in the next revision.

Thus, the APA published a revised DSM-III in 1987 (DSM-III-R, 1987). One of the important changes in the DSM-III-R was that former *'abuse'* criteria were shifted into the *'dependence'* category. By grouping behavioral dysfunctions with physiological processes in a polythetic diagnostic set, the conceptualization of the new *'dependence category'* stood in contrast to the earlier view that physiological symptoms were both necessary and sufficient for a dependence diagnosis. The DSM-III-R went even further in separating physiological dependence from the diagnosis of *'Dependence'* explicitly stating that: "surgical patients [who] develop a tolerance to prescribed opioids and experience withdrawal symptoms without showing any signs of impaired control over their use of opioids are not considered to fall in the category of Substance Dependence" (DSM-III-R, 1987; Widiger & Smith, 2012). However, recommended changes or elimination of the *'abuse category'* and incorporation of elements into a newly expanded *'dependence category'* (Rounsaville *et al.*, 1986) were rejected. Only seven years later, with the attempt to overcome some significant limitations such as differences in reliability and external validity, incorrect assumptions about the relationship between abuse and dependence, and the problem of *'diagnostic orphan'* (individuals with symptoms for whom neither diagnosis was met) (Beckson & Tucker, 2014), the APA published the fourth edition of the DSM (DSM-IV, 1994). Earlier inconsistencies were clarified regarding the distinction between physiological dependence and

'substance dependence' by specifying that: "Neither tolerance or withdrawal is necessary nor sufficient for a diagnosis of Substance Dependence", hence, specifiers such as "With" or "Without Physiological Dependence" were added (DSM-IV, 1994). Due to these approaches in DSM-IV, the nosology of SUDs has evolved its nature from a *'drug-centered'* to an *'individual-centered'* definition as the behavioral alteration emerges as of major importance for the transition to addiction. The use of the term *'addiction'* was largely avoided in favor of *'dependence'*. For individuals to be considered as drug abusers they had to fulfill at least one out of four abuse criteria, and the endorsement of three or more out of seven dependence criteria was required to be considered an addict.

The DSM-IV-TR made several other, rather minor revisions to the SUDs. It was highlighted that compared to *'substance dependence'*, "the criteria for Substance Abuse do not include tolerance, withdrawal, or a pattern of compulsive use and instead only the harmful consequences of repeated use" (DSM-IV-TR, 2000). Despite those changes, a positive diagnosis is already given when the individual has met at least three criteria independent of their nature. Moreover, the criteria were categorical and did not distinguish in their intensity. Hence, individuals considered as addicts did not necessarily show the same symptoms especially when the drug of abuse differs. Consequently, the categorical diagnosis of DSM-IV-TR did not mirror the dimensional nature of SUDs (Deroche-Gamonet & Piazza, 2014).

A decade of work later the APA released the fifth and most recent iteration of the DSMs in May 2013. (DSM-5, 2013). The removal of the *'Abuse-Dependence'* paradigm and important revisions to the diagnostic criteria themselves represent the most dramatic changes since DSM-III. As it was already recommended for the DSM-III-R (Rounsaville *et al.*, 1986), and

proposed in the influential model of a dependence syndrome published in 1976 by Edwards and Gross (Edwards & Gross, 1976), the DSM-5 conceptualizes a unitary SUD construct, varying only in terms of severity on a continuous scale from mild (2-3 criteria endorsed), moderate (4–5 criteria endorsed) and severe (6 or more criteria endorsed) out of 11 total criteria. The 11 criteria for substance use disorder are divided into four categories of behavior related to impaired control, social impairment, risky use and pharmacological indicators (tolerance and withdrawal) (Table 1). Each specific substance (other than caffeine) is addressed as a separate disorder (e.g., nicotine use disorder, cocaine use disorder), but most substances are diagnosed based on the same overarching criteria. The shift to a unified category measured along a dimension of severity represents a notable change from the post-hoc categorical severity specifiers in DSM-IV-TR and further cements the difference between the now-extinct DSM diagnosis of *'Dependence'* and the medical concept of physiological dependence, a distinction which had been increasingly emphasized over time. Other noteworthy changes were made in the DSM-5, including the addition of the *'craving criterion'*, the elimination of the *'legal problems criterion'*, and the title of the chapter, which now reads *'Substance-Related and Addictive Disorders'*. Despite the use of the term addiction in the title, the text explicitly reveals that "the word [addiction] is omitted from the official DSM-5 substance use disorder diagnostic terminology because of its uncertain definition and its potentially negative connotation" (DSM-5, 2013). For the first time, the *'substance-related and addictive disorders'* chapter was expanded to *'behavioral addictions'* (i.e., Gambling Disorder), suggesting that a behavioral addiction underlies shared neurobiological mechanisms and that gambling disorder symptoms resemble SUDs in some ways. Although gambling disorder is

presently the only condition in the subsection of *'non-substance-related disorders'* in the category of *'substance-related and addictive disorders'*, other conditions were considered. Notably, *'Internet gaming disorder'* has been included in the DSM-5 as a condition requiring further study (Petry & O'Brien, 2013). However, internet gaming may represent just one facet of problematic use of the internet and the potential impact of other Internet-related behaviors (e.g., social networking, shopping, pornography-viewing, gambling) warrants consideration (Yau *et al.*, 2012). Although not included in the DSM-5, several other non-substance or behavioral addictions have been considered. Specifically, the subjects relating to food, sex, exercise, and shopping were considered but eventually not included as it was concluded that, "at this time there is insufficient peer-reviewed evidence to establish the diagnostic criteria and course descriptions needed to identify these behaviors as mental health disorders."(DSM-5, 2013) (p. 481).

Table 1.
DSM-5 diagnostic criteria for substance use disorders.

A. Impaired control over substance use
1. The individual may take the substance in larger amounts or over a longer period of time than was originally intended.
2. The individual may express a persistent desire to cut down or regulate substance use and may report multiple unsuccessful efforts to decrease or discontinue drug use.
3. The individual may spend a great amount of time obtaining or using the substance or recovering from its effects.
4. Craving is manifested by the individual as an intense urge for the drug that may occur at any time but it is more likely to happen in an environment where the drug has been previously obtained or used.
B. Social, occupational, or recreational detriment
5. Recurrent substance use may result in a failure to fulfil major role obligations at work, school or home.
6. The individual may continue using the substance despite the appearance of social problems caused by the effects of the substance.
7. Important social, occupational, or recreational activities may be given up or reduced because of substance use.
C. Risky use of the substance
8. The individual uses the substance recurrently in physically hazardous situations.
9. Substance use is continued despite knowledge of having a psychological problem that is likely to have been caused by the substance.
D. Pharmacological criteria
10. A significant increase in the dose of the substance is needed to achieve the desired effect, or the effect produced with the usual dose is markedly reduced. This phenomenon is known as tolerance and it greatly varies between individuals and also between substances. It is important to consider that tolerance to different drug-induced effects could develop at different rates.
11. The individual reports physiological signs when blood or tissue concentrations of substance decline after a prolonged or heavy use of the substance. This is known as withdrawal syndrome. At this point the individual will likely consume the substance to relieve the symptoms. Withdrawal signs and symptoms vary greatly across the different classes of substance in part based on the effects of substance consumption.

1.4 Substance use disorder: A chronic brain disease

1.4.1 Substance use disorder: A multi-step pathology

The voluntary intake of drugs of abuse is a highly preserved behavior throughout phylogeny. In fact, most people in developed countries experience with both licit and illicit drugs over their lifetime but only a subset becomes addicted (Anthony *et al.*, 1994; Nutt *et al.*, 2007; Lopez-Quintero *et al.*, 2011). A field study from the early 90s among eight thousand Americans, 15-54 years old, demonstrated that about one third (31.4%) of tobacco smokers had developed tobacco dependence and about 15.4% of drinkers had become alcohol dependent. Among users of the other drugs, about 14.7% had become dependent on average. This value, however, strongly depends on the drug of abuse. The proportion of users becoming addicts ranges from 23.1% for heroin to 16.7% for cocaine and only 9.1% of people that used cannabis (Anthony *et al.*, 1994). Although this study is rather old and applied the criteria from the DSM-III-R to identify addicts, it clearly pointed out the development of SUD as a multi-step pathology that progresses from simple use to addiction throughout progressive deregulations of use (Kreek *et al.*, 2002). The transition to addiction consists of three phases. (1) The occasional, controlled or social use, (2) drug abuse or harmful use, and (3) drug addiction (Figure 2). These three phases are consecutive because entering in one phase is necessary to shift in another, but independent because entering in one phase is not sufficient to get to the next one (Piazza & Deroche-Gamonet, 2013). The first phase is a nonpathological stage in which drug use is rather sporadic, limited to recreational purposes and occupies only a small portion of the behavioral repertoire. The second phase is the first moderate pathological state. Here, the drug intake changes mainly in quantitative terms. The individual's drug use is elevated

in terms of frequency, amount and motivation for the drug. The last phase is the most serious pathological state in which the individual becomes fully addicted. In contrast to the quantitative change from controlled to harmful use, this transition is predominantly marked by a qualitative change. The amount of the drug consumed does not necessarily change, however, drug-taking and -seeking becomes the individual's major goal-directed behavior and replaces the *'normal'* behavioral repertoire. The addicted prone loses control over drug-seeking and -taking, and continues using the drug despite the knowledge of adverse consequences (Koob & Le Moal, 2008b; Piazza & Deroche-Gamonet, 2013). The act of engaging drug-seeking after a period of drug abstinence is termed relapse and defines addiction as a chronic relapsing disorder. Appallingly, between 40-60% of people with SUD relapse even after prolonged abstinence which remains the major clinical health concern (McLellan *et al.*, 2000). A particularly troublesome aspect of drug addiction is that the vulnerability to relapse persists for years even in the absence of repeated drug use. Three main stimuli have been recognized to trigger relapse in humans : (1) the re-exposure to the drug that originated the addiction but also to other drugs of abuse (de Wit, 1996), (2) the presence of drug-associated environmental cues (Carter & Tiffany, 1999), and (3) stressful situations or negative emotional states (Shiffman *et al.*, 1996). Craving is often seen as the emotional state that triggers drug-seeking. However, craving in itself has been difficult to measure in human clinical studies and does not always correlate with relapse (Tiffany *et al.*, 2000).

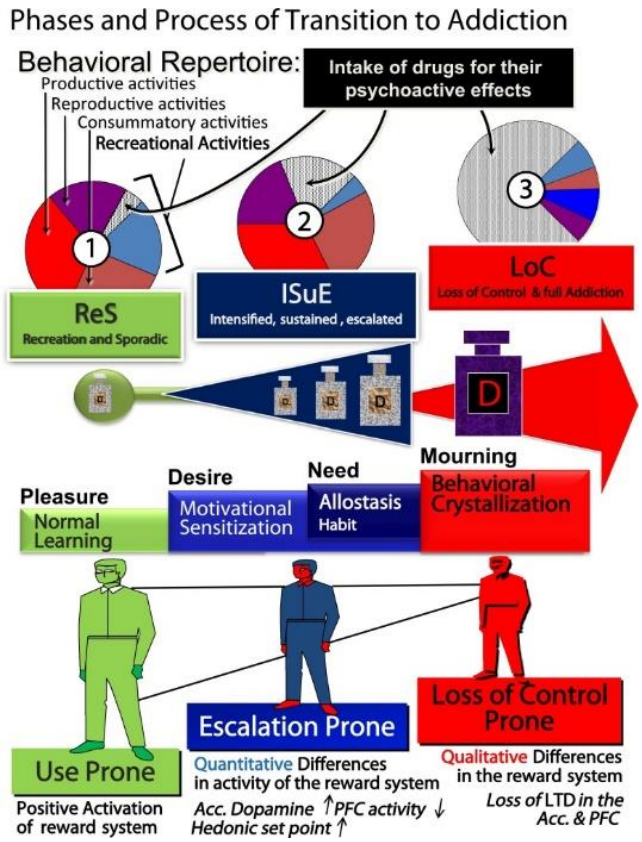

Figure 2. Summary of the phases and processes of transition to addiction. (Piazza & Deroche-Gamonet, 2013). **Abbreviations:** Accumbens (Acc), long-term depression (LTD), prefrontal cortex (PFC)

1.4.2 SUD: A multi-factorial pathology

Once the three different phases of SUD are established, the reasons why a subset of individuals develops SUD but others do not still remain open. The vulnerability to develop SUDs embraces multiple dimensions and is influenced by a combination of environmental and genetic factors whereby both couple with direct drug-induced effects. Importantly, these three components are accompanied by an overarching factor that is time

(Figure 3). Hence it is clear that the vulnerability to develop SUD is, multi-factorial, where multiple genes together drug and environmental factors combine to generate the disorder.

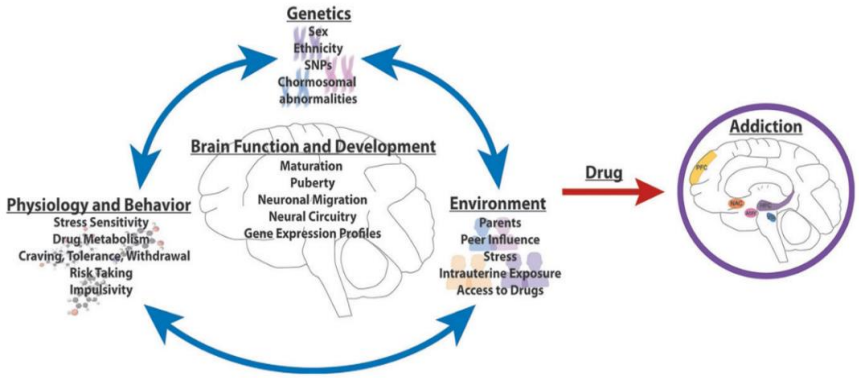

Figure 3. Vulnerabilty factors of substance use disorder.
Addiction is a complex phenotype that is regulated by both genetic and environmental factors. Vulnerability to substance abuse has both genetic and environmental risk factors that act in concert to produce the phenotype, although exposure to drugs of abuse (indicated with the red arrow) is necessary for the behavioral phenotype to emerge (Walker & Nestler, 2018).

Environmental factors include all factors that are not of genetic nature. Among the most important ones stress and adverse life events are found (Koob & Le Moal, 2008a; Peña *et al.*, 2014). Epidemiological studies further demonstrated that vulnerability to SUD increases as a function of lower education, unmarried status, peer influences, chaotic home and domestic abuse, drug availability and numerous other socio-demographic variables (Grant *et al.*, 2001; Crum *et al.*, 2005; Kessler *et al.*, 2005; Swendsen *et al.*, 2009). A person's income and education can influence the type of drug of abuse. Indeed, more than 80% of smokers live in low- and middle-income countries (WHO, 2017). Probands with less education and with an individual income lower than $35,000 reported higher rates of nicotine

use. Respondents who completed at least some college education or with an individual income equal or higher than $70,000 reported higher rates of alcohol, cannabis or cocaine use (Lopez-Quintero *et al.*, 2011). Indeed, alcohol use disorders are more prevalent in high-income countries with the highest prevalence in the European region and the region of the Americas (WHO, 2018).

On the other hand, a large body of evidence for a robust genetic contribution (e.g. drug-sensitivity and -metabolism) to addiction has come from classical family, twin, and adoption studies in humans (Walker & Nestler, 2018) Indeed, the estimated overall heritability of vulnerability to addiction for all abused drugs is approx. 50% (Wang *et al.*, 2012).It was shown that siblings of ethanol-dependent individuals presented a higher vulnerability to develop alcohol use disorder when compared to controls (Bierut *et al.*, 1998), and descendants of alcoholics were five times more likely to be alcohol dependent (Midanik, 1983). Although only a few studies focused on other drugs of abuse, it is suggested that first-degree relatives of substance abusers have higher rates of addiction when compared to controls (Bierut *et al.*, 1998; Merikangas *et al.*, 1998). This further substantiates the importance of a genetic predisposition for the development of SUDs and the complex multifactorial origin of this disease. However, one drawback of all these studies is the difficulty in distinguishing the contribution of genetic variance in individuals vs. environmental factors. One possibility to avoid this bias is using data from twin studies utilizing monozygotic and dizygotic twins, who presumably share much of the same environmental influences, to quantify the contribution of heritable factors. If the development of SUD is more similar in monozygotic than in dizygotic twins, then genetic factors contribute to a high extent. However, it would be a polygenetic

component if the coherence between monozygotic twins is lower than 100%. If the outcome is similar between both types of twins, then environmental factors contribute to the disorder. Twin studies estimate that the heritability of alcohol use disorder ranges from 40% to 60% (Schuckit, 2009; van der Zwaluw & Engels, 2009), and ranges from 30% to 80% for other drugs of abuse (Tsuang *et al.*, 1996; Kendler *et al.*, 2000, 2006; Agrawal *et al.*, 2005; Pergadia *et al.*, 2006). The heritability of smoking initiation and nicotine use disorder (NUD) is estimated to be 50% and 59%, respectively (Li & Burmeister, 2009).

As already mentioned, an individual's vulnerability is multidimensional. Hence, there are several risk factors including age, comorbidity with other psychopathological conditions, gender and inter-racial differences (not discussed) that are influenced by both environmental factors and genetics. Indeed, the adolescence stage represents the phase of greatest vulnerability for SUD, increasing its prevalence about six-fold when drug on-set occurs at the age of 13 to 18 (Merikangas *et al.*, 2010). In this period of cortical brain development, many important cognitive and emotional functions are still maturing which promote vulnerable phenotypes, such as novelty- and sensation-seeking, risk-taking, mood-instability or poor inhibitory control (Crews *et al.*, 2007). Indeed, a dramatic maturational process ongoing in adolescence is the prefrontal cortex (PFC) development, including its dopamine (DA) innervation. DA axons grow from the striatum to the prefrontal cortex, the only known case of long-distance axon growth during adolescence (Hoops & Flores, 2017). These axons are particularly vulnerable to environmental effects, including recreational drug use during adolescence and are strategically localized to profoundly influence prefrontal cortex structure and function (Hoops & Flores, 2017) Importantly, adolescence on-set substance use is a

significant predictor of SUDs over the lifespan (Grant & Dawson, 1998). Thus, the age at which smoking begins can influence the total years of smoking, the number of cigarettes smoked in adulthood, and the likelihood of quitting. Individuals reporting any lifetime psychiatric disorder, including mood, anxiety, conduct, personality disorder or ADHD have higher rates of nicotine, alcohol, cannabis, and cocaine use. Moreover, people with a family history of a SUD or having a diagnosis of a SUD possess a higher vulnerability to develop drug addiction (Lopez-Quintero *et al.*, 2011). Furthermore, there are significant gender differences in the past 12-month prevalence of alcohol use disorders. In 2016, an estimated 2.3 million deaths and 106.5 million DALYs were attributable to the consumption of alcohol among men whereby women experienced 0.7 million deaths and 26.1 million DALYs attributable to alcohol consumption. Globally an estimated 237 million men and 46 million women have alcohol use disorders (WHO, 2018). The genetic contribution for nicotine varies between 60% for men and 51% for women in the United States whereas in an Australian sample heritability estimates were 33% in men, but 67% in women (Heath *et al.*, 1993). Males are less likely to transition from nicotine use to NUD than females, and more likely to transition from alcohol and cannabis use to SUD (Lopez-Quintero *et al.*, 2011).

Interestingly, evidence suggests that earlier stages of drug use are seemingly influenced to a greater extent by environmental factors whereas genetic factors play a greater role in the severity of substance abuse (Midanik, 1983; Tsuang *et al.*, 1996; Kendler & Prescott, 1998; Rhee *et al.*, 2003; Vink *et al.*, 2005; Fowler *et al.*, 2007), highlighting the multi-factorial nature of the addiction phenotype.

The overarching risk factor that accompanies all vulnerability factors is time (Figure 4). Indeed, the probability of transition to addiction is very small after the first year of substance use onset (2.0% for nicotine, alcohol and cannabis users and 7.1% for cocaine users). The probability estimates of transition to addiction a decade after use onset are already moderate (15.6% among nicotine users, 14.8% among cocaine users, 11.0% among alcohol users, and 5.9% among cannabis users) that is consistent with other field studies (Anthony *et al.*, 1994; Nutt *et al.*, 2007). However, lifetime cumulative probability estimates indicated that 67.5% of nicotine users, 22.7% of alcohol users, 20.9% of cocaine users, and 8.9% of cannabis users would develop SUD on those substances at some time in their life (Lopez-Quintero *et al.*, 2011).

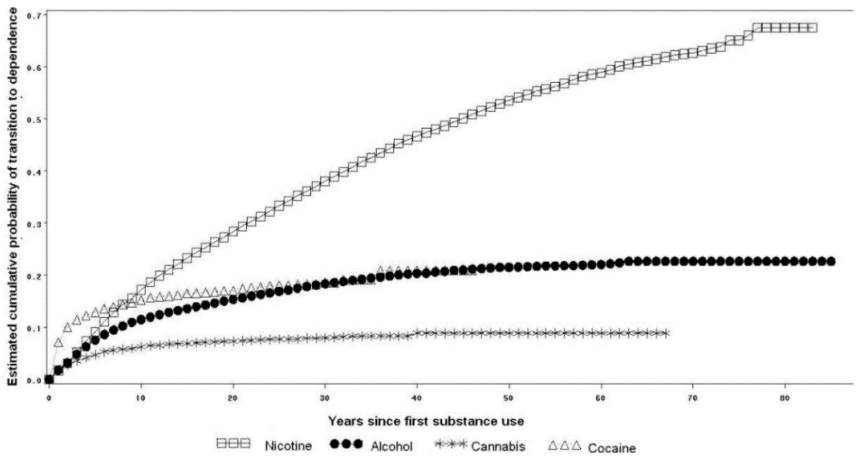

Figure 4. Cumulative probability of transitioning to dependence on nicotine, alcohol, cannabis and cocaine among users of these substances.
(Lopez-Quintero *et al.*, 2011).

1.4.3 Substance use disorder: A multi-faceted pathology

The above-discussed time-dependent individual vulnerability interacts with the direct pharmacokinetic and -dynamic effects of drugs of abuse. Although almost all drugs of abuse are known to target common neurobiological substrates (Nestler, 2005), the mechanisms by which every drug acts on its substrates differs, and hence leads to specific neurobiological effects that are translated into specific pathological behaviors (Camí & Farré, 2003). For instance, cocaine addicts show mainly behavioral criteria whereas heroin and alcohol addicts also show pharmacological symptoms. Individuals addicted to alcohol often show daily episodes or elongated days of heavy drinking, whereas smokers present a highly titrated intake of nicotine just during their waking hours. Similarly, abstinence in alcoholics and heroin addicts induces a severe somatic and emotional withdrawal syndrome, whereas cocaine abstinence is predominantly characterized by negative emotional states such as dysphoria, irritability and intense craving. These behavioral differences observed mainly occur due to the distinct pharmacological properties of different drugs of abuse (Camí & Farré, 2003). Besides, the abuse potential largely depends on the pharmacokinetic and physicochemical properties of a drug (Camí & Farré, 2003). Water solubility facilitates the injection of a drug, whereas liposolubility increases the passage through the blood-brain barrier. Volatility favors the inhalation of drugs in vapor form, and heat resistance favors smoking of the drug (Farré & Camí, 1991). Rapid onset and intensity of effect increase the abuse potential (Mumford *et al.*, 1995; Roset *et al.*, 2001), and drugs that quickly reach high brain concentrations have usually a higher abuse potential. Accordingly, smoking crack cocaine is more addictive than the intranasal administration of cocaine (Hatsukami & Fischman, 1996; Farré

et al., 1998). Finally, the biologic half-life of the drug is also directly related to its potential for abuse. Therefore, high self-administration rates and early emergence of withdrawal symptoms have been observed in drugs with a rapid clearance rate. Heroin, for example, produces more abrupt and intense withdrawal syndromes than methadone does (Camí & Farré, 2003).

2 Behavioral models of addiction

Whereas clinical research in human addicts has been helpful to elucidate the extent, demographics, and severity of SUD, much of the recent progress in understanding the neurobiology of addiction has derived from the results obtained in a variety of increasingly sophisticated animal models. The validity of animal models is assessed by three criteria, the face-, construct- and predictive-validity (Sanchis-Segura & Spanagel, 2006). Face validity means that a model recapitulates important anatomical, biochemical, neuropathological, or behavioral features of the human disease. Construct- or etiologic-validity refers to the disease relevance of the methods by which a model is constructed. In the ideal situation, researchers would achieve construct validity by recreating in an animal the etiologic processes that cause the disease in humans and thus replicate neural and behavioral features of the illness. Predictive- or pharmacological-validity signifies that a model responds to treatments in a way that predicts the effects of those treatments in humans (Nestler & Hyman, 2010). Although no animal model of addiction totally emulates the human condition, critical features of the process of drug addiction can be reliably measured in animal studies, including the intracranial electric self-stimulation paradigms, the place conditioning methods as well as the self-administration techniques, among others (Sanchis-Segura & Spanagel, 2006). These models were predominantly used to assess the neurobiological substrates underlying the hallmarks of early stages of addiction such as the reinforcing effects of drugs of abuse and, in some cases, the aversive aspects of drug withdrawal. However, more recent studies have been adapted their design to study the neurobiological substrates that underly characteristics of full developed addiction, including the loss of control over drug intake (Ahmed & Koob, 1998),

continuing drug use despite adverse consequences (Deroche-Gamonet *et al.*, 2004), and the relapse to drug-seeking and -taking after protracted abstinence (Shaham *et al.*, 2003).

2.1 Intracranial electric self-stimulation

Early work using the intracranial electric self-stimulation (ICSS) paradigm was fundamental for the identification of the brain reward circuitry (Olds & Milner, 1954). Although reward self-stimulation involves widespread brain circuits, the most sensitive sites involve the trajectory of the medial forebrain bundle that connects the ventral tegmental area (VTA) to the basal forebrain (Olds & Milner, 1954). In the ICSS procedure, animals self-stimulate reward-related brain areas by lever-pressing or nose-poking, due to intracranial electrodes that were implanted into reward-related brain areas prior to the experiment. During the first sessions, the threshold of the minimum current needed to promote intracranial self-stimulation is estimated. Once a stable baseline is established, a rewarding such as drugs of abuse decrease the self-stimulation threshold, whereas aversive drugs or stimuli, such as drug withdrawal, elevate the threshold for self-stimulation (Figure 5) (Markou *et al.*, 1993). Thus, ICSS methods are useful to investigate drug reward and withdrawal but have not been used as animal models of reinstatement of drug-seeking behavior.

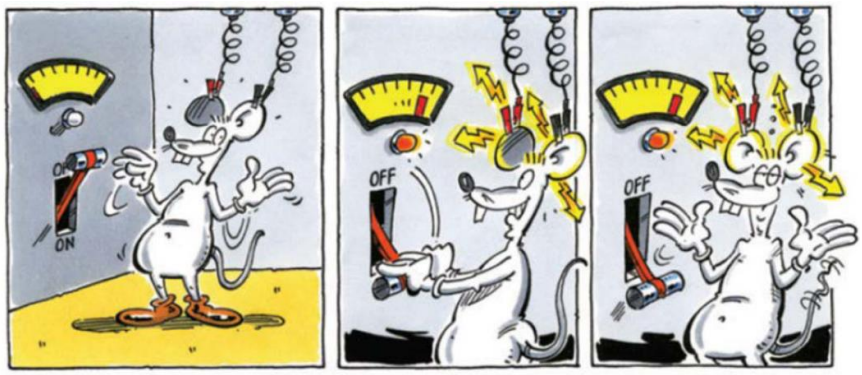

Figure 5. Intracranial self-stimulation paradigm.
(adapted from Sanchís-Segura and Spanagel, 2006).

2.2 Conditioned place preference and aversion

In the place conditioning models, animals are exposed to an apparatus generally consisting of two initially neutral environments that can differ in characteristics, such as color, texture, odor, and lighting (Bardo & Bevins, 2000). The experimental procedure is divided into three consecutive phases (Figure 6). Animals are first allowed to freely explore both environments whereby the time spent in each compartment is recorded. In the conditioning phase, animals are administered with the drug of abuse and exposed to one specific environment. In contrast, the other compartment is paired with vehicle pretreatment. After several conditioning sessions, the initially neutral compartment is then associated with the drug of abuse and acts now as a drug-associated stimulus. On the test day, animals (usually in a drug-free state) have free access to both compartments and the preference/avoidance for one of the two environments is evaluated. A drug with rewarding properties will typically induce place preference (positive score), whereas a drug with aversive effects or withdrawal from chronic drug administration will mainly

produce place aversion (negative score). Although drug consumption in humans can induce conditioned approach/avoidance to specific drug-related stimuli, conditioned place preference (CPP) and conditioned place aversion (CPA) are not intended to model any particular feature of human behavior (Sanchis-Segura & Spanagel, 2006)(Sanchís-Segura and Spanagel, 2006). CPP and CPA are mainly used as an indirect measure of the rewarding or aversive effects of a drug. Two variables with different implications are usually analyzed using this paradigm: the acquisition and the expression of place preference. The acquisition phase has been proposed to be mainly related to learning and memory mechanisms, whereas the expression phase would be more linked to incentive motivation, memory recall or sign tracking. More recently, CPP models have been modified to test reinstatement procedures as well (Aguilar *et al.*, 2009). Reinstatement studies usually involve an extinction phase after the acquisition period. In the extinction phase, the animals are exposed to the previously drug-paired context while in a drug-free state (Aguilar *et al.*, 2009). Using this model, an extinguished CPP has been shown to be robustly reinstated by a non- contingent administration of a drug or by exposure to stressful stimuli (Aguilar *et al.*, 2009). However, some of the effects obtained in the place conditioning paradigms may reflect state-dependent learning due to discriminative properties of the test drug rather than rewarding effects (Tzschentke, 2007), which represents a limitation for the interpretation of the reinstatement models based on these paradigms.

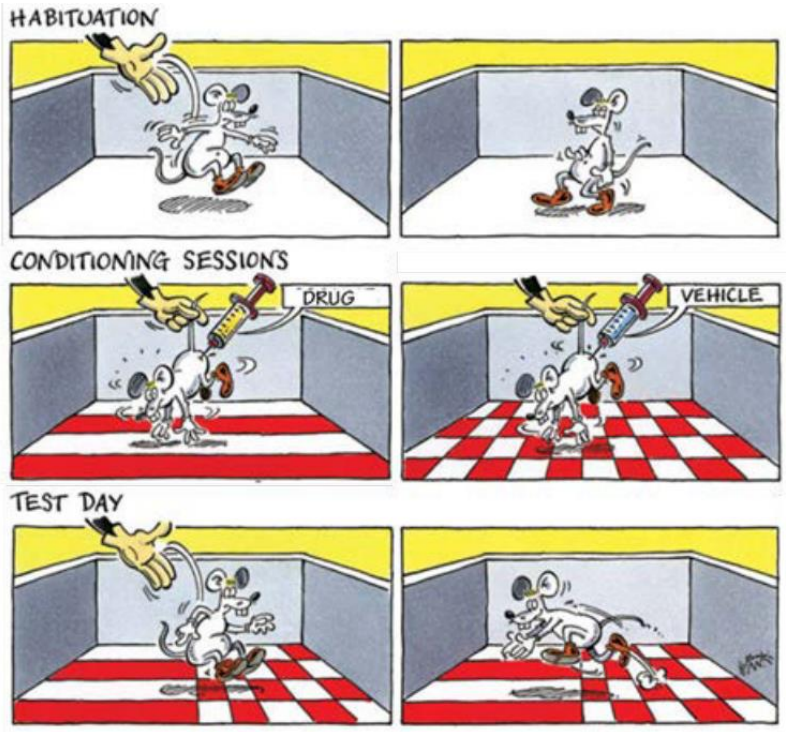

Figure 6. Conditioned place preference paradigm.
(adapted from Sanchís-Segura and Spanagel, 2006).

2.3 Operant self-administration

Operant self-administration is the gold standard in addiction research in rodents. Indeed, drugs that are self-administered by animals correspond well with those that have high abuse potential in humans (Collins *et al.*, 1984) and it is thought to be the behavioral model with the highest predictive validity (O'Connor *et al.*, 2011). It bears a close resemblance to human drug-taking, involves similar forms of conditioning and learning (Maldonado, 2002), and the neural chemistry and anatomical substrates underlying drug self-administration are assumed to be similar in these animal models and in human addicts (Sanchis-Segura & Spanagel, 2006). Another advantage of this technique is that the experimenter intervention

is minimal. Consequently, this technique is widely used in preclinical research and seems to be adequate for identifying common neural mechanisms and developing useful strategies for the treatment of SUD (Sanchis-Segura & Spanagel, 2006). In operant self-administration procedures, the operant chamber consists of two manipulandi that are typically levers or nose-pokes, and devices that deliver the reinforcer (Figure 7). The reinforcer can be delivered by different routes of administration according to the drug of study, including, intravenous, intracranial, intragastric and oral delivery. Typically, alcohol and food studies use oral self-administration, whereas intravenous self-administration is widely used to determine the reinforcing properties of most drugs of abuse, including opioids, psychostimulants, cannabinoids, and nicotine. For intravenous drug self-administration studies, animals are implanted with an intravenous catheter and are trained to self-administer the drug for various days in an operant box. The manipulandi transmit the operant responses and are randomly divided into *'active'* and *'inactive'*. A response in the inactive manipulandum lacks any programmed consequences, but will provide important control procedures for non-specific motor and motivational actions, such as modifications in exploratory activity and locomotion (Sanchis-Segura & Spanagel, 2006; Thomsen & Caine, 2007). A response in the active manipulandum is linked to the delivery of the drug. Moreover, the active manipulandum can be paired with other stimuli (e.g. light or tone), which improves the learning of the operant behavior and are often used as a drug-associated cue.

2.3.1 Fixed and progressive ratio schedule of reinforcement

Positive reinforcement is the obtainment of a reward by fulfilling a behavioral task. Commonly used schedules of reinforcement are either

fixed or progressive (Johanson, 1978; Spealman & Goldberg, 1978; Katz, 1989). In a fixed ratio (FR) schedule of reinforcement, the animal receives the drug when a preselected number of active lever presses or nose-pokes is fulfilled. Rodents on a simple schedule of continuous reinforcement, such as FR1 (one lever-press or nose poke delivers one drug infusion) will develop a highly stable pattern of drug self-administration in a limited access situation (Maldonado *et al.*, 1993). The use of different schedules of reinforcement in intravenous self-administration provides information about the reinforcing strength of the drug.

Under a progressive ratio (PR) schedule of reinforcement, the active responses required to obtain the reinforcer escalate following an arithmetic progression (Figure 7). The highest response rate accomplished to obtain a reinforcement is called *'breakpoint'* and is thought to be a reliable measurement of the motivation of an animal to obtain the reinforcer (Richardson & Roberts, 1996).

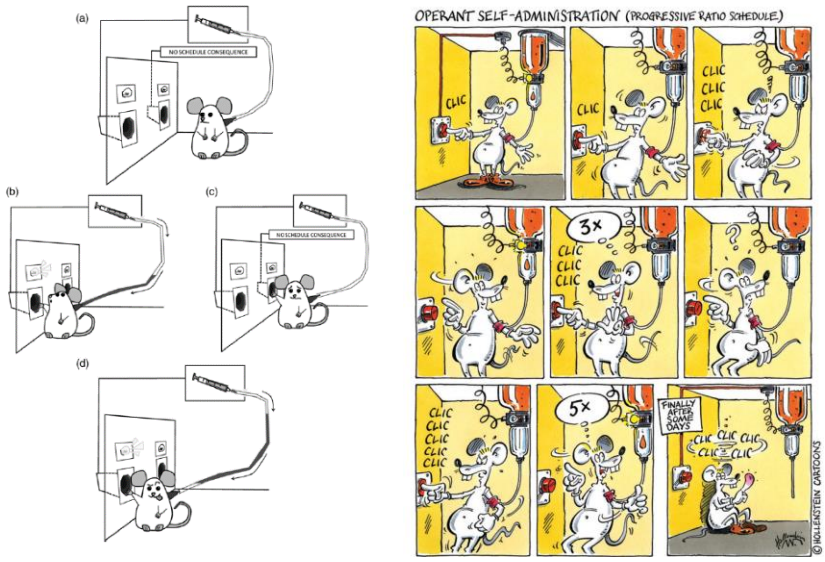

Figure 7. Drug self-administration paradigm.
Animation of a fixed (left panel) and progressive ratio (right panel) schedule in operant behavior. (Sanchis-Segura & Spanagel, 2006; Martin-García *et al.*, 2014)

2.3.2 The yoked control procedure

The yoked control procedure is a research design used in operant conditioning experiments in which matched research subjects are yoked (joined together) by receiving the same reinforcement but with different contingencies (Salkind, 2010). In other words, the yoked control animal receives the same amount of reward at the same time, although, there is no contingency between its responding and the reward delivery. Only the experimental animal can accomplish rewards by active responding. The utility of this procedure is to disentangle goal-directed behavior to obtain a reward and unspecific responding due to drug effects. Hence, the response rate of an experimental animal will be higher if the response-reward contingency is contributing to the observed response rate. In more recent operant conditioning procedures, one experimental animal is usually linked to two yoked control animals (Figure 8). One that receives the same reward as the experimental animal (yoked drug) and another that receives only the vehicle (yoked vehicle). This experimental design allows to further distinguish between neurobiological changes caused by the pharmacological properties of the drug of abuse (yoked drug vs. yoked vehicle) and modifications induced by behavioral repertoires such as goal-directed or motivated behaviors, reward-conditioning and the reinstatement of drug-seeking behavior (experimental animal vs. yoked drug) (Martin *et al.*, 2006; Gipson *et al.*, 2013; Guegan *et al.*, 2013).

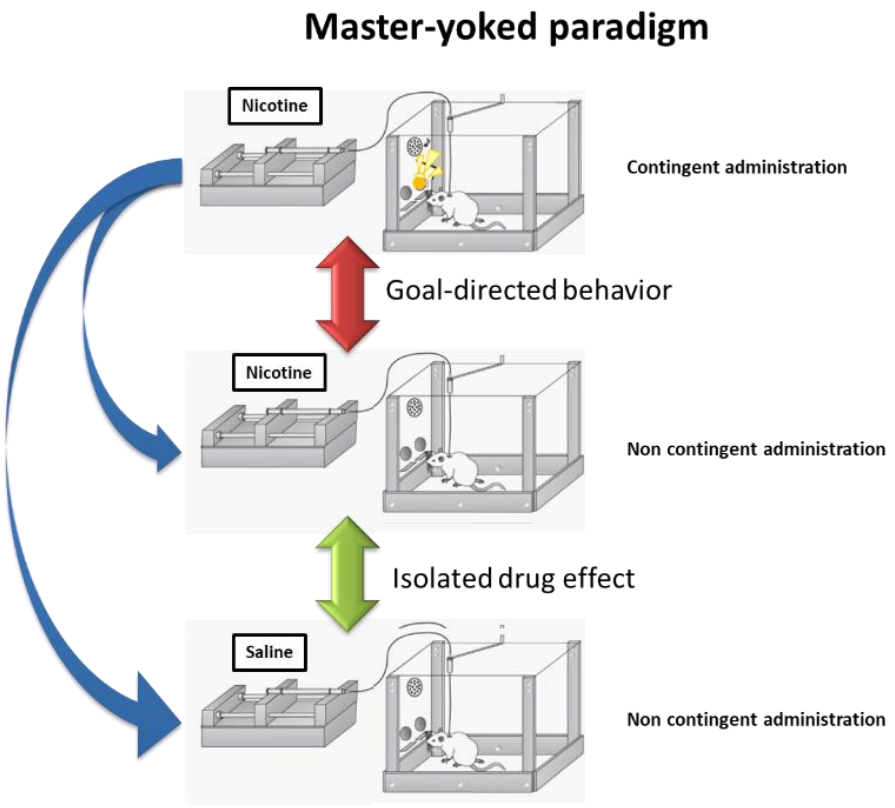

Figure 8. Animation of the yoked-control procedure.

2.3.3 Reinstatement model of drug relapse

Most animal studies on drug relapse are based on reinstatement models (Davis & Smith, n.d.; Shaham *et al.*, 2003; Epstein *et al.*, 2006), whereby reinstatement refers to the recovery of a learned response that occurs when a subject is exposed to some particular stimuli after the extinction of such a response (Bouton & Swartzentruber, 1991). The main strength of this method is that reinstatement in laboratory animals is induced by the same three conditions reported to provoke relapse in humans. Accordingly, craving and relapse to drug-taking and -seeking in human

addicts are mainly triggered by the re-exposure to the drug of abuse (de Wit, 1996), stressful situations (Shiffman *et al.*, 1996) and drug-associated cues (Carter & Tiffany, 1999).

The reinstatement model of relapse is divided into three experimental phases (Figure 9) (Shalev *et al.*, 2002; Shaham *et al.*, 2003). First, animals are trained to acquire and maintain drug self-administration in operant conditioning chambers. During the self-administration phase, a stimulus-reward association is established. Second, operant behavior is extinguished. Extinction testing sessions are identical to training sessions except that operant responses result in no programmed consequences, which means that no drug is delivered or is substituted by saline (Yan & Nabeshima, 2009). This might initially lead to a burst of responses (depending on the drug), but over the course of this extinction phase responding will gradually decrease (De Vries & Schoffelmeer, 2005). Extinction procedures can provide measures of the motivational properties of drugs by assessing the persistence of drug seeking-behavior in the absence of response-contingent drug availability. Measures provided by an extinction paradigm reflect the degree of resistance to extinction, including the duration of extinction responding, and the total number of responses emitted during the entire extinction session. Resistance to extinction and high responding rates on the active manipulandum (especially at the beginning of extinction phase) are related with high motivation to seek the drug. Although the possible mechanisms underlying the resistance to extinction in mice remain unclear (Yan & Nabeshima, 2009), the resistance to extinction in mice is similar to the case in human addicts (Childress *et al.*, 1993; Gilpin *et al.*, 1997; McKay *et al.*, 2001). After the extinction of drug-reinforced behavior, reinstatement of drug-seeking behavior can be determined (Yan

& Nabeshima, 2009). It has been reported that non-contingent drug injections administered after extinction can induce reinstatement of drug-seeking in cocaine-, heroin-, ethanol- and nicotine-trained animals (Chiamulera *et al.*, 1996; Lê *et al.*, 1998; Self & Nestler, 1998).

Animal models of stress-induced reinstatement elicit a strong recovery of extinguished drug-seeking behavior in the absence of further drug availability (Ahmed & Koob, 1997; Shaham *et al.*, 2003; Yan & Nabeshima, 2009). Stress-induced reinstatement of drug-seeking is been realized by intermittent foot shock stimuli, restraint stress, pharmacological agents that induce stress (e.g. yohimbine), or food deprivation (Shalev *et al.*, 2010). Stress-induced reinstatement has been reported in cocaine-, heroin-, ethanol-, food- and nicotine-trained animals (Erb *et al.*, 1996; Shaham, 1996; Ahmed & Koob, 1997; Plaza-Zabala *et al.*, 2012).

On the other hand, drug-associated cues can be defined as neutral motivational stimuli, which acquire motivational properties through associations with a primary reinforcer. In this paradigm, responses on the active lever in the acquisition phase result in a drug infusion paired with the presentation of a brief stimulus (light or tone). Thus, drug-associated stimuli can elicit drug-seeking behavior in experimental animals. Subsequent re-exposure to a drug-associated stimulus after extinction produces a strong recovery of responding at the active manipulandum in the absence of any further drug availability (Yan & Nabeshima, 2009). Cue-induced effect on reinstatement has been reported in cocaine-, heroin-, ethanol-, nicotine-, cannabinoid- and food-trained animals (De Vries & Schoffelmeer, 2005; Soria *et al.*, 2008; Martin-García *et al.*, 2009, 2011).

In addition, contextual stimuli have also been applied to induce reinstatement. Under these situations, rodents are first trained to self-administer the drug in a context with specific cues that reveals the

availability of the reinforcer, and the operant behavior is extinguished in a different context that contains other specific cues. The re-exposure of the animal to the drug-paired context reinstates drug-seeking behavior (Crombag *et al.*, 2008).

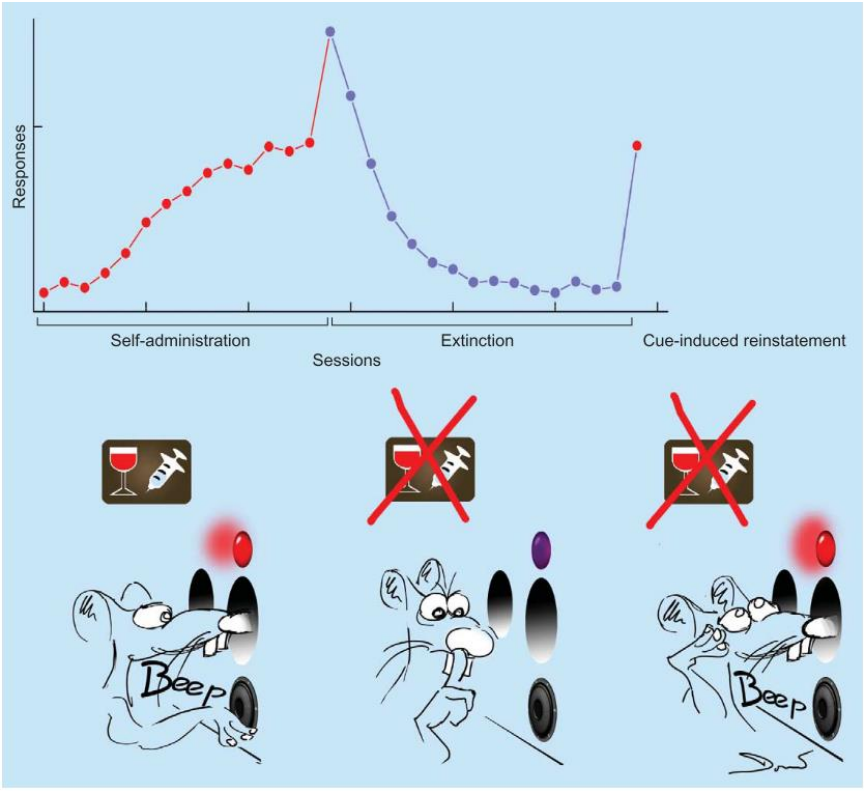

Figure 9. Animation of cue-induced reinstatement of drug-seeking behavior.
(De Vries & Schoffelmeer, 2005)

3 The mesocorticolimbic pathway

The mesocorticolimbic system (Figure 10) is defined as the neural pathway that connects the ventral tegmental area (VTA) with two principal targets, the nucleus accumbens (NAc) and the medial prefrontal cortex (mPFC). This neuronal pathway is responsible for evaluating and integrating the environmental and emotional stimuli that lead to the appropriate activation of motor patterns supporting different types of motivated behaviors (Pistillo *et al.*, 2015). It is suggested that DA transmission critically contributes to the codification of the motivational value and salience of a given stimulus and facilitates reward-induced learning that further promotes recurrent drug-taking (Cardinal & Everitt, 2004; Wise, 2004; Bromberg-Martin & Hikosaka, 2011). However, the differential activation of γ-aminobutyric acid (GABA)ergic, glutamatergic and cholinergic signaling modulates DA signaling and provides crucial biological substrates for motivated behaviors. DAergic, GABAergic, glutamatergic and cholinergic signaling converge in and are integrated by medium spiny neurons (MSNs) in the NAc, which in turn activate and/or inhibit specific motor patterns. (Markou, 2008; D'Souza & Markou, 2013; Koob & Volkow, 2016). Furthermore, additional brain areas that are interconnected with the mesocorticolimbic pathway play also essential roles in the acute and chronic effects of drugs of abuse. These areas include the caudate putamen, amygdala (AMG) and related structures of the so-called 'extended-amygdala' (which comprise the central nucleus of the amygdala (CeA), the bed nucleus of the stria terminalis (BNST) and a transition zone in the medial (shell) subregion of the NAc), (not shown), the laterodorsal tegmentum (LDTg), the lateral habenula (LHb), the mediodorsal thalamus (MDT), the rostromedial tegmentum (RMTg), the subthalamic nucleus (not shown), the ventral hippocampus (vHPC) (not

shown), and the ventral pallidum (VP) (not shown) (Figure 10) (Cooper *et al.*, 2017). Research over the last years using opto- and chemogenetics in transgenic mice, neural tracing tools and electrophysiological studies made clear that the canonical models for mesocortical signaling and its subsequent role in SUD are oversimplified (Pistillo *et al.*, 2015; Cooper *et al.*, 2017; Kupchik & Kalivas, 2017; Klawonn & Malenka, 2019). Therefore, new perspectives of the reward system that will guide future treatment strategies for SUD and other related mental health disorders are required.

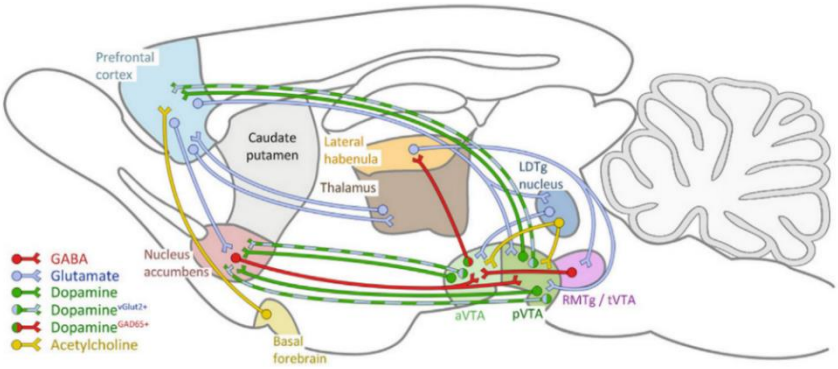

Figure 10. A simplified diagram of the main connections to and from the mesocorticolimbic system, in a sagittal section of rodent brain.
Glutamatergic, dopaminergic, cholinergic and GABAergic projections are in blue, green, yellow and red, respectively (Pistillo *et al.*, 2015). **Abbreviations:** laterodorsal tegmentum (LDTg), the rostromedial tegmentum (RMTg), anterior-lateral ventral tegmental area (aVTA), posterior-medial ventral tegmental area (pVTA)

3.1 The ventral tegmental area

The VTA is located in the ventral midbrain and can be divided into two principal subregions, the anterior-lateral ventral tegmental area (aVTA) and the posterior-medial ventral tegmental area (pVTA), and a further subregion called the tail of the VTA or rostromedial tegmental nucleus (RMTg) (Pistillo *et al.*, 2015).

The VTA comprises two main cellular populations, the DAergic and the GABAergic neurons (Johnson & North, 1992a). DA neurons are characterized by the presence of the DA-synthesizing enzyme tyrosine hydroxylase (TH), account for 60-65% of all VTA cells and are present in both subregions of the VTA. GABAergic interneurons and projection neurons account for 30-35% and express the GABA-synthesizing enzyme glutamic acid decarboxylase (GAD) (Swanson, 1982; Nair-Roberts *et al.*, 2008).

Nevertheless, the two-cell type canonical model of the VTA is actually more complex. GABAergic neurons are divided into projection neurons and interneurons. The projection neurons send inhibitory inputs to the NAc, PFC and the lateral habenula (LHb) (Van Zessen *et al.*, 2012; Stamatakis *et al.*, 2013). GABAergic interneurons contact and tonically inhibit DA neurons within the VTA (Johnson & North, 1992b; Carr & Sesack, 2000; Margolis *et al.*, 2012). Furthermore, there are some DA-GABA hybrid neurons that express both TH and the GAD65 isoform. GABA is loaded into synaptic vesicles by the DA vesicular transporter VMAT2 and co-released in the synapses together with DA (Tritsch & Sabatini, 2012). Another subpopulation of VTA DA neurons expresses the vesicular glutamate transporter vGluT2 and their stimulation leads to the appearance of glutamatergic excitatory postsynaptic currents in MSNs of the NAc (Chuhma *et al.*, 2004) and pyramidal neurons of the mPFC (Lavin *et al.*, 2005; Gorelova *et al.*, 2012). In addition, there is also a small portion of neurons in the VTA (2-9%) that express vGLUT2 mRNA but neither TH or GAD mRNA (Yamaguchi *et al.*, 2007; Nair-Roberts *et al.*, 2008; Taylor *et al.*, 2014), suggesting a subpopulation of glutamatergic neurons in the VTA.

The 2 most extensively studied VTA DA neuron subtypes to date are those that project to the ventral striatum (mesolimbic) and the mPFC

(mesocortical), yet, there are additional projection sites, including the AMG, the hippocampus (HPC) and the BNST. Interestingly, distinct VTA circuits generate reward or aversion. Indeed, VTA DA neurons are by no means a homogenous population, but sub-serve contrasting functions in the motivational control through connections with distinct circuits. Accordingly, a rewarding stimulus (e.g. cocaine) selectively modulates excitatory inputs to mesolimbic VTA DA neurons. In contrast, an aversive stimulus (e.g. hind paw formalin injection) selectively modulates synaptic inputs onto mesocortical VTA DA neurons (Lammel *et al.*, 2011).

VTA neurons receive GABAergic glutamatergic and cholinergic inputs from various brain areas. The main GABAergic transmission originates from the NAc, RMTg, and GABAergic interneurons, among others. These projections make up at least 70% of the synaptic input onto DA neurons (Kalivas *et al.*, 1993; Charara *et al.*, 1996; Omelchenko & Sesack, 2005; Tepper *et al.*, 2007; Watabe-Uchida *et al.*, 2012). The remaining 30% are glutamatergic inputs from the mPFC (see section 3.3), LTDg, LHb, AMG (not shown) and lateral hypothalamus (not shown), and cholinergic inputs deriving from the LTDg and the pedunculopontine tegmental nucleus (not shown) (Figure 11) (Pistillo *et al.*, 2015).

Tonic GABA input is sufficient to suppress burst firing even with excitatory inputs intact (Lobb *et al.*, 2010; Jalabert *et al.*, 2011). Optogenetic inactivation of GABA releasing neurons within the VTA was shown to be reinforcing while activation was aversive. Local GABAergic transmission, but not projection neurons to the NAc, is thought to modulate this effect. Indeed, activation of GABA VTA neurons led to decreased DA release in the NAc and reward behavior, whereby terminal activation of GABA neurons projecting to the NAc increased only GABAergic signaling in the NAc but failed to alter reward behavior (Tan *et al.*, 2012; Van Zessen *et al.*,

2012). Furthermore, local GABA neurons were shown to increase their firing in response to aversive stimuli (Tan *et al.*, 2012). In agreement, activation of GABA neurons disrupted reward behavior and reduced excitability of VTA DA neurons *in vitro* and *in vivo* (Van Zessen *et al.*, 2012). Excitatory inputs into the VTA can generate, as previously explained, either reward or aversion depending on the activation of mesolimbic (see section 3.2) or mesocortical (see section 3.3) VTA circuits, respectively. Activation of glutamatergic and cholinergic excitatory neurons in the LDTg, which preferentially synapse onto aVTA DA neurons that project to the NAc lateral shell, increased reward behavior (Omelchenko & Sesack, 2005; Lammel *et al.*, 2012). In contrast, activation of the LHb, a brain area that is in control of inhibiting DA cell activity in response to the absence of expected rewards (Omelchenko *et al.*, 2009), induced aversive behavior (Lammel *et al.*, 2012). Indeed, glutamatergic neurons from the LHb activate mesocortical VTA DA neurons and inhibit mesolimbic DA neurons indirectly by activating GABAergic neurons in the RMTg (Lammel *et al.*, 2012). Interestingly, this inhibitory pathway can be suppressed by a relatively restricted cell population of GABA-DA hybrid neurons of the aVTA. These neurons were shown to release only GABA-mediated inhibitory synaptic transmission but no detectable DA (Stamatakis *et al.*, 2013). Thus, activation of this pathway suppressed the firing of postsynaptic LHb neurons, which in turn enhanced the spontaneous firing of VTA DA neurons *in vivo* and produced reward-related behavior (Stamatakis *et al.*, 2013). Hence, it is suggested that inhibitory signaling by these hybrid DA-GABAergic neurons act to suppress LHb output under rewarding conditions.

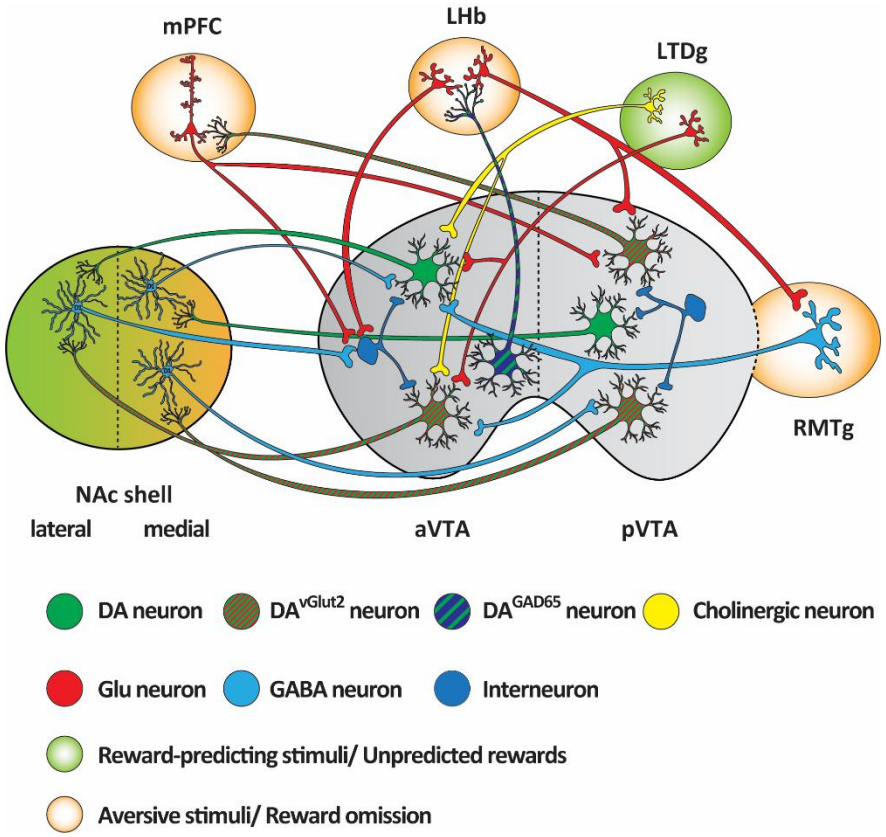

Figure 11. Illustration of major inputs and outputs to and from the VTA.
Activation and inhibtion of mesolimbic and mesocortical VTA DA neurons. For a detailed description see text above.
Abbreviations: γ-aminobutyric acid (GABA), anterior-lateral ventral tegmental area (aVTA), dopamine (DA), glutamate (Glu), glutamic acid decarboxylase 65 (GAD65), laterodorsal tegmentum (LTDg), Lateral habenula (LHb), medial prefrontal cortex (mPFC), nucleus accumbens (NAc), posterior-medial ventral tegmental area (pVTA), rostromedial tegmentum (RMTg), vesicular glutamate transporter 2 (vGlut2),

3.2 The striatum

The striatum is the largest structure of the basal ganglia. It is a critical component of motor and reward systems and coordinates multiple aspects of cognition, including both motor and action planning, decision-making, motivation, reinforcement, and reward perception (Ferré *et al.*,

2010; Taylor *et al.*, 2013; Yager *et al.*, 2015). The striatum is a highly heterogeneous brain area with cell-specific and region-specific differences (Cachope & Cheer, 2014; Yang *et al.*, 2018). It comprises a dorsal and a ventral portion. The dorsal striatum takes part in the nigrostriatal pathway but receives also inputs from cortical areas, including the orbital frontal cortex. The latter pathway was recently shown to drive compulsive reinforcement (Pascoli *et al.*, 2018).

The ventral portion of the striatum is a key node of the mesocorticolimbic pathway (Volkow et al. 2017) and contains different subdivisions known as the core, and the lateral and medial shell, which have different anatomical connectivity and functions (Pistillo *et al.*, 2015; Yang *et al.*, 2018). MSNs are the principal neuronal population in the NAc. They represent 95% of the nerve cells and are expressed in all three sub-divisions. The remaining 5% consist of a very heterogeneous population of interneurons, including tonically active cholinergic interneurons neurons (CINs) and GABAergic interneurons (Tepper & Bolam, 2004).

MSNs are GABAergic projection neurons that can be divided into two classes defined by their expression of either D1- or D2- like DA receptors (Gerfen *et al.*, 1990; Gerfen & Surmeier, 2011). D1 and D2 MSNs in the dorsal striatum are thought to have separate projections, with D1 MSNs constituting the direct pathway leading to an increasing thalamocortical drive, and D2 MSNs forming the indirect pathway that leads to a depression of thalamocortical activity. However, recent experiments showed that NAc MSNs do not necessarily follow the canonical model for the dorsal striatum. D1-MSNs comprise a significant portion of the classical indirect pathway by synapsing on VP neurons that project to the VTA (Kupchik *et al.*, 2015). On the other hand, D2-MSNs target VP neurons that innervate the thalamus directly. Thus, these D2-MSNs make a direct

pathway through the VP that disinhibits the thalamus (Cazorla *et al.*, 2013; Saunders *et al.*, 2015). Curiously, some 15% of VP cells project to both the ventral mesencephalon and the thalamus (Tripathi *et al.*, 2013), converging the direct and indirect pathway on the same neurons (Figure 12).

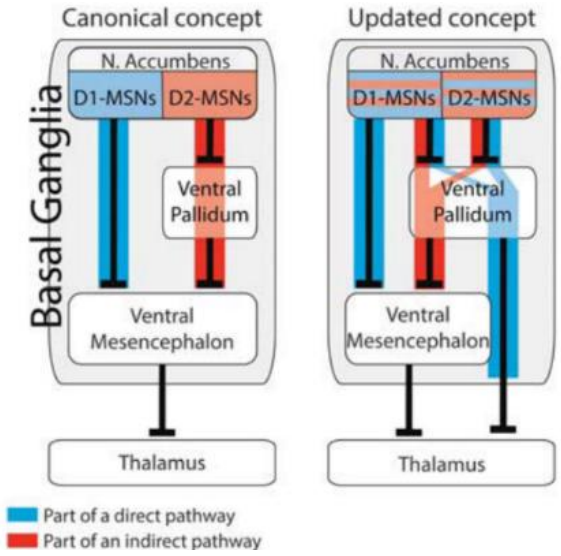

Figure 12. Canonical and novel concepts of the direct and indirect pathways of the nucleus accumbens.
(Kupchik & Kalivas, 2017). **Abbreviations:** Medium spiny neurons (MSNs)

In addition to this cellular heterogeneity, there is also a regional heterogeneity among the NAc core, and lateral and medial shell with distinct drug-associated behaviors and plasticity (Saddoris *et al.*, 2013). MSNs in the NAc core appear to be critical for assigning a motivational value to discrete stimuli associated with reward or aversion, particularly updating these values as circumstances change. In contrast, MSNs in the NAc shell drive behavioral responses to repeated exposure to rewarding experiences, such as chronic drug administration (Meredith *et al.*, 2008).

Furthermore, D1 MSNs in the NAc lateral shell mainly synapse onto VTA GABA neurons in the aVTA, resulting in a disinhibition of DA neurons that project back to the NAc lateral shell. In contrast, D1-MSNs in the medial shell subdivision generate direct inhibitory control over mesolimbic DA neurons in the lateral and medial VTA (Figure 13) (Yang *et al.*, 2018).

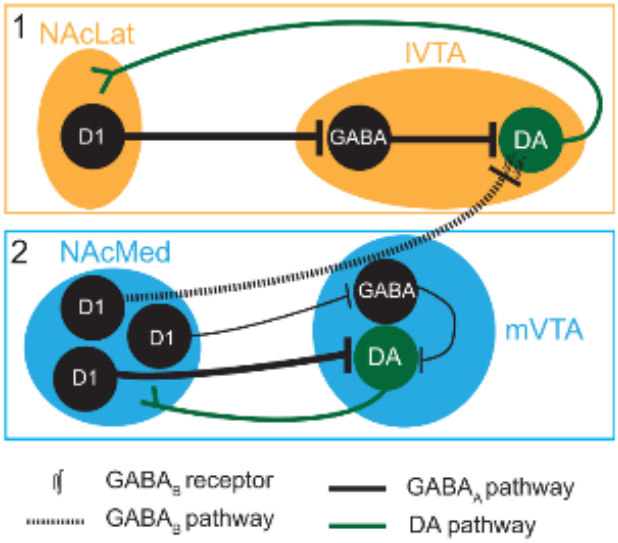

Figure 13. Wiring diagram illustrating direct and indirect feedback loops in the mesolimbic DA system.
(Yang *et al.*, 2018). **Abbreviations:** γ-aminobutyric acid (GABA), dopamine (DA), medial nucleus accumbens shell (NacMed), medial ventral tegmental area (mVTA), lateral nucleus accumbens shell (NacLat), lateral ventral tegmental area (lVTA),

In the NAc, it is indispensable to mention accumbal DA transmission that is thought to be responsible for the pleasurable effects of drugs of abuse and natural rewards. Indeed, all classes of drugs of abuse increase levels of extracellular dopamine in the NAc, despite their marked differences in cellular targets (Di Chiara & Imperato, 1988; Nestler, 2005). The role of D2 receptors is still contradictory. It was shown that the lack of D2 DA receptors blunted the rewarding effects of opioids (Maldonado *et al.*,

1997). In contrast, other studies showed that DA stimulation of high-affinity D2 receptors is not enough for drug reward (Caine *et al.*, 2002; Norman *et al.*, 2011) and that these receptors might even limit drug reward (Durieux *et al.*, 2009). The activation of low-affinity D1 receptors is necessary for the rewarding effects of drugs (Caine *et al.*, 2007) and for triggering conditioned responses (Zweifel *et al.*, 2009), concluding that only phasic DA transmission causes reward. In accordance with these experiments, positron emission tomography studies in humans have shown that fast and steep release of DA into the ventral striatum is associated with the subjective sensation of the so-called high (Volkow *et al.*, 2003).

Besides DA signaling, the NAc receives a large amount of glutamatergic input from a variety of limbic and cortical regions, some of the most notable being mPFC, vHPC, and BLA (Sesack & Grace, 2010; Floresco, 2015). Recent studies exhibited that optogenetic activation of the mentioned inputs to the NAc is reinforcing (Stuber *et al.*, 2011, 2012; Otis *et al.*, 2017) These findings could suggest that any excitatory input to the NAc is reinforcing regardless of the different behavioral roles of the brain areas providing the inputs. However, Zhu *et al.* recently reported that activation of glutamatergic inputs from the paraventricular nucleus of the thalamus causes aversion and that these inputs, like the PFC, vHPC, and BLA inputs, appear to synapse on both NAc D1 and D2 MSNs (Figure 14) (Zhu *et al.*, 2016).

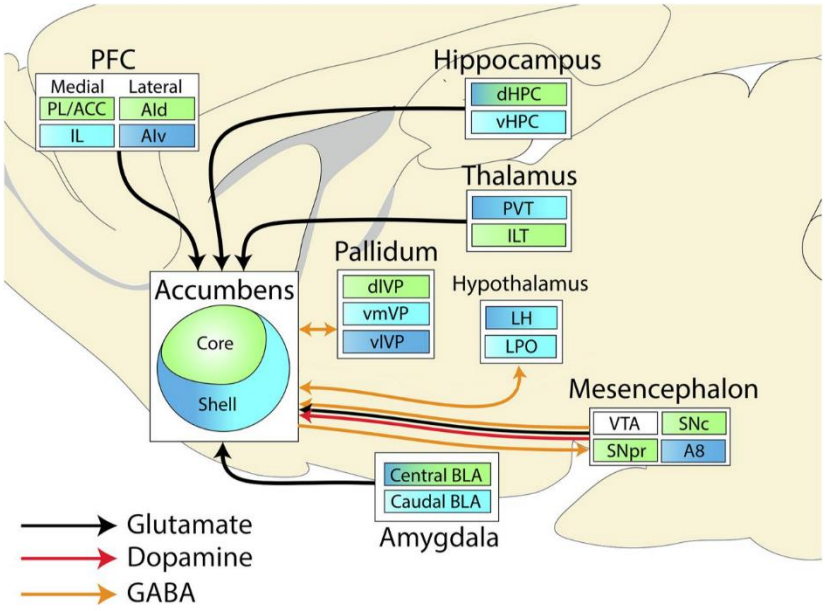

Figure 14. Illustration of major inputs and outputs to and from the NAc.
The NAc receives inputs from cortical, allocortical, thalamic, midbrain, and brainstem structures. In turn, it sends projections to other basal ganglia nuclei, nuclei in the mesencephalon, the hypothalamus, and the extended amygdala. Note that many structures project from different subareas to the NAcore or NAshell. For clarity, these projections have been color coded as projecting to the NAcore (green), medial NAshell (light blue), or lateral NAshell (dark blue); in reality, many regions project to both the NAcore and NAshell along topographical gradients (e.g., dorsoventral projections from the hippocampus terminating from lateral to medial parts of the accumbens; shown as color gradients in the figure). A number of regions project uniformly throughout the accumbens and are marked white (Scofield et al., 2016). **Abbreviations:** retrorubral area (A8), anterior cingulate cortex (ACC), dorsal anterior insular (AId), ventral anterior insular (AIv), dorsal hippocampus (dHPC), dorsolateral ventral pallidum (dlVP), dorsal raphe nucleus (DRN), infralimbic cortex (IL), interlaminar nuclei of the thalamus (ILT), locus coeruleus (LC), lateral hypothalamus (LH), lateral preoptic area (LPO), nucleus of the solitary tract (NTS), prelimbic cortex (PL), pedunculopontine nucleus (PPN), paraventricular nucleus of the thalamus (PVT), ventrolateral ventral pallidum (vlVP), ventromedial ventral pallidum(vmVP), substantia nigra pars compacta (SNc), substantia nigra pars reticulata (SNpr).

In contrast to striatal DAergic and glutamatergic activity, which originates mainly from inputs to the striatum, sources of striatal ACh release are mostly from CINs that account for about 2–5% of all striatal neurons (Descarries *et al.*, 1997; Descarries & Mechawar, 2000). CINs preferentially synapse with MSNs and other CINs (Graybiel *et al.*, 1994; Morris *et al.*, 2004) but also activate neuroglia-form cells (NGF) interneurons (Figure 15A). The role of CINs in the NAc is to modulate the sub- and supra-threshold responses of MSNs to cortical and/or thalamic excitation, particularly in reward-related activities (Tepper & Bolam, 2004). They express both the vesicular acetylcholine transporter (vAChT) and distinct vesicular glutamate transporter 3 (vGluT3), and are able to store and release both acetylcholine (ACh) and glutamate (Higley *et al.*, 2011; Nelson *et al.*, 2014). In accordance, the stimulation of CINs led to glutamatergic excitatory postsynaptic currents in MSNs, which could be elicited by either ACh and glutamate co-release or ACh release that stimulates the adjacent DA terminals that co-release glutamate (Higley *et al.*, 2011; Lenz & Lobo, 2013). Indeed, CINs critically modulate local DA release in the NAc (see section 4.2.2) (Exley & Cragg, 2008; Cachope & Cheer, 2014; Kosillo *et al.*, 2016; Mateo *et al.*, 2017).

GABAergic interneurons comprise an additional type of interneurons. In contrast to the homogenous population of CINs, different GABAergic interneuronal classes have been identified in the NAc (Figure 15A). Striatal GABAergic interneurons fall into two main categories according to their electrophysiological properties. The fast-spiking interneurons (FSIs) and the persistent and low-threshold spike (PLTSs) interneurons (Kawaguchi, 1993). Neurochemically, FSIs express the calcium-binding protein parvalbumin, whereas PLTS interneurons express neuropeptides such as somatostatin (SOM), neuropeptide Y (NPY), and the enzyme nitric oxide

synthase (NOS). In addition, about 20% of NPY-expressing interneurons have the electrophysiological properties of NGFs (Ibáñez-Sandoval *et al.*, 2011), and PLTS also include a class of GABAergic interneurons that express TH and co-release DA (Ibáñez-Sandoval *et al.*, 2010). The most studied GABAergic interneurons by far are the FSIs (Gittis & Kreitzer, 2012). FSIs modulate MSNs by a feedforward mechanism due to their early activation at lower thresholds than MSNs (Mallet *et al.*, 2005). They make strong and dense synapses to both types of MSNs and inhibit their firing. A single FSI inhibits an estimated total of 135–541 MSNs (Koós & Tepper, 1999). Under normal conditions, FSIs preferentially target the MSNs of the direct pathway (Gittis & Kreitzer, 2012). However, upon DA depletion, FSI axons sprout to form new axons specifically onto MSNs of the indirect pathway, which causes an inversion of the normal pathway-selectivity of FSIs (Gittis *et al.*, 2011). At the same time, the connectivity and unitary strength of lateral inhibition between MSNs decreases (Figure 15B) (Taverna *et al.*, 2008). Although these local inhibitory dynamics are described in models of Parkinson disease, they most likely contribute to the long-lasting changes due to chronic exposure to drugs of abuse since DA signaling is dramatically changed after chronic drug use.

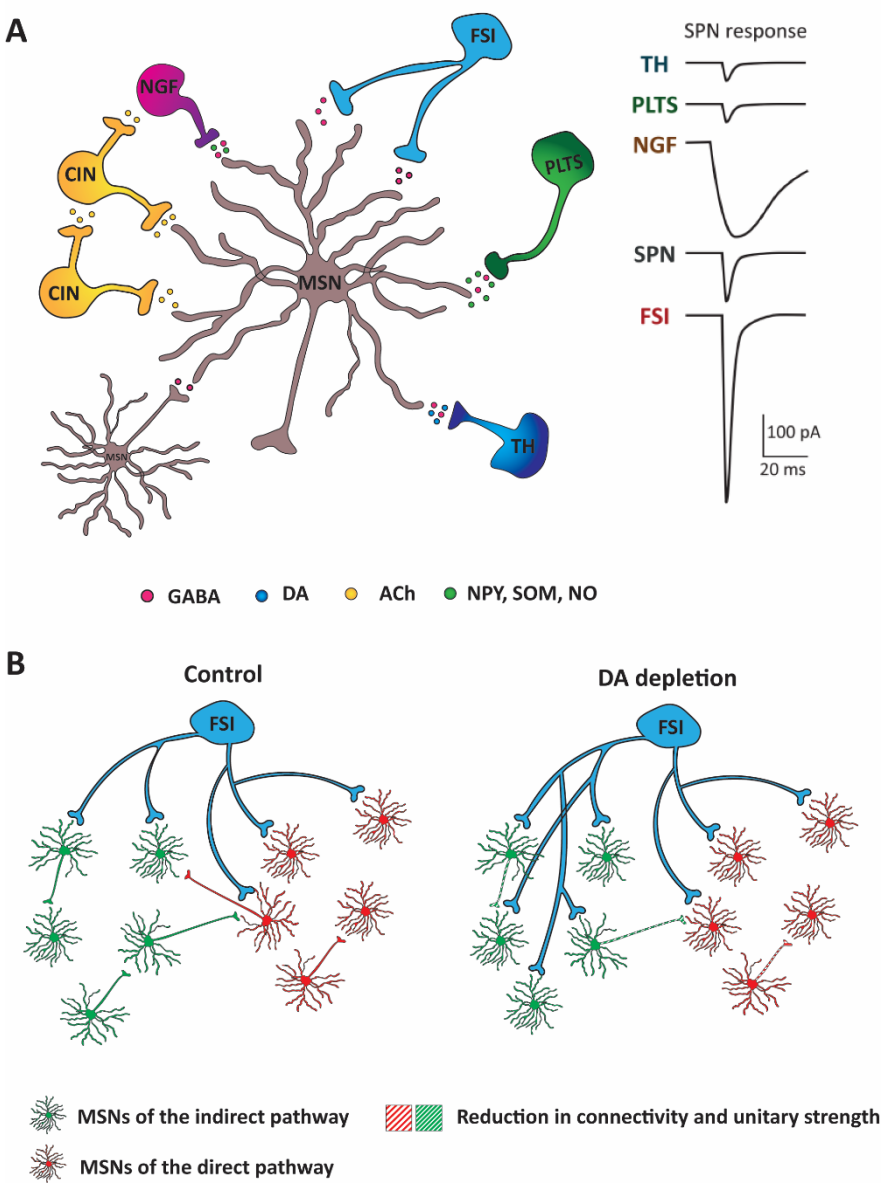

Figure 15. Local control of MSNs by GABAergic and cholinergic interneurons.
A: Different classes of striatal neurons that contribute to the local inhibitory networks. Illustration comparing the typical time course and amplitudes of unitary inhibitory postsynaptic currents observed in spiny projection neurons (SPNs) from each class of inhibitory neuron. **B:** Summary of changes in GABAergic microcircuits following dopamine depletion adapted from (Gittis & Kreitzer, 2012). **Abbreviations:** Acetylcholine (ACh), cholinergic interneuron (CIN), Dopamine (DA), Fast spiking interneuron (FSI), γ-aminobutyric acid (GABA), Medium spiny neuron (MSN), Neural glial form (NGF), Neuropeptide Y (NPY), nitric oxide (NO), Persistent and low-threshold spike (PLTS), Somatostatin (SOM), Tyrosine hydroxylase (TH)

3.3 The medial prefrontal cortex

The PFC is a brain area involved in attention, cognitive flexibility, decision-making, and is further associated with executive control and thought to mediate goal-directed behaviors, such as the seeking to obtain reward-related substances (Groenewegen & Uylings, 2000; Miller, 2000; Kalivas *et al.*, 2005; Stahl, 2013). Among these functions is the control of behavior, including attention, response inhibition, planning, and decision-making (Balleine & Dickinson, 1998; Miller & Cohen, 2001; Dalley *et al.*, 2004; Euston *et al.*, 2012). In addition, mPFC functions regulate the balance between execution and inhibition of behavior, and dysregulation of these functions is at the core of addiction (Goldstein & Volkow, 2011).

In rodents, the mPFC is typically referred to as structures located along the medial wall of the PFC (Groenewegen *et al.*, 1997; Heidbreder & Groenewegen, 2003; Dalley *et al.*, 2004; Kesner & Churchwell, 2011). The mPFC can be divided into four main areas, including the precentral area, the anterior cingulate cortex, the prelimbic cortex (PLC) and the infralimbic cortex (ILC) (Heidbreder & Groenewegen, 2003). In addition, the dorsal agranular insular and dorsolateral orbitofrontal cortex are often included as mPFC structures, despite their lateral location, due to interconnections with the PLC and the ILC. (Condé *et al.*, 1995; Vertes, 2004; Kesner & Churchwell, 2011; Watson *et al.*, 2011). Like other cortical areas, the mPFC is divided into six horizontally arranged layers, however, it is noteworthy that layer IV is different in rodents and primates (Uylings *et al.*, 2003).

Two main neuronal cell types comprise the mPFC, including the excitatory glutamatergic pyramidal projection neurons which represent 80%-90% of the total population, and a variety of inhibitory interneurons that can be functionally divided in FSIs and non-fast spiking interneurons (NFSIs). FSIs

and NFSIs are expressed in all cortical layers. FSIs tonically inhibit pyramidal neurons, whereas the NFSIs are involved in modulating the activity of FSIs (Makram *et al.*, 2004; Yuste, 2005; Druga, 2009). Pyramidal neurons are located in layers II, III, V and VI spreading their axons vertically towards the deeper layers. The apical dendrites are extended towards the superficial layers, whereas the basal dendrites contact with deeper layers (Pistillo *et al.*, 2015).

Pyramidal neurons and interneurons receive DA, glutamatergic, GABAergic and cholinergic inputs from cortical areas, the VTA, the thalamus, the AMG, the HPC, and the basal forebrain in a layer-specific manner. In a similar manner, pyramidal neurons project back to these areas to form microcircuits (Riga *et al.*, 2014; Moorman *et al.*, 2015; Pistillo *et al.*, 2015). More specifically, thalamic neurons were shown to drive fast and robust synaptic responses in layer I interneurons and pyramidal neurons (Cruikshank et al., 2012), and about 20% of the cholinergic and GABAergic afferents from the basal forebrain make contact with the neuronal processes of layer I and a smaller fraction with those of layer II-III (Henny & Jones, 2008). In addition, thalamocortical afferents synapse onto cholinergic fibers, where glutamate stimulates the generation of the cholinergic transients necessary for the detection and storage of environmental stimuli (Sarter *et al.*, 2014). Optogenetic studies demonstrated that layer II pyramidal neurons of the PLC receive functional inputs from the contralateral mPFC, midline thalamic nucleus, BLA, and vHPC (Little & Carter, 2012). These neurons, and those from layer III project back to the BLA and take part in intracortical circuits with other pyramidal neurons and interneurons (Douglas & Martin, 2004; Gabbott *et al.*, 2005).

Layer V neurons receive inputs from the thalamus and other cortical areas. Cholinergic and GABAergic afferents from the basal forebrain project mainly to layers V and VI (Henny & Jones, 2008). DA terminals from the pVTA are densest in layers V and VI, where they make symmetric synapses on pyramidal neurons and, to a lesser extent, on interneurons (Lammel *et al.*, 2008). In addition, DA synapses are typically in close apposition with asymmetric glutamatergic synapses in the mPFC. These synaptic triads are proposed to be responsible for the direct glutamatergic impact on DA transmission (Pistillo *et al.*, 2015). Pyramidal neurons from layer V and VI comprise the main output to subcortical areas, including the pVTA, the NAc, and MDT. Glutamatergic cortico-cortico circuits and feedback projections to the MDT control working memory and perception of sensory stimuli (Goldman-Rakic, 1995), whereby the neurons projecting to the pVTA and the NAc are involved in the evaluation of these stimuli, and the implementation of behavioral responses (Carr & Sesack, 2000; Gabbott *et al.*, 2005). Cortical inputs to the NAc are further associated with the modulation of goal-directed behavior and inhibitory control (Figure 16) (Stahl, 2013).

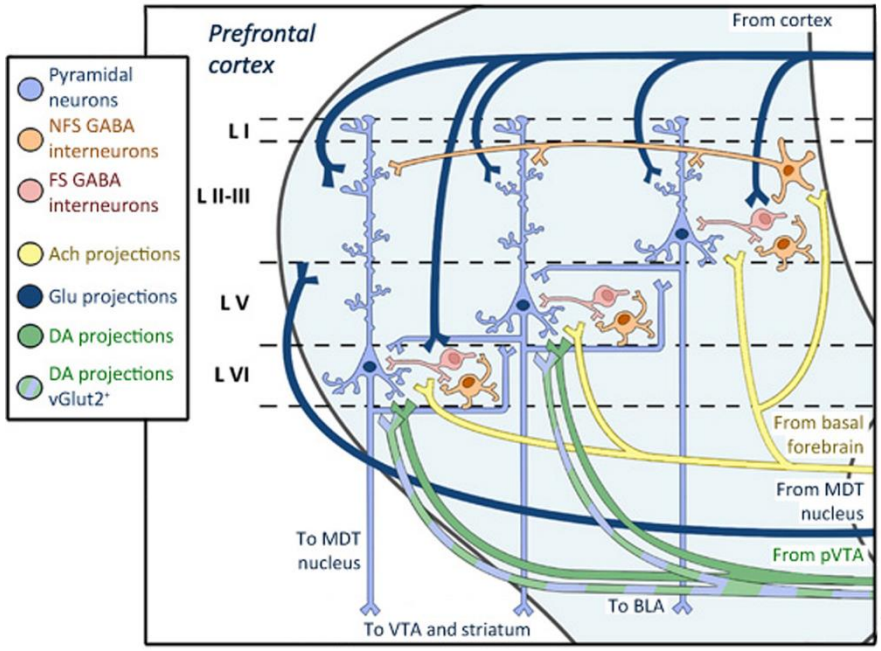

Figure 16. Main inputs to and outputs from the neuronal populations of the prefrontal cortex.
Inputs to glutamatergic pyramidal neurons and different types of interneurons in the PFC, and the outputs from pyramidal neurons to subcortical areas (Pistillo *et al.*, 2015). **Abbreviations:** Acetylcholine (Ach), basolateral amygdala (BLA), dopamine (DA), glutamate (Glu), fast-spiking (FS), Mediodorsal thalamus (MDT), non-fast-spiking (NFS), posterior-medial ventral tegmental area (pVTA), vesicular glutamate transporter 2 (vGlut2),

Besides the layer-specific connectivity of the mPFC. Pyramidal neurons of the PLC and the ILC possess different projection patterns, particularly with respect to the density of their projections to reward-related brain regions (Figure 17) (Vertes, 2004, 2006). Indeed, PLC neurons project predominantly to the NAc core, while ILC pyramidal neurons synapse almost exclusively with cells in the NAc shell (Sesack *et al.*, 1989; Berendse *et al.*, 1992; Vertes, 2004, 2006). Similarly, PLC fibers send their projections primarily to the capsular central amygdala and BLA. In contrast, projection sites of the ILC are widely distributed throughout the

AMG, including the medial, basomedial, cortical and central amygdala nuclei (Beckstead, 1979; Hurley *et al.*, 1991; Vertes, 2004, 2006). Lastly, the PLC lightly innervates the brainstem, including the VTA, and the posterior and lateral hypothalamus, whereas the ILC sends dense projections to the dorsomedial hypothalamus, perifornical region, posterior and supramammillary nuclei (Sesack *et al.*, 1989; Hurley *et al.*, 1991; Vertes, 2004, 2006). Importantly, mPFC projections typically follow a dorsal-ventral gradient. For example, ventral regions of PLC tend to innervate both core and shell regions of NAc (Figure 17) (Heidbreder & Groenewegen, 2003).

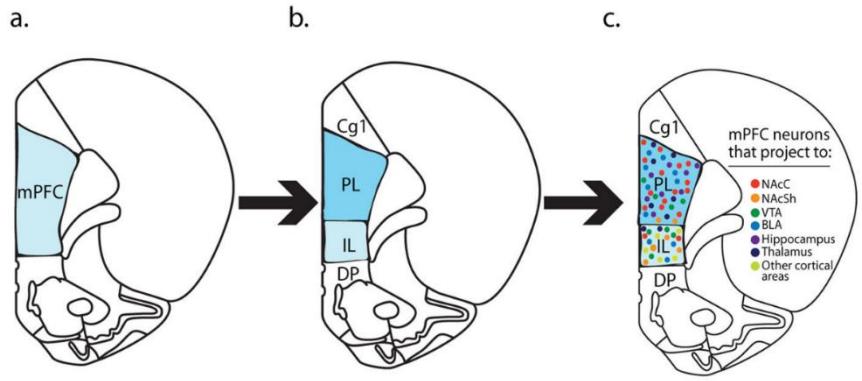

Figure 17. Progressive conceptualizations of mPFC differentiation.
A: mPFC as a unified structure. **B:** Structural distinctions within the mPFC emerge. **C:** Only specific neuronal ensembles within PLC and ILC based on their projection targets are necessary for particular behaviors, not the region as a whole (Moorman *et al.*, 2015). **Abrreviations:** anterior cingulate cortex, area 1 (Cg1), basolateral amygdala (BLA), dorsal peduncular cortex (DP), Infralimbic cortex (ILC), medial prefrontal cortex (mPFC), nucleus accumbens core (NAcC), nucleus accumbens shell (NAcSh), prelimbic cortex (PLC), ventral tegmental area (VTA)

The differential projection patterns of the PLC and the ILC result in differential modulation of motivated behaviors, including seeking, extinction, and reinstatement of seeking-behavior in rodent models of relapse. It was supposed that pyramidal neurons of the PLC drive drug-seeking whereby the neurons of the ILC inhibit drug-seeking. Recent studies, however, revealed that the canonical dichotomy is more complex than previously suggested. Both PLC and ILC have been shown to drive and inhibit drug-seeking, and other types of behaviors, depending on a range of factors, including the behavioral context, the drug-history of the animal, and the type of drug investigated. This heterogeneity of findings may reflect multiple sub-circuits within each of these mPFC areas supporting unique functions as shown in other mesocorticolimbic areas (Moorman *et al.*, 2015).

4 Neurobiology of nicotine use disorder

The complex behaviors that define the addicted state arise from time-dependent, drug-induced neuroadaptations in specific brain circuits that contribute to the enduring nature of the addictive disorders (Koob & Volkow, 2016). The initially rewarding effects produced by acute drug intake involve many relatively transient changes in neuronal function that precede a habit formation over time and fosters excessive drug-seeking, eventually (Nestler, 2005; Koob & Volkow, 2016). Due to repeated drug insults, relatively stable changes in synaptic physiology occur that further triggers opponent-process responses that diminish reward function and increase the brain stress systems (Koob & Le Moal, 2008a). These changes can remain virtually permanent, leading to a stable state of high vulnerability to relapse even after long periods of abstinence that characterizes an addictive disorder. Research of the last decades focused mainly on the mesocorticolimbic pathway to understand the neurobiological mechanisms that underly SUD and to alleviate this severe relapsing brain disease.

4.1 Nicotine

4.1.1 Pharmacological properties of nicotine

(S)-3-[1-Methylpyrrolidin-2-yl] pyridine (Figure 18), better known as nicotine, is an alkaloid found in many members of the solanaceous family of plants, where it acts as a natural insecticide (Soloway, 1976; Dome *et al.*, 2010). It was first isolated in 1828 from tobacco plants *(Nicotiana tabacum*) by Posselt and Reimann. Nicotine accounts for 95% of the alkaloid content in tobacco leaves. The predominant isomeric form of nicotine is the pharmacologically active (S)-isomer meanwhile the (R)-

isomer only accounts for 0.1 to 0.3% of the total nicotine content (Armstrong *et al.*, 1998). Chemically, nicotine is a tertiary amine composed of a pyridine and a pyrrolidine ring (Figure 18) (Henningfield & Zeller, 2006). It is a weak base (pKa = 8.0) (Fowler, 1954) and its absorption across biological membranes depends on the pH of the medium. Smoking is a highly efficient form of nicotine administration and produces high concentrations (100–500 nM) in the brain that are comparable to those seen after nicotine intravenous administration (Hukkanen *et al.*, 2005). Briefly, cigarette smoke (pH: 5.5-6) is inhaled into the lungs (pH: 7.4), where the alkaline fluid of the surface of the alveoli buffers the pH of smoke, allowing nicotine to be absorbed into the pulmonary circulation. After absorption, nicotine enters the bloodstream (pH: 7.4) and is distributed throughout body tissues (Hukkanen *et al.*, 2005). Interestingly, a puff of smoked tobacco delivers high levels of nicotine to the brain in 10 to 20 seconds, faster than intravenous administration, producing rapid rewarding effects through the activation of the mesocorticolimbic DA system (see section 4.3.1) (Benowitz, 1990). Nicotine gets rapidly and extensively metabolized primarily by the liver enzyme cytochrome P450, isoform 2A6 to cotinine (Figure 18) (Matta *et al.*, 2007). Rodents display a faster nicotine metabolism and they are less sensitive to the effects of nicotine. The plasma half-life ($t_{1/2}$) of nicotine in humans averages about 2 hours while the $t_{1/2}$ in rats is 45 min and 6-7 min in mice (Hukkanen *et al.*, 2005). Therefore, it is important to adjust nicotine doses and to select a route of administration that approximates human exposure when setting up a murine model of nicotine addiction (Matta *et al.*, 2007). Indeed, the rapid rate of nicotine delivery by smoking in humans can be mimicked in rodents by intravenous injections, which presents similar distribution kinetics (Hukkanen *et al.*, 2005). Accordingly, it has been shown that rats

(Corrigall & Coen, 1989) and mice (Galeote *et al.*, 2009; Martin-García *et al.*, 2009) will readily self-administer nicotine if delivered as a rapidly injected intravenous bolus, rather than a slower infusion.

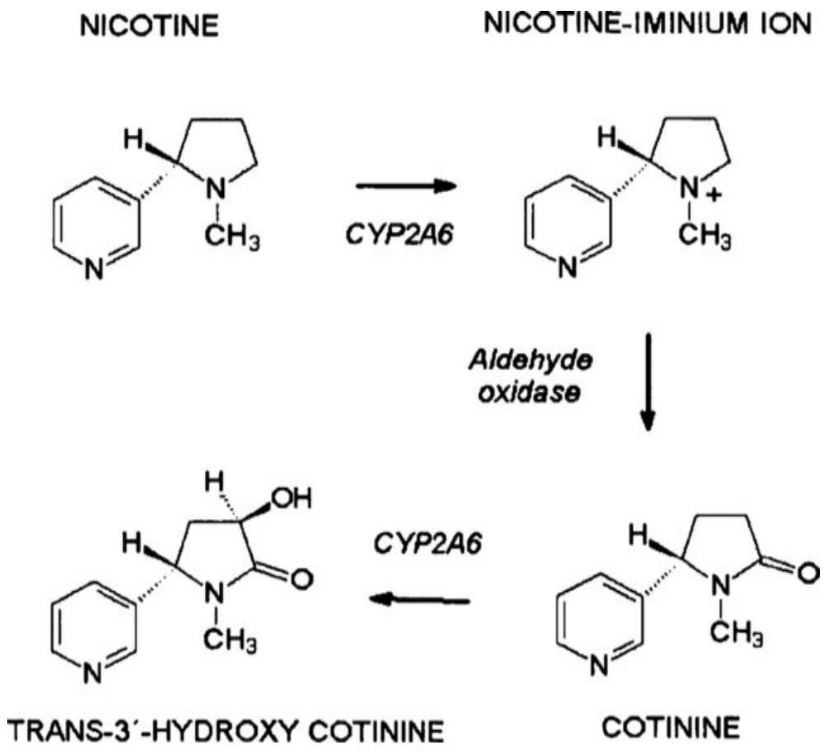

Figure 18 Chemical structure and primary metabolism of (S)-3-[1-Methylpyrrolidin-2-yl] pyridine (nicotine).

4.1.2 Nicotinic acetylcholine receptors

Cholinergic receptors perform major roles in neural transmission within the somatic and autonomic nervous systems. Nicotinic receptors are divided into two subtypes, N1 and N2. N1 may also be referred to as the peripheral or muscle receptor type, while N2 is known as the central or neuronal receptor subtype (Kalamida *et al.*, 2007). The N1 receptor is located in skeletal muscle at the neuromuscular junction performing the action of voluntary muscle movement (Papke, 2014). N2 is located within the peripheral and central nervous systems. For the purpose of this work, nicotinic acetylcholine receptors (nAChRs) refer only to N2 receptors when not indicated differently.

4.1.2.1 Anatomical and subcellular distribution

nAChRs are widely distributed throughout the central and peripheral nervous systems. They are expressed by neurons, microglia, and astrocytes (Egea *et al.*, 2015; Maurer & Williams, 2017). They are further expressed in non-neuronal cells including keratinocytes, endothelial cells, digestive, respiratory, and immune cells (Albuquerque *et al.*, 2009; Kawashima *et al.*, 2015).

In parallel to the brain cholinergic pathways, nAchRs present a widespread distribution throughout the CNS, including brain areas associated with nicotine addiction (Figure 19) (Tuesta *et al.*, 2011). Their distribution profile, however, is not uniform. nAChRs are predominantly expressed at presynaptic and/or preterminal localization, and modulate the release of almost all classes of neurotransmitter. However, some nAChRs have also been found at dendritic, somal, axonal and post-synaptic sites (Dani & Bertrand, 2007; Albuquerque *et al.*, 2009) Consequently, their activation

can have opposite modulatory effects on the same circuit depending on their location.

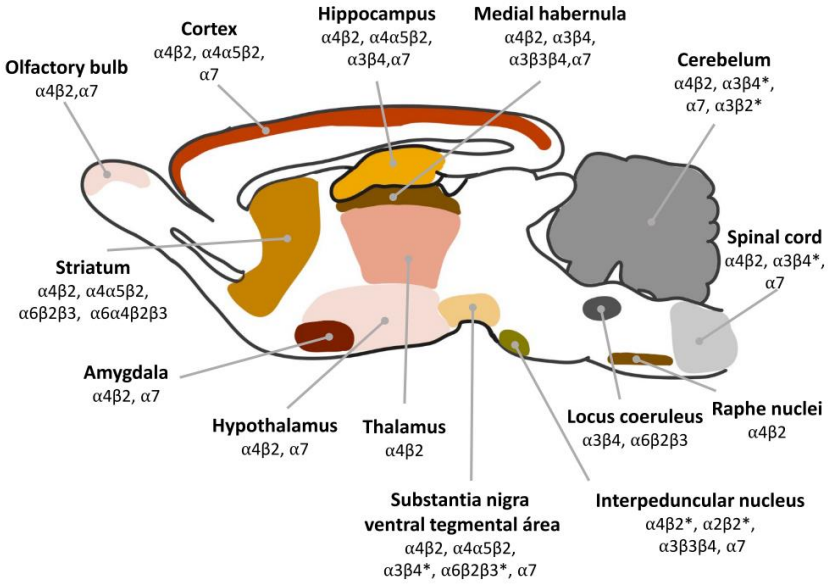

Figure 19. Distribution of nicotinic acetylcholine receptors in the rodent central nervous system. (Gotti *et al.*, 2006)

4.1.2.2 Structure and subtypes

nAChRs belong to the superfamily of pentameric ligand-gated ion channels and are endogenously activated by the neurotransmitter acetylcholine (Millar & Gotti, 2009). Due to the diversity of possible combinations out of eight α (α2– α7, α9, α10) and three β (β2– β4) neuronal subunits, they are involved in a variety of physiological processes (Gotti & Clementi, 2004). The different subunits can form homo- and hetero-oligomeric receptors arranged by 5 membrane-spanning subunits that form a central cationic pore that is permeable not only to monovalent Na^+ and K^+ but also to Ca^{2+} ions (Figure 20) (Albuquerque *et al.*, 2009). Neuronal nAChRs can be

divided into two classes: First, the α-bungarotoxin-sensitive subtypes made up of the α7, α9, and α10 subunits, which can be homomeric or heteromeric. Second, the α-bungarotoxin-insensitive receptors, which are heteromeric combinations of α2-6 and β2–4 subunits. The alpha subunits can conform homo-oligomeric and hetero-oligomeric receptors because these subunits contain the ligand-binding site. In contrast, beta subunits only arrange hetero-oligomeric receptors that exhibit 2 ligand binding sites at the interface between α and β subunit (Figure 20) (Nicolas *et al.*, 2001).

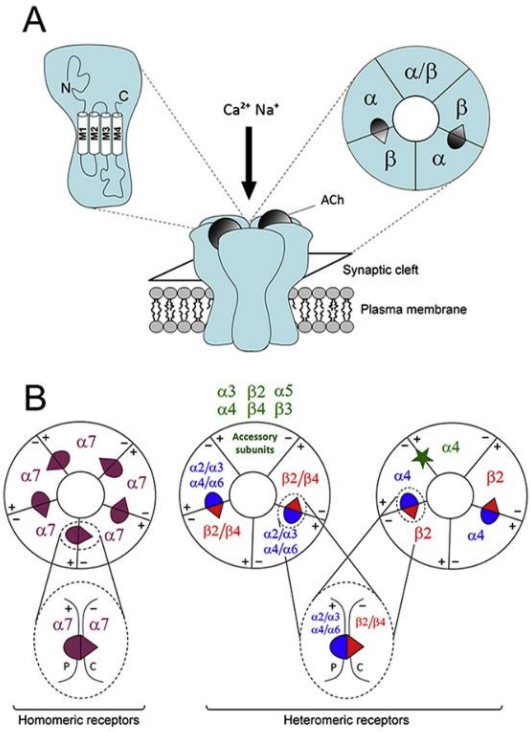

Figure 20. Basic structure of neuronal nicotinic receptors.
A-Left: Diagram showing the topography of nAChR subunits. The extracellular amino terminal portion is followed by three hydrophobic transmembrane domains (M1-M3), a large intracellular loop, and then a fourth hydrophobic transmembrane domain (M4). Middle) The arrangement of nAChR subunits in an assembled receptor. **A-Right:** Localization and organisation of the ACh binding sites in a heteromeric receptor. **B-Left:** Structure of homopentameric and heteropentameric neuronal subtypes. The pentameric arrangement of nAChR subunits in an α7 homopentameric subtype; **B-Middle:** heteromeric receptor subtype; **B-Right:** $(\alpha4)_3(\beta2)_2$ subtype. The localizations of the subunit interfaces of the orthosteric binding sites are indicated, together with the primary component P(+)carried by the α subunits and the complementary component C(-)carried by an α or non-α subunit. In addition to the two orthosteric sites, the $(\alpha4)_3(\beta2)_2$ subtype has a binding site at the α4α4 interface (star). (Zoli *et al.*, 2015)

4.1.2.3 Activation and desensitization

Upon binding of the endogenous neurotransmitter ACh, the open conformation of nAChRs stabilizes and positive-charged ions enter the cell which favors the emergence of action potentials leading to the release of multiple neurotransmitters (Dajas-Bailador & Wonnacott, 2004; Dani & Bertrand, 2007). In addition, activity-dependent modulation of circuits and intracellular enzymatic processes are associated with nAChR activation, as well (Mckay *et al.*, 2007). By modulating activity-dependent events, nAChRs are key modulators of synaptic plasticity that is involved in attention, learning and memory (Dani *et al.*, 2001; Ge & Dani, 2005). Multiple subtypes of nAChRs can be expressed by the same neuronal population and overlapping distribution of different nAChR subtypes can be found in different brain areas. The balance between nicotine-mediated activation and desensitization of specific subtypes of nAChRs can influence the functional and behavioral responses to nicotine exposure (Picciotto *et al.*, 2008)

Three main functional states have been described for nAChRs upon agonist binding: (1) closed at rest, (2) open pore when conducting cations in response to agonists and (3) closed desensitized when unresponsive to agonist(s) (Dani & Heinemann, 1996). The state of a receptor is highly dynamic and depends on a variety of factors, including the nAChR subtype, the agonist concentration and the rate of the agonist application (Figure 22) (Dani & Heinemann, 1996; Giniatullin *et al.*, 2005).

At moderate or high agonist concentrations, nAChRs are first activated and can then desensitize with subsequent recovery upon agonist removal. This ‘classical desensitization’ develops quickly in a millisecond range. In contrast, at low agonist concentrations, nAChRs can switch to a desensitized state even without apparent receptor activation. This ‘high-

affinity desensitization' is a rather slow process in a second to minute range and is, therefore, more likely to be generated than classical desensitization. This kinetic model suggests the transition into the desensitized state from both the open receptor state but also from the agonist-bound closed state. The latter state reveals a high agonist affinity because it can be evoked by low agonist concentrations in a nanomolar range. Hence, this transition receptor conformation could be responsible for generating high-affinity desensitization (Figure 21) (Giniatullin *et al.*, 2005).

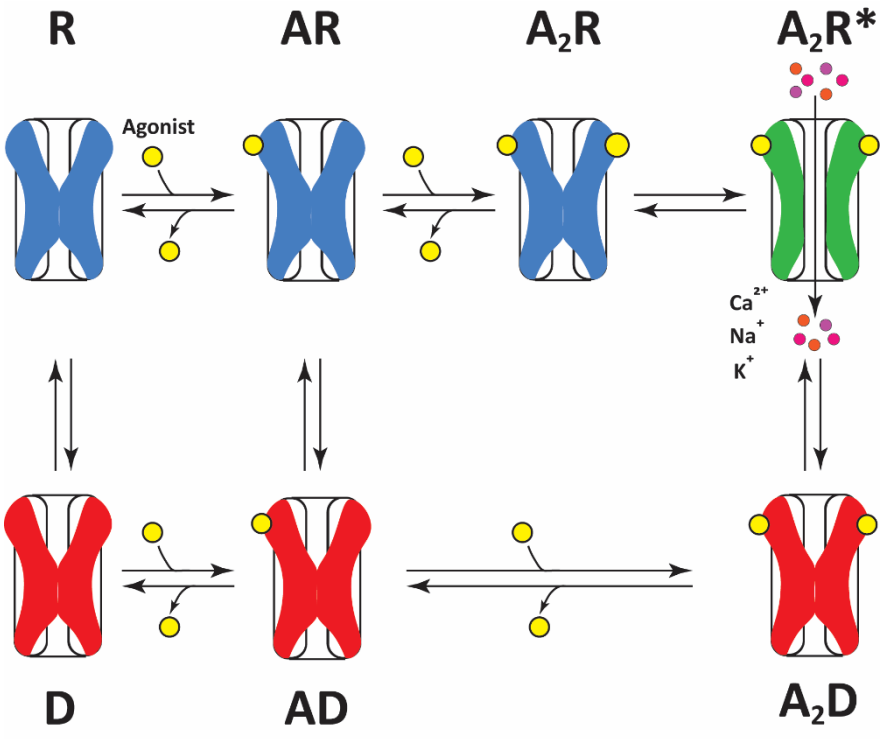

Figure 21. Desensitization of nAChRs.
Binding of two agonist molecules and transition into the desensitized state from both the agonist-bound closed state (AR) and from the open receptor state (A2R*).
Abbreviations: Agonist (A), desensitized state (D), resting state (R), open state (R*)

The prone nAChR for high-affinity desensitization is the α4β2* subtype rather than the α7* or the α3β4* subtype (Taly *et al.*, 2009). Indeed, it was demonstrated that presynaptic effects of low concentrations of nicotine, that were blocked with selective α7*nAChR antagonists, persisted in the continued presence of nicotine in brain slices of rats (Mansvelder *et al.*, 2002) and mice (Wooltorton *et al.*, 2003). In contrast, presynaptic effects that were blocked by selective β2* nAChR agonists desensitized during continued nicotine (Mansvelder & Mcgehee, 2000; Mansvelder *et al.*, 2002). nAChRs are unresponsive or display a decreased response to agonists in the desensitized state, however, desensitized nAChRs reveal a higher affinity for ACh and other ligands than those in the "activatable" state (Heidmann *et al.*, 1983; Quick & Lester, 2002). Indeed equilibrium binding experiments showed increased nicotine binding in the brain after chronic nicotine exposure measured in living human subjects (Staley *et al.*, 2006). Long exposure to nicotinic agonists can produce sustained changes in receptor sensitivity owed to upregulation of both α4β2 and α7-containing neuronal nAChRs by high-affinity desensitization (Figure 22) (Buisson & Bertrand, 2002). Furthermore, different stoichiometric variations may occur in the case of α4β2 subtype, resulting in different functional oligomers. Hence, $(\alpha4\beta2)_2\alpha4$ receptors exhibited lower sensitivity to ACh and faster desensitization than $(\alpha4\beta2)_2\beta2$ (Buisson & Bertrand, 2001; Nelson *et al.*, 2003).

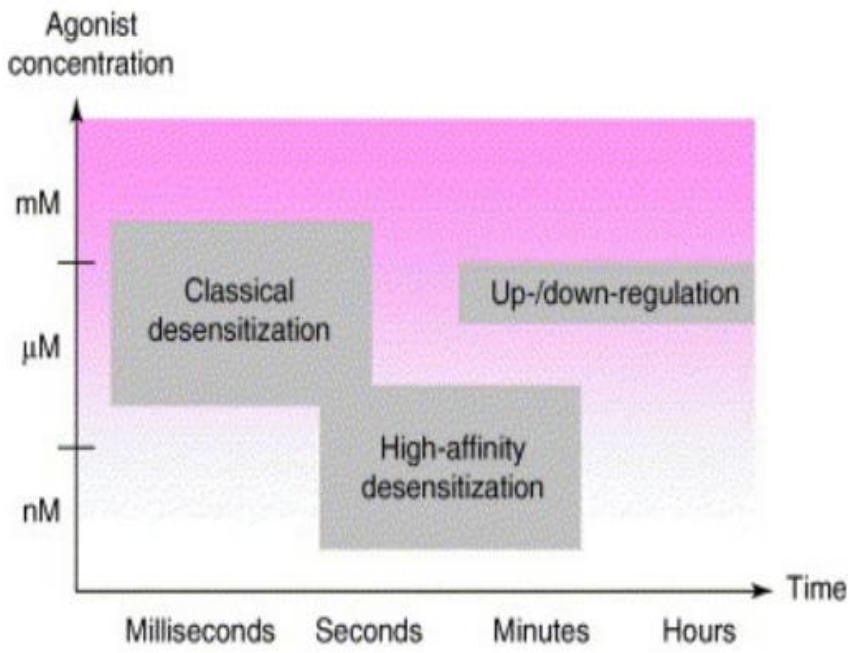

Figure 22. Classical and high-affinity desensitization of nAChRs.
Nicotinic acetylcholine receptor desensitization depends on agonist concentration and exposition time (Giniatullin *et al.*, 2005).

4.2 Cholinergic signaling in the mesocorticolimbic circuit

The cholinergic system is a key modulator of the mesocorticolimbic pathway where it controls the physiology of reward-seeking, motivation, and motor control. This system is also involved in the pathophysiology of several disorders, such as Parkinson's and Huntington's disease, schizophrenia and addiction to drugs of abuse (Cachope & Cheer, 2014). Recent studies were able to asses specific nAChR subtypes in specific cell types in the mesocorticolimbic circuit by means of technological advances in mouse genetics, virus-mediated gene transfer, optogenetic and chemogentic tools, and electrophysiological studies (Markou, 2008; Threlfell & Cragg, 2011; Cachope & Cheer, 2014; Pistillo *et al.*, 2015).

4.2.1 Cholinergic signaling in the ventral tegmental area

Cholinergic signaling acts as an essential *'gate'* in the VTA that switches VTA neurons from tonic to phasic firing which is associated with receiving reward-predicting stimuli or unpredicted rewards (Pistillo *et al.*, 2015).

Almost all nAChR subunits are expressed in midbrain DA neurons, although biochemical and functional analyses have shown that α4β2* and α4α6β2* nAChRs are the two main receptors in DA cell body/dendrite compartment of the ventral midbrain (Champtiaux *et al.*, 2003; Drenan *et al.*, 2008; Gotti *et al.*, 2010). The β2 subunit was shown to play a critical role in cholinergic-induced firing of DA neurons. Activation of somatodendritic β2* nAChRs elicited cell firing. Furthermore, agonist-induced cell-firing was decreased in β2 KO mice but restored by targeted expression of the β2 subunit in the VTA (Mameli-Engvall *et al.*, 2006; Changeux, 2010).

The α5 subunit is also highly expressed on DA cell bodies and dendrites and accounts for about half of the α4β2* nAChRs. The lack of this subunit in α5 KO mice halves the expression of α4* nAChRs (Chatterjee *et al.*, 2013). The α5 subtype does not contribute to the ligand-binding site, but it plays a critical role in defining a receptor's nicotine-sensitivity (Morel *et al.*, 2014).

The α7 subunit is expressed on half of the DA cell bodies and half of the glutamatergic nerve terminals innervating the VTA (Klink *et al.*, 2001). Although they were shown to only tune activation of DA neurons, their activation facilitates glutamate release on DA neurons (Jones & Wonnacott, 2004) which facilitates the burst firing of VTA DA neurons and eventually leads to long-term potentiation (LTP) (Zhao-Shea *et al.*, 2011).

GABAergic interneurons and nerve terminals innervating the VTA express predominantly α4β2 subtypes, where their activation facilitates GABA

release on DA neurons (Marubio *et al.*, 1999; Klink *et al.*, 2001; Changeux, 2010). However, GABA transmission on DA neurons was blocked using a selective α6β2 antagonist suggesting that GABAergic interneurons and/or nerve terminals also express the α6 subunit (Figure 23) (Yang *et al.*, 2011).

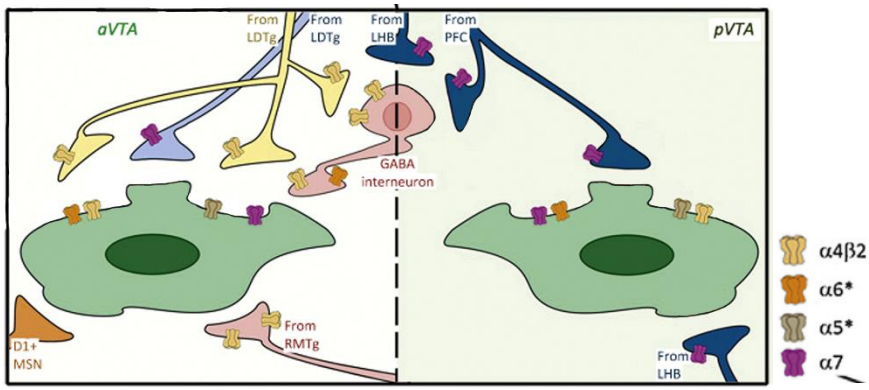

Figure 23. Cholinergic signaling in the VTA.
(Pistillo *et al.*, 2015).

4.2.2 Cholinergic signaling in the striatum

In contrast to the VTA and the mPFC that receive cholinergic signaling from the LTDg, the pedunculopontine tegmental nucleus (PPTg) and the basal forebrain, cholinergic signaling in the striatum is locally controlled by CINs (Descarries *et al.*, 1997; Descarries & Mechawar, 2000). nAChRs are expressed in DAergic, glutamatergic and GABAergic nerve terminals, as well as in GABAergic interneurons in the striatum (Cachope & Cheer, 2014; Pistillo *et al.*, 2015).

Striatal DA axons express a high density of α4, α5, α6, β2 and β3 subunits in an arrangement of two αβ pairs that could be α4β2*, α6β2* and/or α4β4*, plus a fifth subunit that can be α5 or β3 (Champtiaux *et al.*, 2003; Threlfell & Cragg, 2011). In addition, the β2 subunit is included in all

nAChRs expressed on striatal DA projections (Figure 24) (Jones *et al.*, 2001). A significant amount of work has shown that α4*(non-α6*) nAChRs play a prominent role in the dorsal striatum, while α4α6*nAChRs are dominant in the NAc (Exley & Cragg, 2008; Exley *et al.*, 2012). Given the distinct functional role of the dorsolateral and the ventromedial striatum, it has been proposed that such differences could be taken into account as a substrate for region-specific intervention (Threlfell & Cragg, 2011).

Animals treated with the DA neuron-selective toxin 6-hydroxydopamine showed that the major subtypes remaining after DA denervation are the α4β2 and α7 subtypes. The α7 subtype is localized on cortical and thalamic glutamatergic afferents in the NAc (Kaiser *et al.*, 2000; Marchi *et al.*, 2002; Rousseau *et al.*, 2005), whereby α4β2* receptors account for the majority of nAChRs modulating GABA release. α4β2* nAChRs are expressed by GABA releasing nerve endings (Grilli *et al.*, 2009a), soma-dendrites of FSIs (Koós & Tepper, 2002), and GABAergic neurons projecting to MSNs in the striatum (Figure 24) (Liu *et al.*, 2007c)

In contrast, no functional nAChRs have been detected in MSNs (Pisani *et al.*, 2007) and CINs, although α7 and β2 mRNA have been detected in these latter cells (Figure 24) (Azam *et al.*, 2002). Furthermore, CINs express M2 and M4 muscarinic acetylcholine receptors (mAChRs) that are G_i-coupled transmembrane receptors and act as inhibitory autoreceptors. In a similar way to what has been described for nAChRs, mAChRs exhibit some dorso-ventral gradient in their ability to regulate DA release. While M2/M4 receptors are necessary for such regulation in the dorsal striatum, M4 receptors are prevalent in the NAc (Threlfell *et al.*, 2010).

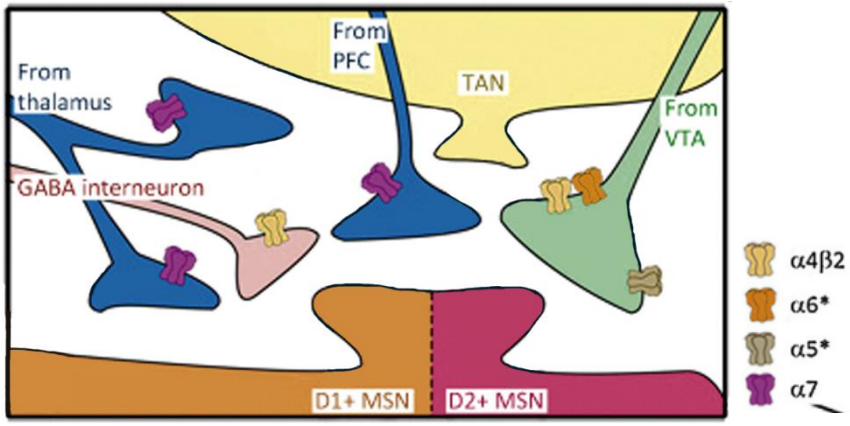

Figure 24. Cholinergic signaling in the NAc.
(Pistillo *et al.*, 2015). **Abbreviations:** Tonically active cholinergic interneuron (TAN).

The involvement of presynaptic nAChRs on DA transmission was demonstrated very early mainly from experiments describing increases of DA release in response to nAChR activation in slices or synaptosomes (Giorguieff *et al.*, 1977; Rapier *et al.*, 1990; Wonnacott *et al.*, 1990). Recent studies using electrochemical methods and optogenetics *in vivo* showed that CINs can trigger DA release in the NAc directly, bypassing ascending activity from DA neurons. Indeed, optogenetic direct activation of CINs and activation of thalamo-striatal inputs, which synchronize CINs, were shown to increase DA levels in the NAc *in vivo* (Cachope *et al.*, 2012; Threlfell *et al.*, 2012). Conversely, CIN activity seems to depend on DA firing. CINs show synchronized breaks in their activity during burst firing of DA neurons (Figure 25) (Schultz, 2002; Morris *et al.*, 2004), concluding that a decrease in cholinergic transmission may enhance DA burst firing. Indeed, it was demonstrated that DA release is increased by ACh at low firing rates of DA neurons. However, ACh decreased DA release at burst firing frequencies due to a form of release depression, called short-term depression (Rice & Cragg, 2004).

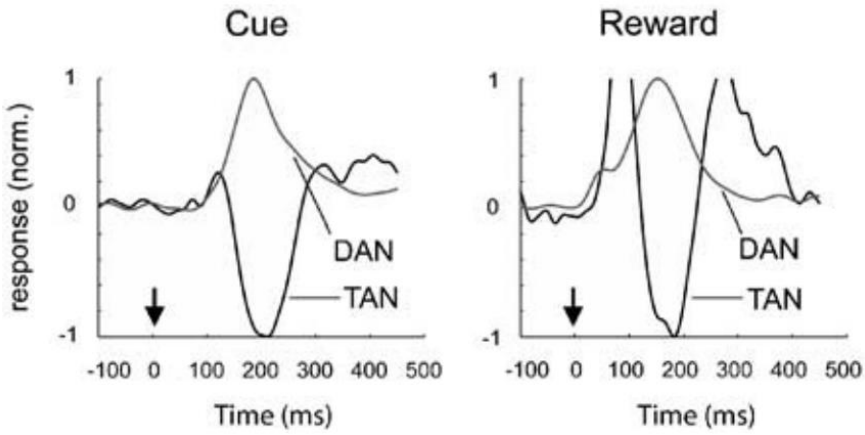

Figure 25. Synchronization of dopaminergic and cholinergic neuron responses to behavioural events.
(Morris *et al.*, 2004; Cragg, 2006). **Abbrevaitions:** Dopamine neurons (DAN) and cholinergic interneurons (tonically active neuron (TAN)

4.2.3 The medial prefrontal cortex

Due to the complex architectural structure and the plethora of neuronal connections and interconnections, the specific role of cholinergic signaling is yet to elucidate. However, different studies over the last decade could demonstrate a cholinergic modulation of prefrontal activity.

DAergic, GABAergic and glutamatergic signaling are modulated by the neurotransmitter Ach in the mPFC that derives from the basal forebrain. This modulation works mainly through volume transmission, although pyramidal neurons in layers V and VI can also be directly excited by cholinergic stimulation (Aracri *et al.*, 2010; Proulx *et al.*, 2014).

α4β2* nAChRs are expressed on DA terminals originating from the pVTA (Livingstone & Wonnacott, 2009; Livingstone *et al.*, 2009), and on pyramidal neurons in layer V and VI (Poorthuis *et al.*, 2013a), where DA terminals are densest. Aside from DA terminals, stimulation of the β2

subunit increased excitatory inputs from thalamocortical terminals to layer V pyramidal neurons (Lambe *et al.*, 2003; Couey *et al.*, 2007), and increases the frequency of GABAergic input from interneurons to pyramidal neurons (Poorthuis *et al.*, 2013b). In addition, only GABAergic interneurons in layer V express the α4α5β2* receptors that are less sensitive to desensitization, whereas layer II, III and VI lack the subunit α5 (Poorthuis *et al.*, 2013b).

α7 nAChRs are expressed on pyramidal neurons, DA terminals and interneurons of all layers except layer VI (Figure 26) (Livingstone *et al.*, 2009; Poorthuis *et al.*, 2013b, a).

In summary, nAChRs stimulate both excitatory and inhibitory neurons in distinct layers. However, due to distinct desensitization profiles of different nAChR subtypes, the net result of cholinergic stimulation is an increase in the activity of layer V and VI pyramidal neurons, whereas, in layers II and III, only interneurons are activated.

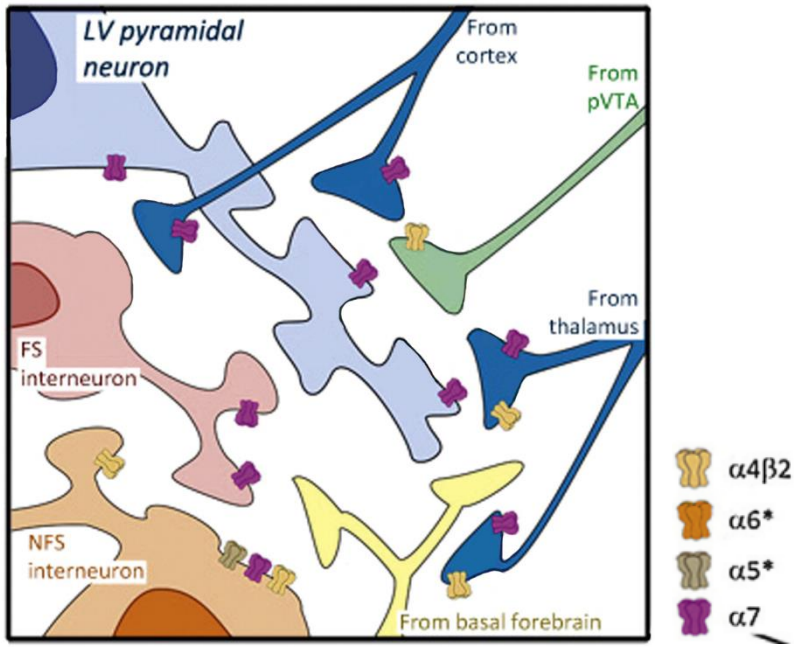

Figure 26. Cholinergic signaling in layer V of the mPFC.
(Pistillo *et al.*, 2015). **Abbreviations:**Fast-spiking (FS), non-fast spiking (NFS), posterior-medial ventral tegmental area (pVTA).

4.3 Stages of nicotine use disorder

Similar to other SUDs, nicotine use disorder is a chronic relapsing brain disease characterized by compulsive tobacco use, loss of control over tobacco consumption, and continuing tobacco use despite its harmful effects. A negative emotional state, craving upon acute withdrawal, and the relapse to nicotine-seeking even after protracted abstinence (Koob & Le Moal, 2008a; DSM-5, 2013).

4.3.1 Nicotine's acute reinforcing effects

Reward is defined herein as any event that increases the probability of a response with a positive hedonic component. In humans, the main reinforcing effects of nicotine are a mild pleasurable rush, mild euphoria,

increased arousal, decreased fatigue and relaxation (Henningfield *et al.*, 1985). In addition, smokers also derive pleasure from the sensory cues associated with smoking (Rose *et al.*, 1985; Perkins *et al.*, 2001; Rose, 2006). Such positive effects play an important role in the initiation and maintenance of tobacco smoking (Markou, 2008). Nicotine has an inverted U-shaped dose-response curve in both humans and animals (Picciotto, 2003; Matta *et al.*, 2007), usually showing reinforcing effects at lower doses (around 0.1 mg/kg in rats or mice) and aversive effects at higher concentrations (>1 mg/kg in rats or mice).

A large body of evidence shows that nicotine, like other drugs of abuse, produces its reinforcing effects through the modulation of the mesocorticolimbic reward system (Markou, 2008). Nicotine self-administration enhances brain reward function demonstrated by decreased ICSS reward thresholds in rats self-administering nicotine (Kenny & Markou, 2006), and acute nicotine administration elevated DA extracellular levels in the ventral striatum, especially in the NAc shell (Di Chiara & Imperato, 1988; Benwell & Balfour, 1992; Pontieri *et al.*, 1996).

These rewarding effects arise mostly due to the modulation of DA neurons within the VTA. Accordingly, nicotine increases the firing rate of mesolimbic DA neurons (Grenhoff *et al.*, 1986; Schilström *et al.*, 2003; Mameli-Engvall *et al.*, 2006), and only intra-VTA but not intra-NAc infusions of nAChR antagonists diminished nicotine-elicited DA outflow in the NAc (Nisell *et al.*, 1994). Furthermore, lesions of mesolimbic DA projections from the VTA to the NAc (Corrigall *et al.*, 1992), and lesions of cholinergic projections from the PPTg to the VTA reduced intravenous nicotine self-administration in rats (Lança *et al.*, 2000).

The mechanisms by which nicotine develops its reinforcing properties in the VTA are complex and critically depend on the desensitization profiles

and region-specific expression patterns of the distinct nAChR subtypes within the VTA. The α6α4β2* nAChRs are proposed to be the primary mediators of nicotine's reinforcing effects in the VTA. DA neurons of the VTA express α6 and β3 subunits together with the α4 and β2 subunits (Zhao-Shea *et al.*, 2011; Leslie *et al.*, 2013), however, DA neurons from the pVTA, that provide the main projection to the NAc, expressed higher levels of α4, α6, and β3 transcripts (Zhao-Shea *et al.*, 2011). α4α6β2β3 appear to have the highest affinity for nicotine (Salminen *et al.*, 2007; Liu *et al.*, 2012), and the presence of the α6 subunit, particularly in α6α4β2* nAChRs, slowed the rate and degree of desensitization compared to α4β2 nAChRs at the low concentrations of nicotine achieved by smokers (Liu *et al.*, 2012). In agreement, Whole-cell recordings of DA neurons in the VTA revealed that pVTA DA neurons showed more burst firing than aVTA DA neurons at low nicotine doses, and were activated at lower nicotine doses than aVTA DA neurons (Zhao-Shea *et al.*, 2011). Consistent with these findings, rats directly self-administered nicotine into the pVTA but not into the aVTA (Ikemoto *et al.*, 2006). Together, these data established a pivotal role for α4α6β2* subtypes expressed on pVTA DA neurons as the primary mediators of the reinforcing properties of nicotine.

The α5 subunits account for half of the α4β2*nAChRs express on DA cell bodies and dendrites (Chatterjee *et al.*, 2013). Although the α5 subunit does not contribute to nicotine binding, it plays a critical role in a receptor's nicotine sensitivity. Slice preparations of the VTA from α5 KO mice were less sensitive to nicotine and nicotinic agonists (Morel *et al.*, 2014). In line with these results, α5 KO mice demonstrated a significantly increased nicotine intake during nicotine self-administration and self-administered nicotine at doses that normally elicit aversion in Wt mice (Fowler & Kenny, 2011; Morel *et al.*, 2014) Moreover, α4α5β2* nAChRs

are less sensitive to the desensitization induced by nicotine (Poorthuis *et al.*, 2013a), thus, maintaining DA neurons active while GABAergic transmission is already suppressed due to receptor desensitization.

Indeed, GABAergic inputs to VTA DA neurons express mainly the high-affinity α4β2 nAChRs. Smoked concentrations of nicotine transiently increase the release of GABA but subsequently depress it for about 1h (Mansvelder *et al.*, 2002), hence, disinhibiting DA neurons.

Glutamatergic input to VTA DA neurons is also enhanced by nicotine through the activation of presynaptic α7 nAChRs (Dani *et al.*, 2000; Mansvelder & Mcgehee, 2000; Mansvelder *et al.*, 2002). Thus, further facilitating the burst firing of VTA DA neurons and eventually leading to LTP at glutamatergic synapses (Saal *et al.*, 2003; Zhao-Shea *et al.*, 2011).

Together, nicotine facilitates DA, GABA and glutamate transmission in the VTA. However, by acting on different nAchR subtypes with distinct desensitization profiles nicotine enhances glutamatergic transmission, while nAchRs on GABA neurons are desensitized, thus shifting the balance of synaptic inputs to excitation and inducing a net activation of the dopaminergic neurons of the VTA (Figure 27) (Mansvelder *et al.*, 2002).

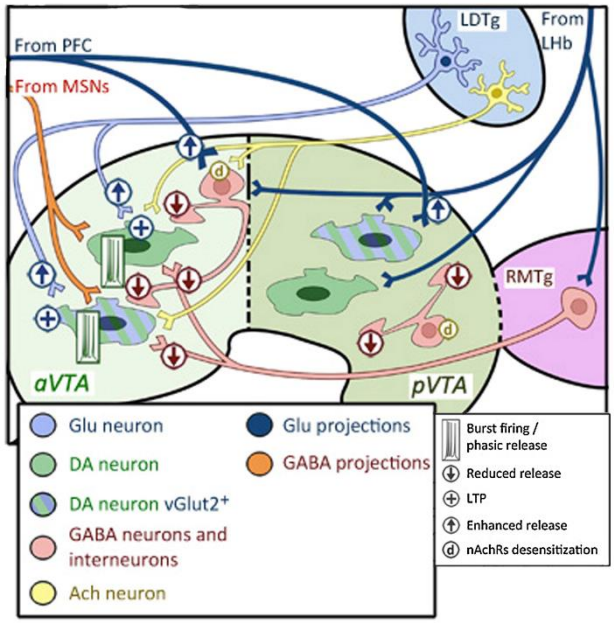

Figure 27. Nicotine's effects in the ventral tegmental area.
Exposure to nicotine increases the release of glutamate from the PFC and probably from LDTg projections and, by desensitizing the α4β2 receptors expressed by GABA terminals and interneurons decreases GABA release. Increased glutamate release induces LTP of glutamate synapses on DA neurons (Pistillo *et al.*, 2015). **Abbreviations:** γ-aminobutyric acid (GABA), anterior-lateral ventral tegmental area (aVTA), acetylcholine (Ach), dopamine (DA), glutamate (Glu), Laterodorsal tegmentum (LTDg), lateral habenula (LHb), long-term potentiation (LTP), medium spiny neurons (MSNs), nicotinic acetylcholine receptors (nAChRs), prefrontal cortex (PFC), posterior-medial ventral tegmental area (pVTA), Rostromedial tegmentum (RMTg), vesicular glutamate transporter 2 (vGluT2).

In the NAc, nicotine modulates DA, GABA and glutamate transmission. The nicotine levels present in smokers desensitize nAChRs at DA terminals in the NAc. Smoked nicotine, therefore, mimics the *'pause'* in the activity of cholinergic interneurons upon DA firing (see section 4.2.2) (Threlfell *et al.*, 2012). Accordingly, in the presence of the nAChR antagonist mecamylamine or nicotine, DA release at low frequencies was decreased, due to nAChR blockage or desensitization, while at high frequencies release was enhanced (Rice & Cragg, 2004). Concluding that the contrast

between tonic and phasic DA is enhanced either a pause in CIN activity, nAChR desensitization by nicotine or block by nAChR antagonists (Figure 28). The first follow up studies using selective nicotinic antagonists have demonstrated that α4β2* and α6β2* nAChRs are responsible for cholinergic effects on the DA terminals in the dorsal and ventral striatum, respectively (Exley & Cragg, 2008). The use of KO mice in more recent studies demonstrated that this increased contrast observed in WT mice is decreased in α6, α4 and β3 subunit KO mice in the NAc core. On the contrary, this increased contrast was sustained in α5 KO mice (Exley *et al.*, 2012). Thus, it is suggested that presynaptic nAChRs serve as dynamic ACh detectors, enhancing the contrast between tonic and burst firing (Rice & Cragg, 2004; Wonnacott, 2008). At the same time, nicotine stimulates burst firing of DA neurons via action at VTA level. The net result is an increased phasic release of DA to the NAc that makes nicotine acting as a powerful artificial reward (Wonnacott, 2008).

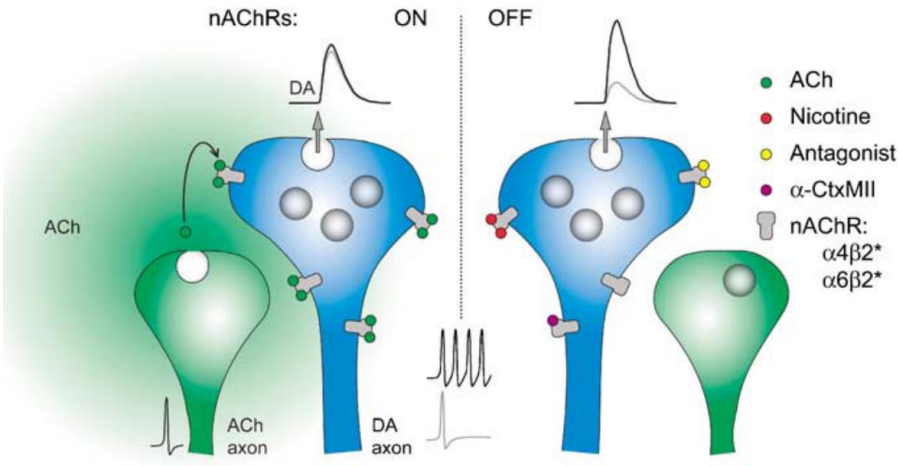

Figure 28. Nicotine's effects in the nucleus accumbens
Left panel: tonic ACh tone at nAChRs on DA axon terminals. **Right panel:** nAChR tone switched off (or reduced) by either a pause in ACh interneuron activity, nAChR desensitization by nicotine or block by nAChR antagonists (Exley & Cragg, 2008). **Abbreviations:** α-conotoxin MII (α-CtxMII), acetylcholine (ACh), dopamine (DA), nicotinic acetylcholine receptors (nAChRs)

Nicotine's effects in the PFC are layer-specific due to a differential nAChR subtypes expression (see section 4.2.3). As already discussed, high-affinity α4β2* nAChRs desensitize already at very low doses whereby the presence of the α5 subunit prevents receptor desensitization at lower doses as it is the case in smokers. Thus, it was shown that the desensitization of α4β2 receptors blocked the response of interneurons in layers II, III and VI, and, to a lesser extent, those of layer V. In contrast, pyramidal neurons expressing α4α5β2 nAChRs in layer VI were much less desensitized by nicotine (Bailey *et al.*, 2010). In agreement, nicotine treatment reduced the response of GABAergic interneurons but had much less effect on the excitability of pyramidal neurons, especially those located in layers V and VI (Poorthuis *et al.*, 2013b). In a similar manner, acute nicotine exposure (300 nM for 10 min to mimic similar conditions to smoking) greatly desensitized the response to ACh of some β2* receptors whereas the response of α7 receptors was unaffected. Thus, the glutamatergic input to mesolimbic areas such as the NAc and the VTA is increased, further enhancing mesocorticolimbic activity (Figure 29).

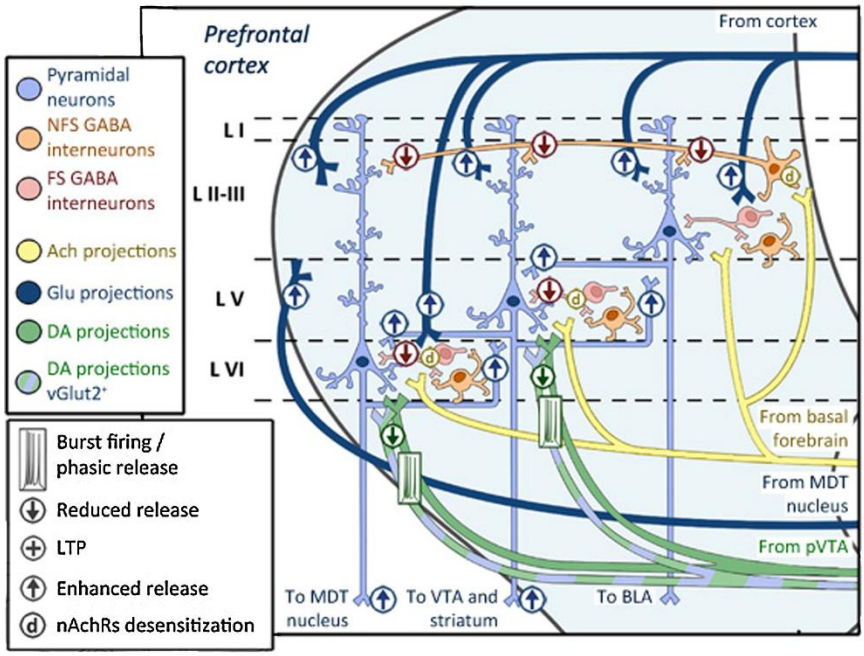

Figure 29 Nicotine's effects in the prefrontal cortex.
Exposure to nicotine increases glutamate release from the cortex and MDT nucleus afferents and pyramidal neuron terminals and reduces tonic but increases phasic release of DA from pVTA projections. Nicotine desensitizes α4β2 receptors on NFSIs and FSIs and decreases GABA release onto pyramidal neurons (Pistillo *et al.*, 2015). **Abbreviations:** γ-aminobutyric acid (GABA), acetylcholine (Ach), Basolateral amygdala (BLA), dopamine (DA), glutamate (Glu), fast-spiking (FS), long-term potentiation (LTP), medial-dorsal thalamus (MDT), nicotinic acetylcholine receptors (nAChRs), non-fast-spiking (NFS), prefrontal cortex (PFC), posterior-medial ventral tegmental area (pVTA), ventral tegmental area (VTA), vesicular glutamate transporter 2 (vGluT2).

Although nicotine acts on nAChRs, glutamatergic signaling plays a central role in the reinforcing effects of nicotine. A big body of evidence showed that the negative modulation of glutamate transmission at pre- or postsynaptic level decreased the reinforcing properties of nicotine. Thus, blocking NMDARs with competitive (Schilström *et al.*, 2000) or non-competitive (Shoaib *et al.*, 1997) antagonists in the VTA decreased nicotine self-administration and the effect of nicotine on ICSS (Kenny *et al.*, 2009). Furthermore, nicotine self-administration was decreased by

blocking the postsynaptically expressed mGluR5 (Kenny *et al.*, 2003). Conversely, activating the presynaptic mGluR2/3 by systemic or intra-VTA administration, decreased nicotine self-administration, while nicotine self-administration itself downregulated mGluR2/3 function in the VTA and the NAc (Liechti *et al.*, 2007).

Glutamatergic signaling to the NAc also plays a key role in the reinforcing and motivational aspects of nicotine. Acute nicotine increases the levels of glutamate (Toth *et al.*, 1993; Reid *et al.*, 2000), and modulates GluR expression (Grilli *et al.*, 2009b, 2012). Accordingly, micro-injections of mGluR5 selective antagonists in the NAc prevented intravenous nicotine self-administration and DA release in both naïve and nicotine exposed rats (Tronci & Balfour, 2011), and activation of the predominant presynaptic mGluR2/3 decreased nicotine self-administration (Liechti *et al.*, 2007). In contrast, intra-NAc shell, but not core injections of NMDAR antagonists increased nicotine intravenous self-administration under both FR and PR schedules of reinforcement, suggesting that NMDARs in the NAc shell negatively regulate the reinforcing and motivational effects of nicotine (D'Souza & Markou, 2014).

4.3.2 Molecular adaptation after chronic nicotine

Chronic drug exposure leads to neuroadaptations in the mesocorticolimbic system in an attempt to restore brain reward normal functioning (Nestler, 2005). Homeostatic adaptations may occur within cells and circuits stimulated by the drug to counteract this chronic pharmacological insult to the brain. Among these adaptations, one of the most pervasive processes is certainly tolerance, or the progressive decrease of the initial drug effect (Koob, 2009). Tolerance often develops towards the rewarding effects of drugs of abuse, leading individuals to

constantly increase the dosage to maintain a stable effect. Indeed, drug addicts often describe their continuing drug use as an attempt to re-experience the initial remembered "high" or "rush" without success (Hyman *et al.*, 2006). Furthermore, amphetamine-induced or methylphenidate-induced striatal dopamine responses are 80% lower in active abusers, and accompanied by lower self-reports of the drug's rewarding effects relative to non-drug-abusing controls (Volkow *et al.*, 2004; Martinez *et al.*, 2007)

With continued nicotine exposure, smokers develop tolerance to some nicotine effects with the consequent need for progressively higher doses of nicotine to obtain the same responses (Wang & Sun, 2005). It has been proposed that desensitization and up-regulation of nAChRs are behind the phenomenon of nicotine tolerance and dependence. Following nicotine binding, nAChRs activate and rapidly enter in a desensitized state (see section 4.1.2.3). During chronic nicotine exposure, smokers exhibit low plasmatic levels of nicotine responsible for maintaining most nAChRs in a desensitized state that interrupts ACh signaling (Wang & Sun, 2005). Moreover, chronic nicotine usage enhances substantially the time that nAChRs need to recover from the desensitized state, contributing to a generalized inactive state of nAChRs in the brain (Picciotto *et al.*, 2008; Dani, 2015). Indeed, a brain image study showed that cigarette smoking, in amounts used by typical daily smokers, maintains near complete saturation, and thus desensitization, of the brain's nAChRs.

Long-term exposure to an agonist usually produces excessive receptor activation that is homeostatically compensated by down-regulation of the receptor (Dani, 2015). Paradoxically, chronic nicotine exposure increases nicotine-binding sites in the brain, a phenomenon termed up-regulation of nAChRs (Cosgrove *et al.*, 2015; Zoli *et al.*, 2015). Indeed, brain studies

in humans (Perry *et al.*, 1999; Mukhin *et al.*, 2008) and animals (Mugnaini *et al.*, 2002; Marks *et al.*, 2004; Moretti *et al.*, 2010) chronically exposed to nicotine have shown that long-term exposure triggers an increase in the number of receptors, particularly high-affinity α4β2 receptors. This up-regulation of nAChRs has been observed in humans, mice and rats and may be a response to the prolonged desensitization of nAChRs (Picciotto *et al.*, 2008). Nicotine-induced up-regulation only occurs in nicotinic, but not muscarinic AChRs and differs among receptor subtypes and brain regions (Gaimarri *et al.*, 2007; Zoli *et al.*, 2015). Indeed, chronic exposure to nicotine up-regulates α4β2 receptors that are primarily expressed on GABAergic neurons (Nashmi & Lester, 2007), but not the α6β2* receptors selectively expressed on DA neurons (Mugnaini *et al.*, 2002; Perry *et al.*, 2007; Moretti *et al.*, 2010; Perez *et al.*, 2013). Nevertheless, upregulated α4β2 receptors are functionally desensitized. Hence, GABA control over DA neuron activity is depressed in smokers (Mansvelder *et al.*, 2002). A reduction in the number and DA-releasing function of α6β2 nAChRs was also revealed in the dorsal striatum and the NAc but not in the olfactory tubercle, whereas a reduction of α4β2 function was observed in both regions even though the number of receptors was markedly up-regulated (Marks *et al.*, 2014). Interestingly, no dose of nicotine caused changes in DA receptor or dopamine transporter (DAT) expression or DAT affinity, suggesting that the functional changes observed were directly dependent on changes in the number and function of nAChRs rather than on intrinsic mechanisms of DA transmission. There is now evidence indicating that the key steps in nicotine-induced up-regulation are receptor assembly, trafficking and cell surface expression (Colombo *et al.*, 2013; Mazzo *et al.*, 2013). Nicotine can affect all of these processes depending on the receptor subtype and circuit in which the receptors are expressed (Nashmi

& Lester, 2007; Zhao-Shea *et al.*, 2013). In contrast, nicotine exposure causes a four- to six-fold higher binding to α4β2 nAChRs that did not correspond with any significant change in the number of surface receptors or changes in the assembly, trafficking, or cell-surface turnover of the receptors. However, upregulation does alter the functional state of the receptor, slowing desensitization and enhancing sensitivity to acetylcholine (Vallejo *et al.*, 2005).

Chronic drug-taking does also lead to an opposing response of inverse tolerance, termed sensitization. Sensitization of the dopamine system is characterized by greater increases in dopaminergic transmission in response to the drug itself or to drug-associated cues (Everitt & Wolf, 2002; Robinson & Berridge, 2008) This process is associated with the emergence of glutamatergic synaptic plasticity mechanisms in the mesocorticolimbic brain circuitry. Drug-induced strengthening of excitatory input may increase the incidence of burst firing (Jones & Bonci, 2005) and support the progressive manifestation of synaptic plasticity in striatal regions that occurs following repeated drug exposure acting to strengthen drug-seeking behaviors (Mameli *et al.*, 2009; Lüscher, 2013). Consistent with this hypothesis, chronic nicotine exposure produces sensitization, increases DA release in the ventral and dorsal striatum and enhances locomotor responses to nicotine challenge (Reid *et al.*, 1998; Cadoni & Di Chiara, 2000; Shim *et al.*, 2001). Nicotine, acting on α7 nAChRs expressed on glutamatergic terminals, leads to LTP as shown by the increase in the ratio of α-amino-3-hydroxy-5-methyl-4-isoxazolepropionic acid receptor (AMPAR)/NMDAR currents at the glutamatergic synapses on DA neurons. (Saal *et al.*, 2003; Zhao-Shea *et al.*, 2011), and glutamatergic synapses in the NAc (Gipson *et al.*, 2013). It is further suggested that chronic nicotine induces a hyperglutamatergic state of the NAc by

modulating its uptake from the synaptic cleft (Warr *et al.*, 1999; Huang & Bergles, 2004). Accordingly, nicotine self-administration decreases the expression of the xCT and glial glutamate transporter 1 in the NAc (Reid *et al.*, 2000; Knackstedt *et al.*, 2009; Schroeder *et al.*, 2011). In addition, Kenny *et al*. found increased levels of GluA1 AMPARs in rats that self-administer nicotine. Nicotine modulates the release of DA and glutamate in the striatum, whereby DA and glutamate inputs converge on the same tripartite synapses of MSNs (Jay, 2003; Sesack *et al.*, 2003). Rats chronically exposed to nicotine showed an increase in length and density of dendritic spines on MSNs (Brown & Kolb, 2001), which is associated with an increase in NMDAR currents in the core but not in the shell of the NAc. Interestingly, the increase in the excitability of the D1-MSNs located in the NAc core and dorsal striatum is greater than in D2 receptor-expressing MSNs (Ávila-Ruiz *et al.*, 2014)

In summary, chronic nicotine exposure leads to enduring neuroadaptations in the cortico-striatal and cortico-VTA glutamatergic brain circuitry, leading to increased glutamatergic transmission in the VTA, NAc, and PFC. Furthermore, basal DA levels are reduced, but the probability of phasic DA release in the NAc is increased. In addition, nicotine desensitizes the majority of nAChRs expressed by GABAergic neurons interfering with the cholinergic control of GABAergic transmission (Wallace & Bertrand, 2013; Li *et al.*, 2014). These alterations result in increased susceptibility to excessive smoking and relapse in smoking-experienced subjects even after long periods of withdrawal (Wise & Koob, 2014).

4.3.3 Cessation of nicotine intake: acute withdrawal

The appearance of an aversive state when the drug of abuse is discontinued is termed withdrawal syndrome and results in recurrent drug use to avoid the negative consequences of drug abstinence (Koob *et al.*, 1997; Koob & Le Moal, 2008b). All drugs of abuse can produce a motivational withdrawal syndromes characterized by chronic irritability, emotional alterations, dysphoria, alexithymia, states of stress, and loss of motivation for natural rewards (Koob & Volkow, 2016). Indeed, brain imaging studies in humans demonstrated a decreased sensitivity of brain reward circuits to stimulation by natural rewards during withdrawal (Garavan *et al.*, 2000), and profound decreases in dopamine release in striatum in detoxified addicts (Volkow *et al.*, 1997, 2007). In rodents, acute drug withdrawal is associated with decreased dopaminergic and serotonergic transmission in the NAc as measured by *in vivo* microdialysis (Weiss *et al.*, 1992), elevated brain reward thresholds in ICSS experiments (Koob *et al.*, 2014), and elevations in stress and anxiety-like responses (Koob & Le Moal, 2005).

Another relevant mechanism during acute withdrawal is the dysregulation of the hypothalamic-pituitary-adrenal axis and the brain stress system. Both are mediated by the corticotropin-releasing factor (CRF) and dysregulated by chronic exposure to all major drugs of abuse. During acute withdrawal, the adrenocorticotropic hormone, corticosterone, and amygdala CRF are elevated (Kreek & Koob, 1998; Koob & Le Moal, 2005, 2008b). Thus, the pharmacological blockade of CRF reversed the anxiogenic-like effects observed during acute withdrawal from all major drugs of abuse (Funk *et al.*, 2006; George *et al.*, 2007; Specio *et al.*, 2008). Therefore, although drug consumption is initially triggered by the positive

reinforcing effects of drugs of abuse, negative reinforcement is a crucial component for maintaining drug use (Koob & Le Moal, 2001).

Smokers also maintain nicotine consumption to avoid or alleviate the distressing withdrawal symptoms rather than to obtain the positive reinforcing effects of nicotine (Koob & Le Moal, 2008b; Koob, 2013). Indeed, nicotine withdrawal syndrome is considered a major cause of relapse into smoking (Le Foll & Goldberg, 2009). Thus, the severity and the duration of withdrawal symptoms have been suggested to predict relapse in abstinent smokers (Killen & Fortmann, 1997; Rukstalis *et al.*, 2005; Allen *et al.*, 2008; Zhou *et al.*, 2009; Ashare & Schmidt, 2014). The wide range of undesirable effects that are produced by smoking cessation can be classified as somatic, affective and cognitive withdrawal symptoms (Hughes & Hatsukami, 1986; Hughes, 2005). Somatic or *'physical'* signs of withdrawal include bradycardia, gastrointestinal discomfort, fatigue, insomnia, and restlessness. The affective or *'emotional'* withdrawal symptoms include depressed mood, irritability, severe craving for nicotine, anxiety and decreased arousal. Cognitive deficits associated with nicotine withdrawal include impairments in attention, working memory and episodic memory (Hughes, 2007; Wesnes *et al.*, 2013; Hall *et al.*, 2015). In general, all these withdrawal signs onset approx. after 4h of the last tobacco consumption, peak within the first few days of abstinence, and could still be observed for weeks (Benowitz, 1992; Hughes, 2007).

Chronic nicotine leads to long-lasting neuroadaptations in various brain areas that promote and sustain recurrent nicotine-taking, whereas nicotine cessation disrupts the equilibrium formerly reached in the presence of nicotine. Like other drugs of abuse, nicotine withdrawal decreases the function of the reward system, which was revealed by dramatically increased reward thresholds in ICSS experiments (Epping-

Jordan *et al.*, 1998), by decreased DA levels in the VTA, NAc (Natividad *et al.*, 2012), and striatum (Zhang *et al.*, 2012), as well as and increases in the function of striatal DATs (Hadjiconstantinou *et al.*, 2011). In agreement, nicotine withdrawal decreased tonic but not phasic activity of VTA DA neurons (Grieder *et al.*, 2012), and decreased both tonic and phasic DA release in the NAc (Zhang *et al.*, 2012). Moreover, like stressful and aversive stimuli, nicotine withdrawal increases DA release in the PFC (Carboni *et al.*, 2000), which may contribute to the anxiety-related behaviors associated with this process.

Nicotine withdrawal also modulates the glutamatergic system, leading to a decreased glutamatergic transmission in the mesocorticolimbic system (Li *et al.*, 2014), compensatory changes in GluRs and a decrease in the NAc proteins involved in glutamatergic signaling. Accordingly, acute nicotine withdrawal resulted in fewer NMDARs in the PFC (Kenny *et al.*, 2009), and decreased mGluR2/3 function in the VTA and NAc (Liechti *et al.*, 2007). Acute withdrawal in rats following nicotine self-administration displayed a decreased expression of the glutamate exchanger xCT in the NAc and VTA and the glial glutamate transporter 1 in the NAc (Knackstedt *et al.*, 2009).

As opposed to the affective symptoms of nicotine withdrawal, the mechanisms and brain regions underlying physical symptoms of nicotine abstinence have not been fully clarified. The habenula and the interpeduncular nucleus play an important role in the somatic symptoms of nicotine withdrawal (Salas *et al.*, 2009). Thus, the nAChR antagonist mecamylamine precipitated nicotine withdrawal in mice chronically treated with nicotine when microinjected into the habenula or interpeduncular nucleus but not into the cortex, VTA and HPC. However, nicotine withdrawal syndrome is absent in α5, β4 or α2 KO mice (Baldwin

et al., 2011; De Biasi & Dani, 2011). Therefore, it has been proposed that signaling through α2*, α5* and β4* containing nAChRs in the habenulo-interpeduncular pathway participates in the manifestation of somatic symptoms of nicotine withdrawal.

4.3.4 Long-term abstinence: Relapse to nicotine consumption

The act of engaging drug-seeking after a period of drug abstinence is termed relapse and defines addiction as a chronic relapsing disorder. A particularly troublesome aspect of drug addiction is that the vulnerability to relapse persists for years even in the absence of repeated drug use, which remains the major clinical health concern (Koob *et al.*, 1997; Koob & Le Moal, 2008a; Koob & Volkow, 2016). Craving is often seen as the emotional state that triggers drug-seeking, however, craving in itself has been difficult to measure in human clinical studies and does not always correlate with relapse (Tiffany *et al.*, 2000).

Abstinent smokers remain vulnerable to relapse even years after cessation of tobacco smoking. Relapse to tobacco can be triggered by a single smoked cigarette (re-exposure) (Liu, 2016). Stress also plays an important role in relapse to smoking. External stressors are important triggers of relapse, and nicotine withdrawal itself produces a “stress-like state” of negative affect (Hughes, 2007; Wardle *et al.*, 2011). Another important factor for the relapse to drug-seeking is the exposure to environmental stimuli previously associated with the abused drug (Franklin *et al.*, 2007; Liu, 2016). Smoking may be particularly effective in establishing the incentive properties of nicotine-associated environmental stimuli (cues), including the smell and taste of cigarettes or contexts where smoking occurs.

The use of animal models has been determinant to advance in the study of the mechanisms underlying relapse. Reinstatement models of relapse in animals have been shown to reinstate drug-seeking behavior by either the re-exposure to the drug, stress or drug-associated conditioned cues (Shaham *et al.*, 2003; Crombag *et al.*, 2008; Venniro *et al.*, 2015).

Drug-induced reinstatement of seeking-behavior in rats involves glutamatergic projections from the PLC to the NAc that is modulated by DA activity through D1 and D2 receptors in the frontal cortex (Everitt & Wolf, 2002). Stress-induced reinstatement of drug-related responding in animal models appears to depend on the activation of both CRF and norepinephrine in elements of the extended AMG and the VTA (Shaham *et al.*, 2000, 2003; Bossert *et al.*, 2005). In contrast, human imaging studies have shown increased activation of the prefrontal cortex and anterior cingulate gyrus during cue-induced craving in smokers (Lee *et al.*, 2005; Goudriaan *et al.*, 2010). Furthermore, cue-induced reinstatement of drug-seeking behavior in rodents involves glutamatergic projections from the PLC, BLA, and ventral subiculum to the NAc, and DA modulation in the BLA and dorsal striatum (Everitt & Wolf, 2002; Vanderschuren *et al.*, 2005). However, these findings are predominantly based on cocaine, heroin and alcohol relapse, much less is known about the reinstatement of nicotine-seeking, and the neurobiological mechanisms involved remain are poorly understood.

The reinstatement of nicotine-seeking in rodents can also be triggered by nicotine-priming (Liu, 2016), stress (Bruijnzeel *et al.*, 2009; Plaza-Zabala *et al.*, 2010; Feltenstein *et al.*, 2012) and environmental cues (Martin-García *et al.*, 2009; Feltenstein *et al.*, 2012; Gipson *et al.*, 2013). However, many studies reported difficulties to reinstate nicotine-seeking by nicotine-priming (Martin-García *et al.*, 2009; Feltenstein *et al.*, 2012). Hence, most

of the knowledge is based on the research of stress and cue-induced reinstatement of nicotine-seeking.

Stress-induced reinstatement was abolished by the blockade of the CRF1 receptor in rats (Bruijnzeel *et al.*, 2009) and mice (Plaza-Zabala *et al.*, 2010) that further establishes the important role of the brain stress system in the addictive properties of nicotine.

The cue-induced reinstatement of nicotine-seeking involves a plethora neurotransmitter systems, including the orexin system (Plaza-Zabala *et al.*, 2013), the endogenous cannabinoid system (Cohen *et al.*, 2005; Gamaleddin *et al.*, 2015), the endogenous opioid system (EOS) (see section 5.6) (Liu *et al.*, 2009), and the GABAergic system (Paterson *et al.*, 2005; Fattore *et al.*, 2009; Vlachou *et al.*, 2011; Lubbers *et al.*, 2014). Nevertheless, research of the last decade mainly focused on the glutamatergic system. Accordingly, pharmacological blockade of the mGluR1 (Dravolina *et al.*, 2007) and mGluR5 decreased cue-induced reinstatement of nicotine-seeking but not food-seeking (Tessari *et al.*, 2004; Bespalov *et al.*, 2005). Furthermore, intra-NAc shell administration of the mGluR2/3s agonist LY379268 and N-acetylcysteine attenuated cue-induced reinstatement of both nicotine- and food-seeking (Liechti *et al.*, 2007; Ramirez-Niño *et al.*, 2013). Lastly, intra-NAc core and systemic injections of specific NMDAR subunit NR2A and NR2B antagonists were shown to abolished cue-induced reinstatement of nicotine-seeking, respectively (Gipson *et al.*, 2013).

Together, these results indicate that negative modulation of glutamatergic transmission attenuates cue-induced reinstatement of nicotine-seeking (D'Souza & Markou, 2013).

5 The endogenous opioid system

The EOS is integrated by opioid receptors (ORs), their endogenous peptide ligands and the enzymes involved in their metabolism. This system is largely distributed through the CNS and peripheral tissues, and plays an important role in the control of multiple physiological and pathophysiological responses to exogenous and endogenous stimuli such as respiration and gastrointestinal motility, nociception, stress, locomotion, emotional behaviors, learning and memory and the regulation of reward circuits, among others (Olson *et al.*, 1991; Bodnar, 2013, 2017).

5.1 Historical overview

Opium is extracted from poppy seeds (*Papaver somniferum*) and consumed for several thousand years to relieve pain and obtain euphoria. Morphine, the most active alkaloid extracted from opium, was the first opioid to be isolated by Friedrich Sertürner in 1805 (Figure 30).

Almost one hundred and seventy years later the existence of membrane receptors for opiate drugs was discovered by three different groups (Pert & Snyder, 1973; Simon *et al.*, 1973; Terenius, 1973). Some years later, different opioid binding sites were identified which let assume that ORs did not constitute a homogenous population. They were distinguished between the μ-opioid receptor (MOR) which was stimulated by morphine, the κ-opioid receptor (KOR) which binds ketocyclazocine, and the sigma type which has a high affinity for SKF-10,047 (Martin *et al.*, 1976). One year later, the δ-opioid receptor (DOR) was identified in mouse vas deferens (Figure 30) (Lord *et al.*, 1977). Additional research revealed that the sigma-type receptor is a non-opioid (see section 6), thus the main types of ORs

are MOR, DOR and KOR (Manallack *et al.*, 1986). The endogenous ligands Met- and Leu-enkephalins were identified in 1975. Altogether, three families of endogenous opioid peptides precursors were identified in the late ’70s, including pre-proenkephalin (PENK), pre-prodynorphin (PDYN) and proopiomelanocortin (POMC) (Figure 30) (Guillemin *et al.*, 1976; Li & Chung, 1976; Goldstein *et al.*, 1979). The genes encoding those precursor families were first isolated in the early ’80s (Nakanishi *et al.*, 1979; Comb *et al.*, 1982; Gubler *et al.*, 1982; Kakidani *et al.*, 1982; Noda *et al.*, 1982). The first opioid receptor gene, encoding the DOR, was isolated by expression cloning in 1992 (Evans *et al.*, 1992; Kieffer *et al.*, 1992), followed by the MOR and KOR genes that were cloned by homology (Figure 30) (Chen *et al.*, 1993; Simonin *et al.*, 1994, 1995). Only a few years later, the first constitutive knock out (KO) mice deficient in EOS components, including the MOR (Matthes *et al.*, 1996), DOR (Filliol *et al.*, 2000) and KOR (Simonin *et al.*, 1998), as well as the endogenous opioid peptide precursors PENK (König *et al.*, 1996) and PDYN (Sharifi *et al.*, 2001) and the endogenous opioid ligand β-endorphin (Rubinstein *et al.*, 1996), have been generated by homologous recombination (Figure 30). On this basis and by Cre loxp recombination, conditional KO mice restricted to primary afferent nociceptive neurons and GABAergic forebrain neurons have been created targeting the MOR (Weibel *et al.*, 2013; Charbogne *et al.*, 2017) and DOR (Figure 30) (Gaveriaux-Ruff *et al.*, 2011; Chung *et al.*, 2015; Reiss *et al.*, 2017). In addition, the 3D crystal structure of all three receptors was elucidated very recently at high-resolution by X-ray crystallography (Figure 30) (Granier *et al.*, 2012; Manglik *et al.*, 2012; Wu *et al.*, 2012).

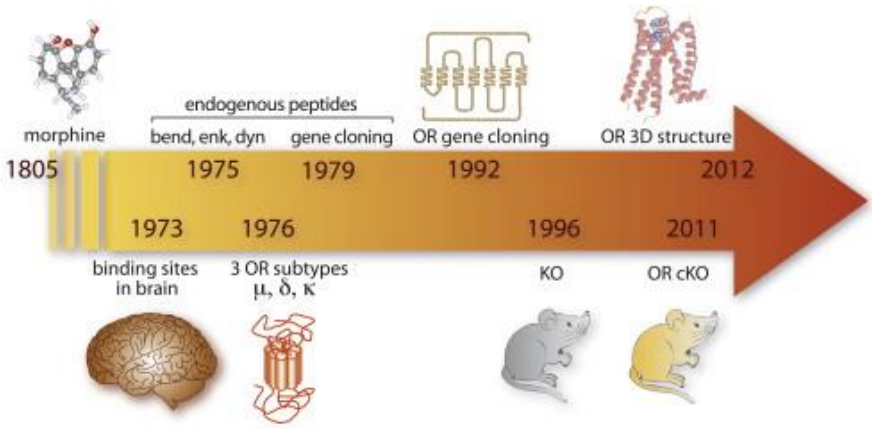

Figure 30. Milestone discoveries in opioid research.
(Charbogne *et al.*, 2014). **Abbreviations:** β-endorphin (bend), conditional knockout (cKO), dynorphin (dyn), enkephaline (enk), knockout (KO), opioid receptor (OR).

5.2 Opioid receptors

5.2.1 Gene and structure

As already mentioned, three classical ORs have been identified and cloned in experimental animals and humans (Kieffer, 1999). A non-classical opioid receptor, the nociceptin or orphanin receptor (NOR or opioid receptor-like 1, ORL-1) was identified later on and was accepted to be part of the ORs family (Bunzow *et al.*, 1994; Mollereau *et al.*, 1994), although it is considered to belong to an 'anti'-opioid system owed to its pharmacological actions (Anton *et al.*, 1996).

ORs belong to the superfamily of G protein-coupled receptors (GPCRs). They possess seven-transmembrane domains for anchorage in the cell membrane, an extracellular N-terminal and an intracellular C-terminal domain (Figure 31). Although each OR receptor is encoded by a unique gene sequence (Oprm1, Oprd1, Oprk1, Oprl1), they present a high homology in the sequence identity in both, transmembrane (73%-76%) and intracellular domains (63%-66%). In contrast, a large divergence is

reported in the extracellular N-domains (34%-40% identity) (Pogozheva *et al.*, 2005; Al-Hasani & Bruchas, 2011; Toll *et al.*, 2016). Furthermore, two subclasses for μ- (μ1,μ2) and δ- (δ1,δ2) opioid receptors and three for κ- (κ1, κ2, κ3,) opioid receptor, generated by post-transcriptional modifications, were reported (Minami & Satoh, 1995). However, the relevance of these subtypes is very polemic. In addition, hetero-dimerization of ORs, particularly δ/κ- (Jordan & Devi, 1999) and μ/δ-dimers (Gomes *et al.*, 2000) was identified. Thus, these new structures result in novel functional properties different from those of μ-, δ- and κ-opioid receptor monomers, which could explain the pharmacological responses of the EOS which do not coincide with those of classical OR monomers. The crystal structures for the inactive and active state of each receptor have been identified with atomic-level details, which allow the definition of the unique opioid binding pockets that maintain ligand preferences (Figure 31) (Granier *et al.*, 2012; Manglik *et al.*, 2012; Thompson *et al.*, 2012; Wu *et al.*, 2012). These findings provide new insights on how different agonists distinctly alter receptor conformations to direct downstream intracellular cascades, which may ultimately lead to more effective pharmacological treatments.

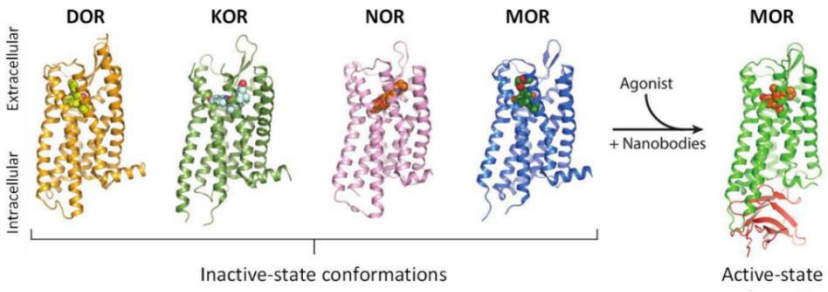

Figure 31. Chrystal structures of inactive states of opioid receptors.
Crystal structures of the inactive states of the DOR, KOR, NOR, and the MOR, and the conformational change of the MOR in the transmembrane domains due to agonist binding that enables intracellular effector molecules to bind and activate signaling cascades that modulate neural function (Corder *et al.*, 2018). **Abbreviations:** δ-opioid receptor (DOR), κ-opioid receptor (KOR), μ-opioid receptor (MOR), nociception receptor (NOR)

5.2.2 Opioid cellular signaling

All four ORs couple to inhibitory pertussis toxin-sensitive G proteins ($G_{\alpha i}$ and $G_{\alpha o}$) (Charbogne *et al.*, 2014). Upon activation by endogenous or exogenous agonists, the two G protein subunits $G_{\alpha,}$ and $G_{\beta\gamma}$ dissociate from one another and subsequently engage a variety of effectors and intracellular signaling cascades that typically depress neural excitability. After dissociation, the G_{α} subunit inhibits adenylate cyclase (AC) activity reducing cyclic adenosine monophosphate (cAMP) production (Law *et al.*, 2000). The $G_{\beta\gamma}$ subunit positively modulates the G protein gated inwardly rectifying potassium channels (GIRK) at the postsynaptic level (Wickman & Clapham, 1995; Torrecilla *et al.*, 2002). At the same time, the $G_{\beta\gamma}$ subunit inhibits N-, P/Q- and L-type voltage-gated calcium channels at a presynaptic level (Zamponi & Snutch, 1998). These processes lead to neuronal hyperpolarization, which results in reduced neuronal excitability and inhibition of neurotransmitter release (Figure 32).

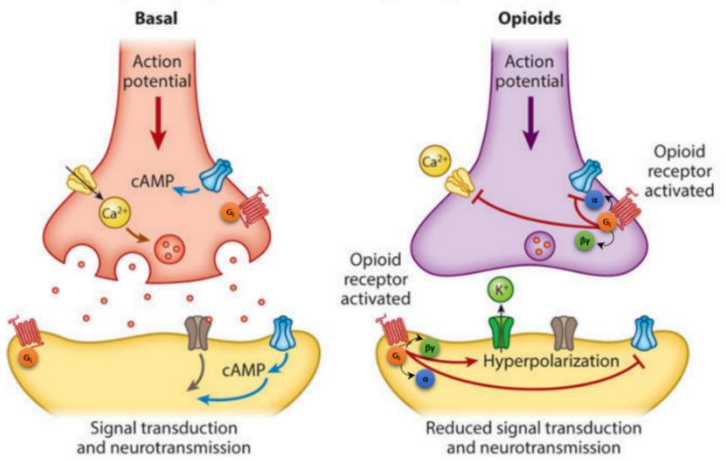

Figure 32. Presynaptic and postsynaptic effect of opioid signaling.
(Corder *et al.*, 2018). **Abbreviations:** Cyclic adenosine monophosphate (cAMP)

Besides the G protein signaling, there is an additional mechanism, called arrestin signaling. The interaction of an OR with arrestin depends on the cellular context, type of agonist, and model system studied (Corder *et al.*, 2018). Upon activation, ORs are phosphorylated by GPCR kinases, leading to the recruitment of β-arrestin 2 or 3. Arrestins are key proteins that bind to phosphorylated GPCRs to regulate their activity through desensitization and internalization. Indeed, mice that lack β-arrestin 2 show enhanced morphine antinociception and increased CPP (Bohn *et al.*, 1999, 2003). It was generally accepted that internalized receptors were inactive (Bohn *et al.*, 1999), however, more recent studies have shown that ORs may still signal from endosomal compartments (Irannejad *et al.*, 2013; Eichel *et al.*, 2016).In addition to the modulation of G protein signaling, evidence exhibited that β-arrestin is a key signal effector mediating an array of cellular and behavioral responses. Phosphorylated arrestin-bound OR complexes trigger critically important downstream signaling cascades, including the mitogen-activated protein kinase (MAPK) cascade (Figure 33) (Al-Hasani & Bruchas, 2011) These MAPKs, which consist of three major proteins, including the extracellular signal regulated kinase 1 and 2 (ERK1/2), c-Jun N-terminal kinase 1–3 (JNK1–3), and p38, notably modulate cell proliferation, differentiation, apoptosis, transcription factor regulation, ion channel regulation, neurotransporter regulation, and protein scaffolding (Raman *et al.*, 2007).

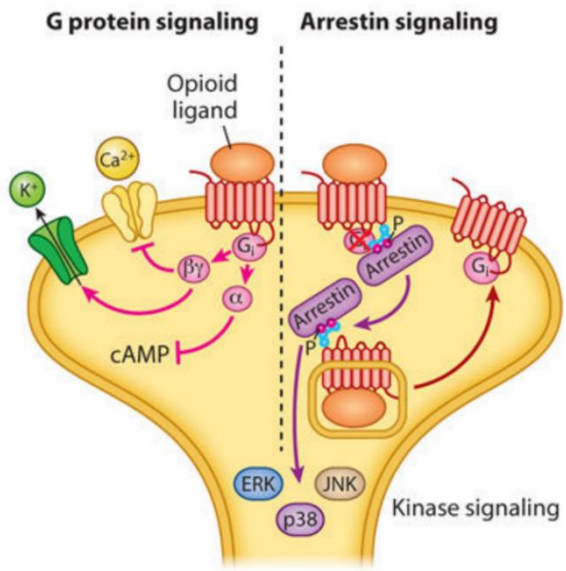

Figure 33. G protein and arrestin signalin upon ligand binding.
(Corder *et al.*, 2018). **Abbreviations:** c-Jun N-terminal kinase (JNK), extracellular signal regulated kinase 1 and 2 (ERK1/2), Cyclic adenosine monophosphate (cAMP)

5.2.3 Anatomical and subcellular distribution

Opioid receptors are widely distributed throughout the central and peripheral nervous system (Mansour *et al.*, 1988; Stein & Lang, 2009). In the CNS ORs are expressed primarily in the cortex, limbic system, and brain stem (Mansour *et al.*, 1994; Neal *et al.*, 1999), whereby each component has a distinct expression pattern. On the one hand, ligand autoradiography and in situ hybridization studies have determined the opioid binding sites (receptor protein). On the other hand, the distribution of cell bodies that express ORs was based on the detection of mRNA (Le Merrer *et al.*, 2009). Interestingly, the sites of OR expression (mRNA) generally match the distribution of binding sites (protein), suggesting that many neurons that synthesize ORs are local neurons (Le Merrer *et al.*, 2009).

The binding sites for MORs, DORs, and KORs overlap in most structures, nevertheless, some structures exhibit higher expression of one receptor subtype over the others. Accordingly, MORs are the most expressed opioid receptor in the AMG, but not in the central nucleus of the AMG, thalamus, mesencephalon, and some brain stem nuclei. KORs are the most represented receptors in the basal anterior forebrain, including the claustrum and endopiriform cortex, olfactory tubercle, striatum, preoptic area, hypothalamus, and pituitary gland. DORs are highly expressed in the striatum and are the most abundant receptors in the olfactory tract (olfactory bulbs, anterior olfactory nucleus, olfactory tubercle, medial AMG) and the cortices, including the whole neocortex and regions of the AMG that derive ontogenically from the cortex (basolateral, cortical, and median nuclei) (Figure 34) (Le Merrer *et al.*, 2009; Lutz & Kieffer, 2013).

In addition, ORs have also been found in immune cells and various peripheral tissues including the gastrointestinal system, dermis, and epidermis (around hair follicles), bone, joint tissue and in dental pulp (Bigliardi & Bigliardi-Qi, 2014). In these tissues, they are expressed in sensory and sympathetic fibers where they modulate different physiological effects (Mansour *et al.*, 1988; Przewłocki & Przewłocka, 2001).

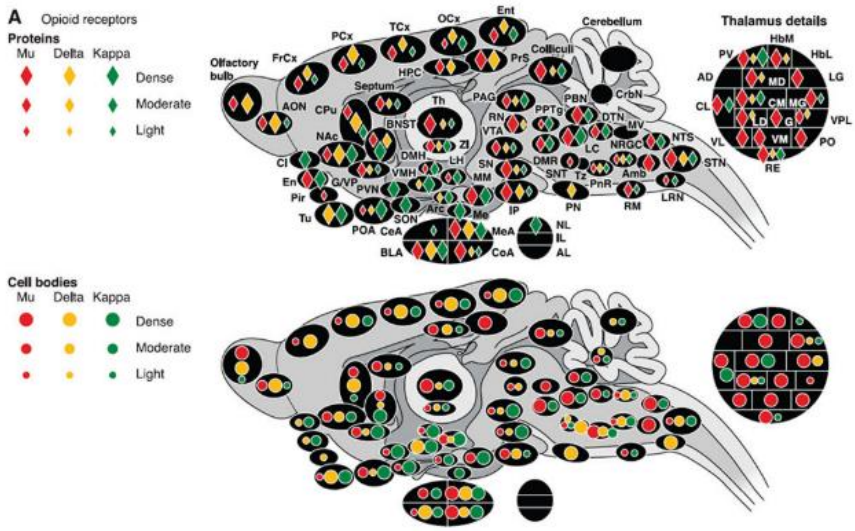

Figure 34. Anatomical distribution of opioid receptors in the rodent brain
(Le Merrer *et al.*, 2009). **Abbreviations:** Nucleus ambiguous(Amb), anterodorsal thalamus (AD), anterior lobe pituitary (AL), anterior olfactory nucleus (AON), arcuate nucleus hypothalamus (Arc), basolateral amygdala (BLA), bed nucleus of the stria terminalis (BNST), central nucleus of amygdala (CeA), claustrum (CI), centrolateral thalamus (CL), centromedial thalamus (CM), cortical nucleus of amygdala (CoA), caudate putamen (CPu), cerebellar nuclei (CrbN), dorsomedial hypothalamus (DMH), dorsal and medial raphe´(DMR), dorsal tegmental nucleus (DTN), endopiriform cortex (En), entorhinal cortex (Ent), frontal cortex (FrCx), nucleus gelatinosus of thalamus (G), globus pallidus/ventral pallidum (G/VP), lateral habenula (HbL), medial habenula (HbM), hippocampus (HPC), intermediate lobe of pituitary (IL), interpeduncular nucleus (IP), locus coeruleus (LC), laterodorsal thalamus (LD), lateral geniculate of thalamus (LG), lateral hypothalamus (LH), lateral reticular nucleus (LRN), mediodorsal thalamus (MD), median eminence (Me), median nucleus of amygdala (MEA), medial geniculate (MG), medial mammillary nucleus (MM), medial vestibular nucleus (MV), nucleus accumbens (NAc), neuronal lobe of pituitary (NL), nucleus reticularis gigantocellularis (NRGC), nucleus tractus solitarius (NTS), occipital cortex (OCx), periaqueductal gray (PAG), parietal cortex (PCx), piriform cortex (Pir), pontine nucleus (PN), pontine reticular (PnR), posterior thalamus (PO), preoptic area (POA), pedunculopontine nucleus (PPTg), presubiculum (PrS), paraventricular thalamus (PV), paraventricular hypothalamus (PVN), reuniens thalamus (RE), red nucleus (RN), raphe´ magnus (RM), supraoptic nucleus (SON), substancia nigra (SN), sensory trigeminal nucleus (SNT), spinal trigeminal nucleus (STN), temporal cortex (TCx), thalamus (Th), olfactory tubercle (Tu), trapezoid nucleus (Tz), ventrolateral thalamus (VL), ventromedial thalamus (VM), ventromedial hypothalamus (VMH), ventroposterolateral thalamus (VPL), ventral tegmental area (VTA), zona incerta (ZI)

5.3 Endogenous opioid peptides

5.3.1 Gene and structure

ORs are activated by four major families of endogenous opioid ligands, including β-endorphin, enkephalins, dynorphins and nociceptin/orphanin FQ (Figure 35) (Kieffer & Gavériaux-Ruff, 2002; Corder *et al.*, 2018).

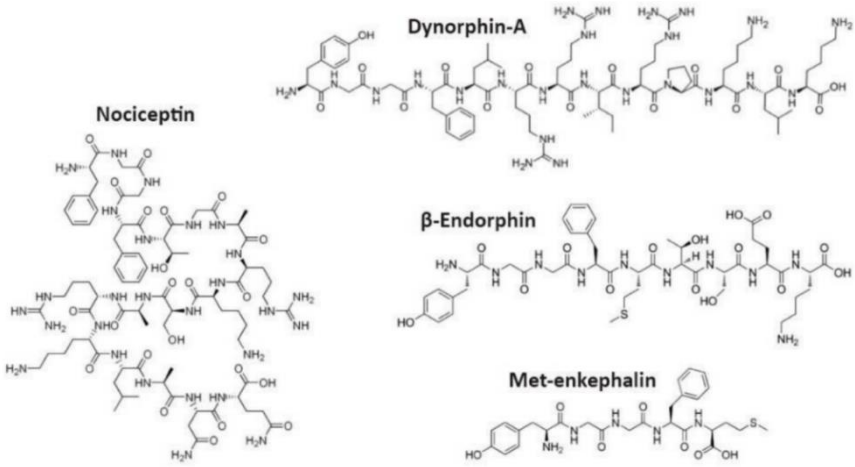

Figure 35. Chemical structures of the four main classes of opioid peptides.
β- endorphin, met-enkephalin, dynorphin-A and nociceptin (Corder *et al.*, 2018).

These opioid peptides derive from four major families of endogenous opioid peptide precursors, including POMC, PENK, PDYN, and PNOC, respectively (Corder *et al.*, 2018). The precursors are characterized by repeatedly having certain amino acid sequences along their structure and thus generating several active peptides due to enzymatic cleavage.

Accordingly, POMC can be spliced into β-endorphin, as well as adrenocorticotropic hormone (ACTH), melanotropic hormones (MSHs) and Met-enkephalin. PENK is the main precursor for Met-enkephalin, Leu-

enkephalin and the related heptapeptide Met-enkephalin-Arg(6)-Phe(7) and octapeptide Met-enkephalin-Arg(6)-Gly(7)-Leu(8). Dynorphin A, dynorphin B and α- and β-neo-endorphin, as well as Leu-enkephalin, are derived from PDYN (Patey & Rossier, 1986; Flórez, 2007), and nociceptine, nocistatin and orphanin FQ2 are the active peptides after cleavage of PNOC (Figure 36) (Flórez, 2007). In addition, two additional short peptides, endomorphin-1 and -2, that display a high selective affinity for MORs were reported (Zadina *et al.*, 1997). However, neither the genes nor the precursor peptides for their endogenous synthesis have been identified.

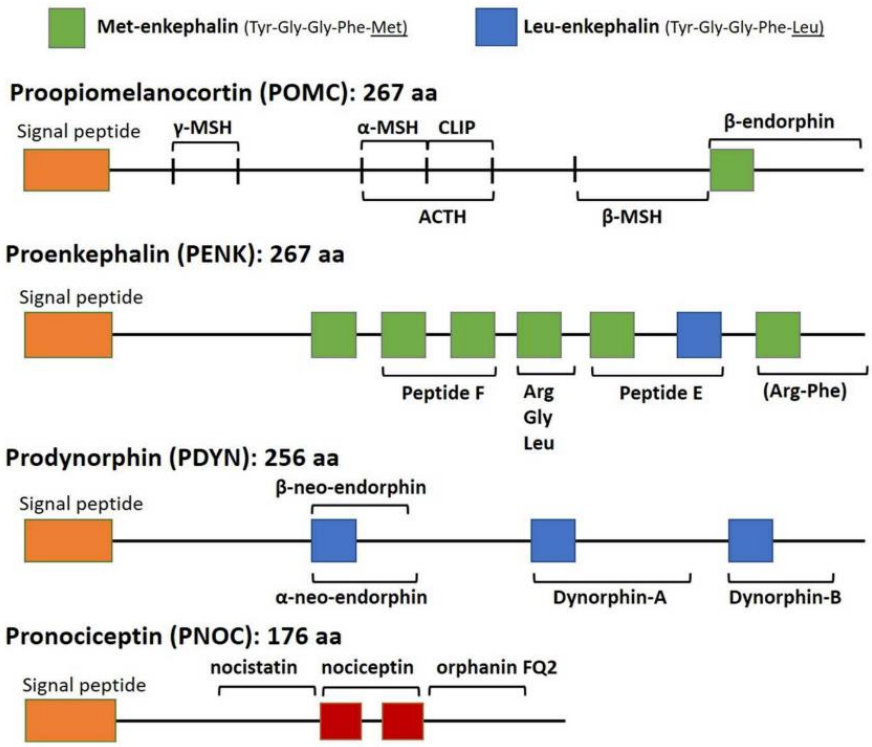

Figure 36. Precursor proteins of opioid peptides.
(adapted from Flórez, 2007). **Abbreviations:** Adrenocorticotropic hormone (ACTH), Corticotropin-like intermediate peptide (CLIP), Melanocyte stimulating hormone (MSH)

The endogenous opioid peptides all contain the enkephalin sequence Tyr-Gly-Gly-Phe-Met/-Leu at their N-terminus, however, they exhibit different affinities for each OR. β-endorphin is the main endogenous ligand for MORs but also binds to DORs and KORs with less affinity. The affinity of met- and leu-enkephalins is 20-fold higher to DORs than to MORs, the dynorphins are the putative endogenous ligands for KORs, and nociceptin exhibits a high and selective affinity for NORs (Table 2) (Roth-Deri *et al.*, 2008).

Contrasting with the tight, spatially controlled synaptic transmission of small-molecule transmitters such as glutamate or dopamine, opioids are thought to rely on volumetric release into synaptic and extra-synaptic spaces and diffuse toward their receptors (Duggan, 2000; Banghart & Sabatini, 2012; Chavkin, 2013). Indeed, electron microscopy illustrates that most MORs are extra-synaptic, being hundreds of microns away from release sites (Svingos *et al.*, 1996; Glass *et al.*, 2009). This implies that opioid synapses may include a much broader area than typical fast transmitter synapses.

Table 2. The affinity of opioid ligands for opioid receptors.
Affinity from - (no affinity) to +++ (high affinity)**. Adapted from** (Kieffer, 1995; Roth-Deri *et al.*, 2008).

Precursor protein	Opioid peptide	MOR	DOR	KOR	NOR
POMC	β-endorphin	+++	++		
PENK	Met-enkephalin	++	+++		
	Leu-enkephalin	++	+++		
PDYN	Dynorphin-A	++		+++	
	Dynorphin-B	+	+	+++	
	α-neoendorphin	+	+	+++	
	β-neoendorphin	+	+	+++	
	Leu-enkephalin	++	+++		
PNOC	Nociceptin				+++

5.3.2 Anatomical and subcellular distribution

Opioid peptides are widely distributed throughout the central and peripheral nervous system (Mansour *et al.*, 1988; Stein & Lang, 2009). The distribution of opioid peptide-containing neuronal fibers and cell bodies has been assessed by immunohistochemistry, while in situ hybridization studies completed the mapping of opioid cell bodies (Le Merrer *et al.*, 2009). Mismatches exist between the distribution of opioid peptide immunoreactivity and the localization of cell bodies. The discrepancies between peptide and cell body maps suggest that an important proportion of opioid peptides is released by projecting neurons (Le Merrer *et al.*, 2009). Indeed, the opioid precursors are packaged into dense core vesicles

in the soma and transported down to axon terminals. Precursor proteins are cleaved during this process into opioid peptides (Corder *et al.*, 2018). Opioid peptide immunoreactivity in projection fibers overlaps largely with the localization of ORs. PENK is the most abundant and widely distributed opioid precursor and is best detected in the thalamus, where it overlaps with MORs. PDYN is also widespread with the highest concentration in the NAc but near absence in the thalamus. POMC shows a more restricted distribution and is absent from cortical structures except for the AMG (Figure 37) (Le Merrer *et al.*, 2009).

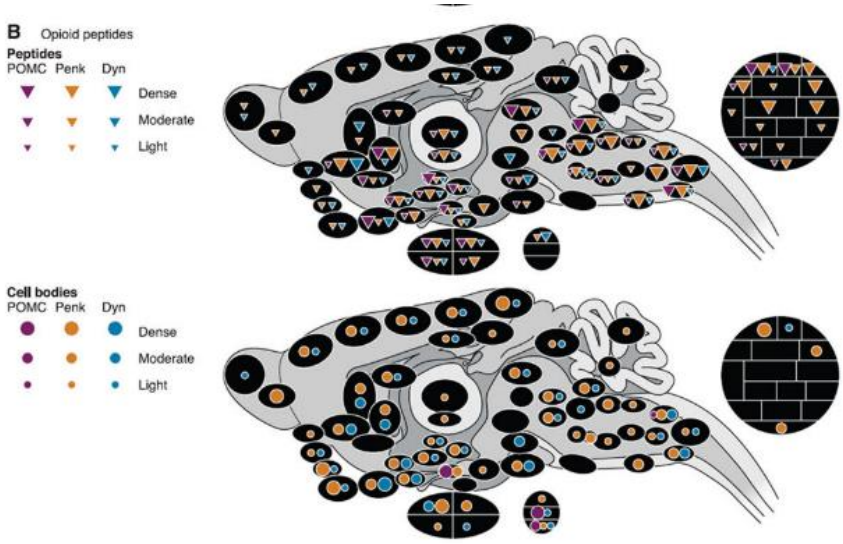

Figure 37. Anatomical distribution of opioid peptides in the rodent brain.
(Le Merrer *et al.*, 2009). See abbreviations in Figure 34

5.4 The physiological role of the endogenous opioid system

The EOS in the control of multiple physiological responses due to its widespread distribution in the central and peripheral nervous system(Bodnar, 2017). Thus, the EOS has been the subject of a vast number of investigations. The control of pain is probably the most well studied physiological function. However, this system is involved in a wide range of functions related to behavior, such as reward and addiction, stress and social status, learning and memory, mental and mood disorders, food intake, gastrointestinal transit, respiratory, cardiovascular and immunological functions, among others (Bodnar, 2017). For the aim of this thesis, we will focus our attention on the role of the EOS in nicotine addiction.

5.5 Opioid signaling in the mesocorticolimbic circuit

Due to its high expression within the mesocorticolimbic pathway, the EOS is strongly involved in the modulation of mood, motivation, reinforcement, learning, and memory (Shippenberg *et al.*, 2007; Bodnar, 2017). The EOS modulates mesocorticolimbic activity mostly by inhibiting neuronal activity upon receptor activation (see section5.2.2). However, ORs modulate both the rewarding and aversive properties of opioids due to their differential expression patterns (Arbuthnott, 1992)..

Systemic administration of MOR agonists increased DA release in the NAc (Di Chiara & Imperato, 1988; Yoshida *et al.*, 1999). Furthermore, several studies used intracerebral micro-injections to better assess the specific brain areas in which MORs develop their rewarding properties. Accordingly, VTA micro-injections of MOR agonists enhanced basal DA release in the NAc (Spanagel *et al.*, 1992; Devine *et al.*, 1993; Yoshida *et al.*, 1999), an effect blocked by pretreatment with a selective MOR

antagonist (Devine *et al.*, 1993). In contrast, MOR antagonists alone in the VTA decreased accumbal DA (Spanagel *et al.*, 1992). MORs are highly expressed on GABAergic terminals in the VTA and GABA input to DA neurons is reduced by the activation of MORs, resulting in an increase in the firing rate of DA neurons. The disinhibition of DA neurons upon MOR activation was originally thought to be mediated by local interneurons (Johnson & North, 1992b). However, more recent studies found a dense opioid sensitive GABA input to DA neurons from the RMTg (Jhou *et al.*, 2009; Kaufling *et al.*, 2009), and morphine increased VTA DA neuron firing through the activation of VTA MOR receptors expressed on afferents from the RMTg (Jalabert *et al.*, 2011). A follow-up study selectively activated the three major GABAergic inputs onto DA neurons (Interneurons, NAc, RMTg) (Figure 11) and demonstrated that MOR agonist-induced GABAergic depression was pathway-dependent with the strongest effect on GABAergic projection neurons originating in the RMTg (Matsui *et al.*, 2014). VTA-injections of a DOR agonist also increase basal accumbal DA levels that was reversed by DOR antagonists (Devine *et al.*, 1993). KOR agonists microinjected in the VTA had no effect, but decreased DA levels when systemically administered, indicating a lack of a regulatory role of KORs in the VTA (Devine *et al.*, 1993).

ORs also play a crucial role in the control of the reward circuit in the NAc. Indeed, local administration of MOR agonists in the NAc increased DA levels in the NAc as well. The DA increase could be reversed by systemic administration of non-specific OR antagonist and intra-NAc injections of a MOR antagonist (Yoshida *et al.*, 1999). MOR antagonists in the NAc could also block electrically evoked DA release in the NAc further substantiating the important role of MORs in regulating DA release (Gómez-A *et al.*, 2019). Similar to the VTA, DOR agonists also increased basal accumbal DA

(Hirose *et al.*, 2005). More strikingly, δ_2- but not δ_1-antagonists were able to decrease MOR agonist-induced DA increases (Yoshida *et al.*, 1999; Hirose *et al.*, 2005). Suggesting that activated MORs may interact with δ_2-opioid receptors. In contrast to MORs and DORs, stimulation of KOR within the NAc decreased DA release, whereas their selective blockade markedly increased basal DA release (Spanagel *et al.*, 1992). In agreement, in vitro studies have shown that KOR activation inhibited electrically evoked DA release in the NAc (Heijna *et al.*, 1992; Yokoo *et al.*, 1992). More recent evidence indicated that KORs regulate DA uptake (Thompson *et al.*, 2000). Indeed, KORs are co-localized with DATs in NAc nerve terminals (Svingos *et al.*, 2001). Autoradiographic studies have shown that DAT density and the maximal velocity of transport are reduced for at least three days following cessation of repeated KOR agonist treatment (Thompson *et al.*, 2000; Collins *et al.*, 2001), suggesting that in contrast to acute KOR activation, down-regulation of DAT may occur as a consequence of chronic KOR agonist exposure.

Whereas reward-modulatory opioid actions have been intensively studied in subcortical sites such as the NAc, the role of cortical opioid transmission has received comparatively little attention. Systemic administrations of MOR agonists were found to mainly inhibit the spontaneous firing of cells in the mPFC, which could be reversed by a MOR antagonist. Electrophoretic application of a selective MOR agonist reproduced the effects of systemic morphine to a more limited degree (Giacchino & Henriksen, 1996). In a follow-up study, the authors demonstrated that systemic administration of a MOR agonists attenuate mPFC excitatory response to glutamate, but not to ACh. Furthermore, electrophoresed MOR agonists into the mPFC attenuated the response of prefrontal cortical cells to activation of excitatory afferents from the mediodorsal

thalamus, and to a lesser degree, from the BLA and HPC. Both modulations were reversed by MOR antagonists (Giacchino & Henriksen, 1998)

5.6 Involvement of the endogenous opioid system in SUD: Focus on nicotine

The involvement of the EOS in SUDs was intensively studied over the last three decades. A large body of evidence proposes the EOS as a promising target to treat SUDs of all major legal and illicit drugs of abuse, including opiates, alcohol, nicotine, psychostimulants and also palatable food (Trigo *et al.*, 2010; Charbogne *et al.*, 2014). A detailed description would reach beyond the scope of this work, hence this work will mostly focus on nicotine.

The EOS is thought to have a crucial role in mediating nicotine's rewarding and aversive effects, although nicotine is actively acting on nAChRs. However, nicotine can activate the EOS due to the ability of nAChRs to facilitate neurotransmitter release (see section 3), including endogenous opioids at central and peripheral levels. Indeed, plasma concentrations of β-endorphin were increased in rats (Conte-Devolx *et al.*, 1981), and humans (del Arbol *et al.*, 2000) by nicotine administration. In agreement, β-endorphin concentration was elevated in the hypothalamus of rodents after acute nicotine administration (Marty *et al.*, 1985). Furthermore, mRNA levels of PDYN and MOR were also elevated in the mouse striatum after chronic nicotine administration (Wewers *et al.*, 1999), and acute nicotine increased and chronic nicotine administration decreased PENK mRNA expression in striatum and HPC (Houdi *et al.*, 1998), however, PENK protein expression in the striatum was increased after both acute and chronic nicotine administration (Dhatt *et al.*, 1995). Upon nicotine withdrawal, PENK mRNA was shown to be increased in the striatum and

HPC (Houdi *et al.*, 1998). This accumulated evidence let to the assumption that the EOS could also be involved in the reinforcing properties of nicotine. Indeed, CPP was decreased in KO mice deficient in PENK, β-endorphin, MOR and DOR (Berrendero *et al.*, 2002a, 2005; Walters *et al.*, 2005; Trigo *et al.*, 2009; Berrendero *et al.*, 2012). In accordance, systemic and intra-VTA infusions of a MOR antagonist abolished nicotine-induced elevations in DA extracellular levels in the NAc (Tanda & Di Chiara, 1998). Similarly, nicotine-elicited enhancement of DA transmission in the NAc is absent in mice lacking PENK (Berrendero *et al.*, 2005), and DOR (Berrendero *et al.*, 2012) In agreement, nicotine self-administration was also decreased in DOR KO mice and a selective DOR antagonist dose-dependently attenuated nicotine self-administration (Berrendero *et al.*, 2012), further substantiating the notion that DOR/PENK signaling contributes to the reinforcing properties of nicotine. In contrast, the KOR/dynorphin system seems to play an opposite role in nicotine reward as treatment with a KOR agonist reduced the number of infusions obtained by nicotine self-administering rats (Ismayilova & Shoaib, 2010), and mice lacking PDYN showed enhanced sensitivity to nicotine self-administration (Galeote *et al.*, 2009), which suggests that the KOR/dynorphin system mediates nicotine's aversive effects. In addition, the use of MOR and DOR antagonists (Balerio *et al.*, 2005) and knockout mice lacking β-endorphin (Trigo *et al.*, 2009) revealed that these receptors are mediating the anxiolytic- and anxiogenic-like effects of nicotine.

The EOS is also involved in the withdrawal syndromes induced by nicotine. In humans, the opioid antagonist, naloxone has been reported to induce somatic signs of withdrawal in heavy chronic smokers (Krishnan-Sarin *et al.*, 1999). In rodents, opioid antagonists precipitated somatic manifestations of withdrawal in nicotine-dependent animals (Balerio *et*

al., 2004). MOR/PENK signaling seems to be specifically involved in the somatic manifestations of nicotine withdrawal since the withdrawal signs were attenuated in chronically nicotine-treated PENK (Berrendero *et al.*, 2005) and MOR KO (Berrendero *et al.*, 2002a) mice. In contrast, no differences were observed comparing wild-type controls and mice lacking PDYN (Galeote *et al.*, 2009), DOR (Berrendero *et al.*, 2012), and β-endorphin (Trigo *et al.*, 2009). However, another study indicated increased activity of striatal, particularly accumbal, dynorphinergic neurons during nicotine withdrawal resulting in enhanced peptide release and compensatory synthesis that might be responsible, in part, for the emergence of the negative affective states observed during nicotine withdrawal (Isola *et al.*, 2008).

The involvement of the EOS in nicotine relapse is almost unknown. Pretreatment with KOR antagonist norbinaltorphimine elicited stress-induced but not nicotine-induced reinstatement of CPP (Jackson *et al.*, 2013). Another study could block cue-induced nicotine reinstatement by opioid antagonist naltrexone (Liu *et al.*, 2009), which indicates an involvement of the EOS in nicotine relapse, but it is still unknown neither which opioid receptor nor which endogenous ligand particularly mediates nicotine reinstatement.

6 The sigma-1 receptor

6.1 Historical overview

Sigma receptors were discovered in 1976 by Martin *et al.* (Martin *et al.*, 1976). Initially, these receptors were misclassified as an opioid receptor subtype sensitive to phencyclidine due to the cross-reactivity of some opioid ligands. Sigma receptors are now considered to be unique non-opioid and non-phencyclidine binding sites present in the CNS and peripheral organs distinct from other known neurotransmitter or hormone receptors (Quirion *et al.*, 1992). Based on pharmacological and molecular differences, the sigma receptor was classified into two subtypes, the sigma-1 receptor (Sig-1R) and the sigma-2 receptor (Sig-2R) (Hellewell & Bowen, 1990; Quirion *et al.*, 1992). Although the Sig-2R was identified as progesterone receptor membrane component 1 (Xu et al., 2011), recent studies showed that the Sig-2R and the progesterone receptor membrane component 1 are two distinct molecular entities (Abate *et al.*, 2015; Chu *et al.*, 2015; Pati *et al.*, 2017). In 2017, the gene sequence that codes for the Sig-2R was identified and its identity was revealed as transmembrane protein 97, a binding partner of the lysosomal cholesterol transporter NPC1 (Alon *et al.*, 2017). Sig-2Rs are proposed to be involved in mechanisms underlying proliferation, apoptosis, dendritogenesis, synaptogenesis and neuronal plasticity, activation of cytochrome P450, and steroid signalling, among others (Cahill, 2007; Lösel *et al.*, 2008; Rohe *et al.*, 2009). This work has been focused on Sig-1Rs as a potential target for the treatment of SUD.

6.2 Gene and structure

The Sig-1R was first cloned in 1996 from guinea pig liver (Hanner *et al.*, 1996), and later from human cell lines (Kekuda *et al.*, 1996), human brain (Prasad *et al.*, 1998), rat brain (Seth *et al.*, 1998; Mei & Pasternak, 2001) and mouse kidney and brain (Seth *et al.*, 1997; Pan *et al.*, 1998). In humans, the Sig-1R gene is located on chromosome 9 (chromosome 4 in mice, and 5 in rats) and is translated into a protein of 223 amino acids with a molecular mass of approx. 24 kDa. The Sig-1R sequence is highly homologous across species (90% identity and 95% similarity) and shares no homology with any known mammalian protein (Hanner *et al.*, 1996; Kekuda *et al.*, 1996; Seth *et al.*, 1997, 1998). The Sig-1R has two alpha-helical transmembrane segments with both protein termini on the cytoplasmic side of the plasma membrane or in the lumen of the endoplasmic reticulum (ER), whereby the C-terminus possesses chaperone activity that prevents protein aggregation (Hayashi & Su, 2007). Beside the chaperone activity, Sig-1Rs own two binding sides, the steroid binding domain like (SBDL) I and the SBDLII, that are located at the inner surface of the membrane, allowing hydrophobic molecules to interact with the receptor (Figure 38). Sig-1R binding studies have revealed high affinities for a variety of naturally occurring compounds such as steroids and neuropeptides. However, the endogenous ligands for the Sig-1R are as yet unknown (Fontanilla *et al.*, 2008).

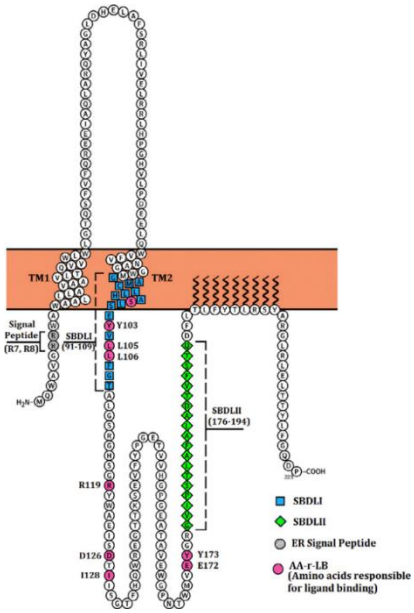

Figure 38 The putative structural model of the Sig-1R.
Sig-1R contains two hydrophobic transmembrane regions with the N- and C- terminals in the intracellular side of the plasma membrane or in the ER lumen. Circles represent amino acids and the numbers correspond to the serial number of the residues. (Bolshakova *et al.*, 2016). **Abbreviations:** steroid binding domain like (SBDL), endoplasmatic reticulum (ER)

6.3 Anatomical and subcellular distribution

Sig-1Rs are widely expressed throughout the central and peripheral nervous systems. In the CNS, Sig-1Rs are concentrated in specific brain areas involved in memory, emotion, sensory and motor functions, such as the HPC, hypothalamus, olfactory bulb, several cortical layers of the PFC, periaqueductal gray, locus coeruleus and rostroventral medulla (McCann *et al.*, 1994; Alonso *et al.*, 2000). Sig-1Rs are further present in peripheral tissue, including the digestive tract (Samovilova & Vinogradov, 1992), liver (Hellewell *et al.*, 1994), kidney (Hellewell *et al.*, 1994), sexual organs (Jansen *et al.*, 1992), skin (Sánchez-Fernández *et al.*, 2013), adrenal glands

(Hayashi & Su, 2007) and the heart (Ela *et al.*, 1994; Bhuiyan & Fukunaga, 2011).

The location of the Sig-1Rs in the subcellular compartment is dynamic in nature, and hence, they are found in several membranes (Hayashi & Su, 2005a, b). Binding experiments using Sig-1R radioligands showed that Sig-1Rs are especially enriched in microsomal membranes (McCann & Su, 1990; Cagnotto *et al.*, 1994) suggesting that they are mainly located in the ER membrane in the rat brain. Further research substantiated these results by immunohistochemical studies showing the presence of Sig-1Rs in the ER in neurons (Alonso *et al.*, 2000) and glial cells (Palacios *et al.*, 2003; Hayashi & Su, 2005a; Jiang *et al.*, 2006). The amino acid sequence of the Sig-1Rs has a double-arginine ER retention signal on the N-terminus (Figure 38). At the ER level, Sig-1Rs are located at the interface between mitochondria and ER at the mitochondria-associated ER membrane. Upon activation, they can redistribute to other subcellular compartments, such as the plasma or the nuclear membrane (Morin-Surun *et al.*, 1999; Hayashi & Su, 2001). This dynamic relocation possibly increases the number or type of proteins that can be targeted by the Sig-1R s (Zamanillo *et al.*, 2013).

6.4 Sigma-1 receptor cellular signaling

Sig-1Rs are ligand-regulated chaperones that interact with other proteins to modulate their activity and are thought to lack their own specific signaling machinery (Su & Hayashi, 2003; Tsai *et al.*, 2009; Su *et al.*, 2010). The best characterized chaperoning effect of Sig-1Rs occurs at the mitochondrial-associated ER membrane. There, under normal resting conditions, Sig-1Rs form a complex *via* direct protein-protein interactions with the binding immunoglobulin protein/78 kDa glucose-regulated

protein (BiP), another ER chaperone (Hayashi & Su, 2007). Their association and disassociation are regulated by oxidative stress, depletion of Ca^{2+} in the ER (Hayashi & Su, 2007; Hayashi *et al.*, 2011), activation of inositol-1,4,5-triphosphate (IP_3) receptors via G_q-coupled metabotropic receptors, and ligand binding (Figure 39) (Su *et al.*, 2010). At the mitochondrial-associated ER membrane, once dissociated from BiP, Sig-1Rs can interact with unstable IP_3 receptors, thus preventing IP_3 receptor degradation and ensuring proper Ca^{2+} influx into the mitochondria, which plays a central role in energy production (Figure 39) (Hayashi & Su, 2007; Tsai *et al.*, 2009; Zamanillo *et al.*, 2013).

Following pharmacological treatments or during cellular stress, Sig-1Rs can switch their client proteins from those at the mitochondrial-associated ER membrane to others at the plasmalemma, the plasma membrane, or nuclear envelopes (Hayashi & Su, 2003a, b; Mavlyutov & Ruoho, 2007; Hayashi & Fujimoto, 2010). Thus, electrophysiological studies showed that activated Sig-1Rs decreased potassium outward currents, and this effect was reversible by the Sig-1R antagonists (Soriani *et al.*, 1999b, a; Hayashi & Su, 2005b). Sig-1Rs also modulate several types of presynaptic Ca^{2+} channels in rat sympathetic and parasympathetic neurons (Hayashi *et al.*, 2000a; Zhang & Cuevas, 2002), and cardiac voltage-gated sodium channels (hNav1.5) (Langa *et al.*, 2003; Johannessen *et al.*, 2009).

In addition to ion channels, Sig-1R activation enhanced the BDNF signaling on the phospholipase C-IP_3-Ca^{2+} pathway in cortical neurons (Yagasaki *et al.*, 2006). PLC hydrolyzeS phosphatidylinositol 4,5-biphosphate into diacylglycerol and IP_3 (Morin-Surun *et al.*, 1999). IP_3 then binds to IP_3 receptors in the ER to promote Ca^{2+} efflux into the cytoplasm.

Sig-1R activation also facilitates the phosphorylation of the NR1 subunit of NMDARs at protein kinase C (PKC)-dependent (Ser^{890} and Ser^{896}) and

protein kinase A (PKA)-dependent (Ser^{897}) sites (Kim *et al.*, 2008; Roh *et al.*, 2008), thus, potentiating NMDAR currents. Direct physical interaction of the Sig-1R with the C terminal of the NMDAR NR1 subunit has been described (Balasuriya *et al.*, 2013; Rodríguez-Muñoz *et al.*, 2015). In addition, Sig-1Rs also modulate NMDAR activity through an indirect mechanism by inhibiting small conductance Ca^{2+}-activated potassium channels, which in turn potentiate NMDAR currents (Martina *et al.*, 2007). Furthermore, the activation of Sig-1Rs diminishes the association of the neuronal nitric oxide synthase (nNOS) with the NR2 subunit of the NMDAR by reducing the recruitment of nNOS to the membrane fraction and its interaction with the postsynaptic density protein-95 (Yang *et al.*, 2010). Previous studies suggested that Sig-1Rs do not seem to directly interact with G-proteins (Wilke *et al.*, 1999; Aydar *et al.*, 2002). However, a functional and physical association of the Sig-1Rs have been recently reported with MORs, DA D1 and D2 receptors and with mAChRs, indicating a possible universal role for the Sig-1Rs in modulating GPCR agonist function and/or GPCR trafficking (Figure 39) (Kim *et al.*, 2010; Navarro *et al.*, 2010, 2013; Sánchez-Blázquez *et al.*, 2014).

Although free forms of Sig-1Rs have not been found in the cytoplasm, Sig-1Rs indirectly modulate intracellular kinases and synthases. The Sig-1R-induced rise of intracellular Ca^{2+} results in a decreased phosphorylation of nNOS, which in turn increases enzymatic activity and increased levels of nitric oxide. As a gas, nictric oxide can freely diffuse to neighbored cells and stimulate the soluble guanylate cyclase to produce cyclic guanosine monophosphate. This mechanism leads to PKC activation, which phosphorylates and consequently activates NMDARs and ERK1/2 (Figure 39) (Roh *et al.*, 2011).

At the nucleus, Sig-1R activation modulates the reactive oxygen species-induced expression of transcription factors, including NF-κβ, cAMP response element binding protein (CREB) and c-fos. Consequently, Sig-1Rs transcriptionally regulate the gene expression of several proteins related to inflammation, nociception, neuronal survival, synaptogenesis and neurogenesis, such as nNOS, inducible nitric oxide synthase, the antiapoptotic protein Bcl-2, BDNF and interleukins 8/10 (Figure 39) (Yang *et al.*, 2007; Meunier & Hayashi, 2010; Hayashi *et al.*, 2011).

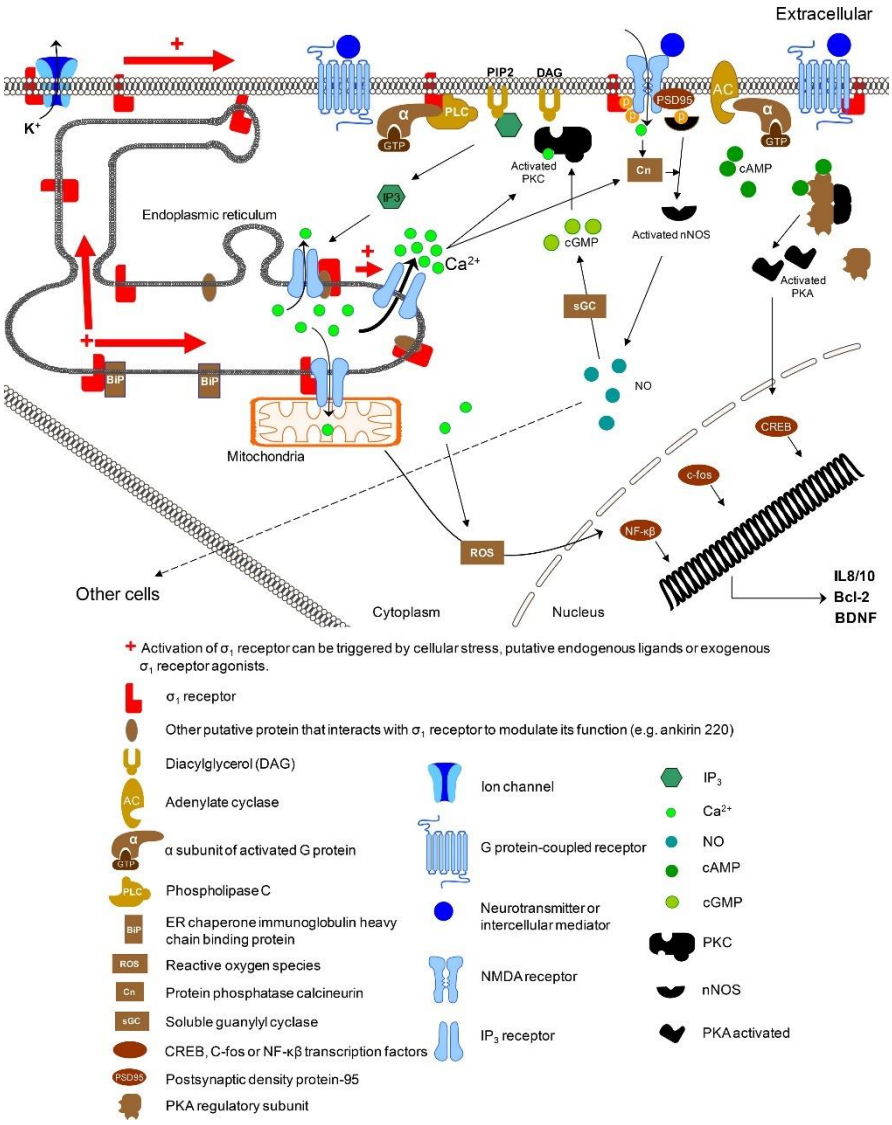

Figure 39. Signal transduction pathways modulated by Sigma-1 receptor activation. (Zamanillo *et al.*, 2013). **Abbreviations:** Binding immunoglobulin protein (BiP), brain-derived neurotrophic factor (BDNF), cAMP response element binding protein (CREB), cyclic adenosine monophosphate (cAMP), cyclic guanine monosphosphate (cGMP), endoplasmic reticulum (ER), guanosine triphosphate (GTP), interleukins 8/10 (IL8/10), neuronal nitric oxide synthase (nNOS), nitric oxide (NO), protein kinase C (PKC), phospholipase C (PLC), nuclear factor-κB (NF-κB)

6.5 Involvement of sigma-1 receptors in drug addiction

Under normal physiological conditions, most target proteins are not affected by Sig-1Rs, but when they become conformationally unstable, disturbed or stressed, the Sig-1R chaperone can assist and modulate their activity (Hayashi *et al.*, 2000b; Su & Hayashi, 2003; Su *et al.*, 2010). Therefore, Sig-1Rs are proposed to be involved in neurological diseases, including schizophrenia, depression and anxiety, cognitive deficits, neurodegenerative disorders, pain (Cobos *et al.*, 2008; Maurice & Su, 2009; Zamanillo *et al.*, 2013; Nguyen *et al.*, 2017), and addiction to drugs of abuse (Katz *et al.*, 2016; Quadir *et al.*, 2019). In addition, some unrelated indications such as cardioprotection (Bhuiyan & Fukunaga, 2011) or cancer (Aydar *et al.*, 2004; Spruce *et al.*, 2004) have also been suggested.

Relatively little is known about the involvement of Sig-1Rs in SUD. The interest of elucidating the role of Sig-1Rs in the addictive properties of cocaine started in 1988 when Sharkey *et al.* reported that cocaine binds to Sig-1Rs. Although the affinity of cocaine for Sig-1Rs is in the µM range, the authors argued that brain concentrations reached in cocaine consumers would be sufficient to bind Sig-1Rs (Sharkey *et al.*, 1988). Few years after this discovery, first studies reported that Sig-1R antagonists blocked acute cocaine-induced locomotor stimulation (Menkel *et al.*, 1991), as well as sensitized locomotor responses to cocaine (Ujike *et al.*, 1992; Witkin *et al.*, 1993), and the convulsive effects and lethality induced by cocaine (Liu *et al.*, 2007b). The same effects were also attenuated by antisense oligodeoxynucleotides against Sig-1Rs (Matsumoto *et al.*, 2002). In addition to cocaine, methamphetamine binds to both subtypes of sigma receptors (Itzhak, 1993), with a 22-fold preferential affinity for the Sig-1R subtype (Nguyen *et al.*, 2005). Similar to the results obtained with cocaine, Sig-1R antagonists significantly attenuated the locomotor stimulatory

effects of methamphetamine (Nguyen *et al.*, 2005), and methamphetamine-induced behavioral sensitization in rats (Takahashi *et al.*, 2000).

Several groups also reported that cocaine-induced CPP was blocked by different Sig-1R antagonists (Romieu *et al.*, 2000, 2002, 2003; Matsumoto *et al.*, 2011; Xu *et al.*, 2012). In contrast, Sig-1R antagonists failed to block cocaine self-administration across a range of doses of either antagonist (Martin-Fardon *et al.*, 2007) or cocaine (Hiranita *et al.*, 2010, 2011). One possible reason for this discrepancy may be due to differences between species since all the studies that assessed cocaine-induced CPP used mice, whereas the self-administration studies were conducted in rats. Those discrepancies could also be due to the difference of non-contingent administration in a paradigm of CPP *vs.* contingent cocaine self-administration. In a further assessment, moderate effects of a Sig-1R antagonist were reported on the reinstatement induced by cocaine priming after cocaine self-administration in rats (Martin-Fardon *et al.*, 2007).

Interestingly, pretreatment with Sig-1R agonists produced a dose-related potentiation of cocaine self-administration in rats (Hiranita *et al.*, 2010). This leftward shift of cocaine self-administration was similar to the effects of dopamine uptake inhibitors on cocaine self-administration (Schenk, 2002; Barrett *et al.*, 2004). In addition, Sig-1R agonists also potentiated cocaine-induced locomotor stimulant effects and increased the total time of cocaine-evoked convulsions in rats (Matsumoto, 2009). Since Sig-1R agonists enhance the effects of psychostimulants, it was hypothesized that Sig-1R agonists may produce psychoactive effects. However, Sig-1R agonists alone lacked substantive effects on behavioral procedures related to drug abuse, such as locomotor activation (Maj *et al.*, 1996;

Skuza & Rogóz, 2009) or place conditioning (Romieu *et al.*, 2002; Mori *et al.*, 2014). In agreement with these results, self-administration of Sig-1R agonists in naïve animals also failed (Hiranita *et al.*, 2013).

Another possibility to assess the reinforcing properties of a certain drug is a substitution procedure (Johanson & Balster, 1978). In this approach, animals are trained to respond for drugs known to maintain responding, such as cocaine. Once responding is stable, the drug is substituted by the compound of interest. If saline is substituted, responding tends to decline to low self-administration rates. In contrast, when a reinforcing test compound is substituted, responding may be maintained. Using this procedure, Sig-1R agonists established a stable self-administration pattern in cocaine and methamphetamine trained animals, but not in heroin, ketamine or food trained animals (Hiranita *et al.*, 2010, 2013). The authors suggest that the induction of the reinforcing effects of previously inactive Sig-1R agonists may be related to the DAT since cocaine and methamphetamine produce their reinforcing properties by acting on DAT (Hiranita *et al.*, 2013; Katz *et al.*, 2016).

The expression of Sig-1Rs was evaluated after acute or chronic treatment with psychostimulants. mRNA analysis demonstrated a significant increase in Sig-1R mRNA in the NAc but not in the caudate putamen, PFC, or cerebellum after repeated cocaine treatment (Romieu *et al.*, 2002). Following methamphetamine self-administration, Sig-1Rs were upregulated in the midbrain and Sig-1R mRNA was decreased in the frontal cortex and increased in the HPC of animals actively self-administering methamphetamine, but not in the yoked methamphetamine-exposed or saline-control rats (Stefanski *et al.*, 2004). Furthermore, protective doses of Sig-1R antagonists have been shown to prevent changes in gene expression that are induced by cocaine (Matsumoto *et al.*, 2003).

Sig-1R antagonists also inhibit the increase in locomotor activity induced by ethanol (Maurice *et al.*, 2003). In agreement, Sig-1R KO mice demonstrated less sensitivity to the dose-dependent locomotor stimulating effects of alcohol when compared to WT mice (Valenza *et al.*, 2016). However, treatment with a Sig-1R agonist lacked an effect on alcohol-induced locomotion (Maurice *et al.*, 2003). Although alcohol has high reinforcing effects in humans, it is difficult to establish reliable alcohol-drinking patterns in rodents. Therefore, many alcohol-related studies use Scripps Research Institute Sardinian alcohol-preferring rats (Scr:sP), a line that was selectively bred to drink high amounts of alcohol (Colombo *et al.*, 2006). Interestingly, this line has elevated protein levels of Sig-1R in the NAc compared to outbred Wistar rats. This increase returned to baseline after 4 weeks of home-cage alcohol-drinking (Blasio *et al.*, 2015). In agreement with these findings, Sig-1R antagonist diminished alcohol consumption in Scr:sP rats without affecting total fluid intake or food intake (Sabino *et al.*, 2009a; Blasio *et al.*, 2015), however, Sig-1R KO mice displayed higher ethanol intake compared to WT mice (Valenza *et al.*, 2016). Daily systemic treatment with the unspecific Sig-1/2R agonist facilitated binge-like drinking under an operant FR1 schedule and this response was blocked by a Sig-1R antagonist (Sabino *et al.*, 2011). In agreement, alcohol self-administration was decreased by the same antagonist in a dose-dependent manner when given alone (Sabino *et al.*, 2009b), and the breakpoint under an operant PR schedule was increased by Sig-1R agonist and decreased by Sig-1R treatment (Sabino *et al.*, 2009b, 2011). Furthermore, Sig-1R mRNA in the NAc was decreased in ethanol-dependent Wistar rats during acute withdrawal and ethanol naïve Scr:sP rats compared to ethanol naïve Wistar rats (Sabino *et al.*, 2009b).

Sig-1Rs are also involved in alcohol craving and relapse, which are Alcohol often tested using a paradigm of alcohol deprivation. Here, alcohol deprived animals temporary increase the ratio of ethanol/total fluid intake and the voluntary intake of ethanol solutions over baseline drinking conditions when ethanol access is reinstated. Sig-1R antagonist blocked the alcohol deprivation effect in alcohol deprived Scr:sP rats (Sabino *et al.*, 2009a). Furthermore, ethanol-induced CPP could be reinstated with intraventricular injections of a Sig-1R agonist. In agreement, Sig-1R antagonism blocked both alcohol- and Sig-1R agonist-induced reinstatement of place preference (Bhutada *et al.*, 2012).

The implication of Sig-1Rs in nicotine addiction is almost unknown. It was demonstrated that nicotine- and nicotinic agonist-induced catecholamine release and Ca^{2+} entry was decreased by Sig-1R ligands in adrenal chromaffin cells (Paul *et al.*, 1993; Brindley *et al.*, 2017). To our knowledge, the involvement of Sig-1Rs in the reinforcing properties of nicotine was tested in only one study (Horan *et al.*, 2001). Interestingly, the authors demonstrated that the Sig-1R agonist SA 4503 decreased nicotine-induced CPP. However, a different study showed that the acquisition of place preference induced by morphine, cocaine, and methamphetamine was attenuated using the same Sig-1R agonist whereas (+)-pentazocine, a selective Sig-1R agonist, was inactive (Mori *et al.*, 2012). Thus, more studies are needed to verify whether the effect SA 4503 was mediated by Sig-1Rs.

Objectives

Objective 1

1. To evaluate the implication of *pre*-proenkephalin in the reinforcing properties and the motivation for nicotine, as well as its implication in the cue-induced reinstatement of nicotine-seeking.
2. To study the participation of *pre*-proenkephalin in nicotine-induced neuroplasticity.
3. To elucidate the involvement of pathway-specific glutamate transmission to the NAc core in the reinforcing properties of nicotine.

Objective 2

1. To evaluate the phenotypical differences associated with the genetic deletion of the sigma-1 receptor.
2. To study the involvement of the sigma-1R in the reinforcing properties and the motivation for nicotine, as well as its implication in the cue-induced reinstatement of nicotine-seeking.
3. To investigate the implication of the sigma-1R in the reinforcing properties and the motivation for palatable food, as well as its implication in the cue-induced reinstatement of palatable food-seeking.

Material and methods

Animals

In a first study, we used homozygous KO mice deficient in PENK on a C57BL/6J background and their respective WT littermates (König *et al.*, 1996). In a second study, C57BL/6J WT mice (Jackson Laboratories) and C57BL/6J constitutive Sig-1R KO mice (Langa *et al.*, 2003), provided by HARLAN laboratories, were used.

In both studies, mice were 8-12 weeks old at the beginning of the experiments and of male sex. Individuals were housed individually in a temperature- (21 ± 1 °C) and humidity-controlled (55 ± 10%) room. All experiments were conducted during the dark phase of a 12-h light/dark reverse cycle (light off at 08:00 a.m., light on at 8:00 p.m.). Food and water were available ad libitum during the whole experiment. Mice were allowed to acclimate to the vivarium (minimum 1 week) before starting experimental procedures. Animal procedures were conducted in strict accordance with the guidelines of the European Communities Directive 2010/63/EU regulating animal research and were approved by the local ethical committee (CEEA-PRBB).

Drugs

All solutions were diluted with or dissolved in sterile 0.9% physiological saline when not indicated differently.

(-)-Nicotine hydrogen tartrate salt (Glentham Life Sciences) was dissolved and the pH was adjusted with NaOH to 7.4. For anesthesia, ketamine hydrochloride (100 mg/ml) (Imalgène; Merial Laboratorios S.A.) and medetomidine hydrochloride (1 mg/ml) (Domtor; Esteve, Spain) stock solutions were mixed and diluted to a final concentration of 10mg/ml and

0.2mg/ml, respectively. The anesthetic mixture was administered intraperitoneally (i.p.) (10ml/kg). Atipamezole hydrochloride (5mg/ml) (Revertor; Virbac, Spain) and meloxicam (5mg/ml) (Metacam; BoehringerIngelheim, Rhein) were diluted and administered subcutaneously (s.c.) at doses of 2.5 mg/kg and 2mg/kg, respectively. Gentamicin (40mg/ml) (Genta-Gobens; LaboratoriosNormon, Spain) was diluted and administered i.p. at 1mg/kg as an antibiotic solution. Thiopental sodium (Braun Medical S.A, Barcelona, Spain) was dissolved in distilled water and delivered by intravenous (i.v.) infusion of 0.05 ml through the catheter. Clozapine-N-oxide (CNO) (Palex medical, Barcelona, Spain) was dissolved in sterile 0.9% physiological saline and administered i.v. at a dose of 1mg/kg. The Sig-1R antagonist 1-[2-(3,4-Dichlorophenyl)ethyl]-4-methylpiperazine dihydrochloride (BD 1063) (Laboratories Esteve, Barcelona, Spain) was dissolved in hydroxypropyl methylcellulose and administered s.c. at a dose of 10mg/kg (correction factor: 1.27).

Surgery

Study 1

Intravenous catheter insertion

For catheter surgery, mice were anesthetized with a ketamine/medetomidine mixture and implanted with indwelling i.v. silastic catheters as previously described (Soria *et al.*, 2008). Briefly, a 6 cm length of silastic tubing (0.3 mm inner diameter, 0.6 mm outer diameter) was fitted to a 22-gauge steel cannula that was bent at a right angle and then embedded in a cement disk with an underlying nylon mesh. The catheter tubing was inserted 1.3 cm into the right jugular vein and

anchored with suture. The remaining tubing ran subcutaneously to the cannula, which exited at the midscapular region. All incisions were sutured and coated with antibiotic ointment. Animals were allowed to rest for 4 days prior to self-administration procedures.

Virus vector microinjection

Mice were anesthetized with a ketamine/medetomidine mixture and placed into a stereotaxic apparatus (KOPF instruments). Coordinates to target the PLC, NAc core and the BLA were chosen according to Paxinos and Franklin. (PLC) AP +1.98 mm, ML ±0.3 mm, DV -2.3 mm; (NAc core) AP +1.34 mm, ML ±1 mm, DV -4.6 mm, (BLA) AP -1.34, ML± 2.9, DV -4.8.

For injections in the PLC and NAc core, a bilateral injection cannula (33-gauge internal cannula, Plastics One, UK), and a single injection cannula for the BLA were used. In both cases, cannulas were connected to a polyethylene tubing (PE-20, Plastics One, UK) that was attached to a 10 µl microsyringe (Model 1701 N SYR, Cemented NDL, 26 ga, 2 in, pointstyle 3, Hamilton company, NV).

Specific inhibition of projection sites from the PLC to the NAc core and BLA to NAc core were achieved by bilateral injections of the AAV-hM4Di-DREADD into the PLC (under control of the hSyn promoter) or BLA (under control of the CaMKIIα promoter) and an injection of the AAV-retrograde-Cre into the NAc core.(under control of pmSyn1 promoter) Each hemisphere was injected with 0.2 µl (PLC) and 0.4 µl (NAc core and BLA) at a constant rate of 0.05 µl/min (PLC) or 0.1 µl/min (NAc core and BLA) by using a microinfusion pump (Harvard Apparatus, Holliston, MA) over 4 min followed by an additional 10 minutes to allow diffusion of viral particles away from the injection site and to prevent reflux. Injection needles were

slowly withdrawn during 10 additional min. The successful injection was monitored by the displacement of an air bubble along with the tubing.

Viral vectors

We used the following vectors: AAV-retrograde-Cre (AAV pmSyn1-EBFP-Cre; 6×10^{12} vg/mL) (Addgene (viral prep # 51507-AAVrg)) for the NAc core. AAV-hM4Di-DREADD (AAV8-hSyn-DIO-hM4D(Gi)-mCherry, 1.21E+13 gc/ml) for PLC, (AAV8-CamKII-DIO-hM4D(Gi)-mCherry , 8,6E+12) for BLA and AAV-control-DREADD (AAV8-hSyn-DIO-mCherry, 1.19E+13 gc/ml) for both areas (Viral Vector Production Unit of Universitat Autònoma de Barcelona).

Study 2

Intravenous catheter insertion

Surgery was implemented as described in study 1.

Experimental procedures

Study 1

Experiment 1

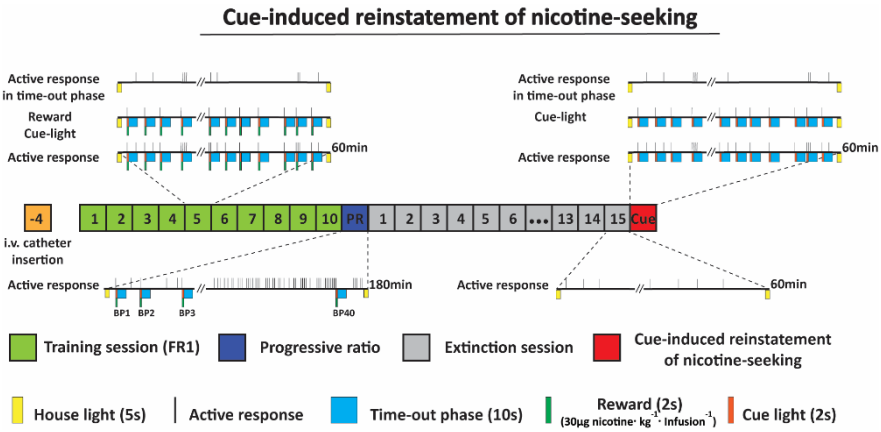

Figure 40. Experimental procedure of experiment 1.
Relapse model of nicotine-seeking

Cue-induced reinstatement of nicotine-seeking

Nicotine's reinforcing properties, the motivation for nicotine, and cue-induced reinstatement of nicotine-seeking were evaluated in PENK KO mice and WT littermates in an operant model of cue-induced reinstatement validated in our laboratory.

After recovery from indwelling catheter insertion. PENK KO mice and their WT littermates were first trained to self-administer nicotine (30µg/kg/Inf (free base)) during 10 daily sessions under an FR1 schedule of reinforcement. The maximum session duration was 1h or whenever mice reached the maximum amount of reinforcements (50). A reward was obtained by nose-poking the active hole. The i.v. drug infusion was paired

with the presentation of a cue-light (2 sec.) above the active nose-poke and followed by a 10 sec. time-out period where responses had no consequences but were recorded. Acquisition criteria for operant responding were fulfilled when mice earned at least 5 reinforcements in three consecutive sessions with less than 30% deviation from the average number of infusions, and a discrimination index ((active responses – inactive responses) / (active responses + inactive responses)) between nose-pokes higher than 0.6. After 10 sessions under an FR schedule, we tested the motivation for nicotine in a PR schedule following an exponential equation. (Series: 1-2-3-5-12-18-27-40-60-90-135-200-300-450-675-1000). The maximum length of a PR session was 3h or whenever a mouse did not respond on the active hole during 1h. Thiopental test was applied subsequently and mice that did not show prominent signs of anesthesia directly after i.v. infusion were excluded from the experiment.

Experiment 2

Nicotine-induced structural plasticity

Nicotine-induced structural plasticity changes in dendritic spine density and morphology were evaluated. We used a yoked control procedure to better assess whether the obtained changes in structural plasticity derive from motivated behavior to obtain nicotine or from the drug alone.

Yoked control procedure

A new cohort of PENK KO mice and their WT littermates were divided into three groups: (1) Master Nicotine, (2) Yoked Nicotine and (3) Yoked Saline. PENK KO mice and WT littermates of the Master Nicotine group were trained to acquire and maintain nicotine self-administration, as described above, for 12 consecutive days, followed by a PR session. Animals in the Yoked groups were exposed to the operant conditioning chamber, whereby nose-poking had no programmed consequences but was recorded. However, mice received non-contingent nicotine or saline infusions (Yoked Nicotine or Yoked Saline, respectively) whenever their corresponding experimental subject (Master Nicotine group) actively obtained a contingent nicotine infusion.

Ballistic labeling with the fluorescent dye DiI

Immediately after the PR schedule of nicotine self-administration on day 13, mice were deeply anesthetized with a ketamine/medetomidine mixture. Animals were rapidly perfused intracardially with 4% paraformaldehyde (PFA) in a Na2HPO4/ NaH_2PO_4/NaCl buffer (pH 7.4) (PBS), using a peristaltic pump delivering at 20 ml/min. Initially, 20 ml of 0.1 M PBS were perfused followed by 40 ml of 4% PFA. Brains were quickly removed from the skull and postfixed in PFA 4% for 10 minutes and stored in PBS 0.1 M at 4ºC overnight.

Brain coronal sections (100 µm) containing the NAc (from bregma 1.54 mm to bregma 1.10 mm) were obtained by using a vibratome (Leica SM 2000R, Nussloch, Germany) and stored in a cryoprotectant solution (34.4% glycerol (85%), 30% ethylene glycol, 20% PB 0.5M and 15.6%distilled water) at -20ºC until processed for fluorescent labeling.

Brain samples were washed three times for 15 min in PBS 0.1M to remove all possible remains of the cryoprotectant solution and labeled by ballistic

delivery of the fluorescent dye DiI (Biotium, Fremont, CA, USA) using a gene gun apparatus (Helios Gene Gun System, Bio-Rad, Munich, Germany). Once labeled with the DiI fluorophore, tissues were kept in PBS 0.1M at 4ºC overnight to facilitate diffusion of the dye and then post-fixed with 4% PFA for 2 hours at 4ºC to further preserve the structures.

Sections were placed on microscope gelatin-coated slides and coverslipped with mounting medium (Mowiol, Sigma Aldrich, Germany) for the following confocal analysis.

Dendritic spine analysis

Images were acquired with a confocal microscope (Leica TCS SP5 II, Leica Microsystems, Wetzlar, Germany) using an immersion lens (63x). Individual MSNs of the NAc core and shell were chosen for spine analysis based on the following criteria previously described by Lee *et al.* (Lee *et al.*, 2006). (1) There was minimal or no overlap between labeled cells to correctly differentiate dendrites of each neuron, (2) cells used for analysis must have at least three visible primary dendrites, and (3) only distal dendrites (from secondary dendrites to terminal dendrites) with a minimum length of 25µm were examined. 8 to 10 dendrites were analyzed for each animal per area of interest.

Pictures were obtained at different z levels (0.13µm depth intervals) of dendrites from the core and shell of the NAc. The images taken were then deconvoluted with Huygens Essential software (Scientific Volume Imaging, B.V, Hilversum, Netherlands) to improve the resolution and diminish noise.

Measurements of dendrites and dendritic spines were made using NeuronStudio analysis software (Computational Neurobiology and Imaging Center, New York, USA). Protrusions from dendrites were semi-

automatically classified into five types based on their morphology (Figure 41): Class 1, also called stubby protuberances, lacked a large spine head and did not appear to have a neck (ratio length/width < 2.5 and spines which did not overcome 0.5 µm in length). Class 2, or mushroom-shaped spines, were characterized by a short neck and a large head (length between 0.5 and 2 µm; ratio head/neck bigger than 1.1; head diameter bigger than 35 µm); Class 3, or thin spines, had elongated spine necks with small heads (length between 0.5 and 3 µm; ratio head/neck bigger than 1.1; head diameter minor to 35µm). Class 4, or filopodia extensions, lacked a spine head and had a large neck (length between 0.5 and 3.5µm; ratio length/width > 2.5); and class 5, or branched spine, had elongated spine necks with two or more spine heads (detected manually).

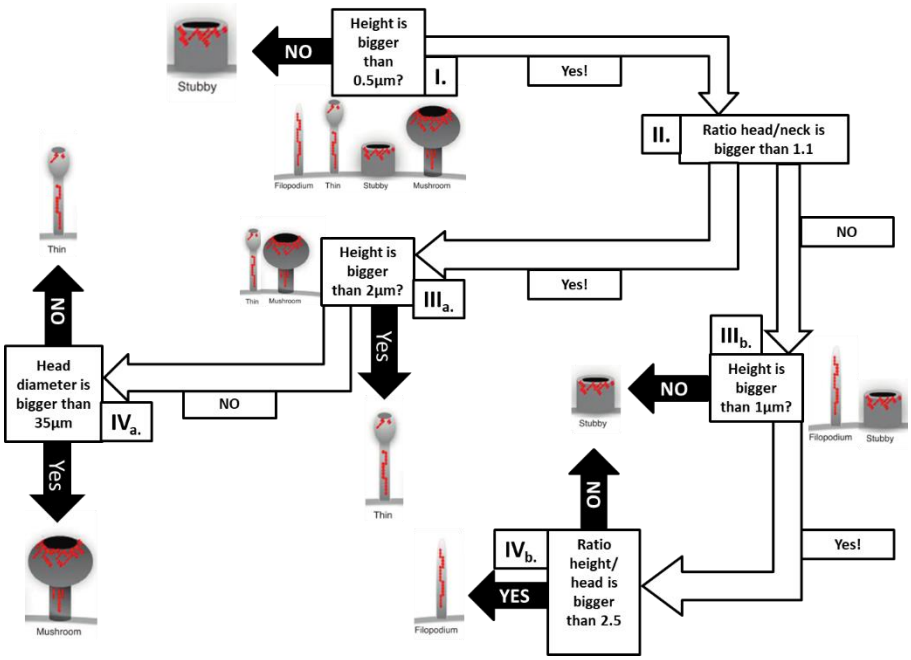

Figure 41. Algorithm for semi-automatic spine classification.

Experiment 3

Pathway-specific chemogenetic inhibition of glutamatergic projections to the nucleus accumbens core during nicotine self-administration

To inhibit pathway-specific glutamatergic transmission in the NAc core, WT mice were injected with the retrograde AAVr pmSyn1-EBFP-Cre into the NAc core, and the CRE-dependent AAV8-hSyn-DIO-hM4D(Gi)-mCherry or the AAV8-CamKII-DIO-hM4D(Gi)-mCherry into the PLC or BLA, respectively (see Virus vector microinjection). Hence, only glutamatergic neurons that project to the NAc core expressed the G_i-coupled designer receptor exclusively activated by designer drugs (DREADD) in the PLC or BLA.

WT animals expressing G_i-coupled DREADDs or control DREAADs were trained to acquire and maintain nicotine self-administration for 12 consecutive days under an FR1 schedule of reinforcement, followed by a test of motivation for nicotine under a PR schedule. PLC-NAc core and BLA-NAc core pathways were inhibited by DREADD activation *via* i.v. injections of clozapine N-oxide (CNO) (1mg/kg, i.v.) or saline immediately before each training session.

Histological studies to determine virus expression sites

Coronal brain sections were obtained as previously described (see Ballistic labeling with the fluorescent dye DiI). Briefly, immediately after the PR session on day 13, mice were deeply anesthetized with a ketamine/medetomidine mixture and rapidly perfused intracardially with 4% PFA. Brains were quickly removed from the skull and postfixed in PFA 4% for 10 minutes and stored in PBS 0.1 M at 4ºC overnight. Brain coronal sections (100 µm) containing the PLC (from bregma 2.34mm to bregma 1.54mm), NAc (from bregma 1.54 mm to bregma 1.10 mm)and BLA (from bregma -0.7 mm to bregma -1.82 mm) were obtained by using a vibratome and stored in a cryoprotectant solution at -20ºC until processed for fluorescent labeling.

Expression of AAV8-hSyn-DIO-hM4D(Gi)-mCherry and AAV8-CamKII-DIO-hM4D(Gi)-mCherry were visualized directly in the confocal microscope. mCherry is a bright red monomeric fluorescent protein that was clearly visualized in our experimental conditions without performing an immunofluorescence.

Cre-recombinase expression was detected by immunofluorescence using an anti-Cre recombinase antibody (1:500, Merck). Brain samples were washed three times for 15 min in PBS 0.1M to remove all possible remains

of the cryoprotectant solution. Sections were incubated with the primary antibody in 3% normal donkey serum and 0.3% Triton X-100 in 0.1 M PB (NDS-T-PB) overnight at 4°C. Next day, sections were incubated with the secondary antibody (1:1000, Invitrogen, A21202) at room temperature in NDS-T-PB for 2h. After incubation, sections were rinsed and mounted onto glass slides coated with gelatin in DAPI containing mounting medium.
The stained sections of the brain were analyzed at 10× objective using a Leica TCS SPE inverted confocal microscope. ImageJ software was used for visualization of virus expression sites. The threshold was adjusted to distinguish the particles from the background.

Study 2

Experiment 1

Phenotypical characterization of Sig-1R KO mice

Locomotion

Locomotor activity was assessed by using actimetry boxes (9 × 20 × 11 cm) (Imetronic, Lyon France) in a low luminosity room (5 lux), and with white noise. Each box contained two lines of photocells located 2 cm and 6 cm above the floor to measure horizontal and vertical movements, respectively. Mice were injected with either BD 1063 (10mg/kg) or saline 1h prior to the test. Subjects were then individually placed in the boxes and their activity was evaluated for 2h.

Anxiety-like behavior

Elevated plus maze test was performed using a black Plexiglas apparatus with 2 open (45 lux) and 2 closed (5 lux) arms (both 29 cm long x 5 cm

wide), set in cross from a neutral central square (5x5 cm) that was elevated 40 cm above the floor. The number of entries and the percentage of time spent in the open arms was determined for 5 min, as previously reported (Busquets-Garcia *et al.*, 2011).

The light/dark box was carried out as previously described (Filliol *et al.*, 2000). A Plexiglas box comprising a small dark compartment (10 lux) and a large lit compartment (500 lux) separated by a connecting 4 cm long tunnel was used. Floor lines separated the light compartment into three equal zones, from the tunnel to the opposite wall, designated as proximal, median and distal zones. The time spent in the lit compartment, as well as total and distal entries to the lit compartment, were registered for 5 min.

Novel object recognition test

The novel object recognition test was performed as previously described (Puighermanal *et al.*, 2009). Briefly, the test was performed in a V-shaped maze for two consecutive days. On day one, mice were habituated for 9 min to the maze in which the task was performed. On the second day, 2 identical objects (chess pieces) were presented to the mice, and the time spent exploring each object was recorded. After three hours mice were placed in the maze again for 9 min, one of the familiar objects was replaced with a novel object and the total time spent exploring each of the two objects (novel and familiar) was computed. Exploration time was counted when the orientation of the mice's nose pointed to the object at a distance of less than 2 cm. A discrimination index was calculated as the difference between the times spent exploring the novel (O_n)and familiar object (O_f) divided by the total time exploring the two objects ((O_n - O_f) / (O_n + O_f)). A higher discrimination index is considered to reflect greater memory retention for the familiar object.

Sensation-seeking

WT and Sig-1R KO mice were trained similarly to the acquisition protocol used in the drug and food self-administration paradigm. Responding on the active manipulandum resulted in the presentation of the cue-light (2 sec.) above the active nose-poke. Neither extinction training nor the reinstatement of seeking behavior was performed in this cohort of mice.

Experiment 2

Reinstatement of cue-induced nicotine-seeking behavior

WT and Sig-1R knockout mice were first trained to self-administer either nicotine (30µg/kg/Inf (free base)) or saline during 10 daily sessions (5 days of FR1, followed by 5 days of FR3). The maximum session duration was 2h or whenever mice reached the maximum amount of reinforcements (50). A reward was obtained by nose-poking the active hole. The i.v. drug/saline infusion was paired with the presentation of a cue-light (2 sec.) above the active nose-poke and followed by a 10 sec. time-out period where responses had no consequences but were recorded. Acquisition criteria for operant responding were fulfilled when mice earned at least 10 reinforcements in three consecutive sessions with less than 30% deviation from the average number of infusions, and a discrimination index ((active responses – inactive responses) / (active responses + inactive responses)) between nose-pokes higher than 0.8. After 10 sessions under an FR schedule, we tested the motivation for either nicotine or saline in a PR schedule following an exponential equation. (Series: 1-2-3-5-12-18-27-40-60-90-135-200-300-450-675-1000). Mice were injected with either the selective the Sig-1R antagonist BD 1063 (10mg/kg s.c., free base) or saline 1h prior to the test. The maximum length of a PR session was 4h

or whenever a mouse did not respond on the active hole during 1h. Thiopental test was applied subsequently and only mice that showed patency of catheter, and accomplished acquisition criteria (only nicotine groups) were moved to the extinction phase. The first extinction session occurred 48h after the thiopental test to avoid any possible influence of thiopental residual effects. During the extinction phase, experimental conditions were similar to acquisition sessions except that neither nicotine/saline nor the drug-associated cue (cue-light) was available after active responding. Mice had to reduce active responding to a 30% (average of 3 consecutive days) compared to the average of the 3 last acquisition sessions. Mice were given 2h daily extinction sessions during at least 10 consecutive days or until extinction criterion was achieved. After extinction, seeking behavior was reinstated by environmental cues. Cue-induced reinstatement was conducted under the same conditions used in the acquisition phase except that nicotine/saline was not delivered. Three responses on the active manipulandum in this phase led to the presentation of the cue-light for 2s. The reinstatement criterion was achieved when responding in the active NP was tripled compared to extinction responding.

Sample collection

Mice were sacrificed by cervical dislocation directly after cue-induced reinstatement sessions. Brain areas, including the mPFC and the NAc, were quickly dissected and snap-frozen at -80ºC. The brain tissue was further processed for immunoblot and qPCR analysis.

Immunoblot

Frozen tissues were minced and biotinylated as previously described (Ferrario *et al.*, 2011). Briefly, brain samples were added to an ice-cold aCSF with 1 mM of the biotin derivative sulfo-NHS-SS-biotin (Thermo Scientific, Rockford, IL), a cleavable and water-soluble biotinylation reagent specific for primary amino groups. Brain samples were incubated at 4°C with gentle agitation for 30 min. The reaction was quenched by adding glycine (100 mM). After 10min of incubation at 4ºC, the suspension was centrifuged at 14000 rpm at 4 ºC for 2 min. The supernatant was removed, the remaining pellet was re-suspended in lysis buffer (25 mM HEPES pH 7.4, 500 mM NaCl, 2 mM EDTA, 20 mM NaF, ,1 mM PMSF, 0.1% Nonidet (v/v), 1µg/ml aprotinin, 1 µg/ml leupeptin, 1µg/ml pepstatin), and sonicated. Protein contents in the supernatants were determined by DC-micro plate assay (Bio-Rad, Madrid, Spain) following the manufacturer's instructions. The biotinylated proteins were recovered by adding 100µg of the protein content of each sample to 37.5µl of high capacity NeutrAvidin Agarose beads (Thermo Scientific). The suspension was incubated overnight at 4ºC on an end-over-end rotator. Bound proteins were isolated from the non-biotinylated (unbound) fraction by centrifugation (3000 rpm, 1 min) and rinsed several times in ice-cold lysis buffer. The biotinylated fraction was then dissolved in 2X Laemmli sample buffer (Bio-Rad) containing β-mercaptoethanol (355mM) and was heated up to 97ºC for 3 min to break the avidin-biotin bond and release the biotinylated proteins from the beads. Samples were centrifuged (10000 rpm, 5 min), hence unbound biotinylated proteins were separated by a centrifugal filter unit (0.45mm, #UFC30HV00, Millipore, Billerica, MA) to remove the beads. Blots containing equal amounts of protein samples (membrane enriched or total protein content) were probed for different primary

antibodies: anti-NR1 (1:2000, Novus Biologicals, NB300-118), anti-phospho-NR1(Ser890) (1:500, Cell signaling, 3381), phospho-NR1(Ser896) (1:500,Abcam, Ab75680), phospho-NR1(Ser897) (1:1000, MERCK, ABN99), anti-NR2A (1:2000, Merck Millipore, AB1557B), anti-NR2B (Merck Millipore, AB1557P, 1:1000), anti-GluR1 (1:2000, Abcam, Ab31232), anti-GluR2 (1:2000, Sigma-Aldrich, Sab4300232), anti-mGluR2/3, (1:1000, Millipore, 06-676), anti-MOR (1:500, Santa-Cruz, sc-15310), anti-LynX1(1:5000, LS Bio, LS-C145872), anti-phosphor-ERK1/2 (1:500, Cell signaling, 9101), anti-ERK1/2 (1:2000, Cell signaling, 9102), anti-phosphor-CREB (1:1000, Millipore, 06519), anti-NFκB p50/p105 (1:2000, Abcam, ab32360), anti-ΔFosB (1:1000, Abcam, ab11959), anti-n-Cadherin (1:10000, Abcam, ab18203), anti-Actin (1:5000, Santa Cruz, sc-47778), and anti-GAPDH (Santa Cruz, sc-32233; 1:10000). Antibodies against the nAChR α4 and β2 subunits were obtained from the Gotti laboratory (Instituto di neuroscienze, Milan). Bound primary antibodies were detected using horseradish peroxidase-conjugated antibodies to rabbit or mouse antibodies (Cell signaling, 7074; 1:2000 or Santa Cruz Technologies, sc-2005; 1:2000, respectively) and visualized by enhanced chemiluminescence detection (Clarity Western ECL Substrate, Bio-Rad, 1705061). When necessary, Immobilon-P membranes (Millipore, IPVH09120) were stripped in buffer containing 62.5mM Tris pH 6.5, 2% SDS (vol/vol) and 0.1M beta-mercaptoethanol (vol/vol) for 30 min at 37ºC, followed by extensive washing in 100mM NaCl, 10mM Tris and 0.1% Tween 20 (pH 7.4) before re-blocking and re-probing. The optical density of the relevant immunoreactive bands was quantified after acquisition on a ChemiDoc MP Imaging System (Bio-Rad) controlled by Image Lab Touch Software (Bio-Rad). For quantitative purposes, the optical density values for phosphorylated proteins were normalized to the total protein content

(phosphorylated + unphosphorylated) of the same sample, and GAPDH and Actin were used as housekeeping controls. Data were expressed as a fold change of the control WT saline-vehicle group.

Gene expression analysis by real-time PCR

Total RNA was isolated from frozen (-80ºC) mPFC and NAc with TRIzol reagent plus RNA purification kit (Ambion, AM1924) and subsequently retrotranscribed to cDNA with the High-capacity cDNA reverse transcription kit (Applied Biosystems, 4368814). Gene expression of Sig-1R and "Mm00441480_m1" for GluT1 by real-time PCR. Quantitative analysis of gene expression was measured with TaqMan Gene Expression assays "Mm01223547_g1" for Sig-1R and (Applied Biosystems, Madrid, Spain) as a double-stranded DNA-specific fluorescent dye and performed on the ABI Prism 7900 HT (Applied Biosystems, Waltham, United States). HPRT was used as a housekeeping gene, detected with TaqMan gene expression assay "Mm00446968_m1". Data for each target gene were normalized to HPRT, and the fold change in target gene mRNA abundance was determined by the $2^{(-\Delta\Delta Ct)}$ method (Livak & Schmittgen, 2001).

Experiment 3

Reinstatement of cue-induced food-seeking behavior

Cue-induced reinstatement of palatable food (TestDiet, Richmond, IN, USA) was conducted in similar conditions as described for the cue-induced reinstatement of nicotine-seeking behavior with the difference that the reward obtained was a 20 mg highly palatable isocaloric chocolate-flavored pellet paired with a 2 sec. light-stimulus above the active nose-poke. These pellets had a similar caloric value (3.44 kcal/g: 20.6% protein, 12.7% fat, 66.7% carbohydrate) of standard maintenance diet provided to

mice in their home cage (3.52 kcal/g: 17.5% protein, 7.5% fat, 75% carbohydrate) with some slight differences in their composition: addition of chocolate flavor (2% pure unsweetened cocoa) and modification in the sucrose content.

Statistical analysis

Study 1

All data are presented as mean ± SEM. Statistical analyses were performed using the Statistica 6.0 software (StatSoft, Tulsa OK, USA). Behavioral studies and dendritic spine analysis were analyzed using one-, two- or three-way ANOVA followed by Newman-Keuls post hoc analysis.

Study 2

Behavioral data was expressed and analyzed as described in Study 1. The proteomic and mRNA analysis were performed using two-way ANOVA followed by Fischer's LSD post hoc analysis.

Results

Study 1

Effect of genetic deletion of *pre-proenkephalin* on acquisition and maintenance of nicotine self-administration

In a first approach, we used an operant model of cue-induced reinstatement to evaluate the implication of PENK in the reinforcing properties and the motivation for nicotine, as well as in the cue-induced reinstatement of nicotine-seeking.

PENK KO mice and WT littermates were trained to self-administer nicotine in 10 consecutive 1h training sessions under an FR1 schedule of reinforcement. Three-way ANOVA repeated measures demonstrated a significant main effect of genotype [$F_{(1,72)}$ = 45.50; $p<0.001$], nose-poke [$F_{(1,72)}$ = 97.62; $p<0.001$], and of day [$F_{(9,648)}$ = 19.90; $p<0.001$]. Significant interactions were revealed between genotype and nose-poke [$F_{(1,72)}$ = 23.86; $p<0.001$], genotype and day [$F_{(9,648)}$ = 2.43; $p<0.05$], nose-poke and day [$F_{(9,648)}$ = 17.53; $p<0.001$], and among all three factors [$F_{(9,648)}$ = 4.18; $p<0.001$]. Subsequent Newman-Keuls *post hoc* analysis revealed that active responding was significantly decreased in PENK KO mice compared to WT littermates on day 9 ($p<0.01$) and day 10 ($p<0.05$). No differences were obtained on the inactive manipulandum (Figure 42A). One-way ANOVA revealed a significant effect of genotype on the area under the curve of active responses [$F_{(1,72)}$ = 36.03; $p<0.001$]. Subsequent *post-hoc* analysis (Newman-Keuls) demonstrated a significant decrease of active responses in PENK KO mice compared to WT littermates ($p<0.001$) (Figure 42B).

The motivation for nicotine was evaluated under a PR schedule of reinforcement, one-way ANOVA revealed a significant effect of genotype [$F_{(1,72)}$ = 12,54; $p<0.001$]. *Post-hoc* analysis (Newman-Keuls) showed a

significantly decreased breakpoint in PENK KO mice compared to WT littermates ($p<0.001$) (Figure 42C).

The percentage of mice that fulfilled acquisition criteria was strikingly decreased in PENK KO mice compared to WT littermates [$\chi^2= 22.18$; $p<0.001$] (Figure 42D).

Only mice that fulfilled acquisition criteria were moved to extinction training. In the extinction phase, PENK KO and WT mice were trained to decrease nose-poking on the active manipulandum to a 30% according to their average responding in the last three days of the acquisition phase. Three-way ANOVA repeated measures revealed significant main effects of nose-poke [$F_{1,33} = 51.98$; $p<0.001$] and day [$F_{9,297} = 8.37$; $p<0.001$] but not of genotype [$F_{1,33} =0.51$; n.s.]. A significant interaction between day and nose-poke [$F_{9,297} = 7.3$; $p<0.001$] but not between day and genotype [$F_{9,297} = 0.2$; n.s.] or nose-poke and genotype [$F_{1,33} = 0.41$; n.s.], neither among all three factors was revealed [$F_{9,297} = 0.71$; n.s.] (Figure 42E). All KO and 86% of WT mice extinguished operant behavior [$\chi^2= 0.93$; n.s.].

Cue-induced reinstatement of nicotine-seeking was tested after a minimum of 15 daily extinction session or whenever the extinction criterion was reached. Nicotine-seeking behavior was not modified in PENK KO mice (Two-way ANOVA repeated measures, nose-poke: [$F_{1,29} = 66.54$; $p<0.001$]; genotype: [$F_{1,29} = 0.85$; n.s.]; interaction: [$F_{1,29} = 0.54$; n.s.]) (Figure 42F).

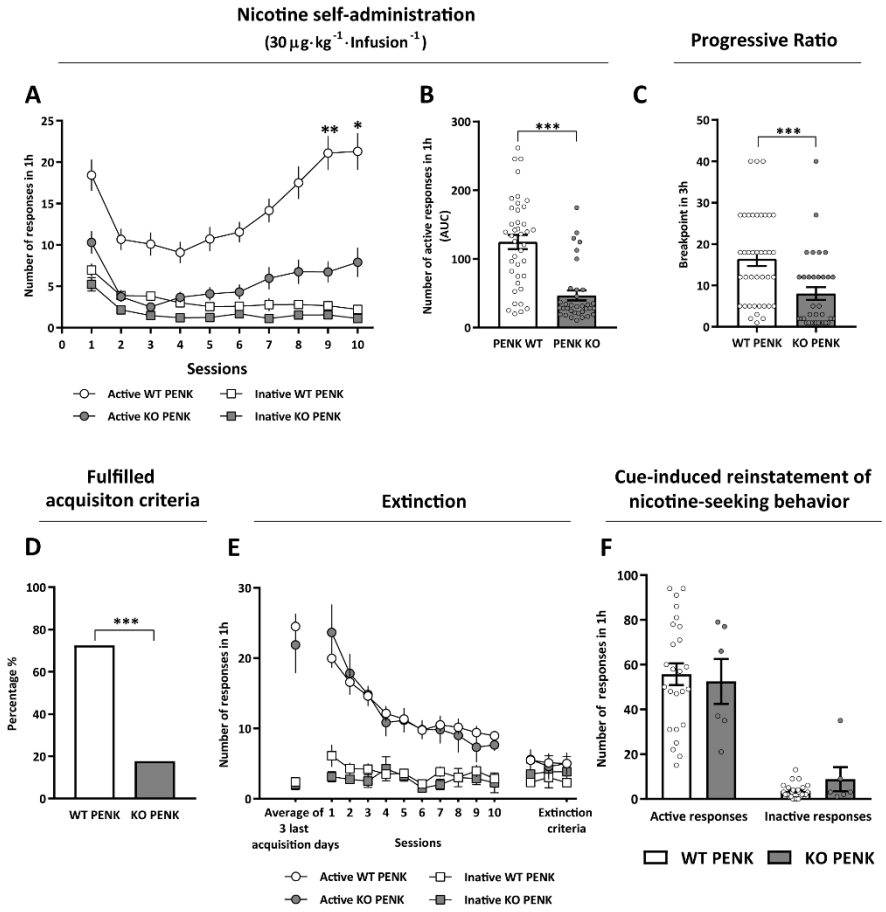

Figure 42. Effect of genetic deletion of PENK on cue-induced reinstatement of nicotine-seeking behavior.

A: Time course of nicotine self-administration of PENK KO (n=34) and WT littermates (n=40). **B:** Area under the curve of active responding for nicotine. **C:** Test for motivation for nicotine under a progressive ratio schedule. **D:** Percentage of mice that fulfilled all three acquisition criteria after 10 days of operant self-administration maintained by nicotine. **E:** Time course of active and inactive responding of PENK KO (n=6) and WT littermates (n= 29) extinguishing operant behavior after nicotine self-administration. **F:** Cue-induced reinstatement of nicotine-seeking behavior after extinction of operant behavior in PENK KO (n=6) and WT littermates (n= 25). Data are expressed as mean ±SEM. *p<0.05, **p<0.01, ***p<0.001. **Abbreviations:** Knockout (KO), nicotine (NIC), *pre*-proenkephalin (PENK), wild type (WT)

Effect of genetic deletion of *pre-proenkephalin* on nicotine-induced neuroplasticity

After the observation that the lack of PENK strikingly decreased nicotine self-administration. We evaluated the changes in neuroplasticity of MSNs in the NAc core and shell after nicotine self-administration in PENK KO and WT littermates. We used a yoked control procedure to evaluate whether the changes in dendritic spine density and spine morphology are induced by contingent or non-contingent nicotine administration. Therefore, animals of each genotype were divided into three groups according to their contingency. Contingent nicotine administration: Master Nicotine; Non-contingent administration: Yoked Nicotine and Yoked Saline.

Yoked control procedure of nicotine self-administration

PENK KO mice and WT littermates of the Master Nicotine group were trained to self-administer nicotine in 12 consecutive 1h training sessions under an FR1 schedule of reinforcement. Yoked Nicotine and Yoked saline groups received the same amount of either nicotine or saline at the same time according to the Master nicotine group.

Two-way ANOVA revealed a significant effect of genotype [$F_{1.39}$ =4.26; $p<0.05$] and group [$F_{2,39}$ =20.09; $p<0.001$], as well as a significant interaction between both factors [$F_{2,39}$ =9.83; $p<0.001$]. Subsequent *post-hoc* analysis (Newman-Keuls) revealed a significantly increased response rate of WT Master Nicotine mice compared to all groups ($p<0.001$) (Figure 43A).

The motivation for nicotine was evaluated as previously described. One-way ANOVA revealed a significant effect of genotype [$F_{1.13}$ =10.07; $p<0.01$], and *post-hoc* analysis revealed a significantly decreased breakpoint in KO

Master Nicotine mice compared to the WT Master Nicotine group (p<0.01) (Figure 43B).

The percentage of animals that fulfilled acquisition criteria was significantly decreased in mice of the KO Master Nicotine group compared to the WT Master Nicotine group [χ^2= 7.27; p<0.01] (Figure 43C).

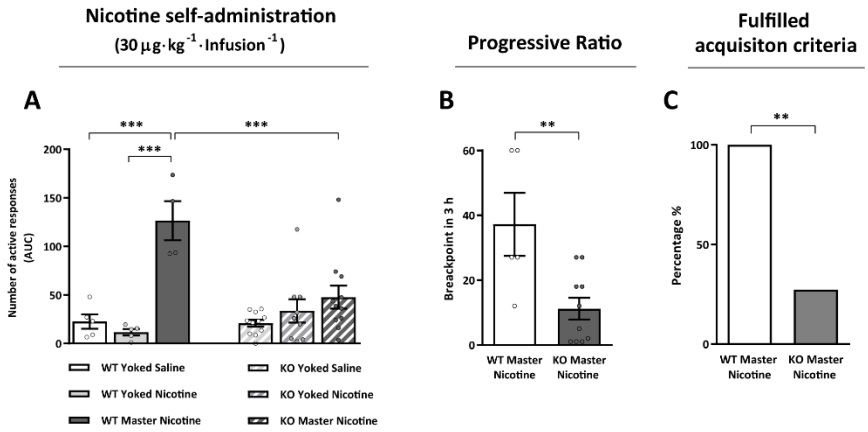

Figure 43. Effect of genetic deletion of PENK on the reinforcing properties and motivation for nicotine.

A: Area under the curve of active responses of WT Master Nicotine (n=5), WT Yoked Nicotine (n=5), WT Yoked Saline (n=5), KO Master Nicotine (n=11), KO Master Yoked (n=9) and KO Yoked Saline (n=11). **B:** Test for motivation for nicotine under a progressive ratio schedule. **C:** Percentage of mice that fulfilled all three acquisition criteria after 12 days of operant self-administration maintained by nicotine. Data are expressed as mean ±SEM. *p<0.05, **p<0.01, ***p<0.001. **Abbreviations:** Knockout (KO), wild type (WT)

Dendritic spine density and spine morphology of MSNs

After the PR session, animals were sacrificed, and samples were processed for morphological analysis of MSNs in the NAc core and shell. We quantified the total dendritic spine density as well as the density of different spine types of 8-10 individual dendrites per animal per area.

Nucleus accumbens core

Two-way ANOVA revealed a significant effect of group [$F_{2,265}$ =9.46; p<0.001] but not of genotype [$F_{1,265}$ =2.86; p=0.09]. The interaction between both factors was significant [$F_{2,265}$ =4.29; p<0.05]. Newman-Keuls *post-hoc* analysis revealed a significantly increased spine density in the WT Master Nicotine group compared to all groups (p<0.001) (Figure 44A).

Furthermore, one-way ANOVA showed a significant effect of group testing the density of thin spines [$F_{5,265}$ =2.42; p<0.05], stubby protuberances [$F_{5,265}$ =4.44; p<0.001], and mushroom-shaped spines [$F_{5,265}$ =4.91; p<0.001], but not of filopodia extensions [$F_{5,265}$ =2.22; p=0.053] or branched spines [$F_{5,265}$ =0.5; n.s.]. Newman-keuls *post-hoc* analysis is shown in Figure 44B.

Nucleus accumbens shell

Similar to the NAc core, two-way ANOVA revealed a significant effect of group [$F_{2,275}$ =3.22; p<0.05] but not of genotype [$F_{1,275}$ =0.84; n.s.], and a significant interaction between both factors [$F_{2,275}$ =8.73; p<0.001]. Newman-Keuls *post-hoc* analysis revealed that mice of the WT Master Nicotine group had significantly increased total spine densities compared to WT Yoked Saline (p<0.01), WT Yoked Nicotine (p<0.001) and KO Master groups (p<0.001) (Figure 45A).

Furthermore, one-way ANOVA showed a significant effect of group on the density of thin spines [$F_{5,275}$ =2.91; p<0.05], mushroom-shaped spines [$F_{5,275}$ =4.52; p<0.001], and branched spines [$F_{5,275}$ =2.27; p<0.05] but not of filopodia extensions [$F_{5,275}$ =1.9; n.s.] or stubby protuberances [$F_{5,275}$ =1.22; n.s.]. Subsequent Newman-keuls *post-hoc* analysis is shown in Figure 45B.

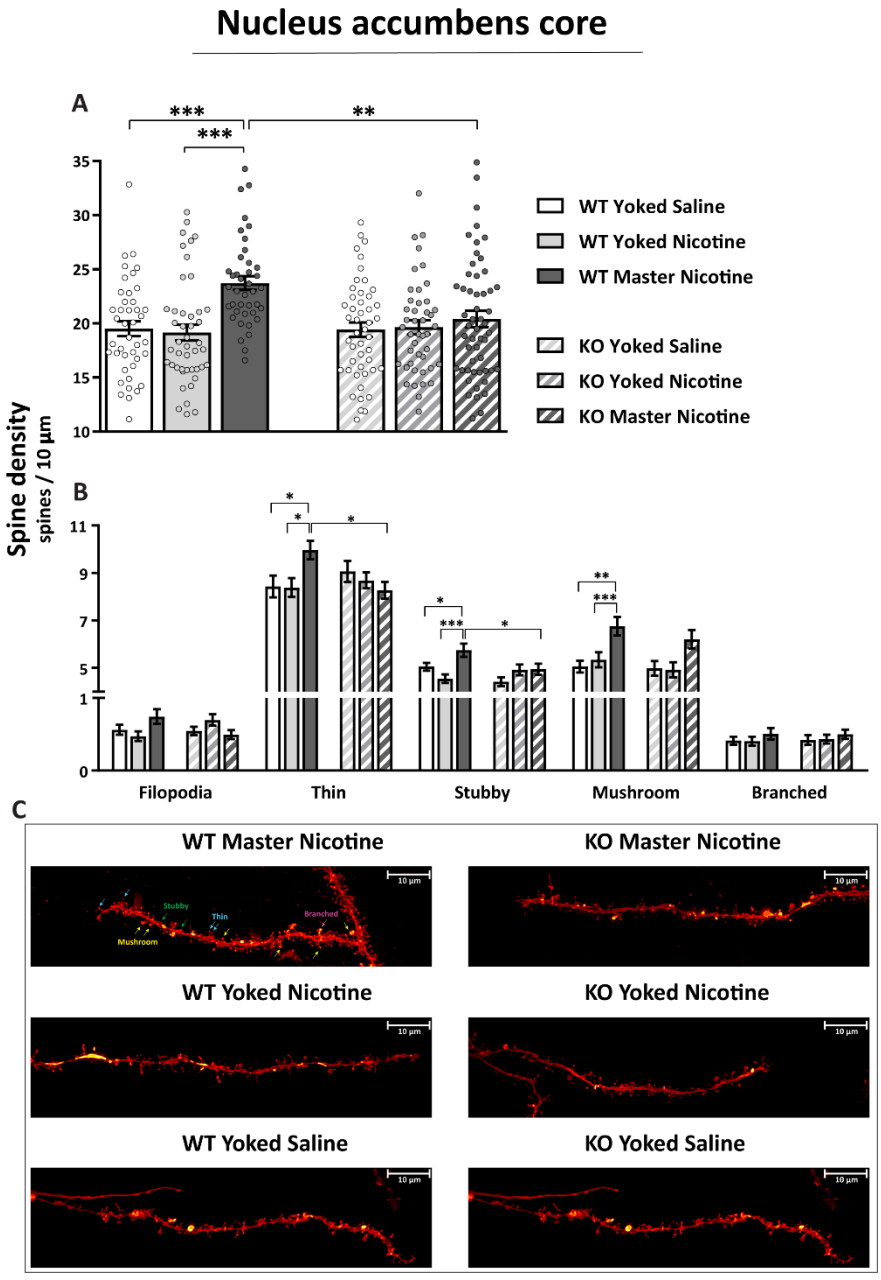

Figure 44. Dendritic spine density and density of spine types in the NAc core
A: Dendritic spine density of WT Yoked Saline (n=42), WT Yoked Nicotine (n=45), WT Master Nicotine (n=40), KO Yoked Saline (n=47), KO Yoked Nicotine (n=44), KO Master Nicotine (n=53). **B:** Density of spine types. **C:** Representative images of individual dendrites from MSNs in the NAc core. Data are expressed as mean ±SEM. *p<0.05, **p<0.01, ***p<0.001. **Abbreviations:** Knockout (KO), wild type (WT)

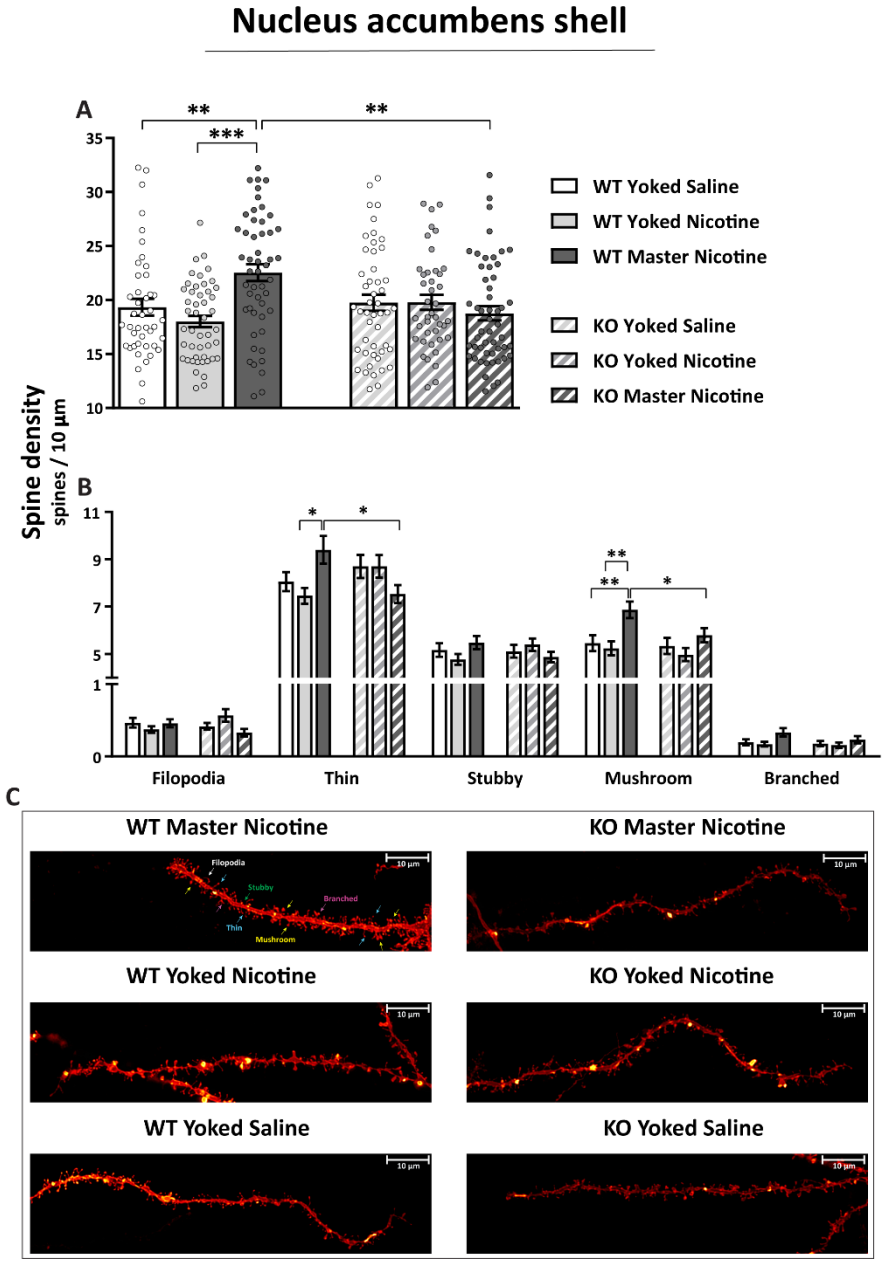

Figure 45. Dendritic spine density and density of spine types in the NAc shell
A: Dendritic spine density of WT Yoked Saline (n=43), WT Yoked Nicotine (n=47), WT Master Nicotine (n=50), KO Yoked Saline (n=48), KO Yoked Nicotine (n=41), KO Master Nicotine (n=52). **B:** Density of spine types. **C:** Representative images of individual dendrites from MSNs in the NAc Shell. Data are expressed as mean ±SEM. *p<0.05, **p<0.01, ***p<0.001. **Abbreviations:** Knockout (KO), wild type (WT)

Pathway-specific chemogenetic inhibition of glutamatergic projections to the nucleus accumbens core

To inhibit pathway-specific glutamatergic transmission in the NAc core, WT mice were injected with the retrograde AAVr pmSyn1-EBFP-Cre into the NAc core, and the CRE-dependent AAV8-hSyn-DIO-hM4D(Gi)-mCherry or the AAV8-CamKII-DIO-hM4D(Gi)-mCherry into the PLC or BLA, respectively. Hence, only glutamatergic neurons that project to the NAc core expressed the G_i-coupled designer receptor exclusively activated by designer drugs (DREADD) in the PLC or BLA (Figure 46A, Figure 47A).

WT animals expressing G_i-coupled DREADDs or control DREAADs were trained to acquire and maintain nicotine self-administration for 12 consecutive days under an FR1 schedule of reinforcement, followed by a test for motivation under a PR schedule. PLC-NAc core and BLA-NAc core pathways were inhibited by DREADD activation with i.v. injections of clozapine N-oxide (CNO) (1mg/kg, i.v.) or saline immediately before each training session.

Effect of chemogenetic inhibition of the PLC-NAc core pathway on nicotine self-administration

Three-way ANOVA repeated measures demonstrated a significant main effect of nose-poke [$F_{(1,19)}$ = 12.43; $p<0.01$] and day [$F_{(11,209)}$ = 12.42; $p<0.001$], but not of group [$F_{(2,19)}$ = 1.83; n.s.]. Significant interactions were revealed between nose-poke and day [$F_{(11,209)}$ = 10.21; $p<0.001$], but not between group and day [$F_{(11,209)}$ = 1.13; n.s.], group and nose-poke [$F_{(2,19)}$ = 0.94; n.s.], or among all three factors [$F_{(11,209)}$ = 1.06; n.s.] (Figure 46B). The area under the curve of active and inactive responses was not significantly different between groups (Two-way ANOVA repeated measures, group:

[$F_{(2,19)}$ = 1.97; n.s.]; nose-poke: [$F_{(1,19)}$ = 11.01; p<0.001]; interaction [$F_{(2,19)}$ = 1.05; n.s.]) (Figure 46C).

After training sessions, we tested the motivation for nicotine under a PR schedule of reinforcement, one-way ANOVA did not reveal a significant effect of group [$F_{(2,19)}$ = 0.14; n.s.] (Figure 46D).

However, inhibition of the PLC-NAc core pathway decreased the percentage of mice that fulfilled acquisition criteria compared to saline [χ^2= 2.86; p = 0.09] and CNO control groups [χ^2= 3.75; p = 0.05]. No differences were obtained between control groups [χ^2= 0.08; n.s.] (Figure 46E).

Effect of chemogenetic inhibition of the BLA-NAc core pathway on nicotine self-administration

Three-way ANOVA repeated measures revealed significant main effects of nose-poke [$F_{(1,42)}$ = 48.15; p<0.001] and day [$F_{(11,462)}$ = 17.41; p<0.001], but not of group [$F_{(2,42)}$ = 1.45; n.s.]. Significant interactions were revealed between nose-poke and day [$F_{(11,462)}$ = 22.6; p<0.001], but not between group and day [$F_{(11,462)}$ = 1.16; n.s.], group and nose-poke [$F_{(2,19)}$ = 0.94; n.s.], or among all three factors [$F_{(11,462)}$ = 0.96; n.s.] (Figure 47B). No differences were obtained comparing the area under the curve of active and inactive responses among groups (Two-way ANOVA repeated measures group: [$F_{(2,42)}$ = 1.49; n.s.]; nose-poke: [$F_{(1,42)}$ = 46.75; p<0.001]; interaction: [$F_{(2,42)}$ = 1.02; n.s.]) (Figure 47C).

The motivation for nicotine was evaluated under a PR schedule of reinforcement. The breakpoint achieved was not modified among groups (One-way ANOVA, group: [$F_{(2,39)}$ = 1.02; n.s.]) (Figure 47D).

The inhibition of glutamatergic transmission from the BLA to the NAc core did not alter the percentage of mice that fulfilled acquisition criteria

compared to saline [χ^2= 0.08; n.s.] and CNO control groups [χ^2= 0.34;n.s.]. No differences were obtained comparing control groups [χ^2= 0.78; n.s.] (Figure 47E).

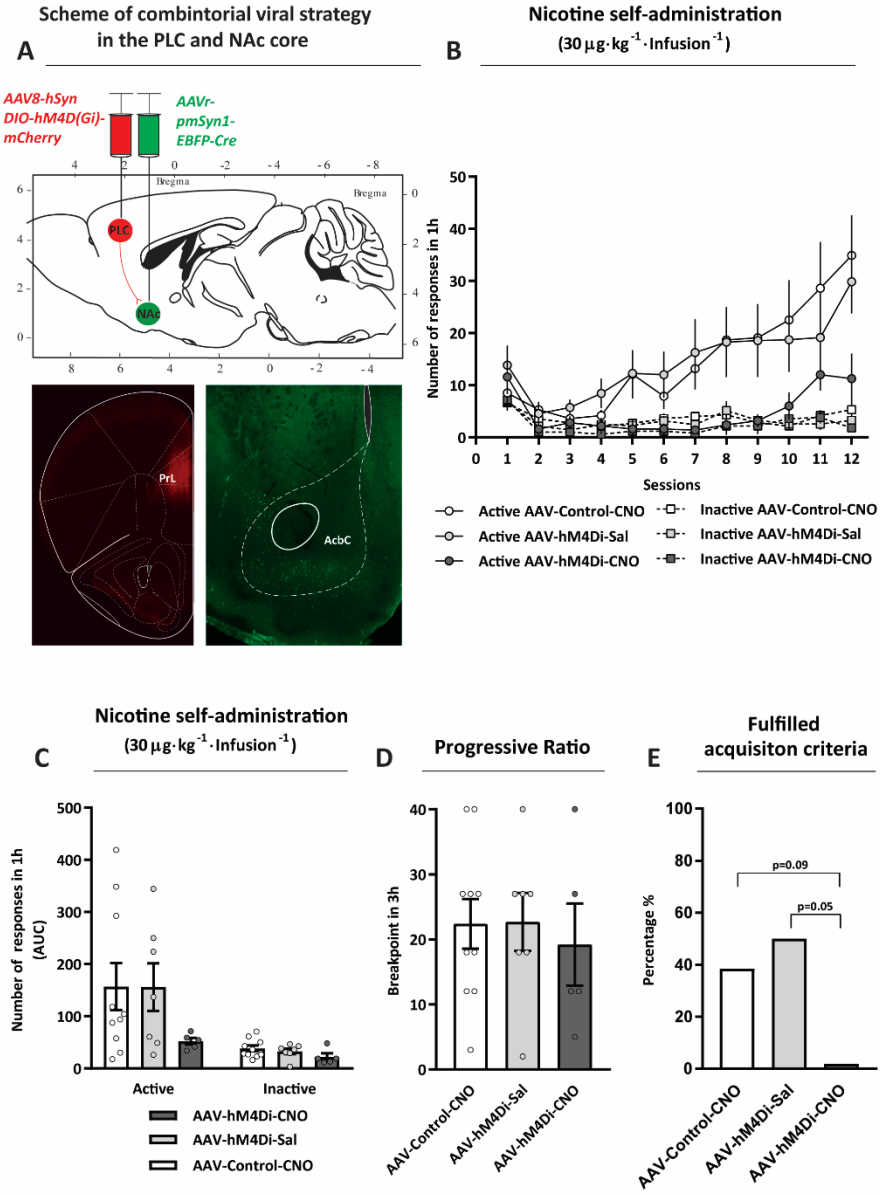

Figure 46. Effect of chemogenetic inhibition of the PLC-NAc core pathway on nicotine self-administration

A: Scheme of combinatorial viral strategy and representative virus expression in the NAc core and PLC. **B:** Time course of nicotine self-administration of AAV-hM4Di-Sal (n=7), and AAV-Control-CNO (n=10) and AAV-hM4Di-CNO (n=5) groups. **C:** Area under the curve. **D:** Break point und a PR schedule of reinforcement. **E:** Percentage of fulfilled acquisition criteria. Data are expressed as mean ±SEM. **Abbreviations:** Adeno associated virus (AAV), clozapine N-oxide (CNO), nucleus accumbens (Nac), prelimbic cortex (PLC), saline (Sal).

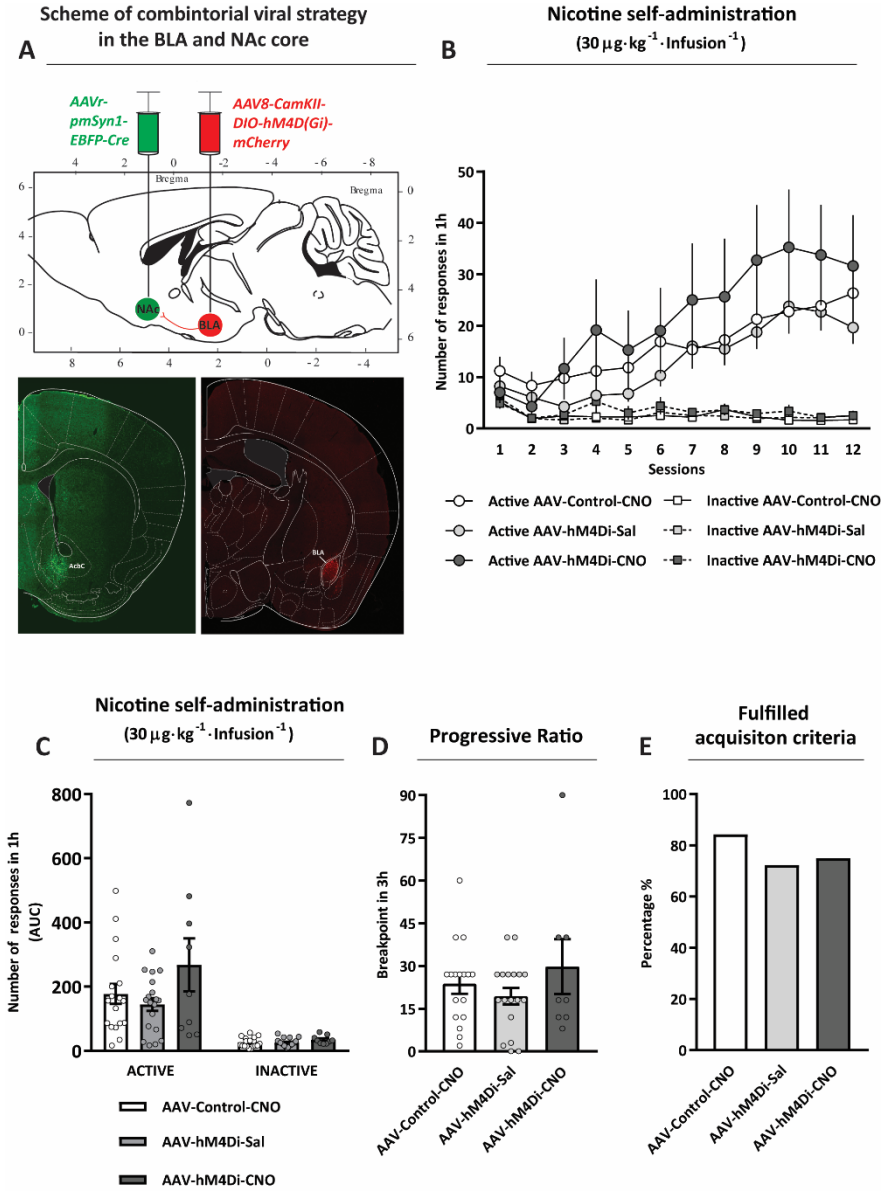

Figure 47. Effect of chemogenetic inhibition of the BLA-NAc core pathway on nicotine self-administration

A: Scheme of combinatorial viral strategy and representative virus expression in the NAc core and BLA. **B:** Time course of nicotine self-administration of AAV-hM4Di-Sal (n=19), and AAV-Control-CNO (n=18) and AAV-hM4Di-CNO (n=8) groups. **C:** Area under the curve. **D:** Break point und a PR schedule of reinforcement. **E:** Percentage of fulfilled acquisition criteria. Data are expressed as mean ±SEM. **Abbreviations:** Adeno associated virus (AAV), Basolateral amygdala (BLA), clozapine N-oxide (CNO), nucleus accumbens (Nac), saline (Sal)

Study 2

Phenotypic characterization of Sigma-1 receptor knockout mice

In a first approach, we characterized the phenotypical differences due to the genetic deletion of the Sig-1R. Sig-1 KO and WT mice were tested for locomotor activity, anxiety-like behavior, short-term memory, and novelty-seeking.

Locomotor activity

One-way ANOVA revealed a significant decrease in horizontal activity [$F_{1,45}$ = 8.52; p<0.01], large movements [$F_{1,45}$ = 11.74; p<0.01] and rearing activity [$F_{1,45}$ = 7.62; p<0.01] in Sig-1R KO mice (Figure 48 A-C).

Anxiety-like behavior

Anxiety-like behavior was tested in the elevated plus-maze and the light/dark box. In the elevated plus-maze, one-way ANOVA revealed that the percentage of time spent in open arms was significantly decreased in KO animals compared to WTs [$F_{1,43}$ = 5.21; p<0.05], as well as the number of total entries [$F_{1,43}$ = 6.16; p<0.05] (Figure 48D, E). In the light/dark box, the time spent in the light area was not significantly different between KO and WT mice [$F_{1,45}$ = 0.54; n.s.], however, the traveled distance was significantly decreased in Sig-1R KO mice [$F_{1,45}$ = 6.59; p<0.05] (Figure 48F, G).

Short-term memory

We used the novel object recognition test to evaluate short-term memory. One-way ANOVA revealed a significantly decreased discrimination index in Sig-1R KO mice compared to WT mice [$F_{1,45}$ = 17.76; p<0.001]) (Figure 48

H). No differences were obtained in total exploration time [$F_{1,45}$ = 1.55; n.s.].

Novelty-seeking

Sig-1R KO and WT mice were tested in an operant model of sensation-seeking to evaluate novelty-seeking and to ensure that Sig-1R KO mice are able to fulfill an operant task despite the phenotypical differences due to the constitutive deletion of the Sig-1R.

Sig-1R KO and WT mice were trained for 10 consecutive days under an FR1 (5 days), and FR3 (5 days) schedule of reinforcement. Three-way ANOVA repeated measures revealed significant main effects of nose-poke [$F_{1,41}$ = 152.72; p<0.001] and day [$F_{9,369}$ = 4.16; p<0.001] but not of genotype [$F_{1,41}$ = 0.09; n.s.]. A significant interaction between day and nose-poke [$F_{9,369}$ = 8.86; p<0.001] and day and genotype [$F_{9,369}$ = 2.45; p<0.05] but not between nose-poke and genotype [$F_{9,369}$ = 0.01; n.s.] or among all three factors [$F_{9,369}$ = 1.66; n.s.] was obtained (Figure 48 I). The area under the curve was tested using a two-way ANOVA repeated measures. Analysis revealed a significant main effect of nose-poke [$F_{1.41}$ = 152.68; p<0.001] but not of genotype [$F_{1,41}$ = 0.05; n.s.]. No significant interaction between both factors was obtained [$F_{1,41}$ = 0.02; n.s.] (Figure 49B). Impulsivity-like behavior was assessed as the number of active responses in the time-out phase (10s) after each presentation of the cue-light. Two-way ANOVA repeated measures demonstrated a significant effect of day [$F_{1,43}$ = 2.03; p<0.05], but not of genotype [$F_{1,43}$ = 0.16; n.s.] or the interaction of both factors [$F_{9,387}$ = 1.89; n.s.] (Figure 48 J). No differences between genotypes were obtained comparing the area under the curve [$F_{1,43}$ = 0.34; n.s.] (Figure 49D).

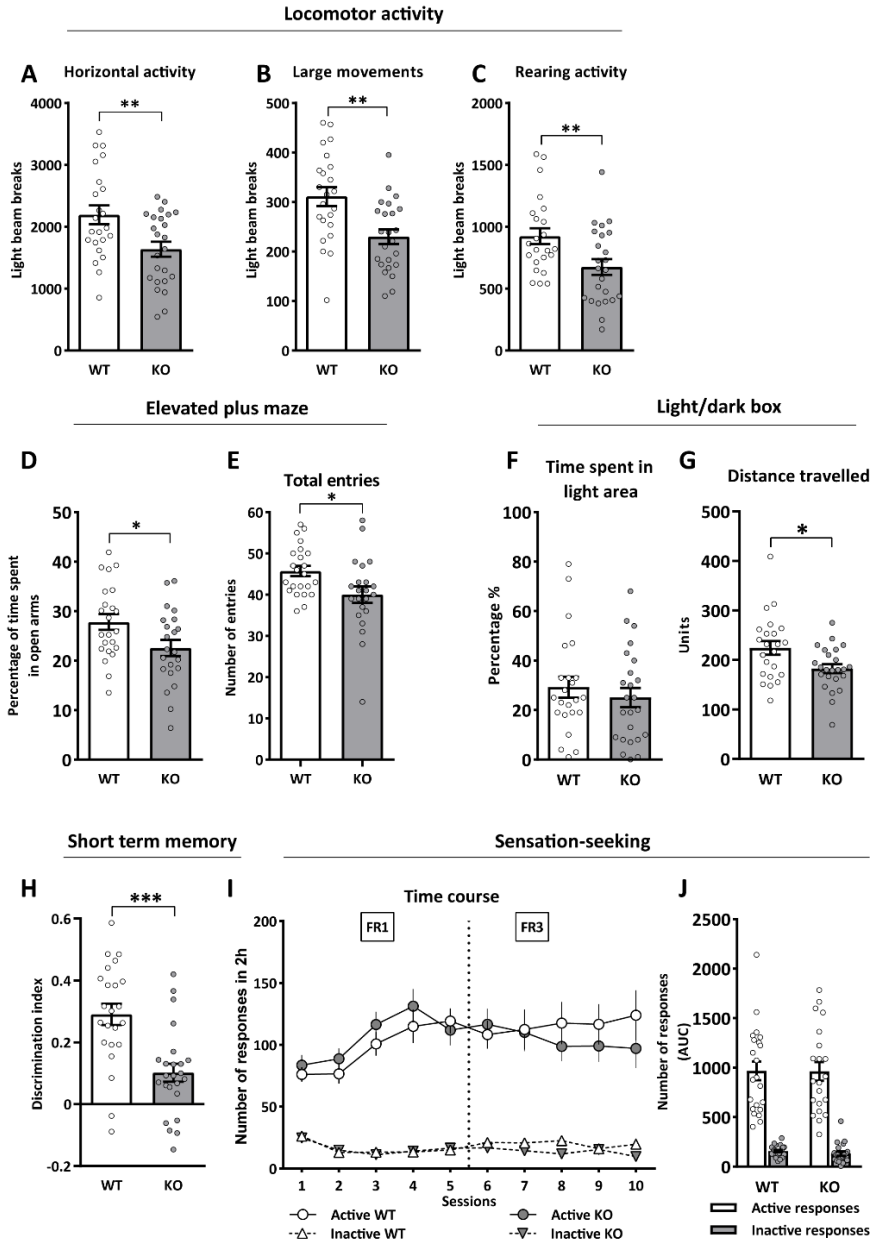

Figure 48. Phenotypic characterization of Sig-1R KO mice.

A-C: Locomotor activity of WT (n=23) and Sig-1R KO (n=24) mice. **D, E:** Anxiety-like behavior of WT (n=23) and Sig-1R KO (n=24) mice in the elevated plus-maze. **F, G:** Anxiety-like behavior of WT (n=23) and Sig-1R KO (n=24) mice in the light/dark box. **H:** Assessment of short-term memory of WT (n=23) and Sig-1R KO (n=24) mice in a novel object recognition test. **I:** Time course of active and inactive responding of WT (n=22) and Sig-1RKO (n=21) mice in an operant model of sensation-seeking. **J:** Area under the curve of active responses Data are expressed as mean ±SEM. *p<0.05, **p<0.01, ***p<0.001. **Abbreviations:** Knockout (KO), wild type (WT).

Impulsivity-like behavior of Sig-R1 KO mice in operant conditioning

Impulsivity-like behavior was tested in different cohorts of WT and Sig-1R KO mice. We used 3 different operant models, including drug-self-administration, food self-administration or a model of sensation-seeking. Operant conditioning was maintained by nicotine or saline with cue-light, palatable food with cue-light or the presentation of the cue-light alone, respectively. Mice were trained for 10 consecutive days under an FR1 (5 days), and FR3 (5 days) schedule of reinforcement to acquire and maintain operant behavior. Impulsivity-like behavior was assessed as the number of active responses in the time-out phase (10s) after each reinforcer.

Operant conditioning maintained by nicotine or saline with cue-light

Three-way ANOVA repeated measures revealed a main effect of genotype [$F_{1,240} = 39.94$; $p<0.001$] and day [$F_{9,2160} = 39.94$; $p<0.001$] but not of drug [$F_{1,240} = 0.76$; n.s.]. No interactions between genotype and drug [$F_{1,240} = 0.10$; n.s.], day and genotype [$F_{9,2160} = 1.47$; n.s.] or among all three factors [$F_{9,2160} = 0.88$; n.s.] were obtained (Figure 49A). Testing the area under the curve, two-way ANOVA showed a significant main effect of genotype [$F_{1,240} = 36.12$; $p<0.001$] but not of drug [$F_{1,240} = 0.51$; n.s.]. No interaction was revealed between both factors [$F_{1,240} = 0.16$; n.s.] (Figure 49B).

Operant conditioning maintained by palatable food

Two-way ANOVA repeated measures revealed a main effect of day [$F_{9,387} = 3.79$; $p<0.001$], but not of genotype [$F_{1,43} = 2.55$; n.s.]. No interaction between genotype and day was obtained (Figure 49C). One-way ANOVA of the area under the curve showed no significant effect of genotype [$F_{1,43} = 2.18$; n.s.] (Figure 49D)

Operant conditioning maintained by cue-light

Two-way ANOVA repeated measures demonstrated a significant effect of day [$F_{9,387}$ = 2.03; p<0.05], but not of genotype [$F_{1,43}$ = 0.16; n.s.] or the interaction of both factors [$F_{9,387}$ = 1.89; n.s.] (Figure 49E). No differences between genotypes were obtained comparing the area under the curve [$F_{1,43}$ = 0.34; n.s.] (Figure 49F).

Effect of Sig-1R antagonist BD 1063 on locomotor activity

After operant training of sensation-seeking was finished, locomotor activity of Sig-1R KO and WT mice was tested 1h after pharmacological treatment with the Sig-1R antagonist BD 1063 (10mg/kg s.c.) or vehicle. BD 1063 (10mg/kg s.c.) did not alter locomotor activity in WT mice: horizontal activity [$F_{1,21}$ = 1.98; n.s.], large movements [$F_{1,21}$ = 1.75; n.s.], and rearing activity [$F_{1,21}$ = 0.08; n.s.] (Suppl.Fig. 1A-C). In contrast, BD 1063 treatment increased large movements in KO mice [$F_{1,21}$ = 10.31; p<0.01] but did not alter their horizontal [$F_{1,21}$ = 1.58; n.s.] and rearing activity [$F_{1,21}$ = 0.63; n.s.] (Suppl.Fig. 1D-F).

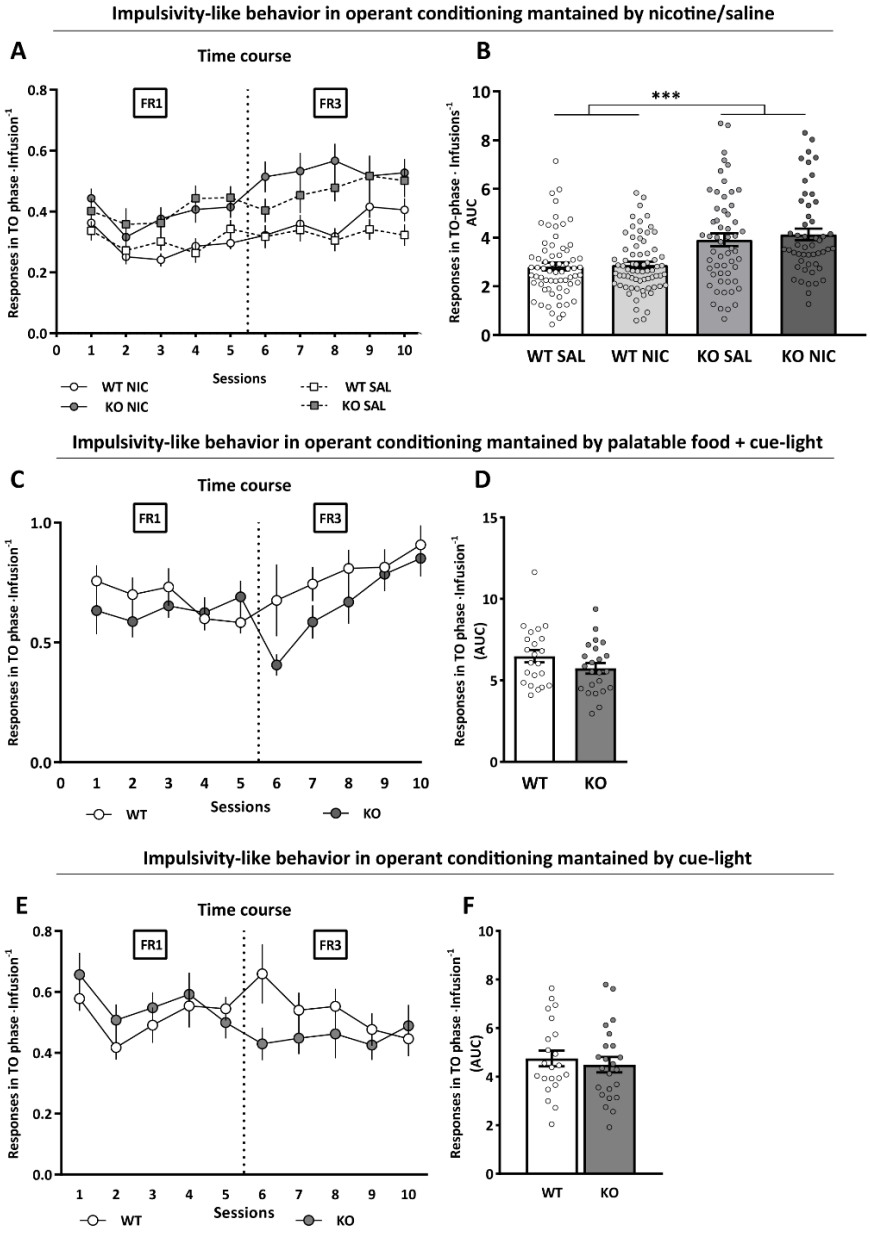

Figure 49. Impulsivity-like behavior of WT and Sig-1R KO mice in different operant behavioral models

A, B: Time course and area under the curve of impulsivity-like behavior of WT and Sig-1R KO mice in operant conditioning maintained by nicotine (n_{WT}=72, n_{KO}=51) or saline (n_{WT}=67, n_{KO}=50). **C, D:** Time course and area under the curve of impulsivity-like behavior of WT (n=22) and Sig-1R KO (n=23) mice in operant conditioning maintained by palatable food. **E, F:** Time course and area under the curve of impulsivity-like behavior of WT (n=22) and Sig-1R KO (n=23) mice in operant conditioning maintained by cue. Data are expressed as mean ±SEM. ***p<0.001. **Abbreviations:** Knockout (KO), wild type (WT).

The implication of Sig-1Rs in the reinforcing properties of nicotine and the cue-induced reinstatement of nicotine-seeking

We used an operant model of cue-induced reinstatement to evaluate the reinforcing properties and the motivation for nicotine, as well as the relapse to nicotine-seeking in WT and Sig-1R KO mice. Furthermore, we tested the ability of the selective Sig-1R antagonist BD 1063 to modify the motivation for nicotine and the reinstatement to nicotine-seeking. Data of operant conditioning maintained by nicotine, extinction and cue-induced reinstatement of nicotine-seeking were analyzed separately for each genotype due to the behavioral differences obtained in locomotor activity, short-term memory, and impulsive- and anxiety-like behavior during the phenotypical characterization.

WT mice were trained to self-administer either nicotine or saline under an FR1 (5 days) and FR3 (5 days) schedule of reinforcement. In the acquisition phase, three-way ANOVA revealed significant main effects of nose-poke [$F_{1,137}$ = 371.1; p<0.001], drug [$F_{1,137}$ = 24.5; p<0.001], and day [$F_{9,1233}$ = 91.33; p<0.001]. Significant interactions between nose-poke and drug [$F_{1,137}$ = 28.82; p<0.001], nose-poke and day [$F_{9,1233}$ = 116.93; p<0.001], drug and day [$F_{9,1233}$ = 16.87; p<0.001] and among all three factors [$F_{9,1233}$ = 19.21; p<0.001] were obtained. Subsequent Newman-Keuls *post-hoc* analysis showed significantly increased active responding of WT mice self-administering nicotine compared to saline control mice on day 7 (p<0.05), 8 (p<0.01), 9 (p<0.001) and 10 (p<0.001). Responses in the inactive manipulandum were unchanged (Figure 50A). One-way ANOVA revealed a significant increase in the area under the curve of active responses in WT animals exposed to nicotine compared to WT mice exposed to saline [$F_{1,137}$ = 24.49; p<0.001] (Figure 50B).

The motivation for nicotine or saline was tested under a PR schedule of reinforcement, WT NIC and WT SAL mice were treated with either vehicle or BD 1063 (10mg/kg s.c.) 1hour prior to testing. Two-way ANOVA demonstrated significant main effects of drug [$F_{1,115}$ = 18.21; p<0.001], and treatment [$F_{1,115}$ = 10.88; p<0.01], and a significant interaction between both factors [$F_{1,137}$ = 4.4; p<0.05]. Subsequent Newman-Keuls *post-hoc* analysis revealed a significantly increased breakpoint in vehicle-treated mice receiving nicotine compared to the saline control group(p<0.001). BD 1063 decreased significantly the motivation for nicotine (p<0.001) but not for saline (Figure 50C).

As expected, the percentage of animals that achieved acquisition criteria was significantly higher in WT mice that self-administered nicotine compared to the saline control group [χ^2= 20.33; p<0.001] (Figure 50D).

In the extinction phase, mice were trained to decrease operant behavior to 30% of the average of the last three days of the acquisition phase. All mice achieved extinction criterion. Furthermore, three-way ANOVA repeated measures revealed significant main effects of nose-poke [$F_{1,102}$ = 317.95; p<0.001], drug [$F_{1,102}$ = 7.53; p<0.01], and day [$F_{9,918}$ =30.65; p<0.001]. A significant interaction between day and nose-poke [$F_{9,918}$ = 64.94; p<0.001] and day and drug [$F_{9,918}$ = 5.38; p<0.001] but not between nose-poke and drug [$F_{1,102}$ = 2.32; p=0.09] was demonstrated. The interaction among all three factors was significant [$F_{9,918}$ = 4.52; p<0.001]. Subsequent Newman-Keuls *post-hoc* analysis showed a significant increase of active responses in WT mice previously exposed to nicotine compared to the saline control group on day 1 (p<0.05) (Figure 50E).

Cue-induced reinstatement of nicotine-seeking was tested after a minimum of 10 daily extinction session or whenever the extinction criterion was reached. WT SAL and WT NIC groups were treated with

either vehicle or BD 1063 (10mg/kg s.c.) 1h prior to cue-induced reinstatement testing. Three-way ANOVA repeated measures demonstrated significant main effects of nose-poke [$F_{1,94}$ = 166.96; p<0.001] and treatment [$F_{1,94}$ = 21.44; p<0.001] but not of drug [$F_{1,94}$ = 0.19; n.s.]. A significant interaction between drug and treatment [$F_{1,94}$ = 9.03; p<0.01] nose-poke and treatment [$F_{1,94}$ = 14.75; p<0.001] but not between nose-poke and drug was revealed [$F_{1,94}$ = 0.19; n.s.]. The interaction among all three factors was also significant [$F_{1,94}$ = 9.18; p<0.01]. Newman-Keuls *post-hoc* analysis revealed a significant increase in the number of active responses comparing vehicle-treated WT mice that were previously exposed to nicotine compared to the vehicle-treated saline control group (p<0.01). Treatment with the Sig-1R antagonist BD 1063 reversed increased responding in WT mice that were exposed to nicotine (p<0.001), and decreased responding compared to the BD 1063-treated control group (p<0.05). No differences were obtained comparing inactive responses (Figure 50F).

KO mice were trained to obtain either nicotine or saline under similar experimental conditions. In the acquisition phase, three-way ANOVA revealed significant main effects of nose-poke [$F_{1,106}$ = 411.62; p<0.001] and day [$F_{9,954}$ = 86.0; p<0.001], but not of drug [$F_{1,106}$ = 3.37; n.s.]. Significant interactions between nose-poke and drug [$F_{1,106}$ = 5.76; p<0.05], nose-poke and day [$F_{9,954}$ = 97.94; p<0.001], drug and day [$F_{9,954}$ = 3.74; p<0.001] and among all three factors [$F_{9,954}$ = 4.23; p<0.001] were obtained. Subsequent Newman-Keuls *post-hoc* analysis did not reveal specific significant differences between active responding of nicotine self-administration compared to saline on any day of FR1 and FR3 (Figure 51A). One-way ANOVA demonstrated a tendency of higher responding comparing the area under the curve of active responses of KO animals self-

administering nicotine compared to saline control animals [$F_{1,106}$ = 3.75; p=0.055] (Figure 51B).

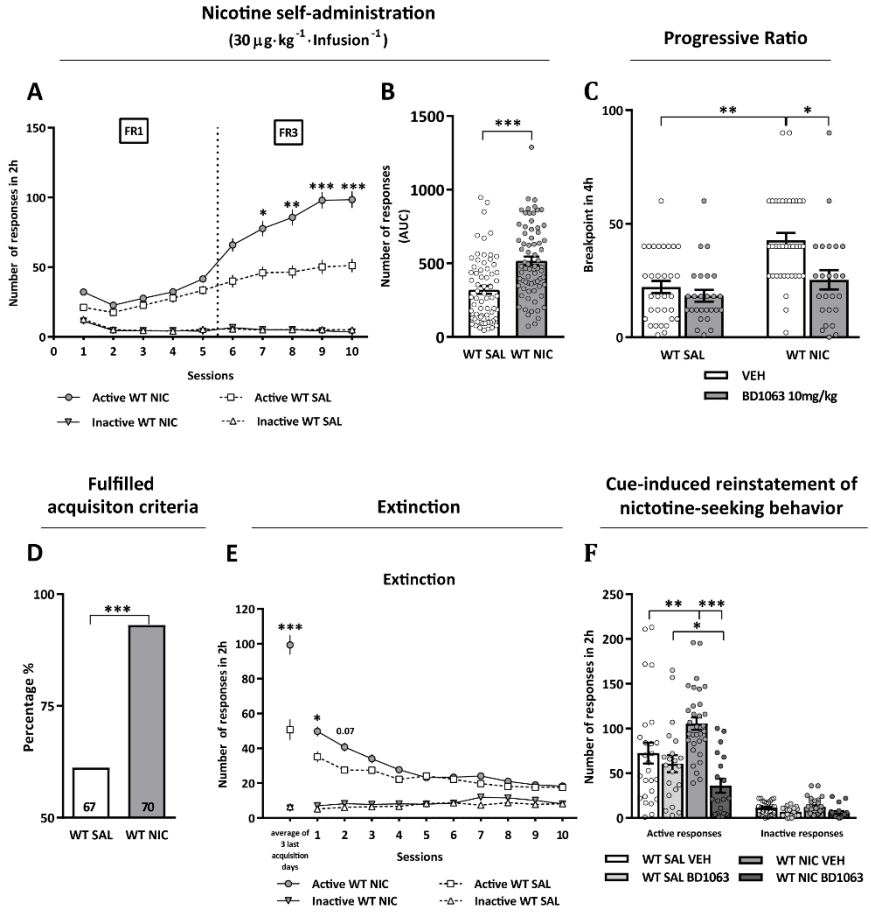

Figure 50. Cue-induced reinstatement of nicotine-seeking behavior in WT mice.
A: Time course of active and inactive responding of WT mice self-administering nicotine (n=70) or saline (67). **B:** Area under the curve of active responding for nicotine or saline. **C:** Test for motivation for nicotine or saline under a progressive ratio schedule. Mice were treated with either BD1063 (10mg/kg s.c.) one hour prior to testing ($n_{WT\ SAL\ VEH}$=32, $n_{WT\ SAL\ BD}$=26, $n_{WT\ NIC\ VEH}$=37, $n_{WT\ NIC\ BD}$=24). **D:** Percentage of mice that fulfilled all three acquisition criteria after 10 days of operant self-administration maintained by nicotine (n=70) or saline (67). **E:** Time course of active and inactive responding of WT mice extinguishing operant behavior after nicotine (n=56) or saline (n=44) self-administration. **F:** Cue-induced reinstatement of nicotine-seeking behavior after extinction of operant behavior. Mice were treated with either BD1063 (10mg/kg s.c.) one hour prior to testing ($n_{WT\ SAL\ VEH}$=22, $n_{WT\ SAL\ BD}$=21, $n_{WT\ NIC\ VEH}$=32, $n_{WT\ NIC\ BD}$=19). Data are expressed as mean ±SEM. *p<0.05, **p<0.01, ***p<0.001. **Abbreviations:** Knockout (KO), nicotine (NIC), saline (SAL), vehicle (VEH), wild type (WT)

The motivation for nicotine or saline was tested under the same conditions as explained for WT mice. Animals were treated with BD 1063 (10mg/kg s.c.) or saline 1h before testing. Two-way ANOVA showed a significant main effect of drug [$F_{1,88}$ = 12.65; p<0.001] but not of treatment [$F_{1.88}$ = 0.14; n.s.] nor the interaction between both factors [$F_{1,88}$ = 0.59; n.s.] (Figure 51C).

No differences were obtained comparing the percentage of fulfilled acquisition criteria between KO animals that self-administered nicotine *vs.* saline [χ^2= 0.36; n.s.] (Figure 51D).

KO NIC and the KO SAL groups underwent extinction training as previously described for WT animals. All KO mice achieved the extinction criterion. Three-way ANOVA repeated measures revealed significant main effects of nose-poke [$F_{1,70}$ = 260.99; p<0.001], drug [$F_{1,70}$ = 7.56; p<0.01], and day [$F_{9,630}$ =37.62; p<0.001], as well as a significant interaction between day and nose-poke [$F_{9,630}$ = 59.03; p<0.001], day and drug [$F_{9,630}$ = 4.65; p<0.001] and nose-poke and drug [$F_{1,70}$ = 12.82; p<0.001]. The interaction among all three factors was significant, as well [$F_{9,630}$ = 5.06; p<0.001]. Subsequent Newman-Keuls *post-hoc* analysis showed a significant increase of active responses in the KO NIC group compared to the KO SAL group on day1 (p<0.01) (Figure 51E).

After a minimum of 10 daily extinction sessions or whenever the extinction criterion was reached mice were tested for cue-induced reinstatement. KO NIC and KO SAL groups were treated with either vehicle or BD 1063 (10mg/kg s.c.) 1h prior to cue-induced reinstatement testing. Three-way ANOVA repeated measures revealed significant main effects of nose-poke [$F_{1,67}$ = 157.75; p=0.001], treatment [$F_{1,67}$= 10.31; p<0.01] and drug [$F_{1,67}$ = 30.14; p<0.001]. A significant interaction between nose-poke and drug [$F_{1,67}$ = 27.20; p=0.001] nose-poke and treatment [$F_{1,67}$ = 8.41; p<0.01], but

not of drug and treatment was obtained [$F_{1,67}$ = 0.27; n.s.] The interaction among the three factors was not significant [$F_{1,67}$ = 0.32; n.s.] (Figure 51F).

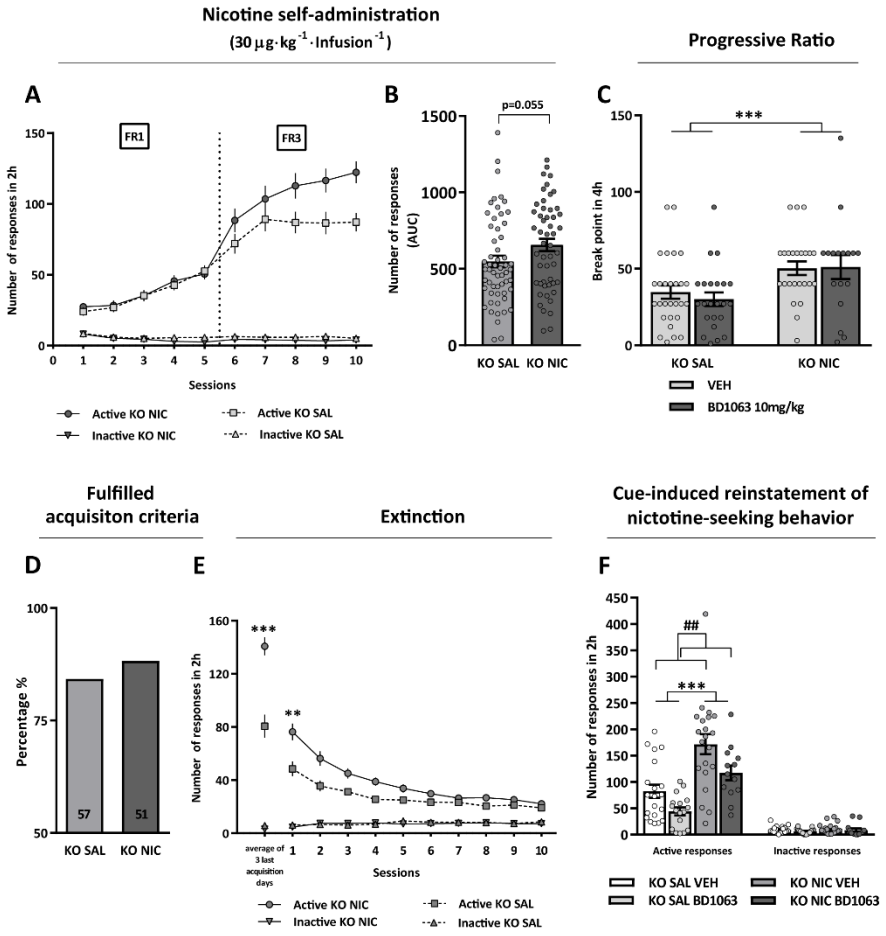

Figure 51 Cue-induced reinstatement of nicotine-seeking behavior in KO mice.
A: Time course of active and inactive responding of KO mice self-administering nicotine (n=51) or saline (57). **B:** Area under the curve of active responding for nicotine or saline. **C:** Test for motivation for nicotine or saline under a progressive ratio schedule. Mice were treated with either BD1063 (10mg/kg s.c.) one hour prior to testing ($n_{KO\ SAL\ VEH}$=28, $n_{KO\ SAL\ BD}$=23, $n_{KO\ NIC\ VEH}$=24, $n_{KO\ NIC\ BD}$=17). **D:** Percentage of mice that fulfilled all three acquisition criteria after 10 days of operant SA maintained by nicotine (n=51) or saline (57). **E:** Time course of active and inactive responding of KO mice extinguishing operant behavior after nicotine (n=34) or saline (n=31) SA. **F:** Cue-induced reinstatement of nicotine-seeking behavior after extinction of operant behavior. Mice were treated with either BD1063 (10mg/kg s.c.) one hour prior to testing ($n_{KO\ SAL\ VEH}$=16, $n_{KO\ SAL\ BD}$=16, $n_{KO\ NIC\ VEH}$=20, $n_{KO\ NIC\ BD}$=13). Data are expressed as mean ±SEM. ***p<0.001. **Abbreviations:** Knockout (KO), nicotine (NIC), saline (SAL), vehicle (VEH), wild type (WT)

The implication of sigma-1 receptors in protein and mRNA expression after cue-induced reinstatement of nicotine-seeking

After cue-induced reinstatement of nicotine-seeking, brain areas including the mPFC and the NAc were dissected and processed for relative protein and mRNA quantification. As explained previously, WT and Sig-1R KO mice were analyzed separately.

Relative mRNA expression in the mPFC

Relative mRNA expression for WT (n=4-7/group) and Sig-1R KO (n=4-6/group) mice was quantified using a TaqMan gene expression assay. Values were normalized to a housekeeping gene. Detailed statistical analysis is shown elsewhere (see

Sig-1R

In the mPFC, WT mice previously exposed to nicotine demonstrated a significant increase in Sig-1R mRNA compared to saline control animals after cue-induced reinstatement of nicotine-seeking ($p<0.01$). Pretreatment with BD 1063 reversed this increase ($p<0.05$). Sig-1R mRNA was not detectable in KO animals (Figure 52A, Table 3).

GluT1

Relative mRNA expression of the GluT1 was significantly increased in WT animals with a history of nicotine self-administration compared to the saline control group ($p<0.01$). The increase was blunted in WT mice treated with BD 1063 ($p<0.01$). No differences were obtained among KO animals (Figure 52B, Table 3).

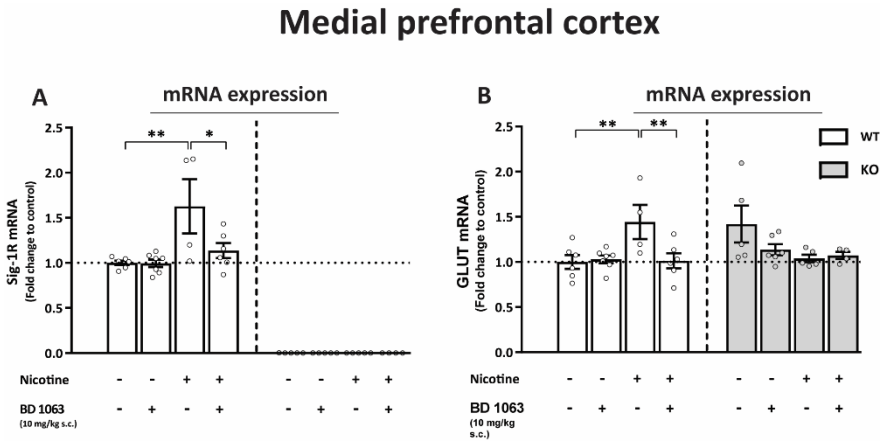

Figure 52. Relative mRNA expression in the mPFC.
A: Sig-1R. **B:** GluT. Data are expressed as mean ±SEM. *p<0.05, **p<0.01. **Abbreviations:** Glutamate transporter (GLUT), sigma-1 receptor (Sig-1R).

Relative protein expression in the mPFC

Relative protein expression was quantified using immunoblot analysis. For membrane proteins, both the relative total and cell surface expression was assessed in WT (n=4-6) and Sig-1R KO (n=4-6) mice. Detailed statistical analysis is shown elsewhere (see

Glutamate receptors

Relative total and cell surface expressions of glutamatergic receptors, including NMDARs, AMPARs, and the mGluR2/3 were assessed after cue-induced reinstatement of nicotine-seeking.

NMDAR

Relative total and cell surface protein expression of the NMDAR subunits NR1, NR2A and NR2B, as well as phosphorylation of the NMDAR NR1 subunit at Ser 890, 896 and 897, were tested in the different groups of WT and KO mice after cue-induced reinstatement of nicotine-seeking.

In KO mice, no significant main effects of drug or treatment, nor a significant interaction between both factors was revealed in KO mice in any protein tested (Table 5).

1. NR1 subunit

Total protein expression was increased in animals treated with BD 1063 compared to vehicle-treated animals ($p<0.05$) after cue-induced reinstatement of nicotine-seeking. This increase was independent of the drug self-administered in the acquisition phase (Suppl.Fig. 2A, Table 5). In contrast, relative cell surface protein expression of the NR1 subunit was significantly increased in animals previously exposed to nicotine compared to saline control groups. Treatment with BD 1063 did not modify cell surface expression (Figure 53A, Table 5).

1.1. p-NR1 (Ser890)

Phosphorylation of the NMDAR subunit NR1 at Ser890 was significantly decreased in vehicle-treated WT mice with a history of nicotine-self-administration when compared to saline control mice treated with vehicle ($p<0.05$). BD 1063 did not modify this decrease but significantly decreased phosphorylation in saline control mice when compared to the vehicle group ($p<0.001$) (Figure 53B, Table 5).

1.2. p-NR1 (Ser896)

Phosphorylation at Ser896 was significantly increased in the vehicle and BD 1063 treated mice that were previously exposed to nicotine compared to saline control groups ($p<0.05$) (Suppl.Fig. 2D, Table 5).

p-NR1 (Ser897)

Phosphorylation at Ser897 was not modified after cue-induced reinstatement of nicotine-seeking (Suppl.Fig. 2G, Table 5).

2. NR2A subunit

Both total and cell surface expressions of the NMDAR subunit NR2A were significantly increased after cue-induced reinstatement of nicotine-seeking in WT mice previously exposed to nicotine compared to saline control groups (total: $p<0.05$; cell surface: $p<0.01$) (Suppl.Fig. 2B, C, Table 5).

3. NR2B subunit

Total and cell surface expression remained unchanged after cue-induced reinstatement of nicotine-seeking (Suppl.Fig. 2E, F, Table 5).

AMPAR

Relative total and cell surface protein expression of the AMPAR subunits GluR1 and GluR2 were tested in WT and KO mice after cue-induced reinstatement of nicotine-seeking.

In KO mice, no significant main effects of drug or treatment, nor a significant interaction between both factors was revealed in KO mice in any protein tested (Table 5).

1. GluR1 subunit

Total protein expression of the AMPAR subunit GluR1 was significantly increased in WT mice treated with vehicle and previously exposed to nicotine after cue-induced reinstatement of nicotine-seeking ($p<0.01$). BD 1063 pretreatment partially inhibited this increase ($p=0.07$) (Suppl.Fig. 2H,

Table 5). Cell surface expression was significantly increased in vehicle-treated mice with a history of nicotine self-administration compared to animals that self-administered saline ($p<0.05$). BD 1063 blocked this effect ($p<0.01$) Figure 53C, Table 5).

2. GluR2 subunit

The AMPAR subunit GluR2 remained unchanged after cue-induced reinstatement of nicotine-seeking (Suppl.Fig. 2I, J, Table 5).

mGluR2/3

In WT mice, total protein expression was significantly increased in vehicle-treated mice previously exposed to nicotine compared to vehicle-treated saline control mice after nicotine relapse. BD 1063 did not modify the protein increase in nicotine-exposed mice but significantly increased protein expression in saline control mice compared to vehicle control mice ($p<0.05$) (Suppl.Fig. 2K, Table 5). Cell surface expression of mGluR2/3 was significantly increased in WT mice with a history of nicotine self-administration compared to saline exposed mice ($p<0.01$). Pretreatment with BD 1063 blunted the observed increase in nicotine exposed animals ($p<0.01$) (Figure 53D, Table 5).

Total protein expression was unchanged in Sig-1R KO mice (Suppl.Fig. 2K, Table 5). However, mGluR2/3 cell surface expression was significantly decreased in mice with a history of nicotine self-administration compared to saline control groups ($p<0.05$) (Figure 53D, Table 5).

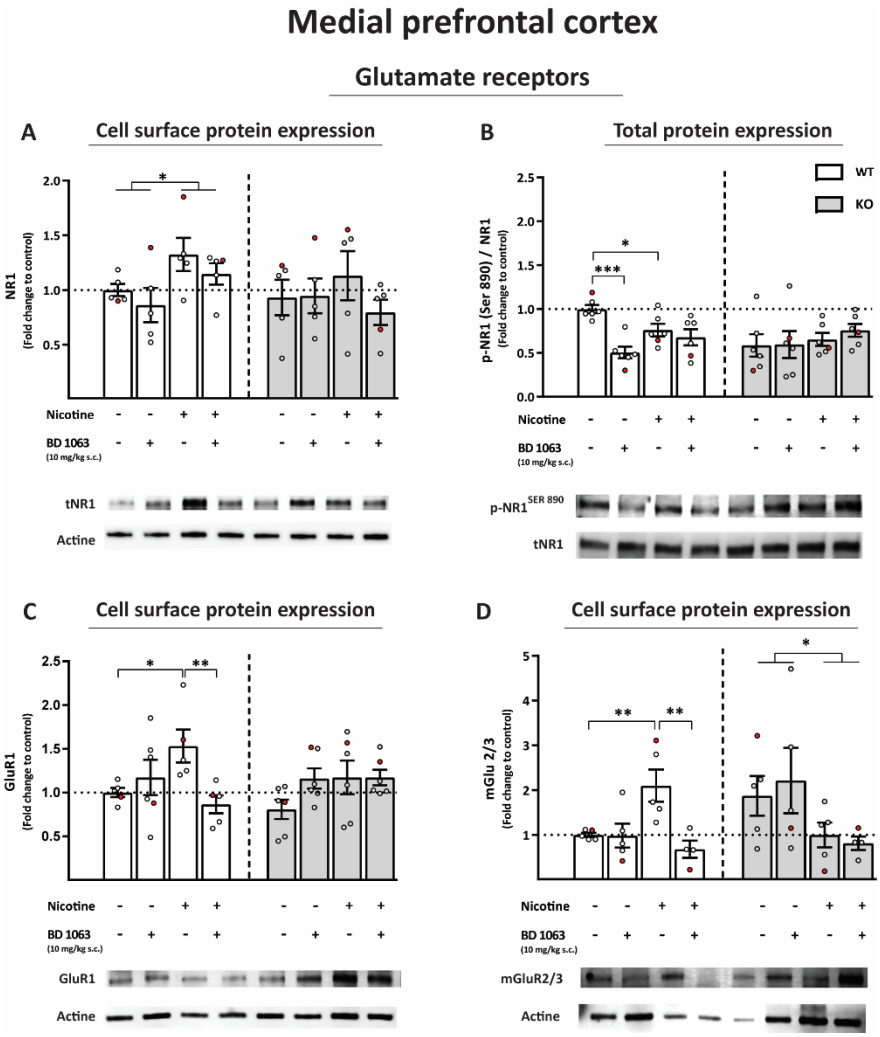

Figure 53 Relative total and cell surface protein expression of glutamate receptors in the mPFC.

A: Cell surface protein expression of the NR1 subunit. **B:** Total protein expression of the p-NR1(Ser890) subunit. **C:** Cell surface protein expression of the GluR1 subunit. **D:** Cell surface protein expression of the mGluR2/3. Data are expressed as mean ±SEM. *p<0.05, **p<0.01, ***p<0.001. **Abbreviations:** Glutamate receptor1 (GluR1), metabotropic glutamate receptor2/3 (mGluR2/3), N-methyl-D-aspartate receptor subunit 1 (NR1), phosphorylated N-methyl-D-aspartate receptor subunit 1 (p-NR1)

μ-opioid receptor

Total protein expression of MORs was significantly upregulated comparing nicotine exposed WT mice to the saline control group ($p<0.01$) after cue-induced reinstatement of nicotine-seeking. This effect was reversed by BD 1063 treatment ($p<0.05$) (Figure 54A, Table 6). At the cell membrane, MOR expression tent to increase after the reinstatement of nicotine-seeking in animals that were previously exposed to nicotine ($p=0.07$). BD 1063 did not change the protein expression of MORs.

No differences in total or cell surface protein expression were obtained comparing Sig-1R KO mice (Figure 54B, Table 6).

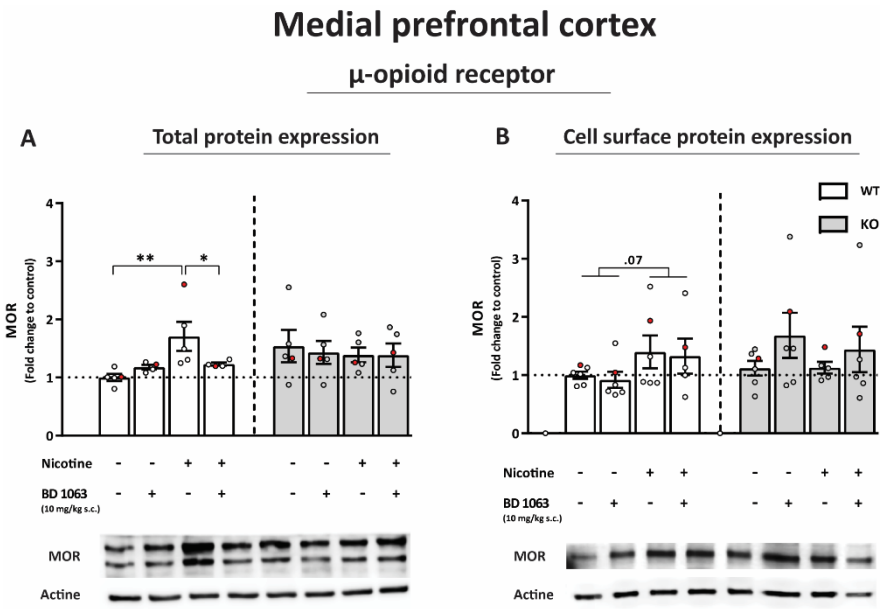

Figure 54. Relative total and cell surface protein expression of the μ-opioid receptor in the mPFC.
A: Total protein expression of the MOR **B:** Cell surface protein expression of the MOR. Data are expressed as mean ±SEM. *p<0.05, **p<0.01. **Abbreviations:** μ-opioid receptor (MOR)

nAChRs and their negative modulator

Relative total and cell surface protein expression of the nAChR subunits α4 and β2, and the negative allosteric modulator of nAChRs LynX1 were quantified in the different groups of WT and KO mice after cue-induced reinstatement of nicotine-seeking.

In KO mice, no significant main effects of drug or treatment, nor a significant interaction between both factors was revealed in KO mice in any protein tested (Table 7).

nAChR

1. *α4 subunit*

Cue-induced reinstatement of nicotine-seeking substantially increased the total protein expression of the α4 nAChR subunit in animals that were previously exposed to nicotine compared to saline control mice ($p<0.001$). BD 1063 partially reversed the increase observed in nicotine-exposed animals ($p=0.06$). BD 1063 did also increase the protein expression in mice that previously self-administered saline ($p<0.001$) (Figure 56A, Table 7).

Cell surface expression was significantly decreased in vehicle-treated mice after the reinstatement of nicotine-seeking compared to the saline control group ($p<0.05$). BD 1063 treatment significantly decreased α4 nAChR subunit expression in control animals ($p<0.05$) (Figure 56B, Table 7).

2. *β2 subunit*

Total protein expression of the β2 nAChR subunit was significantly increased after cue-induced reinstatement of nicotine-seeking in animals with a history of nicotine self-administration compared to saline control groups ($p<0.05$). BD 1063 treatment did not further modify total protein expression (Figure 56C, Table 7).

Cell surface expression of the β2 nAChR subunit was significantly decreased in vehicle-treated mice after cue-induced reinstatement of nicotine-seeking compared to the vehicle-treated control group. BD 1063 treatment did not further modify cell surface protein expression (Figure 56D, Table 7).

LynX1

The total protein expression of LynX1 has significantly decreased in both nicotine exposed groups compared to saline control groups after the reinstatement of nicotine-seeking ($p<0.05$). BD 1063 treatment did not reveal any modifications in the total protein expression (Suppl.Fig. 3A Table 7).

Cell surface expression of LynX1 was unchanged after cue-induced reinstatement of nicotine-seeking (Suppl.Fig. 3B Table 7).

Intracellular effectors and adhesion proteins

Relative total protein expression of p-CREB, p-ERK2, ERK2, NFκB p50, NFκB p105, ΔFosB, and n-cadherin were quantified in the different groups of WT and KO mice after cue-induced reinstatement of nicotine-seeking.

In KO mice, no significant main effects of drug or treatment, nor a significant interaction between both factors was revealed in KO mice in any protein tested.

p-CREB

Total protein expression of p-CREB was significantly increased in vehicle-treated mice after cue-induced reinstatement of nicotine-seeking compared to the saline control group ($p<0.01$). This effect was absent in BD treated mice. mice (Figure 57A, Table 8).

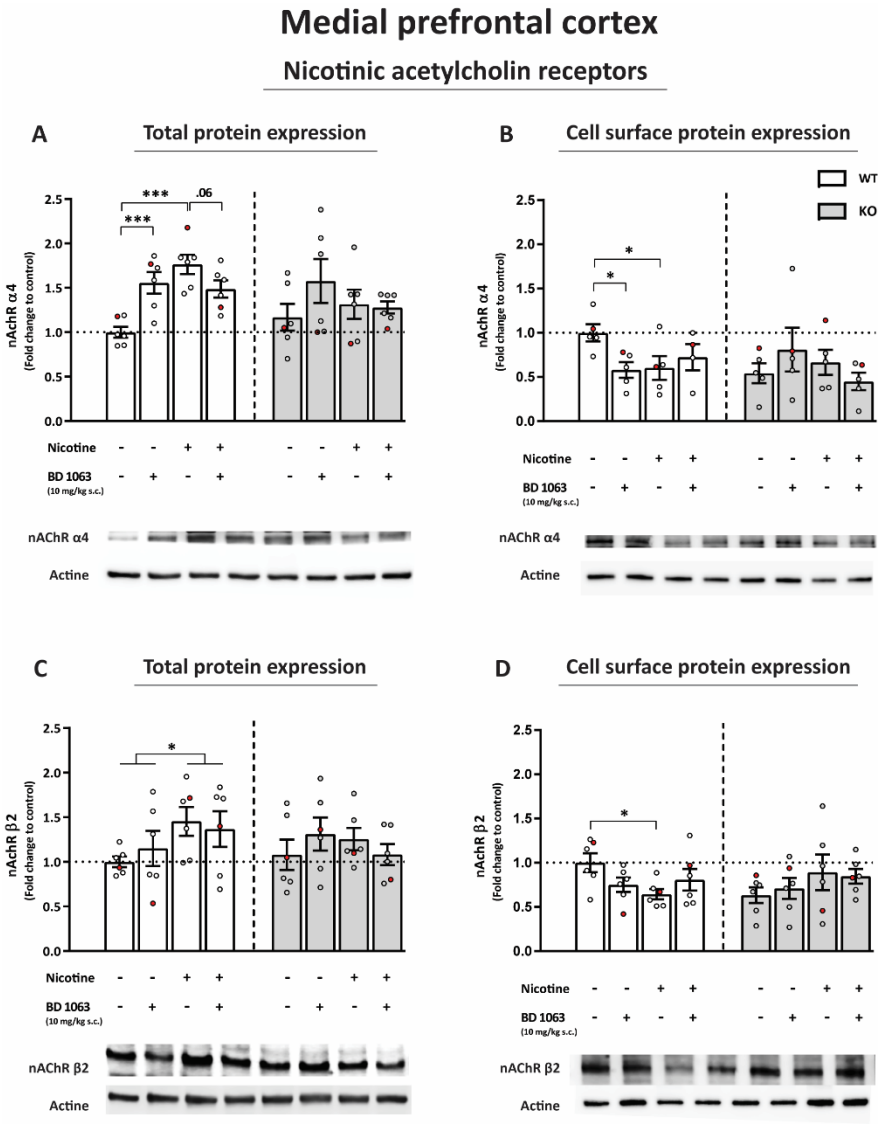

Figure 55. Relative total and cell surface protein expression of nAChRs in the mPFC.
A: Total protein expression of the nAChR α4 subunit. **B:** Cell surface protein expression of the nAChR α4 subunit. **C:** Total protein expression of the nAChR β2 subunit. **D:** Cell surface protein expression of the nAChR β2 subunit. Data are expressed as mean ±SEM. *p<0.05, ***p<0.001. **Abbreviations:** nicotinic acetylcholine receptor (nAChR)

p-ERK2/ERK2

The ratio of p-ERK2/ERK2 was significantly increased in mice that were previously exposed to nicotine compared to saline control groups ($p<0.05$). BD 1063 did not modify the protein expression of p-ERK2 and ERK2 (Figure 57B, Table 8).

NFκB

NFκB p50 total protein expression was unaffected in all groups after cue-induced reinstatement of nicotine-seeking (Suppl.Fig. 3C, Table 8). In contrast, its precursor protein NFκB p105 was significantly increased after the reinstatement of nicotine-seeking in vehicle-treated mice that were previously exposed to nicotine compared to the saline control group ($p<0.01$). The observed increase was blunted due to BD 1063 treatment ($p<0.01$) (Figure 57C, Table 8).

ΔFosB

Total protein expression of ΔFosB remained stable after cue-induced reinstatement of nicotine-seeking. Treatment with BD 1063 significantly decreased ΔFosB expression compared to vehicle-treated groups. (Suppl.Fig. 3D, Table 8).

n-Cadherin

Total protein expression was significantly increased after nicotine relapse in mice with a history of nicotine self-administration compared to saline control groups. BD 1063 treatment lacked effect (Figure 57D, Table 8).

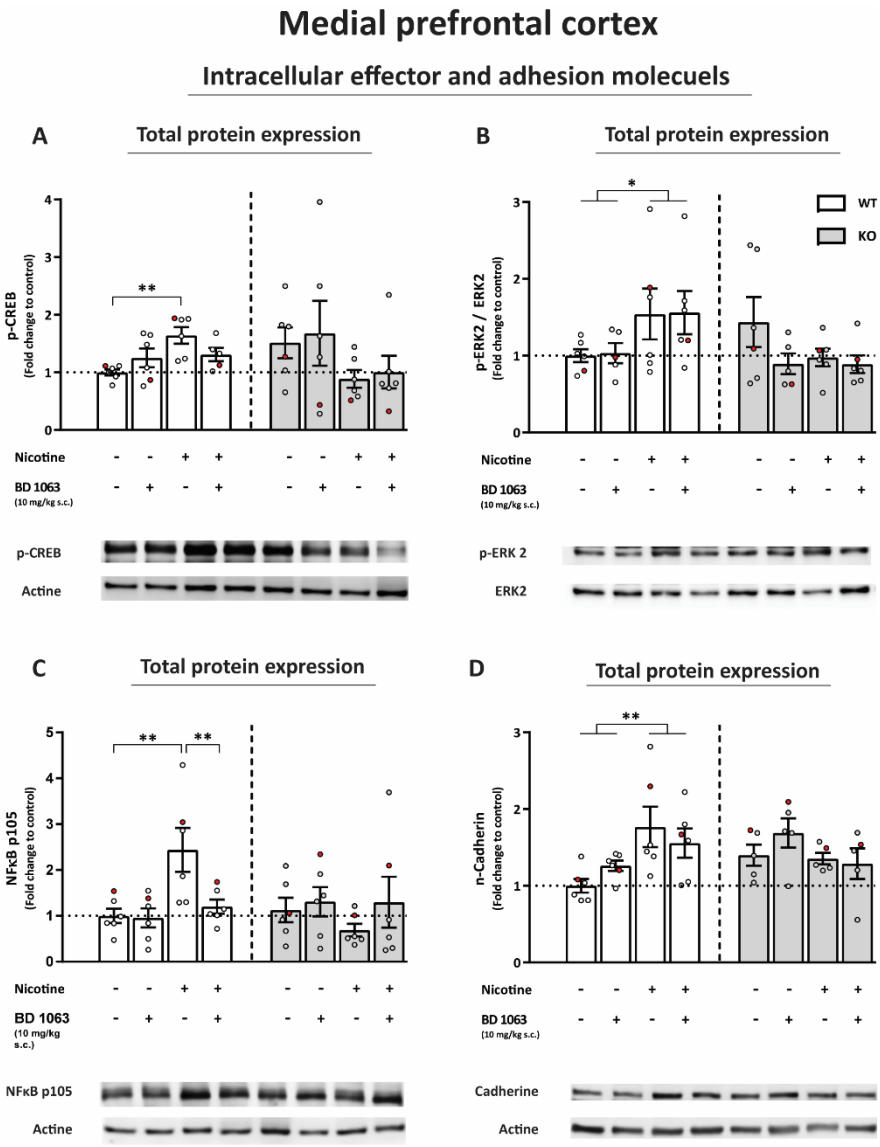

Figure 57. Relative total protein expression of intracellular effectors and adhesion molecules

A: Total protein expression of ppCREB. B**:** Total protein expression of p-ERK normalized to ERK **C:** Total protein expression NFκB p105 **D:** Total protein expression of n-Cadherin. Data are expressed as mean ±SEM. *p<0.05, **p<0.01. **Abbreviations:** Phosphorylated cAMP response element binding protein (p-CREB), nuclear factor kappa-light-chain-enhancer of activated B cells (NFκB), phosphorylated extracellular signal-regulated kinase (p-ERK)

Relative mRNA expression in the NAc

In the NAc, relative mRNA expression of WT (n=4-6) and Sig-1R KO mice (n=3-6) was quantified as previously explained. Detailed statistical analysis is shown elsewhere (see

Sig-1R

Sig-1 mRNA was significantly increased in mice that were exposed to nicotine compared to animals that were exposed to saline ($p<0.01$). BD 1063 had no effect on Sig-1R mRNA expression. Sig-1R mRNA was not detectable in KO animals (Figure 58A, Table 4).

GluT1

Relative mRNA expression of the GluT was significantly decreased after the reinstatement of nicotine-seeking in animals previously self-administering nicotine compared to saline control groups ($p<0.01$). No differences were obtained among KO animals (Figure 58B, Table 4).

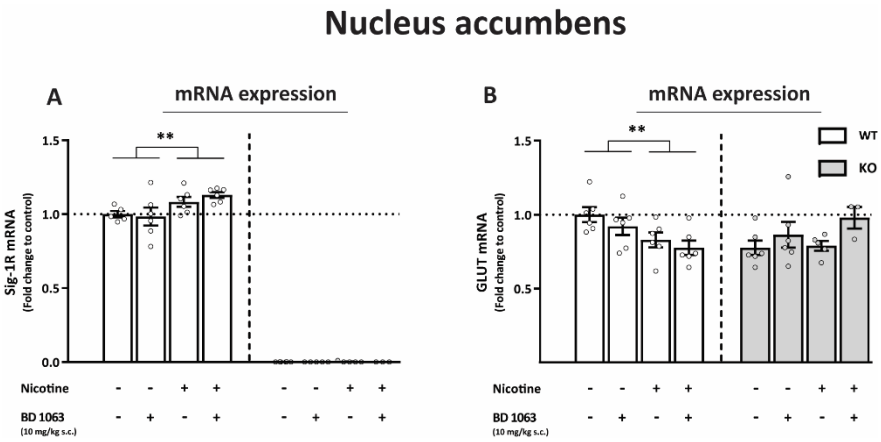

Figure 58 Relative mRNA expression in the NAc.
A: Sig-1R. **B:** GluT. Data are expressed as mean ±SEM. **p<0.01. **Abbreviations:** Glutamate transporter (GLUT), sigma-1 receptor (Sig-1R).

Relative protein expression in the NAc

Relative protein expression of WT (n=4-6) and Sig-1R KO mice (n=4-6) was quantified as previously explained. Detailed statistical analysis is shown elsewhere (see

Glutamate receptors

Relative total and cell surface expression of glutamatergic receptors, including NMDARs, AMPARs and the mGluR2/3 was assessed after cue-induced reinstatement of nicotine-seeking.

NMDAR

Relative total and cell surface protein expression of the NMDAR subunits NR1, NR2A and NR2B, as well as phosphorylation of the NR1 subunit at Ser 890,896 and 897, were tested in WT and KO mice after cue-induced reinstatement of nicotine-seeking.

1. *NR1 subunit*

Total protein expression was significantly increased after nicotine relapse in mice exposed to nicotine compared to saline exposed groups ($p<0.01$). Total protein levels remained unchanged in KO mice (Suppl.Fig. 4A, Table 9).

Cell surface protein expression of the NMDAR NR1 subunit was significantly increased after the reinstatement of nicotine-seeking in vehicle-treated mice that self-administered nicotine prior to extinction compared to saline control mice ($p<0.05$). Pretreatment with BD 1063 blocked the observed increase ($p<0.05$). No differences were observed in the cell surface expression in KO mice (Figure 59A, Table 9).

1.1. p-NR1 (Ser890)

The phosphorylation of the NMDAR subunit NR1 at Ser890 was not altered in any of the experimental groups (Suppl.Fig. 4D, Table 9).

1.2. p-NR1 (Ser896)

Phosphorylation at Ser896 of the NR1 subunit was significantly decreased after the reinstatement of nicotine-seeking in animals previously exposed to nicotine compared to saline control groups ($p<0.05$). BD 1063 did not alter phosphorylation. No differences were obtained comparing groups of Sig-1 KO mice (Suppl.Fig. 4E, Table 9).

1.3. p-NR1 (Ser897)

The phosphorylation of the NMDAR subunit NR1 at Ser897 remained unchanged in all experimental groups (Suppl.Fig. 4F, Table 9).

2. NR2A subunit

Total protein expression of the NR2A subunit was significantly increased in WT mice previously exposed to nicotine compared to saline control groups. Treatment with BD 1063 did not alter protein expression. NR2A was not modified in KO mice (Suppl.Fig. 4B, Table 9).

Cell surface protein expression of the NR2A subunit was significantly increased after the reinstatement of nicotine-seeking in vehicle-treated mice that self-administered nicotine prior to extinction compared to saline control mice ($p<0.01$). Pretreatment with BD 1063 blunted this increase ($p<0.01$). No differences were observed in the cell surface expression in KO mice (Figure 59B, Table 9).

3. NR2B subunit

Total protein expression of the NR2B subunit increased significantly upon reinstatement of nicotine-seeking in vehicle-treated WT mice that had self-administered nicotine in the acquisition phase compared to saline control groups ($p<0.05$). BD 1063 did not alter protein expression. In contrast, NR2B expression was significantly decreased in KO mice that were previously exposed to nicotine compared to saline control groups ($p<0.05$). BD 1063 treatment did not modify protein expression (Suppl.Fig. 4C, Table 9).

Cell surface expression was significantly increased in vehicle-treated WT mice after nicotine relapse compared to saline control mice ($p<0.05$). BD 1063 did not significantly change cell surface expression. In KO mice, cell surface expression of NR2B was significantly decreased after nicotine relapse in mice previously exposed to nicotine compared to saline groups ($p<0.05$) (Figure 59C, Table 9).

AMPAR

Relative total and cell surface protein expression of the AMPAR subunits GluR1 and GluR2 were tested in WT and KO mice after cue-induced reinstatement of nicotine-seeking.

1. GluR1 subunit

Total protein expression after cue-induced reinstatement of nicotine-seeking was strikingly increased in WT mice that were exposed to nicotine compared to saline groups ($p<0.001$) but decreased in KO mice comparing nicotine and saline exposed animals ($p<0.05$) (Suppl.Fig. 4G Table 9).

The cell surface expression did not significantly change after nicotine relapse in any experimental group (Suppl.Fig. 4H Table 9).

2. GluR2 subunit

Total protein expression of the AMPAR subunit GluR2 remained unchanged in all experimental groups (Suppl.Fig. 4I Table 9).

In contrast, cell surface expression significantly increased upon cue-induced reinstatement of nicotine-seeking in WT animals that self-administered nicotine in the acquisition phase compared to saline groups ($p<0.05$). The GluR2 subunit remained unchanged in KO mice (Figure 59D, Table 9).

mGluR2/3

Total and cell surface expression of the mGluR2/3 was not modified in any group after cue-induced reinstatement of nicotine-seeking (Suppl.Fig. 4J, K, Table 9).

μ-opioid receptor

Total and cell surface expression of the MOR was not modified in any group after cue-induced reinstatement of nicotine-seeking (Suppl.Fig. 5A, B, Table 10).

nAChRs and their negative modulator

Relative total and cell surface protein expression of the nAChR subunits α4 and β2, and the negative modulator LynX1 were tested in the different groups of WT and KO mice after cue-induced reinstatement of nicotine-seeking. In KO mice, no significant main effects of drug or treatment, nor a significant interaction between both factors was revealed in KO mice in any protein tested (Table 11).

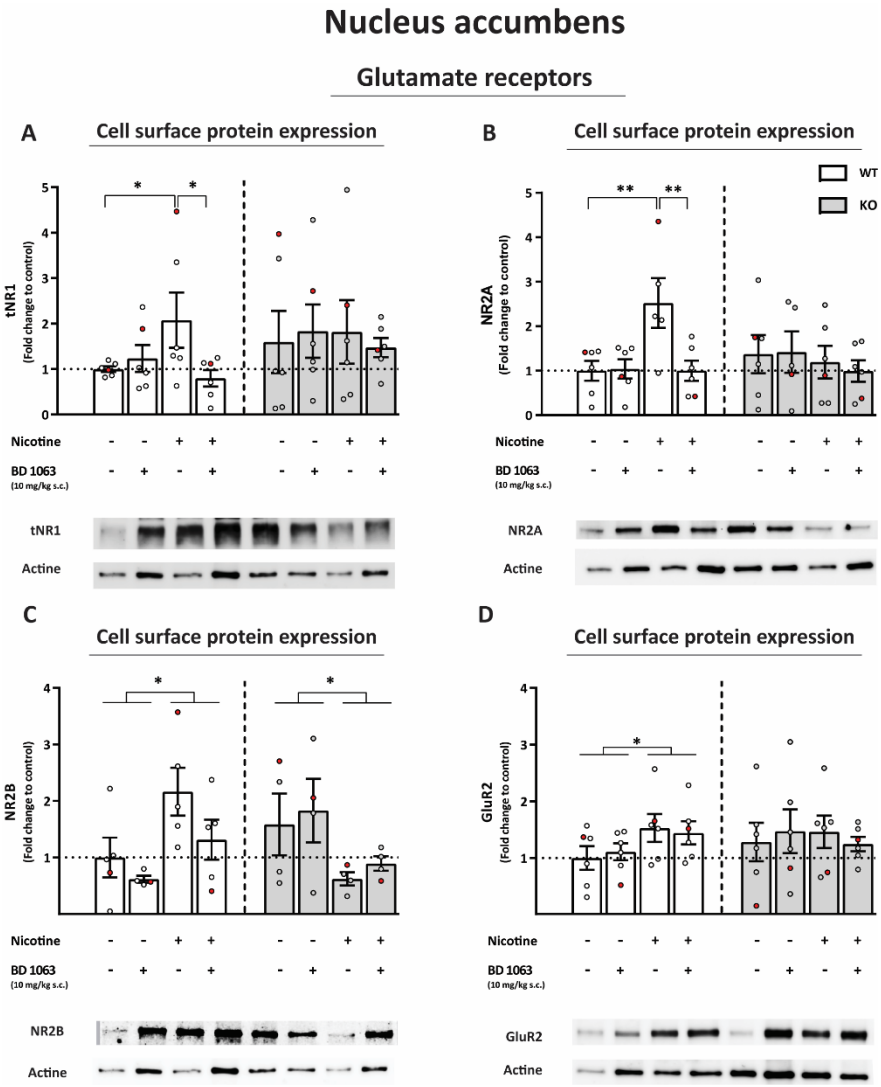

Figure 59. Relative total and cell surface protein expression of glutamate receptors
A: Cell surface protein expression of the NR1 subunit. **B:** Cell surface protein expression of the NR2A subunit. **C:** Cell surface protein expression of the NR2B subunit. **D:** Cell surface protein expression of the GluR2. Data are expressed as mean ±SEM. +p<0.05, **p<0.01. **Abbreviations:** Glutamate receptor2 (GluR2), N-methyl-D-aspartate receptor subunit 1 (NR1).

nAChR

1. *α4 subunit*

Total protein expression of the α4 nAChR subunit was significantly increased upon reinstatement of nicotine-seeking in animals with a history of nicotine self-administration compared to saline control groups ($p<0.01$). (Figure 60A, Table 11).

The same result was obtained for the cell surface expression of the α4 nAChR subunit ($p<0.05$) (Figure 60B, Table 11).

2. *β2 subunit*

The total protein expression of the β2 nAChR subunit was not altered after cue-induced reinstatement of nicotine-seeking (Figure 60C, Table 11).

In contrast, cell surface expression increased significantly in vehicle-treated WT mice exposed to nicotine compared to the vehicle-treated saline control group ($p<0.05$). Pretreatment with BD 1063 blocked this increase ($p<0.05$) (Figure 60D, Table 11).

LynX1

No significant differences were obtained quantifying the total and cell surface protein expression of LynX1 after cue-induced reinstatement of nicotine-seeking (Suppl.Fig. 5D, E, Table 10).

Intracellular effectors and adhesion proteins

Relative total protein expression of p-CREB, p-ERK2, ERK2, NFκB p50, NFκB p105, ΔFosB, and n-cadherin were quantified in the different groups of WT and KO mice after cue-induced reinstatement of nicotine-seeking.

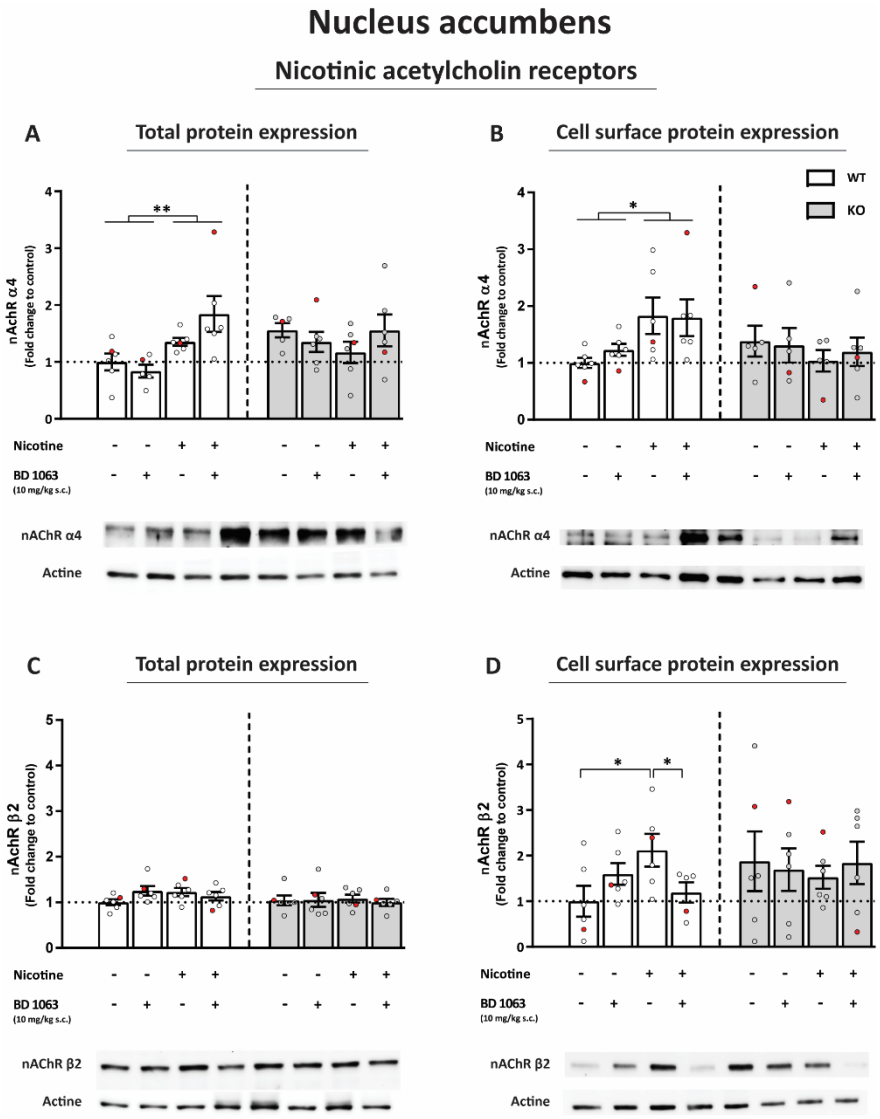

Figure 60 Relative total and cell surface protein expression of nAChRs in the NAc.
A: Total protein expression of the nAChR α4 subunit. **B:** Cell surface protein expression of the nAChR α4 subunit. **C:** Total protein expression of the nAChR β2 subunit. **D:** Cell surface protein expression of the nAChR β2 subunit. Data are expressed as mean ±SEM. *p<0.05, **p<0.01. **Abbreviations:** nicotinic acetylcholine receptor (nAChR)

p-CREB

p-CREB expression increased upon reinstatement of nicotine-seeking in WT mice exposed to nicotine compared to saline control groups ($p<0.05$). BD 1063 did not alter the levels of p-CREB. Protein levels remained unchanged in Sig-1R KO mice (Figure 61A, Table 12).

p-ERK2/ERK2

The ratio of p-ERK2/ERK2 was not modified after cue-induced reinstatement od nicotine-seeking in any experimental group (Suppl.Fig. 5C, Table 12).

NFκB

NFκB p50 protein levels did not alter upon nicotine relapse in any experimental group (Suppl.Fig. 5C, F, Table 12).

Protein levels of NFκB p105 were increased after nicotine relapse in WT but not in KO mice that previously self-administered nicotine in the acquisition phase ($p<0.05$). Bd 1063 did not change the protein expression of NFκB p105 in WT or KO mice (Figure 61C, Table 12).

ΔFosB

Levels of ΔFosB were significantly increased in WT but not in KO mice that were exposed to nicotine compared to saline groups ($p<0.05$) (Figure 61B, Table 12).

n-Cadherin

WT mice exposed to nicotine showed increased protein levels of n-cadherin after the reinstatement of nicotine-seeking compared to saline control mice ($p<0.05$). In contrast, n-cadherin decreased after cue-induced

reinstatement in KO mice that were exposed to nicotine compared to saline control groups ($p<0.05$)) (Figure 61D, Table 12).

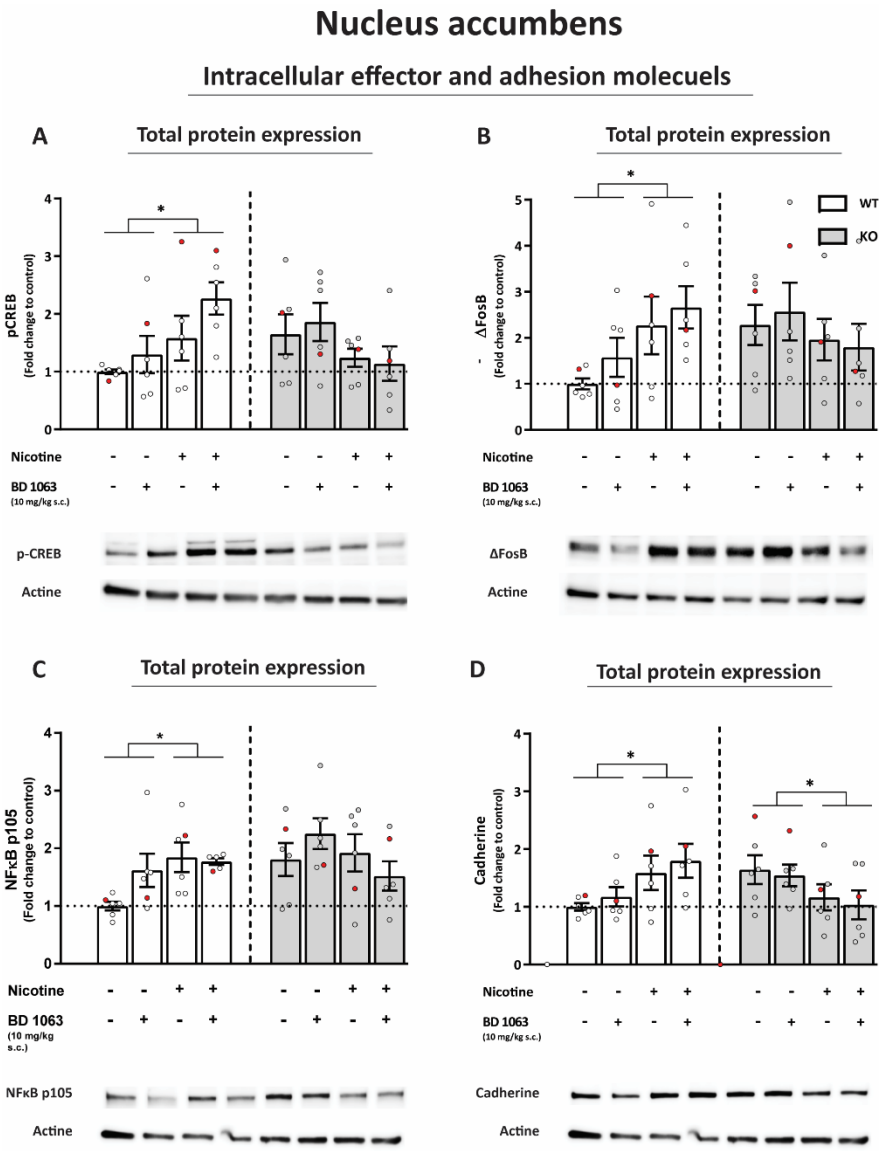

Figure 61 Relative total protein expression of intracellular effectors and adhesion molecules in the NAc.

A: Total protein expression of pCREB. B**:** Total protein expression of ΔFosB. **C:** Total protein expression NFκB p105 **D:** Total protein expression of n-Cadherin. Data are expressed as mean ±SEM. *p<0.05. **Abbreviations:** Phosphorylated cAMP response element binding protein (p-CREB), nuclear factor kappa-light-chain-enhancer of activated B cells (NFκB).

The implication of the Sigma-1 receptor in the reinforcing properties of palatable food and the cue-induced reinstatement of food-seeking

We performed a second study under similar conditions as explained for nicotine, but with chocolate-flavored pellets as reinforcer, to study the involvement of Sig-1Rs in the reinforcing properties and the relapse to a natural reward. Therefore, a new cohort of Sig-1R KO and WT mice were trained to self-administer palatable chocolate-flavored food pellets (20mg/pellet) under an FR1 (5 days), and FR3 (5 days) schedule of reinforcement. In the acquisition phase, three-way ANOVA revealed significant main effects of nose-poke [$F_{1,43}$ = 469.9; p<0.001], day [$F_{9,387}$ = 75.54; p<0.001], but not of genotype [$F_{1,43}$ = 1.61; n.s.]. Furthermore, significant interactions between nose-poke and day [$F_{9,387}$ = 73.73; p<0.001], day and genotype [$F_{9,387}$ = 2.02; p<0.05], among all three factors [$F_{9,387}$ = 1.97; p<0.05] but not between nose-poke and genotype were obtained [$F_{9,387}$ = 1.89; n.s.]. However, subsequent Newman-Keuls *post-hoc* analysis showed no significant differences in active responding between genotypes during the acquisition phase (Figure 62A). Two-way ANOVA repeated measures of the area under the curve demonstrated a significant effect of nose-poke [$F_{1,43}$ = 417.87; p<0.001] but not of genotype [$F_{1,43}$ = 1.37; n.s.], nor a significant interaction between both factors [$F_{1,43}$ = 1.54; n.s.] (Figure 62B).The acquisition criteria were fulfilled by all mice of both genotypes.

The motivation for palatable food was tested under a PR schedule of reinforcement and WT and Sig-1R KO animals were treated with either vehicle or BD 1063 (10mg/kg s.c.) 1h prior to testing. Two-way ANOVA revealed a significant main effect of genotype [$F_{1,41}$ = 4.89; p<0.05], but not

of treatment [$F_{1,41}$ = 1.01; n.s.] nor the interaction between both factors [$F_{1,41}$ = 0.13; n.s.] (Figure 62C).

In the extinction phase, WT and Sig-1R KO mice were trained to decrease operant behavior to 30% of the average of the last three days of the acquisition phase. All mice achieved extinction criterion. Three-way ANOVA repeated measures revealed significant main effects of nose-poke [$F_{1,43}$ = 186.76; p<0.001] and day [$F_{9,387}$ = 44.12; p<0.001], but not of genotype [$F_{1,43}$ = 0.04; n.s.]. The interaction between day and nose-poke was significant [$F_{9,387}$ = 1.97; p<0.001]. No significant interaction between nose-poke and genotype [$F_{1,43}$ = 1.94; n.s.], day and genotype [$F_{9,387}$ = 2.86; p=0.09], or among all three factors was revealed [$F_{9,387}$ = 1.09; n.s.]. (Figure 62F). Mice were tested for cue-induced reinstatement of food-seeking behavior after a minimum of 10 daily extinction session or whenever the extinction criterion was reached. WT and Sig-1R KO mice were treated with either vehicle or BD 1063 (10mg/kg s.c.). Three-way ANOVA repeated measures demonstrated significant main effects of nose-poke [$F_{1,41}$ = 100.16; p<0.001], treatment [$F_{1,41}$ = 7.37; p<0.01], and genotype [$F_{1,41}$ = 4.32; p<0.05]. Furthermore, a significant interaction between genotype and treatment [$F_{1,41}$ = 6.34; p<0.05], nose-poke and treatment [$F_{1,41}$ = 4.1; p<0.05], nose-poke and genotype [$F_{1,41}$= 6.46; p<0.05], as well as the interaction among all three factors was obtained [$F_{1,41}$ = 9.36; p=0.01]. Newman-Keuls *post-hoc* analysis revealed a significant decrease in the number of active responses comparing Sig-1R KO mice (vehicle) to WT mice (vehicle) (p<0.001). In addition, the Sig-1R antagonist decreased significantly active responding of WT mice (p<0.001) but had no effect in Sig-1R KO mice. No differences were obtained in the number of inactive responses among groups (Figure 62G).

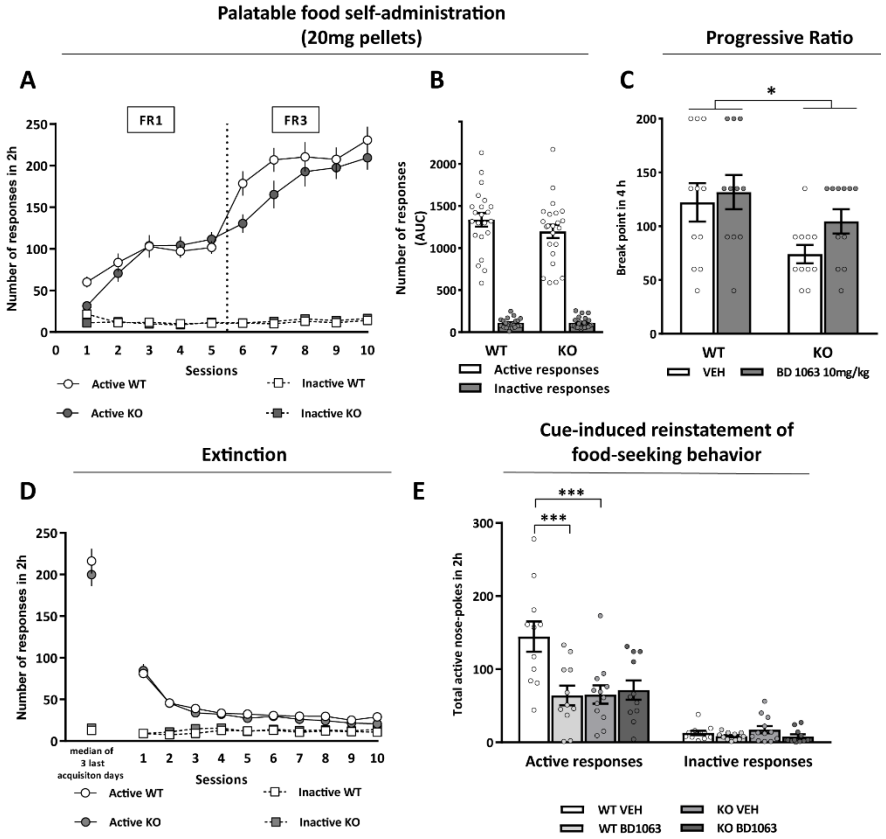

Figure 62. Cue-induced reinstatement of nicotine-seeking behavior.
A: Time course of active and inactive responding of WT (n=22) and Sig-1R KO (n=23) mice of palatable food SA. **B:** Area under the curve of active and inactive responses. **C:** Test for motivation for palatable food under a progressive ratio schedule. Mice were treated with either BD1063 (10mg/kg s.c.) one hour prior to testing ($n_{WT\ VEH}$=11, $n_{WT\ BD}$=11, $n_{KO\ VEH}$=12, $n_{KO\ BD}$=11). **D:** Time course of active and inactive responding of WT (n=22) and Sig-1R KO (n=23) mice extinguishing operant behavior after food self-administration. **E:** Cue-induced reinstatement of food-seeking behavior after extinction of operant behavior. Mice were treated with either BD1063 (10mg/kg s.c.) one hour prior to testing ($n_{WT\ VEH}$=11, $n_{WT\ BD}$=11, $n_{KO\ VEH}$=12, $n_{KO\ BD}$=11). Data are expressed as mean ±SEM. *p<0.05, ***p<0.001. **Abbreviations:** Knockout (KO), vehicle (VEH), wildtype (WT)

Supplementary results

Study 2

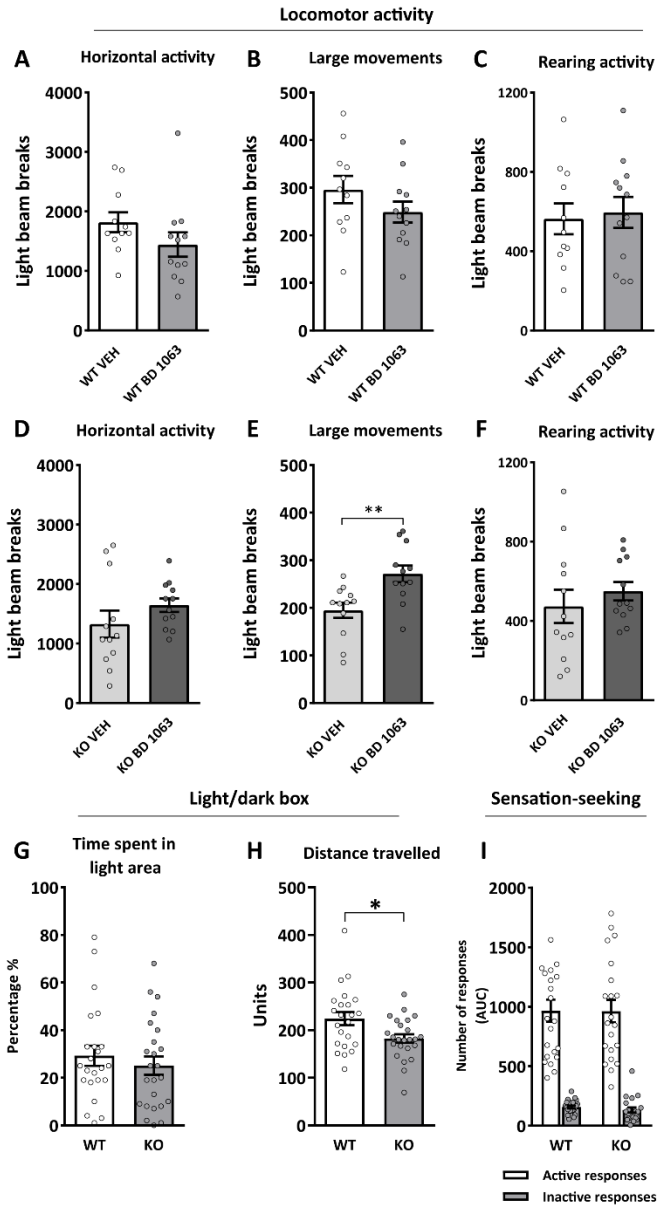

Suppl.Fig. 1. Phenotypic characterization of Sig-1R KO mice.
A-F: Locomotor activity of WT and Sig-1R KO mice treated with BD 1063 (10mg/kg) 1h prior to testin ($n_{WT\ VEH}$=11, $n_{WT\ BD}$=12, $n_{KO\ VEH}$=12, $n_{KO\ BD}$=12). **G, H:** Anxiety-like behavior of WT (n=23) and Sig-1R KO (n=24) mice in a light/dark box. **I:** Operant responding of WT (n=21) and Sig-1R KO (n=21) mice in a model of sensation-seeking. Data are expressed as mean ±SEM. *p<0.05, **p<0.01, ***p<0.001. **Abbreviations:** Knockout (KO), vehicle (VEH), wild type (WT).

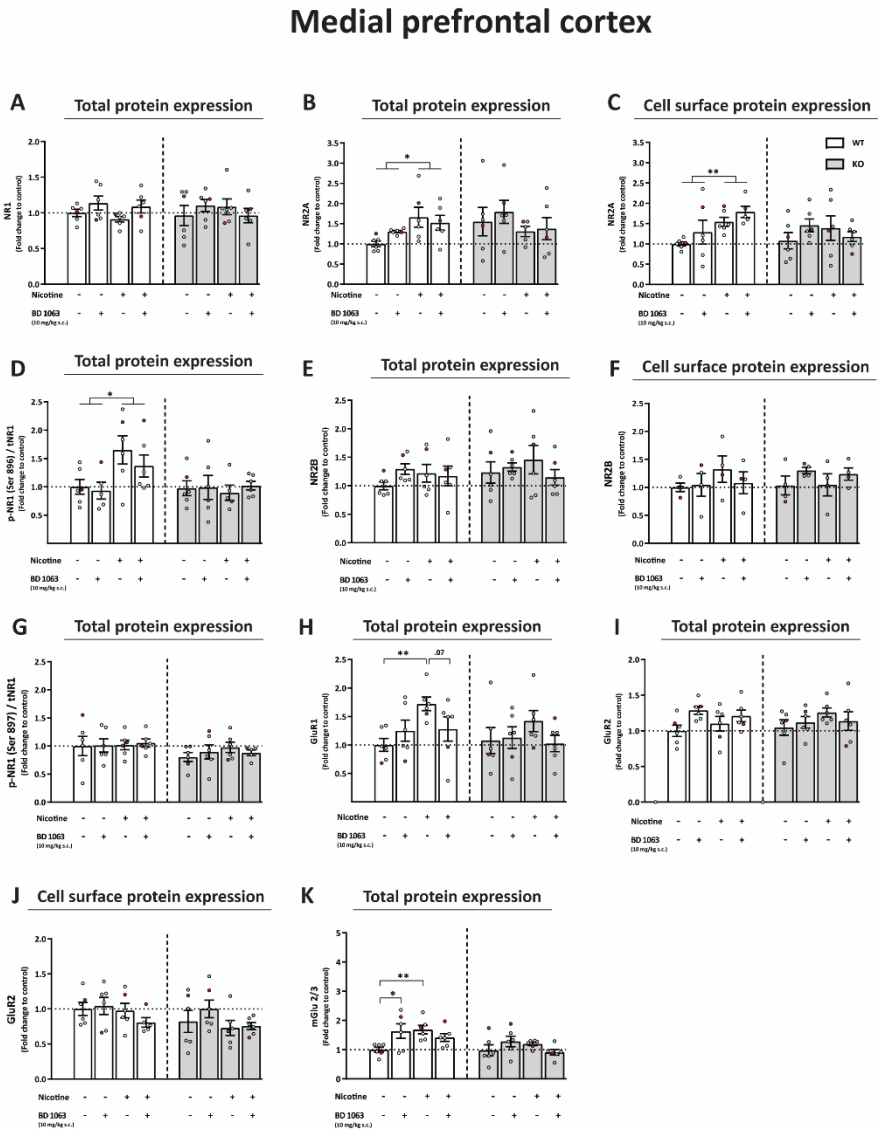

Suppl.Fig. 2.Relative total and cell surface protein expression of glutamate recpetors in the mPFC.

A: Total protein expression of the NR1 subunit. **B, C:** Total and cell surface protein expression of the NR2A subunit. **D:** Total protein expression of the p-NR1(Ser896) subunit. **E, F:** Total and cell surface protein expression of the NR2B subunit. **G:** Total protein expression of the p-NR1(Ser897) subunit. **H:** Total protein expression of the GluR1 subunit. **I, J:** Total and cell surface protein expression of the GluR2 subunit. **K:** Total protein expression of the mGluR2/3. Data are expressed as mean ±SEM. *p<0.05, **p<0.01. **Abbreviations:** Glutamate receptor subunit (GluR), metabotropic glutamate receptor (mGluR), N-methyl-D-aspartate receptor subunit (NR), phosphorylated N-methyl-D-aspartate receptor subunit 1 (p-NR1).

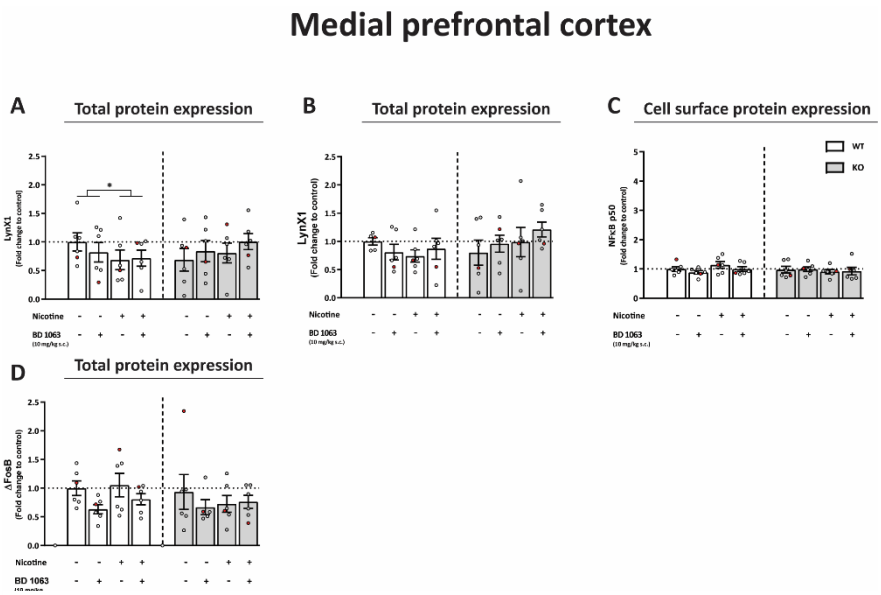

Suppl.Fig. 3. Relative total and cell surface protein expression in the mPFC.
A, B: Total and cell surface protein expression of LynX1. **C:** Total protein expression of NFκB p50. **D:** Total protein expression of ΔFosB. Data are expressed as mean ±SEM. *p<0.05.
Abbreviations: Nuclear factor kappa-light-chain-enhancer of activated B cells (NFκB).

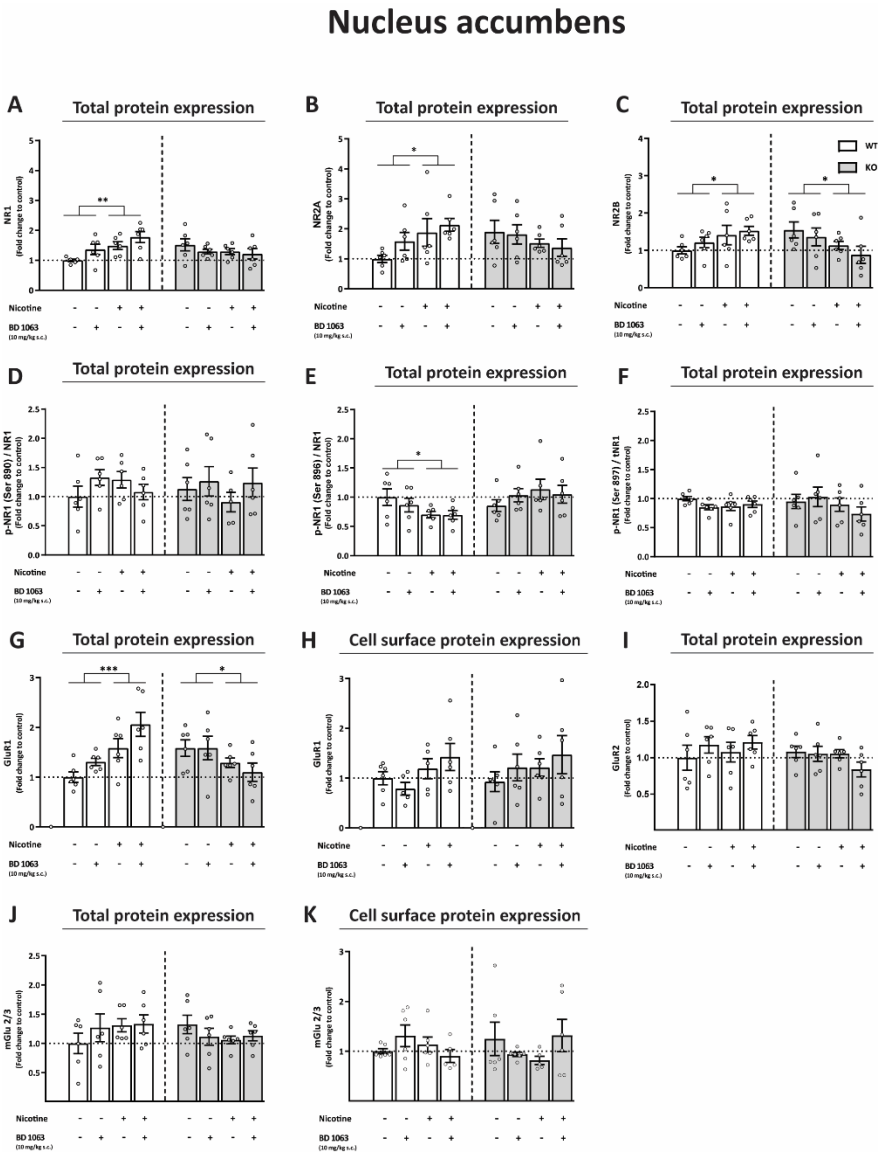

Suppl.Fig. 4. Relative total and cell surface protein expression of glutamate receptors in the NAc

A: Total protein expression of the NR1 subunit. **B:** Total protein expression of the NR2A subunit. **C:** Total protein expression of the NR2B subunit. **D:** Total protein expression of the p-NR1(Ser890) subunit. **E:** Total protein expression of the p-NR1(Ser896) subunit. **F:** Total protein expression of the p-NR1(Ser897) subunit. **G, H:** Total and cell surface protein expression of the GluR1 subunit. **I:** Total protein expression of the GluR2 subunit. **J, K:** Total and cell surface protein expression of the mGluR2/3. Data are expressed as mean ±SEM. *p<0.05, **pz0.01, ***p<0.001. **Abbreviations:** Glutamate receptor subunit (GluR), metabotropic glutamate receptor (mGluR), N-methyl-D-aspartate receptor subunit (NR), phosphorylated N-methyl-D-aspartate receptor subunit 1 (p-NR1).

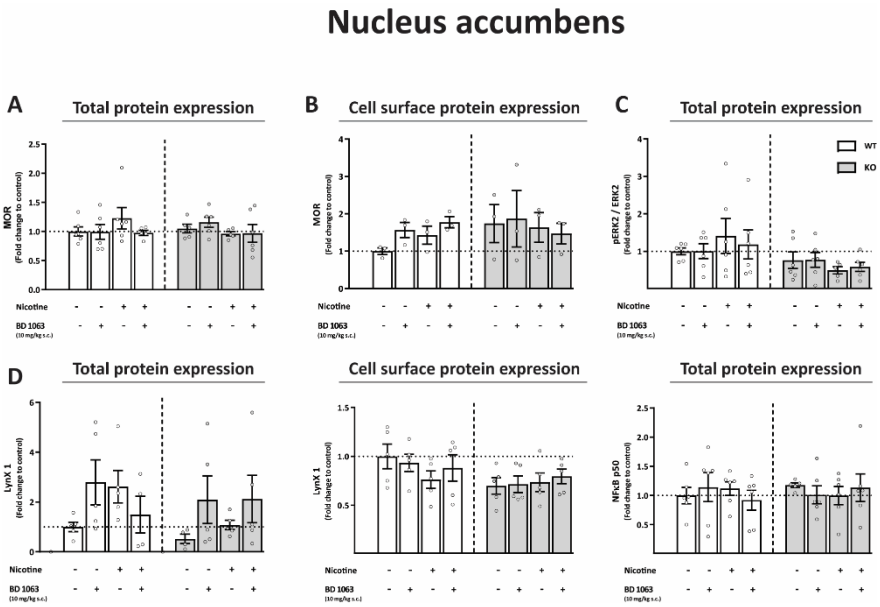

Suppl.Fig. 5. Relative total and cell surface protein expression in the NAc.
A, B: Total and cell surface protein expression of MOR. **C:** Total protein expression of the ratio of p-ERK2/ERK2. **D,E:** Total and cell surface protein expression of LynX1.**F:**Total protein expression of NFκB p50. Data are expressed as mean ±SEM. **Abbreviations:** extracellular signal-regulated kinase (ERK), μ-opioid receptor (MOR), nuclear factor kappa-light-chain-enhancer of activated B cells (NFκB), phosphorylated extracellular signal-regulated kinase (p-ERK)

Table 3. Two-way ANOVA statistical analysis of relative mRNA expression in the mPFC.

Sigma-1 receptor					
Factor names	WT		KO		Figure number
	F(1,19)	p-value	F(1,15)	p-value	
DRUG	**11.19**	**p<0.01**	0.14	n.s.	Figure 46A
TREATMENT	**4.63**	**p<0.05**	0.67	n.s.	
DRUG × TREATMENT	**4.45**	**p<0.05**	1.6	n.s.	
Glutamate transporter					
Factor names	WT		KO		Figure number
	F(1,19)	p-value	F(1,19)	p-value	
DRUG	**5.4**	**p<0.05**	3.17	n.s.	Figure 46B
TREATMENT	**4.74**	p<0.05	1.39	n.s.	
DRUG × TREATMENT	6.**21**	**p<0.05**	1.73	n.s.	

Table 4. Two-way ANOVA statistical analysis of relative mRNA expression in the NAc.

Sigma-1 receptor					
Factor names	WT		KO		Figure number
	F(1,20)	p-value	F(1,15)	p-value	Figure 51A
DRUG	0.21	n.s.	0.72	n.s.	
TREATMENT	**16.55**	**p<0.001**	1.06	n.s.	
DRUG × TREATMENT	**8.46**	**p<0.01**	0.4	n.s.	
Glutamate transporter					
Factor names	WT		KO		Figure number
	F(1,20)	p-value	F(1,16)	p-value	Figure 51A
DRUG	**9.2**	**p<0.01**	0.87	n.s.	
TREATMENT	1.63	n.s.	4.09	n.s.	
DRUG × TREATMENT	0.06	n.s.	0.54	n.s.	

Table 5. Two-way ANOVA statistical analysis of relative total and cell surface protein expression of glutamate receptors in the mPFC.

NR1 Total protein expression					
Factor names	WT		KO		Figure number
	F(1,20)	p-value	F(1,20)	p-value	Suppl. Fig. 2A
DRUG	0.85	n.s.	0.01	n.s.	
TREATMENT	**4.52**	**p<0.05**	0.01	n.s.	
DRUG × TREATMENT	0.07	n.s.	1.41	n.s.	
NR1 Cell surface expression					
Factor names	WT		KO		Figure number
	F(1,16)	p-value	F(1,16)	p-value	Figure 47A
DRUG	**6.16**	**p<0.05**	0.02	n.s.	
TREATMENT	1.65	n.s.	0.88	n.s.	
DRUG × TREATMENT	0.03	n.s.	1.06	n.s.	
p-NR1 (Ser 890) Total protein expression					
Factor names	WT		KO		Figure number
	F(1,20)	p-value	F(1,20)	p-value	Figure 47B
DRUG	0.21	n.s.	1.038	n.s.	
TREATMENT	**16.55**	**p<0.001**	0.26	n.s.	
DRUG × TREATMENT	**8.46**	**p<0.01**	0.68	n.s.	
p-NR1 (Ser 896) Total protein expression					
Factor names	WT		KO		Figure number
	F(1,19)	p-value	F(1,19)	p-value	Suppl. Fig. 2D
DRUG	**8.11**	**p<0.05**	0.03	n.s.	
TREATMENT	0.84	n.s.	0.23	n.s.	
DRUG × TREATMENT	0.32	n.s.	0.14	n.s.	

p-NR1 (Ser 897) Total protein expression					
Factor names	WT		KO		Figure number
	F(1,20)	p-value	F(1,20)	p-value	Suppl. Fig. 2G
DRUG	0.06	n.s.	0.69	n.s.	
TREATMENT	0.03	n.s.	0.001	n.s.	
DRUG × TREATMENT	0.08	n.s.	0.98	n.s.	
NR2A Total protein expression					
Factor names	WT		KO		Figure number
	F(1,20)	p-value	F(1,19)	p-value	Suppl. Fig. 2B
DRUG	**7.64**	**p<0.05**	1.36	n.s.	
TREATMENT	0.28	n.s.	0.3	n.s.	
DRUG × TREATMENT	1.96	n.s.	0.09	n.s.	
NR2A Cell surface expression					
Factor names	WT		KO		Figure number
	F(1,19)	p-value	F(1,20)	p-value	Suppl. Fig. 2C
DRUG	**8.65**	**p<0.01**	0.01	n.s.	
TREATMENT	2.23	n.s.	0.16	n.s.	
DRUG × TREATMENT	0.02	n.s.	2.04	n.s.	
NR2B Total protein expression					
Factor names	WT		KO		Figure number
	F(1,20)	p-value	F(1,20)	p-value	Suppl. Fig. 2E
DRUG	0.14	n.s.	0.02	n.s.	
TREATMENT	0.9	n.s.	0.39	n.s.	
DRUG × TREATMENT	1.73	n.s.	1.36	n.s.	
NR2B Cell surface expression					
Factor names	WT		KO		Figure number
	F(1,12)	p-value	F(1,12)	p-value	Suppl. Fig. 2F
DRUG	0.92	n.s.	0.03	n.s.	
TREATMENT	0.28	n.s.	2.53	n.s.	
DRUG × TREATMENT	0.59	n.s.	0.07	n.s.	
GluR1 Total protein expression					
Factor names	WT		KO		Figure number
	F(1,20)	p-value	F(1,20)	p-value	Suppl. Fig. 2H
DRUG	**5.29**	**p<0.05**	0.4	n.s.	
TREATMENT	0.35	n.s.	0.83	n.s.	
DRUG × TREATMENT	**4.48**	**p<0.05**	1.39	n.s.	
GluR1 Cell surface expression					
Factor names	WT		KO		Figure number
	F(1,17)	p-value	F(1,20)	p-value	Figure 47C
DRUG	0.5	n.s.	2.0	n.s.	
TREATMENT	2.45	n.s.	1.75	n.s.	
DRUG × TREATMENT	**7.06**	**p<0.05**	1.76	n.s.	

GluR2 Total protein expression					
Factor names	WT		KO		Figure number
	F(1,20)	p-value	F(1,20)	p-value	Suppl. Fig. 2I
DRUG	0.02	n.s.	1.32	n.s.	
TREATMENT	**5.93**	**p<0.05**	0.06	n.s.	
DRUG × TREATMENT	1.2	n.s.	0.95	n.s.	
GluR2 Cell surface expression					
Factor names	WT		KO		Figure number
	F(1,19)	p-value	F(1,20)	p-value	Suppl. Fig. 2J
DRUG	1.61	n.s.	2.08	n.s.	
TREATMENT	0.37	n.s.	0.79	n.s.	
DRUG × TREATMENT	1.07	n.s.	0.43	n.s.	
mGluR2/3 Total protein expression					
Factor names	WT		KO		Figure number
	F(1,20)	p-value	F(1,20)	p-value	Suppl. Fig. 2K
DRUG	2.05	n.s.	0.29	n.s.	
TREATMENT	1.26	n.s.	0.003	n.s.	
DRUG × TREATMENT	**7.52**	**p<0.05**	4.32	n.s.	
mGluR2/3 Cell surface expression					
Factor names	WT		KO		Figure number
	F(1,15)	p-value	F(1,15)	p-value	Figure 47D
DRUG	2.52	n.s.	**5.58**	**p<0.05**	
TREATMENT	**8.14**	**p<0.05**	0.06	n.s.	
DRUG × TREATMENT	**7.78**	**p<0.05**	0.3	n.s.	

Table 6. Two-way ANOVA statistical analysis of relative total and cell surface protein expression of the MOR in the mPFC.

MOR Total protein expression					
Factor names	WT		KO		Figure number
	F(1,14)	p-value	F(1,15)	p-value	Figure 48A
DRUG	**6.67**	**p<0.05**	0.02	n.s.	
TREATMENT	1.03	n.s.	0.16	n.s.	
DRUG × TREATMENT	**4.93**	**p<0.05**	0.18	n.s.	
MOR Cell surface expression					
Factor names	WT		KO		Figure number
	F(1,19)	p-value	F(1,19)	p-value	Figure 48B
DRUG	3.6	n.s.	0.15	n.s.	
TREATMENT	0.13	n.s.	2.13	n.s.	
DRUG × TREATMENT	0.0003	n.s.	0.17	n.s.	

Table 7. Two-way ANOVA statistical analysis of relative total and cell surface protein expression of nAChRs and their modulators in the mPFC.

nAChR α4 Total protein expression					
Factor names	WT		KO		Figure number
	F(1,20)	p-value	F(1,20)	p-value	
DRUG	**12.18**	**p<0.01**	0.2	n.s.	Figure 49A
TREATMENT	1.95	n.s.	1.19	n.s.	
DRUG × TREATMENT	**17.49**	**0.001**	1.71	n.s.	
nAChR α4 Cell surface expression					
Factor names	WT		KO		Figure number
	F(1,15)	p-value	F(1,16)	p-value	
DRUG	1.17	n.s.	0.07	n.s.	Figure 49B
TREATMENT	1.64	n.s.	0.02	n.s.	
DRUG × TREATMENT	**5.42**	**p<0.05**	2.22	n.s.	
nAChR β2 Total protein expression					
Factor names	WT		KO		Figure number
	F(1,20)	p-value	F(1,20)	p-value	
DRUG	**4.69**	**p<0.05**	0.03	n.s.	Figure 49C
TREATMENT	0.01	n.s.	0.04	n.s.	
DRUG × TREATMENT	0.67	n.s.	1.77	n.s.	
nAChR β2 Cell surface expression					
Factor names	WT		KO		Figure number
	F(1,20)	p-value	F(1,20)	p-value	
DRUG	2.44	n.s.	2.29	n.s.	Figure 49D
TREATMENT	0.21	n.s.	0.01	n.s.	
DRUG × TREATMENT	**7.78**	**p<0.05**	0.21	n.s.	
LynX1 Total protein expression					
Factor names	WT		KO		Figure number
	F(1,20)	p-value	F(1,20)	p-value	
DRUG	**8.67**	**p<0.01**	0.3	n.s.	Suppl. Fig. 3A
TREATMENT	0.86	n.s.	0.33	n.s.	
DRUG × TREATMENT	1.46	n.s.	0.001	n.s.	
LynX1 Cell surface expression					
Factor names	WT		KO		Figure number
	F(1,19)	p-value	F(1,20)	p-value	
DRUG	0.26	n.s.	1.24	n.s.	Suppl. Fig. 3B
TREATMENT	0.15	n.s.	2.13	n.s.	
DRUG × TREATMENT	0.86	n.s.	0.03	n.s.	

Table 8. Two-way ANOVA statistical analysis of relative total and cell surface protein expression of intracellular effectors and adhesion molecules in the mPFC.

p-CREB Total protein expression					
Factor names	WT		KO		Figure number
	F(1,19)	p-value	F(1,20)	p-value	Figure 50A
DRUG	**7.52**	**p<0.05**	3.41	n.s.	
TREATMENT	0.09	n.s.	0.16	n.s.	
DRUG × TREATMENT	**5.27**	**p<0.05**	0.005	n.s.	
p-ERK2/ERK Total protein expression					
Factor names	WT		KO		Figure number
	F(1,19)	p-value	F(1,19)	p-value	Figure 50B
DRUG	**5.01**	**p<0.01**	1.35	n.s.	
TREATMENT	0.01	n.s.	2.48	n.s.	
DRUG × TREATMENT	0.001	n.s.	1.3	n.s.	
NFκB p50 Total protein expression					
Factor names	WT		KO		Figure number
	F(1,20)	p-value	F(1,20)	p-value	Suppl. Fig. 3C
DRUG	2.21	n.s.	0.42	n.s.	
TREATMENT	2.37	n.s.	0.03	n.s.	
DRUG × TREATMENT	0.02	n.s.	0.001	n.s.	
NFκB p105 Total protein expression					
Factor names	WT		KO		Figure number
	F(1,20)	p-value	F(1,20)	p-value	Figure 50C
DRUG	**8.83**	**p<0.01**	0.4	n.s.	
TREATMENT	**5.12**	**p<0.05**	1.26	n.s.	
DRUG × TREATMENT	**4.44**	**p<0.05**	0.36	n.s.	
ΔFosB Total protein expression					
Factor names	WT		KO		Figure number
	F(1,20)	p-value	F(1,19)	p-value	Suppl. Fig. 3D
DRUG	0.7	n.s.	0.39	n.s.	
TREATMENT	**5.13**	**p<0.05**	0.1	n.s.	
DRUG × TREATMENT	0.2	n.s.	1.24	n.s.	
n-Cadherin Total protein expression					
Factor names	WT		KO		Figure number
	F(1,20)	p-value	F(1,17)	p-value	Figure 50D
DRUG	**9.54**	**p<0.01**	0.01	n.s.	
TREATMENT	0.02	n.s.	1.27	n.s.	
DRUG × TREATMENT	1.9	n.s.	0.01	n.s.	

Table 9. Two-way ANOVA statistical analysis of relative total and cell surface protein expression of glutamate receptors in the NAc.

NR1 Total protein expression					
Factor names	WT		KO		Figure number
	F(1,20)	p-value	F(1,20)	p-value	Suppl. Fig.4A
DRUG	**9.86**	**p<0.01**	1.09	n.s.	
TREATMENT	**5.16**	**p<0.05**	1.06	n.s.	
DRUG × TREATMENT	0.07	n.s.	0.25	n.s.	
NR1 Cell surface expression					
Factor names	WT		KO		Figure number
	F(1,20)	p-value	F(1,20)	p-value	Figure 52A
DRUG	0.83	n.s.	0.01	n.s.	
TREATMENT	2.2	n.s.	0.01	n.s.	
DRUG × TREATMENT	**3.43**	**p<0.05**	0.25	n.s.	
p-NR1 (Ser 890) Total protein expression					
Factor names	WT		KO		Figure number
	F(1,20)	p-value	F(1,19)	p-value	Suppl. Fig.4D
DRUG	0.89	n.s.	0.3	n.s.	
TREATMENT	0.15	n.s.	1.06	n.s.	
DRUG × TREATMENT	3.19	n.s.	0.2	n.s.	
p-NR1 (Ser 896) Total protein expression					
Factor names	WT		KO		Figure number
	F(1,20)	p-value	F(1,20)	p-value	Suppl. Fig.4E
DRUG	**5.07**	**p<0.05**	1.14	n.s.	
TREATMENT	0.46	n.s.	0.12	n.s.	
DRUG × TREATMENT	0.39	n.s.	0.89	n.s.	
p-NR1 (Ser 897) Total protein expression					
Factor names	WT		KO		Figure number
	F(1,20)	p-value	F(1,20)	p-value	Suppl. Fig.4F
DRUG	0.46	n.s.	1.72	n.s.	
TREATMENT	1.09	n.s.	0.08	n.s.	
DRUG × TREATMENT	3.0	n.s.	0.8	n.s.	
NR2A Total protein expression					
Factor names	WT		KO		Figure number
	F(1,20)	p-value	F(1,19)	p-value	Suppl. Fig.4B
DRUG	**5.68**	**p<0.05**	1.89	n.s.	
TREATMENT	1.94	n.s.	0.16	n.s.	
DRUG × TREATMENT	0.3	n.s.	0.01	n.s.	

NR2A Cell surface expression					
Factor names	WT		KO		Figure number
	F(1,19)	p-value	F(1,20)	p-value	
DRUG	**5.59**	**p<0.05**	1.68	n.s.	Figure 52B
TREATMENT	**5.59**	**p<0.05**	0.31	n.s.	
DRUG × TREATMENT	**6.17**	**p<0.05**	0.89	n.s.	
NR2B Total protein expression					
Factor names	WT		KO		Figure number
	F(1,20)	p-value	F(1,20)	p-value	
DRUG	**4.76**	**p<0.05**	**4.83**	**p<0.05**	Suppl. Fig.4C
TREATMENT	0.94	n.s.	1.13	n.s.	
DRUG × TREATMENT	0.09	n.s.	0.03	n.s.	
NR2B Cell surface expression					
Factor names	WT		KO		Figure number
	F(1,15)	p-value	F(1,12)	p-value	
DRUG	**7.09**	**p<0.05**	**5.59**	**p<0.05**	Figure 52C
TREATMENT	3.11	n.s.	0.41	n.s.	
DRUG × TREATMENT	0.45	n.s.	0.001	n.s.	
GluR1 Total protein expression					
Factor names	WT		KO		Figure number
	F(1,20)	p-value	F(1,20)	p-value	
DRUG	**16.13**	**p<0.001**	**4.83**	**p<0.05**	Suppl. Fig.4G
TREATMENT	**5.53**	**p<0.05**	0.28	n.s.	
DRUG × TREATMENT	0.26	n.s.	0.29	n.s.	
GluR1 Cell surface expression					
Factor names	WT		KO		Figure number
	F(1,18)	p-value	F(1,20)	p-value	
DRUG	4.37	n.s.	1.0	n.s.	Suppl. Fig.4H
TREATMENT	0.003	n.s.	1.01	n.s.	
DRUG × TREATMENT	1.28	n.s.	0.003	n.s.	
GluR2 Total protein expression					
Factor names	WT		KO		Figure number
	F(1,20)	p	F(1,20)	p	
DRUG	0.18	n.s.	1.9	n.s.	Suppl. Fig.4I
TREATMENT	1.4	n.s.	1.95	n.s.	
DRUG × TREATMENT	0.03	n.s.	1.13	n.s.	
GluR2 Cell surface expression					
Factor names	WT		KO		Figure number
	F(1,20)	p-value	F(1,20)	p-value	
DRUG	**4.42**	**p<0.05**	0.01	n.s.	Figure 52D
TREATMENT	0.003	n.s.	0.002	n.s.	
DRUG × TREATMENT	0.23	n.s.	0.45	n.s.	

mGluR2/3 Total protein expression					
Factor names	WT		KO		Figure number
	F(1,20)	p-value	F(1,20)	p-value	
DRUG	1.14	n.s.	1.08	n.s.	Suppl. Fig.4J
TREATMENT	0.69	n.s.	0.34	n.s.	
DRUG × TREATMENT	0.48	n.s.	1.38	n.s.	
mGluR2/3 Cell surface expression					
Factor names	WT		KO		Figure number
	F(1,20)	p-value	F(1,20)	p-value	
DRUG	0.15	n.s.	0.07	n.s.	Suppl. Fig.4K
TREATMENT	1.0	n.s.	0.000	n.s.	
DRUG × TREATMENT	0.07	n.s.	1.5	n.s.	

Table 10. Two-way ANOVA statistical analysis of relative total and cell surface protein expression of the MOR in the NAc.

MOR Total protein expression					
Factor names	WT		KO		Figure number
	F(1,19)	p-value	F(1,18)	p-value	
DRUG	0.7	n.s.	1.82	n.s.	Suppl. Fig.5A
TREATMENT	1.04	n.s.	0.32	n.s.	
DRUG × TREATMENT	0.93	n.s.	0.25	n.s.	
MOR Cell surface expression					
Factor names	WT		KO		Figure number
	F(1,8)	p-value	F(1,8)	p-value	
DRUG	3.15	n.s.	0.24	n.s.	Suppl. Fig.5B
TREATMENT	**6.43**	**p<0.05**	0.001	n.s.	
DRUG × TREATMENT	0.38	n.s.	0.08	n.s.	

Table 11. Two-way ANOVA statistical analysis of relative total and cell surface protein expression of nAChRs and their modulators in the NAc.

nAChR α4 Total protein expression					
Factor names	WT		KO		Figure number
	F(1,19)	p-value	F(1,19)	p-value	
DRUG	**12.35**	**p<0.01**	0.2	n.s.	Figure 53A
TREATMENT	0.72	n.s.	0.19	n.s.	
DRUG × TREATMENT	2.83	n.s.	2.05	n.s.	

nAChR α4 Cell surface expression					
Factor names	WT		KO		Figure number
	F(1,20)	p-value	F(1,17)	p-value	Figure 53B
DRUG	**8.54**	**p<0.01**	0.8	n.s.	
TREATMENT	0.17	n.s.	0.03	n.s.	
DRUG × TREATMENT	0.31	n.s.	0.2	n.s.	
nAChR β2 Total protein expression					
Factor names	WT		KO		Figure number
	F(1,20)	p-value	F(1,20)	p-value	Figure 53C
DRUG	0.37	n.s.	0.01	n.s.	
TREATMENT	0.83	n.s.	0.1	n.s.	
DRUG × TREATMENT	3.72	n.s.	0.17	n.s.	
nAChR β2 Cell surface expression					
Factor names	WT		KO		Figure number
	F(1,19)	p-value	F(1,20)	p-value	Figure 53D
DRUG	1.39	n.s.	0.05	n.s.	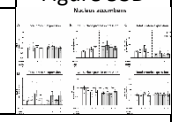
TREATMENT	0.29	n.s.	0.02	n.s.	
DRUG × TREATMENT	**6.33**	**p<0.05**	0.27	n.s.	
LynX1 Total protein expression					
Factor names	WT		KO		Figure number
	F(1,16)	p-value	F(1,16)	p-value	Suppl. Fig.5D
DRUG	1.69	n.s.	0.47	n.s.	
TREATMENT	0.06	n.s.	0.2	n.s.	
DRUG × TREATMENT	0.7	n.s.	0.07	n.s.	
LynX1 Cell surface expression					
Factor names	WT		KO		Figure number
	F(1,15)	p-value	F(1,15)	p-value	Suppl. Fig.5E
DRUG	0.06	n.s.	0.16	n.s.	
TREATMENT	0.25	n.s.	3.22	n.s.	
DRUG × TREATMENT	**4.69**	**p<0.05**	0.13	n.s.	

Table 12. Two-way ANOVA statistical analysis of relative total and cell surface protein expression of intracellular effectors and adhesion molecules in the NAc.

p-ERK2/ERK Total protein expression					
Factor names	WT		KO		Figure number
	F(1,20)	p-value	F(1,20)	p-value	Suppl. Fig.5C
DRUG	0.82	n.s.	0.24	n.s.	
TREATMENT	0.12	n.s.	0.14	n.s.	
DRUG × TREATMENT	0.13	n.s.	0.17	n.s.	
p-CREB Total protein expression					
Factor names	WT		KO		Figure number
	F(1,20)	p-value	F(1,20)	p-value	Figure 61A
DRUG	**7.20**	**p<0.05**	3.70	n.s.	
TREATMENT	2.9	n.s.	0.04	n.s.	
DRUG × TREATMENT	0.45	n.s.	0.59	n.s.	
NFκB p50 Total protein expression					
Factor names	WT		KO		Figure number
	F(1,20)	p-value	F(1,20)	p-value	Suppl. Fig.5F
DRUG	0.09	n.s.	0.03	n.s.	
TREATMENT	0.03	n.s.	0.07	n.s.	
DRUG × TREATMENT	0.94	n.s.	0.27	n.s.	
NFκB p105 Total protein expression					
Factor names	WT		KO		Figure number
	F(1,19)	p-value	F(1,20)	p-value	Figure 61C
DRUG	**5.7**	**p<0.05**	1.19	n.s.	
TREATMENT	1.71	n.s.	0.01	n.s.	
DRUG × TREATMENT	2.79	n.s.	2.24	0.15	
ΔFosB Total protein expression					
Factor names	WT		KO		Figure number
	F(1,20)	p-value	F(1,20)	p-value	Figure 61B
DRUG	**6.94**	**p<0.05**	1.1	n.s.	
TREATMENT	1.17	n.s.	0.01	n.s.	
DRUG × TREATMENT	0.04	n.s.	0.22	n.s.	
n-Cadherin Total protein expression					
Factor names	WT		KO		Figure number
	F(1,20)	p-value	F(1,17)	p-value	Figure 61D
DRUG	**7.09**	**p<0.05**	**4.63**	**p<0.05**	
TREATMENT	0.72	n.s.	0.25	n.s.	
DRUG × TREATMENT	0.01	n.s.	0.004	n.s.	

Discussion

The involvement of PENK in nicotine addiction

Nicotine develops its acute reinforcing properties due to the activation of nAChRs. However, nAChRs desensitize quickly upon repeated nicotine administrations. Thus, neurotransmitter systems other from cholinergic signaling are proposed to participate in the reinforcing properties of nicotine. Indeed, pharmacological and genetic studies have provided evidence for a critical role of the glutamatergic and the EOS in nicotine addiction (Markou, 2008; Trigo *et al.*, 2010; Charbogne *et al.*, 2014)

In the present study, we demonstrated that enkephalins, the most abundant ligands for MORs and DORs, critically contribute to the reinforcing properties of nicotine. Furthermore, we showed a significant increase in dendritic spine density in MSNs of the NAc core and shell after nicotine self-administration. This neuroplasticity mechanism was singularly triggered by contingent nicotine administration and was absent in PENK KO mice. Lastly, we revealed that pathway-specific glutamatergic transmission from the PLC to the NAc core is necessary to acquire and maintain nicotine self-administration.

We demonstrated that the genetic deletion of PENK strikingly decreased the reinforcing properties and the motivation for nicotine. This effect is probably due to the lack of nicotine-induced DA release in the NAc in PENK KO mice (Berrendero *et al.*, 2005). In agreement, nicotine-induced CPP was decreased in MOR, DOR, PENK, and β-endorphin KO mice (Berrendero *et al.*, 2002b, 2005, 2012; Trigo *et al.*, 2009) that further substantiates the pivotal role of MOR- and DOR-signaling in nicotine's reinforcing properties. However, a small subpopulation of PENK KO mice (<20%) acquired nicotine self-administration, indicating that the reinforcing properties of nicotine do not completely depend on opioid signaling,

displaying the multifactorial nature of nicotine's reinforcing effects. This subset of animals reinstated nicotine-seeking behavior similar to WT littermates, suggesting that the mechanisms underlying in the reinforcing properties and the motivation for nicotine are different from those involved in the relapse to nicotine-seeking. In line with our results, cocaine self-administration, but not cue-induced reinstatement of cocaine-seeking, was attenuated in PENK KO mice (Gutiérrez-Cuesta *et al.*, 2014). In contrast, naltrexone attenuated cue-induced reinstatement of nicotine-seeking (Liu *et al.*, 2009), and the genetic deletion of MORs and DORs significantly decreased cue-induced reinstatement of cocaine-seeking (Gutiérrez-Cuesta *et al.*, 2014), thus, we can suggest that β-endorphin modulates the relapse to cocaine- and nicotine-seeking.

In a second approach, we showed that nicotine self-administration significantly increases dendritic spine density in MSNs in the NAc core and shell. More specifically, we observed a significant increase in mushroom and thin spines, which reflects an increase in dendritic spine head diameter and *de novo* formation of spines, respectively (Segal, 2005). In line with our findings, acute nicotine increased glutamatergic levels in the NAc (Toth *et al.*, 1993; Reid *et al.*, 2000). Furthermore, the spine head diameter of dendritic spines in the NAc core and AMPAR/NMDAR currents were increased in rats withdrawn with extinction training from nicotine self-administration. This effect further increased upon cue-induced reinstatement of nicotine-seeking (Gipson *et al.*, 2013). Together, we can suggest that the dendritic spine density of MSNs in the NAc core and shell increases during nicotine self-administration and remains stable throughout extinction, predisposing the NAc in a vulnerable state to engage quickly upon presentation of nicotine-associated cues. The size and shape of individual spines correlate with forms of synaptic plasticity

(Russo *et al.*, 2010). Indeed, the induction of LTP is associated with the formation of new spines and enlargement of existing spines (Matsuzaki *et al.*, 2004; Nägerl *et al.*, 2004; Okamoto *et al.*, 2004). Aside from glutamate, the induction of LTP at cortico-striatal synapses was shown to critically depend on DA signaling (Calabresi *et al.*, 2007), which could explain the absence of nicotine-induced neuroplasticity in PENK KO mice. It would be interesting to know if the genetic deletion of PENK also inhibits nicotine-induced glutamate release in the NAc. We could further demonstrate that the mechanisms underlying neuroplasticity in the NAc are singularly driven by contingent nicotine administration. Indeed, dendritic spine density remained unchanged in Yoked Nicotine mice. This result indicates that goal-directed behavior and conditioning are necessary to induce neuroplasticity in MSNs of the NAc. In agreement, neuroplasticity in the NAc was also abolished in yoked animals after prolonged self-administration of highly palatable food (Guegan *et al.*, 2013), and after prolonged withdrawal from cocaine self-administration (Martin *et al.*, 2006). *In vivo* studies assessing contingent and non-contingent reward-evoked DA and glutamate release in the NAc should give new insights about the mechanisms underlying neuroplasticity in the NAc.

The increase in dendritic spine density is most likely due to a hyper-glutamatergic state in the NAc during nicotine self-administration. Furthermore, negative modulation of pre- and postsynaptic glutamate transmission in the NAc decreased nicotine self-administration (Liechti *et al.*, 2007; Tronci & Balfour, 2011). However, the specific brain areas involved in these processes are as of yet unclear. The NAc receives glutamatergic input from a plethora of limbic and cortical regions, some of the most notable being the mPFC, vHPC, and BLA (Sesack & Grace, 2010; Floresco, 2015). Glutamatergic transmission from the mPFC to the NAc is

largely associated with executive control and thought to mediate goal-directed behaviors, including drug-seeking and preoccupation to obtain drugs of abuse (Kalivas *et al.*, 2005; Koob & Volkow, 2016). Hence, we hypothesized that the PLC-NAc core pathway contributes to the reinforcing properties of nicotine. Indeed, inhibition of the PLC-NAc core pathway decreased nicotine self-administration. Furthermore, the lack of glutamate transmission originating from the PLC completely prevented mice to fulfill acquisition criteria. Indeed, nicotine induces glutamate release via activation of α7 nAChRs that are highly expressed on glutamatergic nerve terminals in the NAc. Glutamatergic afferents from the mPFC and DA neurons are thought to project to the same or close by synapse in the NAc. Thus, cortical glutamate release in the NAc can gate the release of DA from DA fibers in the NAc directly, independently of neuronal activity in the VTA. In agreement, prefrontal cortex input to the NAc readily supports optogenetic self-stimulation (Mateo *et al.*, 2017), and optogenetic activation or inhibition increased or decreased Pavlovian conditioning, respectively (Otis *et al.*, 2017). However, optogenetic activation of glutamatergic fibers in the NAc deriving from the BLA and vHPC was also shown to be reinforcing (Britt *et al.*, 2012; Stuber *et al.*, 2012), which may suggest that an increased glutamatergic tone in the NAc is sufficient to induce reinforcement regardless of the pathway and the different behavioral roles of the brain areas providing these inputs. Thus, to ensure that the reinforcing properties of nicotine specifically depend on glutamatergic transmission from the PLC to the NAc core and not on a specific amount of glutamate, we investigated whether glutamatergic signaling of the BLA-NAc core pathway is also involved in the reinforcing properties of nicotine. We demonstrated that chemogenetic inhibition of glutamatergic inputs from the BLA to the NAc core was not sufficient to

modify nicotine self-administration, although optogenetic stimulation of BLA glutamatergic fibers in the NAc was shown to be reinforcing and inhibition decreased the reinforcing properties of natural rewards (Stuber *et al.*, 2011). Thus, our data suggest that the reinforcing properties of nicotine critically depend on PLC-NAc core activity. However, dendritic spine density was also significantly increased in the NAc shell, therefore, we cannot exclude the importance of the ILC-NAc shell and the vHPC-NAc shell pathway for the reinforcing properties of nicotine. Future studies may evaluate the impact on the PLC-NAc core pathway on nicotine-induced neuroplasticity.

Together, we demonstrated that opioid and glutamatergic signaling critically contributes to the reinforcing properties of nicotine. Furthermore, we revealed that pathway-specific glutamatergic transmission from the PLC to the NAc core is necessary to acquire and maintain nicotine self-administration. Finally, goal-directed behavior and conditioning are required to trigger long-lasting nicotine-induced neuroadaptations, including quantitative and morphological changes in MSN dendritic spines in the NAc core and shell.

The involvement of the sigma-1 receptor in nicotine addiction

Every single drug exposure drives the mesocorticolimbic pathway beyond its physiological limits. Consequently, chronic drug exposure leads to neuroadaptations in the mesocorticolimbic system (Nestler, 2005). These changes can remain virtually permanent, leading to a stable state of high vulnerability to relapse even after protracted abstinence that remains the major clinical health concern in drug addiction. (Koob & Volkow, 2016). In fact, around 80% of former smokers relapse within the first month of abstinence with only 3% of the remaining abstinent at six months (Benowitz, 2010). Current treatments are ineffective (Covey *et al.*, 1999; Piper *et al.*, 2009) and accompanied by important side-effects. Thus, the development of new therapeutic strategies is indispensable. The Sig-1R, a novel receptor type that is thought to lack its own specific signaling machinery, was recently shown to be involved in SUD. Sig-1R antagonists have been demonstrated to decrease the reinforcing properties and the relapse to cocaine- and alcohol-seeking (Katz *et al.*, 2016; Quadir *et al.*, 2019). However, its possible implication in the reinforcing properties of nicotine and the relapse to nicotine-seeking is still unknown. Our study has evaluated the involvement of Sig-1Rs in the addictive properties of nicotine using a reliable operant model of cue-induced reinstatement validated in our laboratory (Martin-García *et al.*, 2009, 2011; Gutiérrez-Cuesta *et al.*, 2014).

We demonstrated that the cue-induced reinstatement of nicotine-seeking was blocked by the Sig-1R antagonist BD 1063. We further showed that nicotine relapse was associated with neurobiological changes in the mPFC and NAc, including Sig-1Rs, glutamatergic, cholinergic and opioid

receptors. These neuroadaptations were absent in Sig-1R KO mice and were partially reversed by BD1063. In a second approach, we demonstrated, using genetic and pharmacological approaches, that Sig-1Rs are also involved in the cue-induced reinstatement of palatable food-seeking.

The reinforcing properties of nicotine are impaired due to the genetic deletion of the Sigma-1 receptor

Our results indicate that the genetic deletion of the Sig-1R does not affect the reinforcing properties of nicotine or palatable food. Operant self-administration is thought to be the gold standard for the evaluation of the reinforcing properties of drugs of abuse (Collins *et al.*, 1984). Sig-1R KO mice displayed cognitive deficits, decreased locomotor activity, and increased anxiety-like behavior. However, we demonstrated by using an operant model of sensation-seeking, that Sig-1R KO mice were able to learn an operant task without any impairment of performance.

Although Sig-1R KO mice displayed a stable pattern of nicotine self-administration, responding for nicotine was not significantly increased compared to the responding for saline of the control group. In contrast, active responding for nicotine was, as expected, strikingly increased in WT mice compared to the saline control group. The high responding is probably due to the detected impulsivity-like phenotype in Sig-1R KO mice in operant drug self-administration. Impulsivity is often related to an impaired reward system which could explain the tendency of increased nicotine intake in Sig-1 KO mice compared to WTs. The first variable that measures impulsivity in the nicotine self-administration paradigm showed increased levels of responding in mutant mice independent of the nicotine or saline group. In contrast, when we measured impulsivity in food self-

administration and sensation-seeking no differences were observed between genotypes. Thus, we cannot conclude that there is a phenotypical modification related to impulsivity due to the lack of Sig-1R. Hence, one could hypothesize that rather than a phenotypical modification in Sig-1R KO mice, the increased response in drug self-administration paradigm may be related to stress induced by the indwelling catheter surgery or the attachment to the tubing.

The Sig-1R antagonist BD1063 but not the genetic deletion of Sig-1Rs decreased the motivation and the cue-induced reinstatement of nicotine-seeking

The Sig-1R antagonist BD1063 strikingly decreased the motivation for nicotine and the cue-induced reinstatement of nicotine-seeking. In contrast, neither the motivation for nicotine nor the reinstatement of nicotine-seeking was attenuated in Sig-1R KO mice. Similar to our findings, alcohol drinking was decreased by BD 1063, but increased in Sig-1R KO mice in a two-bottle choice continuous access paradigm (Blasio *et al.*, 2015; Valenza *et al.*, 2016). Different outcomes of pharmacological and genetic approaches may be expected due to their distinct nature. Indeed, the acute pharmacological blockade at low doses, as used in our experimental design, only partially disrupts receptor function for a determined time frame, whereas the constitutive lifelong lack of a receptor is often accompanied by adaptive modifications of related genes. This may lead to the absence of an expected phenotype, especially in multifactorial diseases such as SUD (El-Brolosy & Stainier, 2017). For example, the lack of ribosomal gene *Rpl22* showed no defects in translation owed to the upregulation of its paralogue, *Rpl22l1*, the

expression of which is normally inhibited by RPL22 (Mulligan *et al.*, 1998). In this context, Sig-2R upregulation may be responsible for the discrepancy between pharmacological and genetic approaches. Although the involvement of Sig-2Rs in nicotine addiction has not been shown yet, their contribution is not fully exclusionary. Another possibility could be that Sig-2Rs may substitute Sig-1R functions in mutant mice, which could explain the absence of a resistant phenotype to the reinforcing properties, motivation for nicotine and the cue-induced reinstatement of nicotine-seeking behavior in the Sig-1R KO mouse. The modification of related genes due to the loss of a negative or positive feedback loop may be the first hypothesis to test when a mutant fails to show a phenotype. The expression of the Sig-2R in the Sig-1R KO mouse has not been elucidated yet. However, binding studies with radioligands of the Sig-2R combined with unlabeled selective Sig-1R ligands, to mask Sig-1R binding, could help to clarify this question.

Besides the significant decrease of reinstated nicotine-seeking in WT mice by BD 1063, this antagonist partially decreased nicotine-seeking behavior in Sig-1R KO mice, which raises questions about the selectivity of BD 1063. BD 1063 binds with more than 70-fold selectivity to Sig-1Rs versus Sig-2Rs and is even more selective towards other tested binding sites (Garcés-Ramírez *et al.*, 2011). However, in the absence of Sig-1Rs, BD 1063 could potentially interact with other binding sites.

A recent study postulated new binding sites for Sig-1R ligands. The authors demonstrated that selective Sig-1R antagonists and agonists, were able to decrease nicotinic agonist-induced nAChRs currents and subsequent catecholamine release in adrenal chromaffin cells (Brindley *et al.*, 2017), an effect that was previously postulated to be selectively mediated by Sig-1Rs (Paul *et al.*, 1993). However, a recent study demonstrated that Sig-1R

ligands block nAChRs directly in adrenal chromaffin cells, and that this mechanism could probably be extrapolated to other cell types (Brindley *et al.*, 2017). The postulated ability of Sig-1R ligands to block nAChRs by a Sig-1R independent mechanism could explain the partially decreased relapse to nicotine-seeking in BD 1063 treated Sig-1R KO mice. In contrast, BD 1063 did not decrease the motivation for nicotine in KO mice. The antagonism of nAChRs in nicotine trained animals is probably not effective at low doses due to a possible development of nAChR desensitization. Indeed, mecamylamine, an unselective nAChR antagonist attenuated cue-induced reinstatement of nicotine-seeking at relatively low doses, however, nicotine self-administration was only moderately decreased in nicotine trained animals even with higher doses of mecamylamine (Liu *et al.*, 2007a). Although our results seem to be in line with this hypothesis, the cue-induced reinstatement of nicotine-seeking was completely blocked by BD1063 in WT mice whereas nicotine-seeking was only slightly decreased in KO mice, concluding that Sig-1R mediated mechanisms are mostly responsible for the attenuation of nicotine relapse. To further investigate the involvement of Sig-1R in the reinstatement of nicotine-seeking, it would be of interest to assess the effect of Sig-1R agonists on the cue-induced reinstatement of nicotine-seeking, as well as the impact of Sig-1R ligands on nAChRs in a Sig-1R *'free'* environment (KOs or knockdowns) to verify whether Sig-1R ligands block nAChRs directly or negatively modulate them *via* Sig-1Rs.

The Sig-1R is involved in the cue-induced reinstatement of palatable food-seeking behavior

We demonstrated the specific involvement of Sig-1Rs in the cue-induced reinstatement of palatable food-seeking behavior. Indeed, the acute Sig-1R antagonism, as well as the genetic deletion of Sig-1Rs, significantly decreased food-seeking after the extinction of operant behavior in food trained animals. BD 1063 did not show any effect in Sig-1R KO mice concluding that these results are mediated by Sig-1Rs. In agreement with our findings, other Sig-1R antagonists decreased the reinstatement of cocaine (Martin-Fardon *et al.*, 2007), alcohol and natural rewards seeking-behavior (Martin-Fardon *et al.*, 2007, 2012). The motivation for palatable food was not affected by BD 1063, but was decreased in Sig-1R KO mice. The decreased motivation for palatable food in Sig-1R KO mice could be influenced by the learning impairment revealed in Sig-1R KO mice. Indeed, KO mice displayed a delayed learning curve in operant food self-administration as shown by a decreased response on the first day of FR1 and FR3 demonstrating that a change of schedule of reinforcement initially impairs the response in KO mice. Another possibility could be that the partial blockade of Sig-1Rs was not sufficient to decrease the motivation for palatable food. Indeed, the low doses of BD 1063 that were used in our experimental design only partially block Sig-1Rs. However, the use of higher doses of BD 1063 can lead to concomitants, such as unspecific receptor binding. In line with this assumption, the breakpoint for palatable food was slightly increased in KO mice treated with BD 1063, which is probably related to the increased locomotor activity caused by BD 1063 in KO but not in WT mice. This result also shows that BD 1063, which is one of the most selective commercially available Sig-1R

antagonists, appears to possess some cross-reactivity at least in the Sig-1R KO mouse.

Sig-1R antagonist BD 1063 inhibits neuroadaptations in the mPFC and NAc leading to nicotine relapse

The cue-induced reinstatement of nicotine-seeking was associated with concomitant neuroadaptations in the mPFC and NAc in WT, but not in KO mice, including Sig-1Rs, glutamatergic, opioid and cholinergic receptors, as well as intracellular effectors downstream of these receptors. These observed neuroadaptations were partially reversed by the Sig-1R antagonist BD 1063 and were mostly absent in Sig-1R KO mice.

Our results suggest an increased activation of the mPFC upon cue-induced reinstatement of nicotine-seeking. Indeed, we observed an overexpression of excitatory glutamatergic receptors, including NMDARs and AMPARs, hypothesizing that this glutamatergic plasticity is due to a hyperglutamatergic state during nicotine relapse. In agreement, increased PFC and anterior cingulate gyrus activity was shown in human imaging studies during cue-induced craving in smokers (Franklin *et al.*, 2007), and reinstatement of nicotine CPP increased FOS protein expression in the PFC (Pascual *et al.*, 2009). Although Sig-1Rs have been shown to interact with NMDARs (Balasuriya *et al.*, 2013; Rodríguez-Muñoz *et al.*, 2015), the increased protein levels of the NMDAR subunits NR1 and NR2A were not modified by BD 1063. This result suggests that these neuroadaptations had been already established due to nicotine self-administration and remained stable during extinction, predisposing the mPFC to quickly facilitate glutamatergic signaling upon presentation of nicotine-associated cues. In agreement, NMDARs were found to be significantly increased

after nicotine self-administration (Wang *et al.*, 2007). Furthermore, the increase of the AMPAR subunit GluR1 was reversed by BD 1063, indicating that this plasticity may be a rapid process during the reinstatement of nicotine-seeking. The rapid change of AMPARs but not of NMDARs could be related to LTP. In line with our suggestion, the adhesion protein n-cadherin was also upregulated suggesting an increased synaptic strength in the mPFC. An increase in synaptic strength is often related to a higher spine head diameter that would facilitate AMPAR receptor insertion.

Increased levels of Sig-1R mRNA were revealed after the reinstatement of nicotine-seeking. This increase was blocked by BD 1063 administrations, suggesting that Sig-1R mRNA increases rapidly upon nicotine relapse. In agreement, Sig-1R mRNA was not modified in the mPFC after repeated cocaine treatment (Romieu *et al.*, 2002) and decreased after methamphetamine self-administration (Stefanski *et al.*, 2004). Thus, the upregulation of Sig-1R mRNA in the mPFC seems to be specific to the cue-induced reinstatement of nicotine-seeking.

The overexpression of GluT mRNA and the predominantly presynaptic mGluR2/3 upon reinstatement of nicotine-seeking, which suggests increased glutamate uptake and decreased glutamate release, respectively, may appear controversial to the hypothesis of a hyperglutamatergic state during the cue-induced reinstatement of nicotine-seeking. Furthermore, systemic administration of mGluR2/3 agonists was shown to decrease reinstatement of nicotine-seeking (Liechti *et al.*, 2007). However, since both neuroadaptations were singularly triggered in WT mice that reinstated nicotine-seeking but not in BD 1063 treated animals, we speculate that these neuroadaptations are rapid compensatory plasticity mechanisms during the cue-induced reinstatement of nicotine-seeking to balance excitatory transmission and

protect cells from excitotoxicity. Compensatory plasticity mechanisms were also described for GABAergic transmission in the mPFC (Lubbers *et al.*, 2014). More specifically, the subunits α1 and γ2 of the $GABA_A$ receptor were upregulated after relapse to nicotine-seeking. However, mPFC microinjections of $GABA_A$ receptor antagonists led to increased reinstatement, whereas mPFC microinjections of $GABA_A$ receptor agonists decreased reinstatement (Lubbers *et al.*, 2014). Thus, these results and ours suggest that increased activation of the mPFC facilitates nicotine-seeking upon presentation of nicotine-associated cues, and that compensatory plasticity mechanisms occur in the mPFC to limit drug-seeking. Protein levels of mGluR2/3 and GluTs could be assessed before cue-induced reinstatement in order to confirm the hypothesis of rapid compensatory plasticity mechanisms in the mPFC.

Opioid signaling in the mPFC seems to be involved in the cue-induced reinstatement of nicotine-seeking. Indeed, we demonstrated that MOR expression was significantly increased after the cue-induced reinstatement of nicotine-seeking. Naltrexone, a selective MOR antagonist, was reported to attenuate cue-induced reinstatement of nicotine-seeking (Liu *et al.*, 2009), and MOR agonists were shown to inhibit GABAergic transmission in the orbitofrontal cortex (Qu *et al.*, 2015). Together with our findings, showing that BD 1063 blocked both reinstatement of nicotine-seeking and overexpression of MORs, we may hypothesize that nicotine relapse leads to MOR overexpression in GABAergic neurons, leading to disinhibition of pyramidal glutamatergic neurons that fosters the hyperactivation of the mPFC.

To our knowledge, protein levels of the α4 and β2 subunit have not been analyzed in the mPFC after cue-induced reinstatement of nicotine-seeking. We demonstrated that the total protein levels of the α4 and the

β2 subunit were increased, although α4 and β2 subunits were significantly decreased at the cell membrane. Thus, we can conclude that α4 and β2 subunits are increased in the cytosol. This result indicates two possible mechanisms of α4β2* nAChRs trafficking in the mPFC. First, α4 and β2 subunits may have been increased at the cell membrane due to nicotine self-administration, remained stable during extinction, but underwent endocytosis upon cue-induced reinstatement of nicotine-seeking, leading to accumulation in the cytosol. Another possibility could be an 'on-demand' expression of both subunits upon reinstatement of nicotine-seeking, meaning that nicotine relapse provokes α4 and β2 subunit production but α4β2* nAChRs could still not be inserted in the cell membrane. Indeed, the assembly nAChRs is a relatively slow and inefficient process that critically dependent upon appropriate subunit folding and requires trafficking of nAChRs from their site of synthesis in the ER to the cell surface (Millar & Harkness, 2008). Little is known about neuroadaptations of nAChRs underlying the enduring vulnerability to relapse produced by continued nicotine use. However, some studies targeted α4β2* nAChRs with systemic administrations of full agonists (Lee *et al.*, 2014), partial agonists (O'Connor *et al.*, 2010) and positive allosteric modulators (Maurer *et al.*, 2017), all of which decreased nicotine-seeking. In contrast, α4β2* nAChR antagonists showed no effect (Liu, 2014). These findings could be in line with the assumption that α4β2* nAChRs are decreased at the cell membrane due to a possible compromised cholinergic signaling after nicotine self-administration. Further studies should be performed using intra-mPFC infusions of cholinergic agents and cell-type-specific assessments to clarify the specific implication of α4β2* nAChRs in nicotine relapse in the mPFC. We further revealed that the expression of both subunits was modified by BD 1063 treatment alone in

WT, but not in KO mice suggesting a Sig-1R mediated modulation of nAChRs in the mPFC.

We observed increased levels of pCREB and pERK2 in WT mice upon cue-induced reinstatement, which supports our findings of increased cellular activation. Indeed, Ca^{2+} entry upon cellular excitation activates intracellular kinases, such as PKC and PKA, and these kinases, among others, activate intracellular effectors that are related to nicotine addiction.

The increased activity of the NAc, suggested by increased levels of NMDARs and AMPARs, is probably a downstream product of the observed hyperactivation of the mPFC. In agreement, extracellular glutamate levels were significantly increased in the NAc core in rats during cue-induced reinstatement of nicotine-seeking (Gipson *et al.*, 2013), and priming induced reinstatement of cocaine (McFarland *et al.*, 2003) and heroin-seeking (LaLumiere & Kalivas, 2008). Furthermore, inactivation of the mPFC by GABA agonists inhibited cocaine- and heroin-induced reinstatement of drug-seeking and glutamate release in the NAc core (McFarland *et al.*, 2003; LaLumiere & Kalivas, 2008). Indeed, the increased expression of the NMDAR subunits NR1 and NR2A, and partially the NR2B subunit, were blunted by BD 1063, which is in line with our findings suggesting that BD 1063 blocked glutamatergic hyperactivation in the mPFC during nicotine-seeking. The increase of the predominantly extrasynaptic NR2B subunit in WT mice may be related to a glutamate overspill that could arise from increased extracellular glutamate levels combined with reduced glutamate reuptake. Indeed, GluT1 mRNA was significantly decreased in the NAc and significantly increased in the mPFC, whereas the NR2B subunit was not modified. The upregulation of n-cadherin is probably related to the observed increase in dendritic spine

head diameter after the reinstatement of nicotine-seeking (Gipson *et al.*, 2013) and after nicotine self-administration (Study 1). Interestingly, the NMADAR subunit NR2B, the AMPAR subunit GluR1, and n-cadherin were decreased in Sig-1R KO mice. These decreases may indicate loss of synaptic strength due to a hypoglutamatergic state. In agreement, we did not observe increased glutamatergic activity in the mPFC activity in mutant mice. The increased levels of AMPAR subunits GluR1 and GluR2 were not reversed by BD 1063, suggesting that AMPARs are already increased during nicotine self-administration or during extinction in the NAc. Previous studies have revealed that AMPAR expression increased in the NAc during withdrawal from cocaine (Kauer & Malenka, 2007).

Sig-1R mRNA was also upregulated in the NAc after the cue-induced reinstatement of nicotine-seeking. However, BD 1063 did not inhibit Sig-1R mRNA upregulation in the NAc, which is in contrast to the results obtained in the mPFC. Taking into account that mRNA transcription is a generally rapid process, our result may suggest that Sig-1R mRNA has already been increased due to chronic exposure to nicotine. In agreement, Sig-1R mRNA was previously reported to significantly increase in the NAc after repeated cocaine treatment (Romieu *et al.*, 2002). These findings may indicate that Sig-1R expression increases in the NAc upon repeated exposure to drugs of abuse and that these changes remain stable during extinction and reinstatement of nicotine-seeking. The NAc is one of the key areas in the CNS responsible for the reinforcing properties of drugs of abuse, thereby, associating previously neutral stimuli with drug availability that induces incentive salience and fosters excessive drug-seeking (Koob & Volkow, 2016). Thus, Sig-1R upregulation in the NAc may be a vulnerability factor for excessive drug-seeking and relapse. Accordingly, Sig-1R protein levels in the NAc are elevated in the alcohol-preferring rat

line Scr: sP (Colombo *et al.*, 2006). The direct modulation of D1 and D2 DA receptors by Sig-1Rs (Navarro *et al.*, 2010, 2013) may be a possible mechanism to foster excessive drug-seeking. In contrast, mPFC activity is strongly related to relapse, which could explain the possible rapid increase of Sig-1Rs in the mPFC during the reinstatement of nicotine-seeking.

We observed increased levels of α4 and β2 nAChR subunits in the NAc in WT, but not in KO mice after the reinstatement of nicotine-seeking. α4 and β2 nAChRs subunits are expressed on both DA terminals and GABAergic interneurons (Cachope & Cheer, 2014). BD 1063 was able to block the increase of the β2, but not α4 subunit, which may indicate a predominant modulation of α6β2* nAChRs that are exclusively expressed on DA terminal in the NAc (Champtiaux *et al.*, 2003; Threlfell & Cragg, 2011). Indeed, endogenous nAChR activation has been recently demonstrated to enhance DA release upon cortical, thalamic and direct activation of CINs (Cachope *et al.*, 2012; Threlfell *et al.*, 2012; Kosillo *et al.*, 2016). Furthermore, intra-NAc infusions of mecamylamine significantly decreased DA release induced by optogenetically evoked glutamate release from the mPFC (Mateo *et al.*, 2017), suggesting that nAChRs directly modulate DA release.

Lastly, the increased expression of pCREB, pERK2, and ΔFosB in the NAc are probably due to the repeated drug insults during nicotine self-administration. In agreement, increased levels of pCREB, pERK2, and ΔFosB were shown after repeated exposure to nicotine (Nestler, 2005).

Together, we showed that the genetic deletion of Sig-1Rs impairs the reinforcing properties of nicotine. Furthermore, acute administration of the Sig-1R antagonist BD 1063 decreased the motivation for nicotine and block the cue-induced reinstatement of nicotine-seeking. However, the specific involvement of Sig-1Rs on these responses is not fully clarified due

to discrepancies between the results obtained using genetic and pharmacological tools. Additional experiments to characterize the Sig-2R expression in the Sig-1R KO mouse, the use of conditional Sig-1R KO mice, an evaluation of the effect of Sig-1R agonists on the cue-induced reinstatement of nicotine-seeking, and binding studies of Sig-1R ligands towards nAChRs should help to clarify whether Sig-1Rs are involved in the cue-induced reinstatement of nicotine seeking.

At a molecular level, we demonstrated that the cue-induced reinstatement of nicotine-seeking is associated with neuroadaptations in the mPFC and NAc, including Sig-1R, glutamatergic, cholinergic and opioid signaling. In agreement with our behavioral results, the observed neuroadaptations were partially reversed by the Sig-1R antagonists BD 1063. It has been proposed that increased corticostriatal activity is a general mechanism underlying the relapse to drug-seeking behavior (McFarland *et al.*, 2003; LaLumiere & Kalivas, 2008; Gipson *et al.*, 2013). In agreement, our molecular results suggest an increased corticostriatal activity during the reinstatement of nicotine-seeking, which was inhibited by the administration of BD 1063. Indeed, BD 1063 and other Sig-1R antagonists have been shown to decrease the relapse to drug-seeking for a variety of drugs of abuse despite their different molecular mechanisms (Katz *et al.*, 2016; Quadir *et al.*, 2019). In fact, we also revealed the specific involvement of Sig-1Rs in the cue-induced reinstatement of palatable food-seeking at a genetic and pharmacological level. Therefore, the ability of BD 1063 to inhibit the neuroadaptations in the corticostriatal pathway during reinstatement of reward-seeking makes the Sig-1R a promising target to prevent relapse, which still remains the major clinical health problem in treating SUD.

Conclusions

The main conclusions of the work presented in this thesis can be summarized as follows:

1. PENK critically mediates the reinforcing properties and the motivation for nicotine, likely by activating MORs and/or DORs. In contrast, the mechanisms underlying the cue-induced reinstatement of nicotine-seeking seems to be independent of PENK.
2. Only contingent nicotine self-administration, but not non-contingent nicotine administration, is associated with a significant increase in dendritic spine density and spine head diameter of MSNs in the NAc core and shell, demonstrating that goal-directed behavior and conditioning are necessary to trigger the mechanisms that underly structural plasticity.
3. The absence of PENK reduces nicotine-induced structural plasticity probably by a DA mediated mechanism.
4. Compromised glutamatergic input from the PLC but not from the BLA to the NAc core was sufficient to decrease nicotine self-administration, demonstrating that glutamatergic transmission to the NAc core critically contributes to the reinforcing properties of nicotine in a pathway-specific manner.
5. The genetic deletion of the Sig-1R produced a phenotype of decreased locomotor activity, increased anxiety-like behavior and impaired short-term memory.
6. The pharmacological acute administration of the Sig-1R antagonist BD1063 blocked the cue-induced reinstatement of nicotine-seeking through inhibition of neuroadaptive changes in the mPFC and NAc, including Sig-1Rs, glutamatergic, cholinergic

and opioid receptors, as well as intracellular effectors related to drug addiction.

7. Sig-1Rs participate in the mechanisms underlying the reinforcing properties and the motivation for nicotine but not palatable food.
8. Sig-1Rs modulate the cue-induced reinstatement of palatable food-seeking. These findings together with other studies indicate that Sig-1Rs are involved in general mechanisms underlying relapse to drug-seeking.

References

Abate, C., Niso, M., Infantino, V., Menga, A. & Berardi, F. **(2015).** Elements in support of the 'non-identity' of the PGRMC1 protein with the σ2 receptor. *Eur J Pharmacol* 758, 16–23. Elsevier.

Agrawal, A., Neale, M. C., Jacobson, K. C., Prescott, C. A. & Kendler, K. S. **(2005).** Illicit drug use and abuse/dependence: modeling of two-stage variables using the CCC approach. *Addict Behav* 30, 1043–1048.

Aguilar, M. A., Rodríguez-Arias, M. & Miñarro, J. **(2009).** Neurobiological mechanisms of the reinstatement of drug-conditioned place preference. *Brain Res Rev* 59, 253–277. Elsevier.

Ahmed, S. H. & Koob, G. F. **(1997).** Cocaine- but not food-seeking behavior is reinstated by stress after extinction. *Psychopharmacology (Berl)* 132, 289–95.

Ahmed, S. H. & Koob, G. F. **(1998).** Transition from moderate to excessive drug intake: change in hedonic set point. *Science* 282, 298–300.

Al-Hasani, R. & Bruchas, M. R. **(2011).** Molecular mechanisms of opioid receptor-dependent signaling and behavior. *Anesthesiology* 115, 1363–81. NIH Public Access.

Albuquerque, E. X., Pereira, E. F. R., Alkondon, M. & Rogers, S. W. **(2009).** Mammalian nicotinic acetylcholine receptors: from structure to function. *Physiol Rev* 89, 73–120.

Allen, S., Bade, T., Hatsukami, D. & Center, B. **(2008).** Craving, withdrawal, and smoking urges on days immediately prior to smoking relapse. *Nicotine Tob Res* 10, 35–45. Narnia.

Alon, A., Schmidt, H. R., Wood, M. D., Sahn, J. J., Martin, S. F. & Kruse, A. C. **(2017).** Identification of the gene that codes for the σ2 receptor. *Proc Natl Acad Sci U S A* 114, 7160–7165.

Alonso, G., Phan, V., Guillemain, I., Saunier, M., Legrand, A., Anoal, M. & Maurice, T. **(2000).** Immunocytochemical localization of the sigma(1) receptor in the adult rat central nervous system. *Neuroscience* 97, 155–70.

Anthony, J. C., Warner, L. A. & Kessler, R. C. **(1994).** Comparative Epidemiology of Dependence on Tobacco, Alcohol, Controlled Substances, and Inhalants: Basic Findings From the National Comorbidity Survey. *Exp Clin Psychopharmacol* 2, 244–268.

Anton, B., Fein, J., To, T., Li, X., Silberstein, L. & Evans, C. J. **(1996).** Immunohistochemical localization of ORL-1 in the central nervous system of the rat. *J Comp Neurol* 368, 229–51.

Aracri, P., Consonni, S., Morini, R., Perrella, M., Rodighiero, S., Amadeo, A. & Becchetti, A. **(2010).** Tonic Modulation of GABA Release by Nicotinic Acetylcholine Receptors in Layer V of the Murine Prefrontal Cortex. *Cereb Cortex* 20, 1539–1555. Narnia.

del Arbol, J. ., Raya Muñoz, J., Ojeda, L., López Cascales, A., Rico Irles, J., Miranda, M. ., Ruiz Requena, M. . & Aguirre, J. . **(2000).** Plasma concentrations of beta-endorphin in smokers who consume different numbers of cigarettes per day. *Pharmacol Biochem Behav* 67, 25–28. Elsevier.

Arbuthnott, G. **(1992).** The mesolimbic dopamine system: From motivation to action: P. Willner and J. Scheel-Krüger (eds). John Wiley & Sons, Ltd, Chichester, 1991. £80. *J Chem Neuroanat* 5, 193–194. Elsevier.

Armstrong, D. W., Wang, X. & Ercal, N. **(1998).** Enantiomeric composition of nicotine in smokeless tobacco, medicinal products, and commercial reagents. *Chirality* 10, 587–591.

Ashare, R. L. & Schmidt, H. D. **(2014).** Optimizing treatments for nicotine dependence by increasing cognitive performance during withdrawal. *Expert Opin Drug Discov* 9, 579. NIH Public Access.

Ávila-Ruiz, T., Carranza, V., Gustavo, L.-L., Limón, D. I., Martínez, I., Flores, G. & Flores-Hernández, J. **(2014).** Chronic administration of nicotine enhances NMDA-activated currents in the prefrontal cortex and core part of the nucleus accumbens of rats. *Synapse* 68, 248–256.

Aydar, E., Palmer, C. P. & Djamgoz, M. B. A. **(2004).** Sigma Receptors and Cancer. *Cancer Res* 64, 5029–5035.

Aydar, E., Palmer, C. P., Klyachko, V. A. & Jackson, M. B. **(2002).** The Sigma Receptor as a Ligand-Regulated Auxiliary Potassium Channel Subunit. *Neuron* 34, 399–410. Cell Press.

Azam, L., Winzer-Serhan, U. H., Chen, Y. & Leslie, F. M. **(2002).** Expression of neuronal nicotinic acetylcholine receptor subunit mRNAs within midbrain dopamine neurons. *J Comp Neurol* 444, 260–274. John Wiley & Sons, Ltd.

Bailey, C. D. C., De Biasi, M., Fletcher, P. J. & Lambe, E. K. **(2010).** The Nicotinic Acetylcholine Receptor α5 Subunit Plays a Key Role in Attention Circuitry and Accuracy. *J Neurosci* 30, 9241–9252.

Balasuriya, D., Stewart, A. P. & Edwardson, J. M. **(2013).** The -1 Receptor Interacts Directly with GluN1 But Not GluN2A in the GluN1/GluN2A NMDA Receptor. *J Neurosci* 33, 18219–18224.

Baldwin, P. R., Alanis, R. & Salas, R. **(2011).** The Role of the Habenula in Nicotine Addiction. *J Addict Res Ther* Suppl 1. NIH Public Access.

Balerio, G. N., Aso, E., Berrendero, F., Murtra, P. & Maldonado, R. **(2004).** Delta9-tetrahydrocannabinol decreases somatic and motivational manifestations of nicotine withdrawal in mice. *Eur J Neurosci* 20, 2737–48.

Balerio, G. N., Aso, E. & Maldonado, R. **(2005).** Involvement of the opioid system in the effects induced by nicotine on anxiety-like behaviour in mice. *Psychopharmacology (Berl)* 181, 260–9.

Balleine, B. W. & Dickinson, A. **(1998).** Goal-directed instrumental action: contingency and incentive learning and their cortical substrates. *Neuropharmacology* 37, 407–419. Pergamon.

Banghart, M. R. & Sabatini, B. L. **(2012).** Photoactivatable neuropeptides for spatiotemporally precise delivery of opioids in neural tissue. *Neuron* 73, 249. NIH Public Access.

Bardo, M. T. & Bevins, R. A. **(2000).** Conditioned place preference: what does it add to our preclinical understanding of drug reward? *Psychopharmacology (Berl)* 153, 31–43. Springer-Verlag.

Barrett, A. C., Miller, J. R., Dohrmann, J. M. & Caine, S. B. **(2004).** Effects of dopamine indirect agonists and selective D1-like and D2-like agonists and antagonists on cocaine self-administration and food maintained responding in rats. *Neuropharmacology* 47, 256–273. Pergamon.

Beckson, M. & Tucker, D. **(2014).** Commentary: Craving Diagnostic Validity in DSM-5 Substance Us. *J Am Acad Psychiatry Law Online* 42, 443–452. Journal of the American Academy of Psychiatry and the Law Online.

Beckstead, R. M. **(1979).** An autoradiographic examination of corticocortical and subcortical projections of the mediodorsal-projection (prefrontal) cortex in the rat. *J Comp Neurol* 184, 43–62. John Wiley & Sons, Ltd.

Benowitz, N. L. **(1990).** Clinical pharmacology of inhaled drugs of abuse: implications in understanding nicotine dependence. *NIDA Res Monogr* 99, 12–29.

Benowitz, N. L. **(1992).** Cigarette smoking and nicotine addiction. *Med Clin North Am* 76, 415–437. Elsevier.

Benowitz, N. L. **(2010).** Nicotine addiction. *N Engl J Med* 362, 2295–303.

Benwell, M. E. & Balfour, D. J. **(1992).** The effects of acute and repeated nicotine

treatment on nucleus accumbens dopamine and locomotor activity. *Br J Pharmacol* 105, 849–56.

Berendse, H. W., Graaf, Y. G.-D. & Groenewegen, H. J. **(1992).** Topographical organization and relationship with ventral striatal compartments of prefrontal corticostriatal projections in the rat. *J Comp Neurol* 316, 314–347. John Wiley & Sons, Ltd.

Berrendero, F., Kieffer, B. L. & Maldonado, R. **(2002a).** Attenuation of nicotine-induced antinociception, rewarding effects, and dependence in mu-opioid receptor knock-out mice. *J Neurosci* 22, 10935–40.

Berrendero, F., Kieffer, B. L. & Maldonado, R. **(2002b).** Attenuation of nicotine-induced antinociception, rewarding effects, and dependence in μ-opioid receptor knock-out mice. *J Neurosci* 22, 10935–10940.

Berrendero, F., Mendizábal, V., Robledo, P., Galeote, L., Bilkei-Gorzo, A., Zimmer, A., Maldonado, R., Mendiza, V., Robledo, P. & other authors. **(2005).** Nicotine-induced antinociception, rewarding effects, and physical dependence are decreased in mice lacking the preproenkephalin gene. *J Neurosci* 25, 1103–12.

Berrendero, F., Plaza-Zabala, A., Galeote, L., Flores, Á., Bura, S. A., Kieffer, B. L. & Maldonado, R. **(2012).** Influence of δ-opioid receptors in the behavioral effects of nicotine. *Neuropsychopharmacology* 37, 2332–44.

Bespalov, A. Y., Dravolina, O. A., Sukhanov, I., Zakharova, E., Blokhina, E., Zvartau, E., Danysz, W., van Heeke, G. & Markou, A. **(2005).** Metabotropic glutamate receptor (mGluR5) antagonist MPEP attenuated cue- and schedule-induced reinstatement of nicotine self-administration behavior in rats. *Neuropharmacology* 49, 167–178. Pergamon.

Bhuiyan, M. S. & Fukunaga, K. **(2011).** Targeting sigma-1 receptor signaling by endogenous ligands for cardioprotection. *Expert Opin Ther Targets* 15, 145–155. Taylor & Francis.

Bhutada, P. S., Mundhada, Y. R., Ghodki, Y. R., Chaware, P., Dixit, P. V, Jain, K. S. & Umathe, S. N. **(2012).** Influence of sigma-1 receptor modulators on ethanol-induced conditioned place preference in the extinction-reinstatement model. *Behav Pharmacol* 23, 25–33.

De Biasi, M. & Dani, J. A. **(2011).** Reward, addiction, withdrawal to nicotine. *Annu Rev Neurosci* 34, 105–30. NIH Public Access.

Bierut, L. J., Dinwiddie, S. H., Begleiter, H., Crowe, R. R., Hesselbrock, V., Nurnberger, J. I., Porjesz, B., Schuckit, M. A. & Reich, T. **(1998).** Familial transmission of substance dependence: alcohol, marijuana, cocaine, and habitual smoking: a report from the Collaborative Study on the Genetics of Alcoholism. *Arch Gen Psychiatry* 55, 982–8.

Bigliardi, P. L. & Bigliardi-Qi, M. **(2014).** *Peripheral Opioids*. *Itch Mech Treat*. CRC Press/Taylor & Francis.

Blasio, A., Valenza, M., Iyer, M. R., Rice, K. C., Steardo, L., Hayashi, T., Cottone, P. & Sabino, V. **(2015).** Sigma-1 receptor mediates acquisition of alcohol drinking and seeking behavior in alcohol-preferring rats. *Behav Brain Res* 287, 315–22. NIH Public Access.

Bodnar, R. J. **(2017).** Endogenous Opiates and Behavior: 2015. *Peptides* 88, 126–188.

Bodnar, R. J. **(2013).** Endogenous opiates and behavior: 2012. *Peptides* 50, 55–95. Elsevier Inc.

Bohn, L. M., Gainetdinov, R. R., Sotnikova, T. D., Medvedev, I. O., Lefkowitz, R. J., Dykstra, L. A. & Caron, M. G. **(2003).** Enhanced rewarding properties of morphine, but not cocaine, in beta(arrestin)-2 knock-out mice. *J Neurosci* 23, 10265–73. Society for Neuroscience.

Bohn, L. M., Lefkowitz, R. J., Gainetdinov, R. R., Peppel, K., Caron, M. G. & Lin, F. T. **(1999).** Enhanced morphine analgesia in mice lacking beta-arrestin 2. *Science* 286, 2495–8.

American Association for the Advancement of Science.

Bolshakova, A. V., Kukanova, E. O., Gainullina, A. N., Zhemkov, V. A., Korban, S. A. & Bezprozvanny, I. B. **(2016).** Sigma-1 receptor as a potential pharmacological target for the treatment of neuropathology. *St Petersbg Polytech Univ J Phys Math* 2, 31–40. No longer published by Elsevier.

Bossert, J. M., Ghitza, U. E., Lu, L., Epstein, D. H. & Shaham, Y. **(2005).** Neurobiology of relapse to heroin and cocaine seeking: an update and clinical implications. *Eur J Pharmacol* 526, 36–50.

Bouton, M. E. & Swartzentruber, D. **(1991).** Sources of relapse after extinction in Pavlovian and instrumental learning. *Clin Psychol Rev* 11, 123–140. Pergamon.

Brindley, R. L., Bauer, M. B., Hartley, N. D., Horning, K. J. & Currie, K. P. M. **(2017).** Sigma-1 receptor ligands inhibit catecholamine secretion from adrenal chromaffin cells due to block of nicotinic acetylcholine receptors. *J Neurochem* 143, 171–182. NIH Public Access.

Britt, J. P., Benaliouad, F., Mcdevitt, R. A., Stuber, G. D., Wise, R. A. & Bonci, A. **(2012).** Synaptic and Behavioral Profile of Multiple Glutamatergic Inputs to the Nucleus Accumbens. *Neuron* 76, 790–803.

Bromberg-Martin, E. S. & Hikosaka, O. **(2011).** Lateral habenula neurons signal errors in the prediction of reward information.

Brown, R. W. & Kolb, B. **(2001).** Nicotine sensitization increases dendritic length and spine density in the nucleus accumbens and cingulate cortex. *Brain Res* 899, 94–100. Elsevier.

Bruijnzeel, A. W., Prado, M. & Isaac, S. **(2009).** Corticotropin-Releasing Factor-1 Receptor Activation Mediates Nicotine Withdrawal-Induced Deficit in Brain Reward Function and Stress-Induced Relapse. *Biol Psychiatry* 66, 110–117.

Buisson, B. & Bertrand, D. **(2001).** Chronic exposure to nicotine upregulates the human (alpha)4((beta)2 nicotinic acetylcholine receptor function. *J Neurosci* 21, 1819–29. Society for Neuroscience.

Buisson, B. & Bertrand, D. **(2002).** Nicotine addiction: the possible role of functional upregulation. *Trends Pharmacol Sci* 23, 130–136. Elsevier Current Trends.

Bunzow, J. R., Saez, C., Mortrud, M., Bouvier, C., Williams, J. T., Low, M. & Grandy, D. K. **(1994).** Molecular cloning and tissue distribution of a putative member of the rat opioid receptor gene family that is not a μ, δ or κ opioid receptor type. *FEBS Lett* 347, 284–288. John Wiley & Sons, Ltd.

Busquets-Garcia, A., Puighermanal, E., Pastor, A., de la Torre, R., Maldonado, R. & Ozaita, A. **(2011).** Differential Role of Anandamide and 2-Arachidonoylglycerol in Memory and Anxiety-like Responses. *Biol Psychiatry* 70, 479–486. Elsevier.

Cachope, R. & Cheer, J. F. **(2014).** Local control of striatal dopamine release. *Front Behav Neurosci* 8, 1–7.

Cachope, R., Mateo, Y., Mathur, B. N., Irving, J., Wang, H., Morales, M., Lovinger, D. M. & Cheer, J. F. **(2012).** Selective activation of cholinergic interneurons enhances accumbal phasic dopamine release: setting the tone for reward processing. *Cell Rep* 2, 33–41.

Cadoni, C. & Di Chiara, G. **(2000).** Differential changes in accumbens shell and core dopamine in behavioral sensitization to nicotine. *Eur J Pharmacol* 387, R23-5.

Cagnotto, A., Bastone, A. & Mennini, T. **(1994).** [3H](+)-pentazocine binding to rat brain sigma 1 receptors. *Eur J Pharmacol* 266, 131–8.

Cahill, M. A. **(2007).** Progesterone receptor membrane component 1: An integrative review. *J Steroid Biochem Mol Biol* 105, 16–36. Pergamon.

Caine, S. B., Negus, S. S., Mello, N. K., Patel, S., Bristow, L., Kulagowski, J., Vallone, D., Saiardi, A. & Borrelli, E. **(2002).** Role of dopamine D2-like receptors in cocaine self-

administration: studies with D2 receptor mutant mice and novel D2 receptor antagonists. *J Neurosci* 22, 2977–88. Society for Neuroscience.

Caine, S. B., Thomsen, M., Gabriel, K. I., Berkowitz, J. S., Gold, L. H., Koob, G. F., Tonegawa, S., Zhang, J. & Xu, M. **(2007).** Lack of Self-Administration of Cocaine in Dopamine D 1 Receptor Knock-Out Mice NIH Public Access. *J Neurosci* 27, 13140–13150.

Calabresi, P., Picconi, B., Tozzi, A. & Di Filippo, M. **(2007, May).** Dopamine-mediated regulation of corticostriatal synaptic plasticity. *Trends Neurosci*.

Camí, J. & Farré, M. **(2003).** Drug Addiction. *N Engl J Med* 349, 975–986.

Carboni, E., Bortone, L., Giua, C. & Di Chiara, G. **(2000).** Dissociation of physical abstinence signs from changes in extracellular dopamine in the nucleus accumbens and in the prefrontal cortex of nicotine dependent rats. *Drug Alcohol Depend* 58, 93–102.

Cardinal, R. N. & Everitt, B. J. **(2004).** Neural and psychological mechanisms underlying appetitive learning: links to drug addiction. *Curr Opin Neurobiol* 14, 156–62.

Carr, D. B. & Sesack, S. R. **(2000).** Projections from the rat prefrontal cortex to the ventral tegmental area: target specificity in the synaptic associations with mesoaccumbens and mesocortical neurons. *J Neurosci* 20, 3864–73.

Carter, B. L. & Tiffany, S. T. **(1999).** Meta-analysis of cue-reactivity in addiction research. *Addiction* 94, 327–40.

Cazorla, M., Delmondes De Carvalho, F., Chohan, M. O., Shegda, M., Chuhma, N., Rayport, S., Ahmari, S. E., Moore, H. & Kellendonk, C. **(2013).** Dopamine D2 receptors regulate the anatomical balance of basal ganglia circuitry.

Champtiaux, N., Gotti, C., Cordero-Erausquin, M., David, D. J., Przybylski, C., Léna, C., Clementi, F., Moretti, M., Rossi, F. M. & other authors. **(2003).** Subunit composition of functional nicotinic receptors in dopaminergic neurons investigated with knock-out mice. *J Neurosci* 23, 7820–9. Society for Neuroscience.

Changeux, J.-P. **(2010).** Nicotine addiction and nicotinic receptors: lessons from genetically modified mice.

Charara, A., Smith, Y. & Parent, A. **(1996).** Glutamatergic inputs from the pedunculopontine nucleus to midbrain dopaminergic neurons in primates:Phaseolus vulgaris-leucoagglutinin anterograde labeling combined with postembedding glutamate and GABA immunohistochemistry. *J Comp Neurol* 364, 254–266. John Wiley & Sons, Ltd.

Charbogne, P., Kieffer, B. L. & Befort, K. **(2014).** 15 years of genetic approaches in vivo for addiction research: Opioid receptor and peptide gene knockout in mouse models of drug abuse. *Neuropharmacology* 76 Pt B, 204–17. Elsevier.

Charbogne, P., Gardon, O., Martín-García, E., Keyworth, H. L., Matsui, A., Mechling, A. E., Bienert, T., Nasseef, T., Robé, A. & other authors. **(2017).** Mu Opioid Receptors in Gamma-Aminobutyric Acidergic Forebrain Neurons Moderate Motivation for Heroin and Palatable Food. *Biol Psychiatry* 81, 778–788. Elsevier USA.

Chatterjee, S., Santos, N., Holgate, J., Haass-Koffler, C. L. & Hopf, F. W. **(2013).** Ventral-Tegmental Area. *PLoS One* 8, 68300.

Chavkin, C. **(2013).** Dynorphin--still an extraordinarily potent opioid peptide. *Mol Pharmacol* 83, 729–36. American Society for Pharmacology and Experimental Therapeutics.

Chen, Y., Mestek, A., Liu, J., Hurley, J. A. & Yu, L. **(1993).** Molecular cloning and functional expression of a mu-opioid receptor from rat brain. *Mol Pharmacol* 44, 8–12.

Chiamulera, C., Borgo, C., Falchetto, S., Valerio, E. & Tessari, M. **(1996).** Nicotine reinstatement of nicotine self-administration after long-term extinction. *Psychopharmacology (Berl)* 127, 102–7.

Di Chiara, G. & Imperato, A. **(1988).** Drugs abused by humans preferentially increase synaptic dopamine concentrations in the mesolimbic system of freely moving rats. *Proc Natl Acad Sci U S A* 85, 5274–8.

Childress, A. R., McLellan, A. T. & O'Brien, C. P. **(1993).** Behavioral therapies for substance abuse. *Int J Addict* 20, 947–69.

Chu, U. B., Mavlyutov, T. A., Chu, M. L., Yang, H., Schulman, A., Mesangeau, C., McCurdy, C. R., Guo, L. W. & Ruoho, A. E. **(2015).** The Sigma-2 Receptor and Progesterone Receptor Membrane Component 1 are Different Binding Sites Derived From Independent Genes. *EBioMedicine* 2, 1806–1813. Elsevier B.V.

Chuhma, N., Zhang, H., Masson, J., Zhuang, X., Sulzer, D., Hen, R. & Rayport, S. **(2004).** Cellular/Molecular Dopamine Neurons Mediate a Fast Excitatory Signal via Their Glutamatergic Synapses.

Chung, P. C. S., Keyworth, H. L., Martin-Garcia, E., Charbogne, P., Darcq, E., Bailey, A., Filliol, D., Matifas, A., Scherrer, G. & other authors. **(2015).** A novel anxiogenic role for the delta opioid receptor expressed in GABaergic forebrain neurons. *Biol Psychiatry* 77, 404–415. Elsevier USA.

Cobos, E. J., Entrena, J. M., Nieto, F. R., Cendán, C. M. & Del Pozo, E. **(2008).** Pharmacology and therapeutic potential of sigma(1) receptor ligands. *Curr Neuropharmacol* 6, 344–66.

Cohen, C., Kodas, E. & Griebel, G. **(2005).** CB1 receptor antagonists for the treatment of nicotine addiction. *Pharmacol Biochem Behav* 81, 387–395. Elsevier.

Collins, R. J., Weeks, J. R., Cooper, M. M., Good, P. I. & Russell, R. R. **(1984).** Prediction of abuse liability of drugs using IV self-administration by rats. *Psychopharmacology (Berl)* 82, 6–13.

Collins, S. L., D'Addario, C. & Izenwasser, S. **(2001).** Effects of κ-opioid receptor agonists on long-term cocaine use and dopamine neurotransmission. *Eur J Pharmacol* 426, 25–34. Elsevier.

Colombo, G., Lobina, C., Carai, M. A. M. & Gessa, G. L. **(2006).** Phenotypic characterization of genetically selected Sardinian alcohol-preferring (sP) and -non-preferring (sNP) rats. *Addict Biol* 11, 324–338. John Wiley & Sons, Ltd (10.1111).

Colombo, S. F., Mazzo, F., Pistillo, F. & Gotti, C. **(2013).** Biogenesis, trafficking and up-regulation of nicotinic ACh receptors. *Biochem Pharmacol* 86, 1063–1073. Elsevier.

Comb, M., Seeburg, P. H., Adelman, J., Eiden, L. & Herbert, E. **(1982).** Primary structure of the human Met- and Leu-enkephalin precursor and its mRNA. *Nature* 295, 663–666. Nature Publishing Group.

Condé, F., Maire-lepoivre, E., Audinat, E. & Crépel, F. **(1995).** Afferent connections of the medial frontal cortex of the rat. II. Cortical and subcortical afferents. *J Comp Neurol* 352, 567–593. John Wiley & Sons, Ltd.

Conte-Devolx, B., Oliver, C., Giraud, P., Gillioz, P., Castanas, E., Lissitzky, J.-C., Boudouresque, F. & Millet, Y. **(1981).** Effect of nicotine on in vivo secretion of melanocorticotropic hormones in the rat. *Life Sci* 28, 1067–1073. Pergamon.

Cooper, S., Robison, A. J. & Mazei-Robison, M. S. **(2017).** Reward Circuitry in Addiction. *Neurotherapeutics* 14, 687–697.

Corder, G., Castro, D. C., Bruchas, M. R. & Scherrer, G. **(2018).** Endogenous and Exogenous Opioids in Pain. *Annu Rev Neurosci* 41, 453. NIH Public Access.

Corrigall, W. A., Franklin, K. B., Coen, K. M. & Clarke, P. B. **(1992).** The mesolimbic dopaminergic system is implicated in the reinforcing effects of nicotine. *Psychopharmacology (Berl)* 107, 285–9.

Corrigall, W. A. & Coen, K. M. **(1989).** Nicotine maintains robust self-administration in rats on a limited-access schedule. *Psychopharmacology (Berl)* 99, 473–8.

Cosgrove, K. P., Esterlis, I., Sandiego, C., Petrulli, R. & Morris, E. D. **(2015).** Imaging

Tobacco Smoking with PET and SPECT, pp. 1–17. Springer, Cham.
Couey, J. J., Meredith, R. M., Spijker, S., Poorthuis, R. B., Smit, A. B., Brussaard, A. B. & Mansvelder, H. D. **(2007).** Article Distributed Network Actions by Nicotine Increase the Threshold for Spike-Timing-Dependent Plasticity in Prefrontal Cortex. *Neuron* 54, 73–84.
Covey, L. S., Glassman, A. H. & Stetner, F. **(1999).** Naltrexone Effects on Short-Term and Long-Term Smoking Cessation. *J Addict Dis* 18, 31–40. Taylor & Francis Group .
Cragg, S. J. **(2006).** Meaningful silences: how dopamine listens to the ACh pause. *Trends Neurosci* 29, 125–31. Elsevier.
Crews, F., He, J. & Hodge, C. **(2007).** Adolescent cortical development: A critical period of vulnerability for addiction. *Pharmacol Biochem Behav* 86, 189–199. Elsevier.
Crombag, H. S., Bossert, J. M., Koya, E. & Shaham, Y. **(2008).** Review. Context-induced relapse to drug seeking: a review. *Philos Trans R Soc Lond B Biol Sci* 363, 3233–43.
Crum, R. M., Chan, Y.-F., Chen, L.-S., Storr, C. L. & Anthony, J. C. **(2005).** Incidence rates for alcohol dependence among adults: prospective data from the Baltimore Epidemiologic Catchment Area Follow-Up Survey, 1981-1996. *J Stud Alcohol* 66, 795–805.
D'Souza, M. S. & Markou, A. **(2014).** Differential role of N -methyl-D-aspartate receptor-mediated glutamate transmission in the nucleus accumbens shell and core in nicotine seeking in rats. *Eur J Neurosci* 39, 1314–1322. John Wiley & Sons, Ltd (10.1111).
D'Souza, M. S. & Markou, A. **(2013).** The 'stop' and 'go' of nicotine dependence: role of GABA and glutamate. *Cold Spring Harb Perspect Med* 3.
Dajas-Bailador, F. & Wonnacott, S. **(2004).** Nicotinic acetylcholine receptors and the regulation of neuronal signalling. *Trends Pharmacol Sci* 25, 317–24.
Dalley, J. W., Cardinal, R. N. & Robbins, T. W. **(2004).** Prefrontal executive and cognitive functions in rodents: neural and neurochemical substrates. *Neurosci Biobehav Rev* 28, 771–784. Pergamon.
Dani, J. A. **(2015).** Neuronal Nicotinic Acetylcholine Receptor Structure and Function and Response to Nicotine. *Int Rev Neurobiol* 124, 3–19.
Dani, J. A. & Bertrand, D. **(2007).** Nicotinic acetylcholine receptors and nicotinic cholinergic mechanisms of the central nervous system. *Annu Rev Pharmacol Toxicol* 47, 699–729.
Dani, J. A. & Heinemann, S. **(1996).** Molecular and cellular aspects of nicotine abuse. *Neuron* 16, 905–8.
Dani, J. A., Radcliffe, K. A. & Pidoplichko, V. I. **(2000).** Variations in desensitization of nicotinic acetylcholine receptors from hippocampus and midbrain dopamine areas. *Eur J Pharmacol* 393, 31–38.
Dani, J. A., Ji, D. & Zhou, F. M. **(2001).** Synaptic Plasticity and Nicotine Addiction. *Neuron* 31, 349–352.
Davis, W. M. & Smith, S. G. **(n.d.).** Role of conditioned reinforcers in the initiation, maintenance and extinction of drug-seeking behavior. *Pavlov J Biol Sci* 11, 222–36.
Deroche-Gamonet, V. & Piazza, P. V. **(2014).** Psychobiology of cocaine addiction: Contribution of a multi-symptomatic animal model of loss of control. *Neuropharmacology* 76 Pt B, 437–49. Elsevier Ltd.
Deroche-Gamonet, V., Belin, D. & Piazza, P. V. **(2004).** Evidence for addiction-like behavior in the rat. *Science* 305, 1014–7.
Descarries, L. & Mechawar, N. **(2000).** Ultrastructural evidence for diffuse transmission by monoamine and acetylcholine neurons of the central nervous system. *Prog Brain Res* 125, 27–47. Elsevier.
Descarries, L., Gisiger, V. & Steriade, M. **(1997).** Diffuse transmission by acetylcholine in

the CNS. *Prog Neurobiol* 53, 603–625. Pergamon.

Devine, D. P., Leone, P., Pocock, D. & Wise, R. A. **(1993).** Differential Involvement of Ventral Tegmental Mu, Delta and Kappa Opioid Receptors in Modulation of Basal Mesolimbic Dopamine Release: In Vivo Microdialysis Studies1. *J Pharmacol Exp Ther* 266, 1236–1246.

Dhatt, R. K., Gudehithlu, K. P., Wemlinger, T. A., Tejwani, G. A., Neff, N. H. & Hadjiconstantinou, M. **(1995).** Preproenkephalin mRNA and methionine-enkephalin content are increased in mouse striatum after treatment with nicotine. *J Neurochem* 64, 1878–83.

Doll, R., Peto, R., Boreham, J. & Sutherland, I. **(2004).** Mortality in relation to smoking: 50 years' observations on male British doctors. *BMJ* 328, 1519.

Dome, P., Lazary, J., Kalapos, M. P. & Rihmer, Z. **(2010).** Smoking, nicotine and neuropsychiatric disorders. *Neurosci Biobehav Rev* 34, 295–342.

Douglas, R. J. & Martin, K. A. C. **(2004).** NEURONAL CIRCUITS OF THE NEOCORTEX. *Annu Rev Neurosci* 27, 419–51.

Dravolina, O. A., Zakharova, E. S., Shekunova, E. V., Zvartau, E. E., Danysz, W. & Bespalov, A. Y. **(2007).** mGlu1 receptor blockade attenuates cue- and nicotine-induced reinstatement of extinguished nicotine self-administration behavior in rats. *Neuropharmacology* 52, 263–269.

Drenan, R. M., Grady, S. R., Whiteaker, P., McClure-Begley, T., McKinney, S., Miwa, J. M., Bupp, S., Heintz, N., McIntosh, J. M. & other authors. **(2008).** In Vivo Activation of Midbrain Dopamine Neurons via Sensitized, High-Affinity α6∗ Nicotinic Acetylcholine Receptors. *Neuron* 60, 123–136.

Druga, R. **(2009).** Neocortical Inhibitory System. *Folia Biol* 55, 201–217.

DSM-5. **(2013).** *Diagnostic and Statistical Manual ofMental Disorders (DSM–5®), 5th ed.* American Psychiatric Publishing: Washington, DC, USA.

DSM-I. **(1952).** *Diagnostic and Statistical Manual: Mental Disorders, 1st ed.* American Psychiatric Association: Washington, DC, USA.

DSM-II. **(1968).** *Diagnostic and Statistical Manual of Mental Disorders, 2nd ed.* American Psychiatric Association: Washington, DC, USA.

DSM-III-R. **(1987).** *Diagnostic and Statistical Manual of Mental Disorders, 3rd rev. ed*. American Psychiatric Association: Washington, DC, USA.

DSM-III. **(1980).** *Diagnostic and Statistical Manual of Mental Disorders, 3rd ed.* American Psychiatric Association: Washington, DC, USA.

DSM-IV-TR. **(2000).** *Diagnostic and Statistical Manual of Mental Disorders, Fourth Edition, Text Revision (DSM-IV-TR)*. American Psychiatric Association: Washington, DC, USA.

DSM-IV. **(1994).** *Diagnostic and Statistical Manual of Mental Disorders, 4th ed*. American Psychiatric Association: Washington, DC, USA.

Duggan, A. W. **(2000).** Neuropeptide spread in the brain and spinal cord. *Prog Brain Res* 125, 369–380. Elsevier.

Durieux, P. F., Bearzatto, B., Guiducci, S., Buch, T., Waisman, A., Zoli, M., Schiffmann, S. N. & de Kerchove d'Exaerde, A. **(2009).** D2R striatopallidal neurons inhibit both locomotor and drug reward processes. *Nat Neurosci* 12, 393–395. Nature Publishing Group.

Edwards, G. & Gross, M. M. **(1976).** *Alcohol dependence: provisional description of a clinical syndrome*. *Med J*.

Egea, J., Buendia, I., Parada, E., Navarro, E., León, R. & Lopez, M. G. **(2015).** Anti-inflammatory role of microglial alpha7 nAChRs and its role in neuroprotection. *Biochem Pharmacol* 97, 463–472.

Eichel, K., Jullié, D. & von Zastrow, M. **(2016).** β-Arrestin drives MAP kinase signalling from clathrin-coated structures after GPCR dissociation. *Nat Cell Biol* 18, 303–10.

NIH Public Access.
El-Brolosy, M. A. & Stainier, D. Y. R. **(2017).** Genetic compensation: A phenomenon in search of mechanisms. *PLoS Genet* 13, e1006780. Public Library of Science.
Ela, C., Barg, J., Vogel, Z., Hasin, Y. & Eilam, Y. **(1994).** Sigma receptor ligands modulate contractility, Ca++ influx and beating rate in cultured cardiac myocytes. *J Pharmacol Exp Ther* 269, 1300–9.
Epping-Jordan, M. P., Watkins, S. S., Koob, G. F. & Markou, A. **(1998).** Dramatic decreases in brain reward function during nicotine withdrawal. *Nature* 393, 76–79. Nature Publishing Group.
Epstein, D. H., Preston, K. L., Stewart, J. & Shaham, Y. **(2006).** Toward a model of drug relapse: an assessment of the validity of the reinstatement procedure. *Psychopharmacology (Berl)* 189, 1–16. NIH Public Access.
Erb, S., Shaham, Y. & Stewart, J. **(1996).** Stress reinstates cocaine-seeking behavior after prolonged extinction and a drug-free period. *Psychopharmacology (Berl)* 128, 408–12.
Euston, D. R., Gruber, A. J. & McNaughton, B. L. **(2012).** The role of medial prefrontal cortex in memory and decision making. *Neuron* 76, 1057–70. NIH Public Access.
Evans, C. J., Keith, D. E., Morrison, H., Magendzo, K. & Edwards, R. H. **(1992).** Cloning of a delta opioid receptor by functional expression. *Science* 258, 1952–5.
Everitt, B. J. & Wolf, M. E. **(2002).** *Psychomotor Stimulant Addiction: A Neural Systems Perspective*.
Exley, R. & Cragg, S. J. **(2008).** Presynaptic nicotinic receptors: a dynamic and diverse cholinergic filter of striatal dopamine neurotransmission. *Br J Pharmacol* 153, 283–297.
Exley, R., Mcintosh, J. M., Marks, M. J., Maskos, U. & Cragg, S. J. **(2012).** Striatal ␣5 Nicotinic Receptor Subunit Regulates Dopamine Transmission in Dorsal Striatum Richard. *J Neurosci* 32, 2352–2356.
Eysenck, H. ., Arnold, W. & Meili, R. **(1975).** *Encyclopedia of Psychology. H. J. Eysenck, W. Arnold, and R. Meili (Eds.). Vol. 1, A-F; Vol. 2, 6-Phas - Z. New York: Herder and Herder (now available from Continuum Books/Seabury Press), 1972. Pp. 396, 390, 401. $22.50 per volume*. *J Hist Behav Sci*. John Wiley & Sons, Ltd.
Farré, M. & Camí, J. **(1991).** Pharmacokinetic considerations in abuse liability evaluation. *Br J Addict* 86, 1601–6.
Farré, M., Terán, M. T., Roset, P. N., Mas, M., Torrens, M. & Camí, J. **(1998).** Abuse liability of flunitrazepam among methadone-maintained patients. *Psychopharmacology (Berl)* 140, 486–95.
Fattore, L., Spano, M. S., Cossu, G., Scherma, M., Fratta, W. & Fadda, P. **(2009).** Baclofen prevents drug-induced reinstatement of extinguished nicotine-seeking behaviour and nicotine place preference in rodents. *Eur Neuropsychopharmacol* 19, 487–498.
Feighner, J. P., Robins, E., Guze, S. B., Woodruff, R. A., Winokur, G. & Munoz, R. **(1972).** Diagnostic criteria for use in psychiatric research. *Arch Gen Psychiatry* 26, 57–63.
Feltenstein, M. W., Ghee, S. M. & See, R. E. **(2012).** Nicotine self-administration and reinstatement of nicotine-seeking in male and female rats. *Drug Alcohol Depend* 121, 240–246.
Ferrario, C. R., Loweth, J. A., Milovanovic, M., Ford, K. A., Galiñanes, G. L., Heng, L.-J., Tseng, K. Y. & Wolf, M. E. **(2011).** Alterations in AMPA receptor subunits and TARPs in the rat nucleus accumbens related to the formation of Ca^{2+}-permeable AMPA receptors during the incubation of cocaine craving. *Neuropharmacology* 61, 1141–51. NIH Public Access.
Ferré, S., Lluís, C., Justinova, Z., Quiroz, C., Orru, M., Navarro, G., Canela, E. I., Franco, R. & Goldberg, S. R. **(2010).** Adenosine-cannabinoid receptor interactions. Implications

for striatal function. *Br J Pharmacol* 160, 443–53. Wiley-Blackwell.

Filliol, D., Ghozland, S., Chluba, J., Martin, M., Matthes, H. W., Simonin, F., Befort, K., Gavériaux-Ruff, C., Dierich, A. & other authors. **(2000).** Mice deficient for delta- and mu-opioid receptors exhibit opposing alterations of emotional responses. *Nat Genet* 25, 195–200.

Floresco, S. B. **(2015).** The Nucleus Accumbens: An Interface Between Cognition, Emotion, and Action NAc: nucleus accumbens. *Annu Rev Psychol* 66, 25–52.

Flórez, J. **(2007).** *El Tratamiento farmacologico del dolor*. Ars Medica.

Le Foll, B. & Goldberg, S. R. **(2009).** Effects of nicotine in experimental animals and humans: an update on addictive properties. *Handb Exp Pharmacol* 192, 335–367.

Fontanilla, D., Hajipour, A. R., Pal, A., Chu, U. B., Arbabian, M. & Ruoho, A. E. **(2008).** Probing the Steroid Binding Domain-like I (SBDLI) of the Sigma-1 Receptor Binding Site Using N-Substituted Photoaffinity Labels † NIH Public Access. *Biochemistry* 47, 7205–7217.

Fowler, C. D. & Kenny, P. J. **(2011).** Intravenous nicotine self-administration and cue-induced reinstatement in mice: effects of nicotine dose, rate of drug infusion and prior instrumental training. *Neuropharmacology* 61, 687–98. NIH Public Access.

Fowler, R. T. **(1954).** A redetermination of the ionization constants of nicotine. *J Appl Chem* 4, 449–452.

Fowler, T., Lifford, K., Shelton, K., Rice, F., Thapar, A., Neale, M. C., McBride, A. & Bree, M. B. M. van den. **(2007).** Exploring the relationship between genetic and environmental influences on initiation and progression of substance use. *Addiction* 102, 413. Wiley-Blackwell.

Franklin, T. R., wang, Z., Wang, J., Sciortino, N., Harper, D., Li, Y., Ehrman, R., Kampman, K., O'Brien, C. P. & other authors. **(2007).** Limbic Activation to Cigarette Smoking Cues Independent of Nicotine Withdrawal: A Perfusion fMRI Study. *Neuropsychopharmacology* 32, 2301–2309. Nature Publishing Group.

Funk, C. K., O'Dell, L. E., Crawford, E. F. & Koob, G. F. **(2006).** Corticotropin-releasing factor within the central nucleus of the amygdala mediates enhanced ethanol self-administration in withdrawn, ethanol-dependent rats. *J Neurosci* 26, 11324–32. Society for Neuroscience.

Gabbott, P. L. A., Warner, T. A., Jays, P. R. L., Salway, P. & Busby, S. J. **(2005).** Prefrontal cortex in the rat: Projections to subcortical autonomic, motor, and limbic centers. *J Comp Neurol* 492, 145–177. John Wiley & Sons, Ltd.

Gaimarri, A., Moretti, M., Riganti, L., Zanardi, A., Clementi, F. & Gotti, C. **(2007).** Regulation of neuronal nicotinic receptor traffic and expression. *Brain Res Rev* 55, 134–143.

Galeote, L., Berrendero, F., Bura, S. A., Zimmer, A. & Maldonado, R. **(2009).** Prodynorphin gene disruption increases the sensitivity to nicotine self-administration in mice. *Int J Neuropsychopharmacol* 12, 615–25.

Gamaleddin, I. H., Trigo, J. M., Gueye, A. B., Zvonok, A., Makriyannis, A., Goldberg, S. R. & Le Foll, B. **(2015).** Role of the endogenous cannabinoid system in nicotine addiction: novel insights. *Front psychiatry* 6, 41. Frontiers Media SA.

Garavan, H., Pankiewicz, J., Bloom, A., Cho, J.-K., Sperry, L., Ross, T. J., Salmeron, B. J., Risinger, R., Kelley, D. & Stein, E. A. **(2000).** Cue-Induced Cocaine Craving: Neuroanatomical Specificity for Drug Users and Drug Stimuli. *Am J Psychiatry* 157, 1789–1798.

Garcés-Ramírez, L., Green, J. L., Hiranita, T., Kopajtic, T. A., Mereu, M., Thomas, A., Mesangeau, C., Narayanan, S., Mccurdy, C. R. & other authors. **(2011).** Sigma receptor agonists: Receptor binding and effects on mesolimbic dopamine neurotransmission assessed by microdialysis 69, 208–217.

Gaveriaux-Ruff, C., Nozaki, C., Nadal, X., Hever, X. C., Weibel, R., Matifas, A., Reiss, D., Filliol, D., Nassar, M. A. & other authors. **(2011).** Genetic ablation of delta opioid receptors in nociceptive sensory neurons increases chronic pain and abolishes opioid analgesia. *Pain* 152, 1238–1248.

Ge, S. & Dani, J. A. **(2005).** Cellular/Molecular Nicotinic Acetylcholine Receptors at Glutamate Synapses Facilitate Long-Term Depression or Potentiation.

George, O., Ghozland, S., Azar, M. R., Cottone, P., Zorrilla, E. P., Parsons, L. H., O'Dell, L. E., Richardson, H. N. & Koob, G. F. **(2007).** CRF-CRF1 system activation mediates withdrawal-induced increases in nicotine self-administration in nicotine-dependent rats. *Proc Natl Acad Sci U S A* 104, 17198–203.

Gerfen, C. R., Engber, T. M., Mahan, L. C., Susel, Z., Chase, T. N., Monsma, F. J. & Sibley, D. R. **(1990).** D1 and D2 dopamine receptor-regulated gene expression of striatonigral and striatopallidal neurons. *Science* 250, 1429–32. American Association for the Advancement of Science.

Gerfen, C. R. & Surmeier, D. J. **(2011).** Modulation of striatal projection systems by dopamine. *Annu Rev Neurosci* 34, 441–466.

Giacchino, J. L. & Henriksen, S. J. **(1996).** Systemic morphine and local opioid effects on neuronal activity in the medial prefrontal cortex. *Neuroscience* 70, 941–949. Pergamon.

Giacchino, J. L. & Henriksen, S. J. **(1998).** Opioid effects on activation of neurons in the medial prefrontal cortex. *Prog Neuro-Psychopharmacology Biol Psychiatry* 22, 1157–1178.

Gilpin, E. A., Pierce, J. P. & Farkas, A. J. **(1997).** Duration of smoking abstinence and success in quitting. *J Natl Cancer Inst* 89, 572–6.

Giniatullin, R., Nistri, A. & Yakel, J. L. **(2005).** Desensitization of nicotinic ACh receptors: Shaping cholinergic signaling. *Trends Neurosci* 28, 371–378. Elsevier Current Trends.

Giorguieff, M. F., Le Floc'h, M. L., Glowinski, J. & Besson, M. J. **(1977).** Involvement of cholinergic presynaptic receptors of nicotinic and muscarinic types in the control of the spontaneous release of dopamine from striatal dopaminergic terminals in the rat. *J Pharmacol Exp Ther* 200.

Gipson, C. D., Reissner, K. J., Kupchik, Y. M., Smith, A. C. W., Stankeviciute, N., Hensley-Simon, M. E. & Kalivas, P. W. **(2013).** Reinstatement of nicotine seeking is mediated by glutamatergic plasticity. *PNAS* 110, 9124–9129.

Gittis, A. H. & Kreitzer, A. C. **(2012).** Striatal microcircuitry and movement disorders. *Trends Neurosci* 35, 557–564.

Gittis, A. H., Hang, G. B., Ladow, E. S., Shoenfeld, L. R., Atallah, B. V, Finkbeiner, S. & Kreitzer, A. C. **(2011).** Rapid target-specific remodeling of fast-spiking inhibitory circuits after loss of dopamine.

Glass, M. J., Vanyo, L., Quimson, L. & Pickel, V. M. **(2009).** Ultrastructural relationship between N-methyl-D-aspartate-NR1 receptor subunit and mu-opioid receptor in the mouse central nucleus of the amygdala. *Neuroscience* 163, 857–67. NIH Public Access.

Goldman-Rakic, P. . **(1995).** Cellular basis of working memory. *Neuron* 14, 477–485. Cell Press.

Goldstein, A., Tachibana, S., Lowney, L. I., Hunkapiller, M. & Hood, L. **(1979).** Dynorphin-(1-13), an extraordinarily potent opioid peptide (endorphin/[Leujenkephalin/pituitary/neuropeptide/endogenous morphine-like peptide). *Proc Natl Acad Sci* 76, 6666–6670.

Goldstein, R. Z. & Volkow, N. D. **(2011).** Dysfunction of the prefrontal cortex in addiction: neuroimaging findings and clinical implications. *Nat Rev Neurosci* 12, 652–669.

Gomes, I., Jordan, B. A., Gupta, A., Trapaidze, N., Nagy, V. & Devi, L. A. **(2000).** Heterodimerization of mu and delta opioid receptors: A role in opiate synergy. *J Neurosci* 20, RC110. NIH Public Access.

Gómez-A, A., Shnitko, T. A., Barefoot, H. M., Brightbill, E. L., Sombers, L. A., Nicola, S. M., Robinson, D. L., Dominick, ‖, Purpura, P. & other authors. **(2019).** Local μ-Opioid Receptor Antagonism Blunts Evoked Phasic Dopamine Release in the Nucleus Accumbens of Rats 10.

Gorelova, N., Mulholland, P. J., Chandler, L. J. & Seamans, J. K. **(2012).** The Glutamatergic Component of the Mesocortical Pathway Emanating from Different Subregions of the Ventral Midbrain. *Cereb Cortex* 22, 327–336.

Gotti, C. & Clementi, F. **(2004).** Neuronal nicotinic receptors: From structure to pathology. *Prog Neurobiol* 74, 363–396.

Gotti, C., Zoli, M. & Clementi, F. **(2006).** Brain nicotinic acetylcholine receptors: native subtypes and their relevance. *Trends Pharmacol Sci* 27, 482–491.

Gotti, C., Guiducci, S., Tedesco, V., Corbioli, S., Zanetti, L., Moretti, M., Zanardi, A., Rimondini, R., Mugnaini, M. & other authors. **(2010).** Behavioral/Systems/Cognitive Nicotinic Acetylcholine Receptors in the Mesolimbic Pathway: Primary Role of Ventral Tegmental Area 62* Receptors in Mediating Systemic Nicotine Effects on Dopamine Release, Locomotion, and Reinforcement.

Goudriaan, A. E., de Ruiter, M. B., van den Brink, W., Oosterlaan, J. & Veltman, D. J. **(2010).** Brain activation patterns associated with cue reactivity and craving in abstinent problem gamblers, heavy smokers and healthy controls: an fMRI study. *Addict Biol* 15, 491–503. Wiley-Blackwell.

Gowing, L. R., Ali, R. L., Allsop, S., Marsden, J., Turf, E. E., West, R. & Witton, J. **(2015).** Global statistics on addictive behaviours: 2014 status report. *Addiction* 110, 904–919. John Wiley & Sons, Ltd (10.1111).

Granier, S., Manglik, A., Kruse, A. C., Kobilka, T. S., Thian, F. S., Weis, W. I. & Kobilka, B. K. **(2012).** Structure of the δ-opioid receptor bound to naltrindole. *Nature* 485, 400–4. NIH Public Access.

Grant, B. F. & Dawson, D. A. **(1998).** Age of onset of drug use and its association with DSM-IV drug abuse and dependence: results from the National Longitudinal Alcohol Epidemiologic Survey. *J Subst Abuse* 10, 163–73.

Grant, B. F., Stinson, F. S. & Harford, T. C. **(2001).** Age at onset of alcohol use and DSM-IV alcohol abuse and dependence: a 12-year follow-up. *J Subst Abuse* 13, 493–504.

Graybiel, A. M., Aosaki, T., Flaherty, A. W. & Kimura, M. **(1994).** The basal ganglia and adaptive motor control. *Science* 265, 1826–31. American Association for the Advancement of Science.

Grenhoff, J. & Svensson, T. H. **(1989).** Pharmacology of nicotine. *Br J Addict* 84, 477–92.

Grenhoff, J., Aston-Jones, G. & Svensson, T. H. **(1986).** Nicotinic effects on the firing pattern of midbrain dopamine neurons. *Acta Physiol Scand* 128, 351–8.

Grieder, T. E., George, O., Tan, H., George, S. R., Le Foll, B., Laviolette, S. R. & van der Kooy, D. **(2012).** Phasic D1 and tonic D2 dopamine receptor signaling double dissociate the motivational effects of acute nicotine and chronic nicotine withdrawal. *Proc Natl Acad Sci U S A* 109, 3101–6. National Academy of Sciences.

Grilli, M., Zappettini, S., Raiteri, L. & Marchi, M. **(2009a).** Nicotinic and muscarinic cholinergic receptors coexist on GABAergic nerve endings in the mouse striatum and interact in modulating GABA release. *Neuropharmacology* 56, 610–614. Pergamon.

Grilli, M., Pittaluga, A., Merlo-Pich, E. & Marchi, M. **(2009b).** NMDA-mediated modulation of dopamine release is modified in rat prefrontal cortex and nucleus accumbens after chronic nicotine treatment. *J Neurochem* 108, 408–416. John Wiley & Sons,

Ltd (10.1111).

Grilli, M., Summa, M., Salamone, A., Olivero, G., Zappettini, S., Di Prisco, S., Feligioni, M., Usai, C., Pittaluga, A. & Marchi, M. **(2012).** In vitro exposure to nicotine induces endocytosis of presynaptic AMPA receptors modulating dopamine release in rat nucleus accumbens nerve terminals. *Neuropharmacology* 63, 916–926.

Groenewegen, H. J. & Uylings, H. B. M. **(2000).** The prefrontal cortex and the integration of sensory, limbic and autonomic information. *Prog Brain Res* 126, 3–28. Elsevier.

Groenewegen, H. J., Wright, C. I. & Uylings, H. B. M. **(1997).** The anatomical relationships of the prefrontal cortex with limbic structures and the basal ganglia. *J Psychopharmacol* 11, 99–106. Sage PublicationsSage CA: Thousand Oaks, CA.

Gubler, U., Seeburg, P., Hoffman, B. J., Gage, L. P. & Udenfriend, S. **(1982).** Molecular cloning establishes proenkephalin as precursor of enkephalin-containing peptides. *Nature* 295, 206–208. Nature Publishing Group.

Guegan, T., Cutando, L., Gangarossa, G., Santini, E., Fisone, G., Martinez, A., Valjent, E., Maldonado, R. & Martin, M. **(2013).** Operant behavior to obtain palatable food modifies neuronal plasticity in the brain reward circuit. *Eur Neuropsychopharmacol* 23, 240–252. Elsevier.

Guillemin, R., Ling, N. & Burgus, R. **(1976).** [Endorphins, hypothalamic and neurohypophysial peptides with morphinomimetic activity: isolation and molecular structure of alpha-endorphin]. *C R Acad Sci Hebd Seances Acad Sci D* 282, 783–5.

Gutiérrez-Cuesta, J., Burokas, A., Mancino, S., Kummer, S., Martin-García, E. & Maldonado, R. **(2014).** Effects of Genetic Deletion of Endogenous Opioid System Components on the Reinstatement of Cocaine-Seeking Behavior in Mice. *Neuropsychopharmacology* 1–15.

Hadjiconstantinou, M., Duchemin, A.-M., Zhang, H. & Neff, N. H. **(2011).** Enhanced dopamine transporter function in striatum during nicotine withdrawal. *Synapse* 65, 91–98.

Hall, F. S., Der-Avakian, A., Gould, T. J., Markou, A., Shoaib, M. & Young, J. W. **(2015).** Negative affective states and cognitive impairments in nicotine dependence. *Neurosci Biobehav Rev* 58, 168–85. NIH Public Access.

Hanner, M., Moebius, F. F., Flandorfer, A., Knaus, H. G., Striessnig, J., Kempner, E. & Glossmann, H. **(1996).** Purification, molecular cloning, and expression of the mammalian sigma1-binding site. *Proc Natl Acad Sci U S A* 93, 8072–7.

Hatsukami, D. K. & Fischman, M. W. **(1996).** Crack cocaine and cocaine hydrochloride. Are the differences myth or reality? *JAMA* 276, 1580–8.

Hayashi, T. & Fujimoto, M. **(2010).** Detergent-resistant microdomains determine the localization of sigma-1 receptors to the endoplasmic reticulum-mitochondria junction. *Mol Pharmacol* 77, 517–28. American Society for Pharmacology and Experimental Therapeutics.

Hayashi, T. & Su, T.-P. **(2003a).** Sigma-1 receptors (sigma(1) binding sites) form raft-like microdomains and target lipid droplets on the endoplasmic reticulum: roles in endoplasmic reticulum lipid compartmentalization and export. *J Pharmacol Exp Ther* 306, 718–25. American Society for Pharmacology and Experimental Therapeutics.

Hayashi, T. & Su, T.-P. **(2003b).** Intracellular dynamics of sigma-1 receptors (sigma(1) binding sites) in NG108-15 cells. *J Pharmacol Exp Ther* 306, 726–33. American Society for Pharmacology and Experimental Therapeutics.

Hayashi, T. & Su, T.-P. **(2007).** Sigma-1 receptor chaperones at the ER-mitochondrion interface regulate Ca(2+) signaling and cell survival. *Cell* 131, 596–610.

Hayashi, T., Maurice, T. & Su, T.-P. **(2000a).** Ca2+ Signaling via ς1-Receptors: Novel Regulatory Mechanism Affecting Intracellular Ca2+Concentration. *J Pharmacol Exp*

Ther 293.

Hayashi, T., Tsai, S.-Y., Mori, T., Fujimoto, M. & Su, T.-P. **(2011).** Targeting ligand-operated chaperone sigma-1 receptors in the treatment of neuropsychiatric disorders. *Expert Opin Ther Targets* 15. NIH Public Access.

Hayashi, T. & Su, T. **(2005a).** The potential role of sigma-1 receptors in lipid transport and lipid raft reconstitution in the brain: Implication for drug abuse. *Life Sci* 77, 1612–1624.

Hayashi, T. & Su, T. **(2005b).** The sigma receptor: evolution of the concept in neuropsychopharmacology. *Curr Neuropharmacol* 3, 267–80. Bentham Science Publishers.

Hayashi, T. & Su, T. P. **(2001).** Regulating ankyrin dynamics: Roles of sigma-1 receptors. *Proc Natl Acad Sci* 98, 491–496. National Academy of Sciences.

Hayashi, T., Maurice, T. & Su, T. P. **(2000b).** Ca(2+) signaling via sigma(1)-receptors: novel regulatory mechanism affecting intracellular Ca(2+) concentration. *J Pharmacol Exp Ther* 293, 788–98.

Heath, A. C., Cates, R., Martin, N. G., Meyer, J., Hewitt, J. K., Neale, M. C. & Eaves, L. J. **(1993).** Genetic contribution to risk of smoking initiation: comparisons across birth cohorts and across cultures. *J Subst Abuse* 5, 221–46.

Heidbreder, C. A. & Groenewegen, H. J. **(2003).** The medial prefrontal cortex in the rat: evidence for a dorso-ventral distinction based upon functional and anatomical characteristics. *Neurosci Biobehav Rev* 27, 555–579. Pergamon.

Heidmann, T., Bernhardt, J., Neumann, E. & Changeux, J. P. **(1983).** Rapid kinetics of agonist binding and permeability response analyzed in parallel on acetylcholine receptor rich membranes from Torpedo marmorata. *Biochemistry* 22, 5452–5459.

Heijna, M. H., Bakker, J. M., Hogenboom, F., Mulder, A. H. & Schoffelmeer, A. N. M. **(1992).** Opioid receptors and inhibition of dopamine-sensitive adenylate cyclase in slices of rat brain regions receiving a dense dopaminergic input. *Eur J Pharmacol* 229, 197–202. Elsevier.

Hellewell, S. B. & Bowen, W. D. **(1990).** A sigma-like binding site in rat pheochromocytoma (PC12) cells: decreased affinity for (+)-benzomorphans and lower molecular weight suggest a different sigma receptor form from that of guinea pig brain. *Brain Res* 527, 244–53.

Hellewell, S. B., Bruce, A., Feinstein, G., Orringer, J., Williams, W. & Bowen, W. D. **(1994).** Rat liver and kidney contain high densities of σ1 and σ2 receptors: characterization by ligand binding and photoaffinity labeling. *Eur J Pharmacol Mol Pharmacol* 268, 9–18. Elsevier.

Henningfield, J. E., Miyasato, K. & Jasinski, D. R. **(1985).** Abuse liability and pharmacodynamic characteristics of intravenous and inhaled nicotine. *J Pharmacol Exp Ther* 234, 1–12.

Henningfield, J. E. & Zeller, M. **(2006).** Nicotine psychopharmacology research contributions to United States and global tobacco regulation: a look back and a look forward. *Psychopharmacology (Berl)* 184, 286–91.

Henny, P. & Jones, B. E. **(2008).** Projections from basal forebrain to prefrontal cortex comprise cholinergic, GABAergic and glutamatergic inputs to pyramidal cells or interneurons. *Eur J Neurosci* 27, 654–670.

Higley, M. J., Gittis, A. H., Oldenburg, I. A., Balthasar, N. & Seal, R. P. **(2011).** Cholinergic Interneurons Mediate Fast VGluT3-Dependent Glutamatergic Transmission in the Striatum. *PLoS One* 6, 19155.

Hiranita, T., Soto, P. L., Tanda, G. & Katz, J. L. **(2010).** Reinforcing effects of sigma-receptor agonists in rats trained to self-administer cocaine. *J Pharmacol Exp Ther* 332, 515–24. American Society for Pharmacology and Experimental Therapeutics.

Hiranita, T., Soto, P. L., Kohut, S. J., Kopajtic, T., Cao, J., Newman, A. H., Tanda, G. & Katz, J. L. **(2011).** Decreases in Cocaine Self-Administration with Dual Inhibition of the Dopamine Transporter and σ Receptors. *J Pharmacol Exp Ther* 339, 662. American Society for Pharmacology and Experimental Therapeutics.

Hiranita, T., Mereu, M., Soto, P. L., Tanda, G. & Katz, J. L. **(2013).** Self-administration of cocaine induces dopamine-independent self-administration of sigma agonists. *Neuropsychopharmacology* 38, 605–15. Nature Publishing Group.

Hirose, N., Murakawa, K., Takada, K., Oi, Y., Suzuki, T., Nagase, H., Cools, A. R. R. & Koshikawa, N. **(2005).** Interactions among mu- and delta-opioid receptors, especially putative delta1- and delta2-opioid receptors, promote dopamine release in the nucleus accumbens. *Neuroscience* 135, 213–25. Pergamon.

Hoops, D. & Flores, C. **(2017).** Making Dopamine Connections in Adolescence. *Trends Neurosci* 40, 709–719. NIH Public Access.

Horan, B., Gardner, E. L., Dewey, S. L., Brodie, J. D. & Ashby, C. R. **(2001).** The selective s 1 receptor agonist , blocks the acquisition of the conditioned place preference response to ž y / -nicotine in rats 1–2.

Houdi, A. A., Dasgupta, R. & Kindy, M. S. **(1998).** Effect of nicotine use and withdrawal on brain preproenkephalin A mRNA. *Brain Res* 799, 257–63.

Huang, Y. H. & Bergles, D. E. **(2004).** Glutamate transporters bring competition to the synapse. *Curr Opin Neurobiol* 14, 346–352. Elsevier Current Trends.

Hughes, J. **(2005).** Effects of abstinence from tobacco: Etiology, animal models, epidemiology, and significance: A subjective review. *Nicotine Tob Res* 9, 329–339. Narnia.

Hughes, J. **(2007).** Effects of abstinence from tobacco: Valid symptoms and time course. *Nicotine Tob Res* 9, 315–327. Narnia.

Hughes, J. R. & Hatsukami, D. **(1986).** Signs and Symptoms of Tobacco Withdrawal. *Arch Gen Psychiatry* 43, 289.

Hukkanen, J., Jacob, P. & Benowitz, N. L. **(2005).** Metabolism and disposition kinetics of nicotine. *Pharmacol Rev* 57, 79–115.

Hurley, K. M., Herbert, H., Moga, M. M. & Saper, C. B. **(1991).** Efferent projections of the infralimbic cortex of the rat. *J Comp Neurol* 308, 249–276. John Wiley & Sons, Ltd.

Hyman, S. E., Malenka, R. C. & Nestler, E. J. **(2006).** Neural Mechanisms of Addiction: The Role of Reward-Related Learning and Memory.

Ibáñez-Sandoval, O., Tecuapetla, F., Unal, B., Shah, F., Koós, T. & Tepper, J. M. **(2010).** Electrophysiological and morphological characteristics and synaptic connectivity of tyrosine hydroxylase-expressing neurons in adult mouse striatum. *J Neurosci* 30, 6999–7016. Society for Neuroscience.

Ibáñez-Sandoval, O., Tecuapetla, F., Unal, B., Shah, F., Koós, T. & Tepper, J. M. **(2011).** A novel functionally distinct subtype of striatal neuropeptide Y interneuron. *J Neurosci* 31, 16757–69. Society for Neuroscience.

Ikemoto, S., Qin, M. & Liu, Z.-H. **(2006).** Primary Reinforcing Effects of Nicotine Are Triggered from Multiple Regions Both Inside and Outside the Ventral Tegmental Area. *J Neurosci* 36, 723–730.

Irannejad, R., Tomshine, J. C., Tomshine, J. R., Chevalier, M., Mahoney, J. P., Steyaert, J., Rasmussen, S. G. F., Sunahara, R. K., El-Samad, H. & other authors. **(2013).** Conformational biosensors reveal GPCR signalling from endosomes. *Nature* 495, 534–8. NIH Public Access.

Ismayilova, N. & Shoaib, M. **(2010).** Alteration of intravenous nicotine self-administration by opioid receptor agonist and antagonists in rats. *Psychopharmacology (Berl)* 210, 211–20.

Isola, R., Zhang, H., Tejwani, G. A., Neff, N. H. & Hadjiconstantinou, M. **(2008).** Dynorphin

and prodynorphin mRNA changes in the striatum during nicotine withdrawal. *Synapse* 62, 448–55.

Itzhak, Y. **(1993).** Repeated methamphetamine-treatment alters brain δ receptors. *Eur J Pharmacol* 230, 243–244. Elsevier.

Jackson, K. J., McLaughlin, J. P., Carroll, F. I. & Damaj, M. I. **(2013).** Effects of the kappa opioid receptor antagonist, norbinaltorphimine, on stress and drug-induced reinstatement of nicotine-conditioned place preference in mice. *Psychopharmacology (Berl)* 226, 763–8.

Jalabert, M., Bourdy, R., Courtin, J., Veinante, P., Manzoni, O. J., Barrot, M. & Georges, F. **(2011).** Neuronal circuits underlying acute morphine action on dopamine neurons. *Proc Natl Acad Sci U S A* 108, 16446–50. National Academy of Sciences.

Jansen, K. L., Elliot, M. & Leslie, R. A. **(1992).** Sigma receptors in rat brain and testes show similar reductions in response to chronic haloperidol. *Eur J Pharmacol* 214, 281–3.

Jay, T. M. **(2003).** Dopamine: a potential substrate for synaptic plasticity and memory mechanisms. *Prog Neurobiol* 69, 375–390. Pergamon.

Jellinek E. M. **(1960).** THE DISEASE CONCEPT OF ALCOHOLISM. *Hillhouse Press Haven, CT,USA*.

Jhou, T. C., Geisler, S., Marinelli, M., Degarmo, B. A. & Zahm, D. S. **(2009).** The mesopontine rostromedial tegmental nucleus: A structure targeted by the lateral habenula that projects to the ventral tegmental area of Tsai and substantia nigra compacta. *J Comp Neurol* 513, 566–596.

Jiang, G., Mysona, B., Dun, Y., Gnana-Prakasam, J. P., Pabla, N., Li, W., Dong, Z., Ganapathy, V. & Smith, S. B. **(2006).** Expression, Subcellular Localization, and Regulation of Sigma Receptor in Retinal Müller Cells. *Investig Opthalmology Vis Sci* 47, 5576.

Johannessen, M., Ramachandran, S., Riemer, L., Ramos-Serrano, A., Ruoho, A. E. & Jackson, M. B. **(2009).** Voltage-gated sodium channel modulation by σ-receptors in cardiac myocytes and heterologous systems. *Am J Physiol - Cell Physiol* 296, C1049. American Physiological Society.

Johanson, C. E. **(1978).** Effects of intravenous cocaine, diethylpropion, d-amphetamine and perphenazine on responding maintained by food delivery and shock avoidance in rhesus monkeys. *J Pharmacol Exp Ther* 204, 118–29.

Johanson, C. E. & Balster, R. L. **(1978).** A summary of the results of a drug self-administration study using substitution procedures in rhesus monkeys. *Bull Narc* 30, 43–54.

Johnson, S. W. & North, R. A. **(1992a).** Two types of neurone in the rat ventral tegmental area and their synaptic inputs. *J Physiol* 450, 455–468. John Wiley & Sons, Ltd (10.1111).

Johnson, S. W. & North, R. A. **(1992b).** Opioids excite dopamine neurons by hyperpolarization of local interneurons. *J Neurosci* 12, 483–8.

Jones, I. W. & Wonnacott, S. **(2004).** Precise localization of alpha7 nicotinic acetylcholine receptors on glutamatergic axon terminals in the rat ventral tegmental area. *J Neurosci* 24, 11244–52.

Jones, I. W., Bolam, J. P. & Wonnacott, S. **(2001).** Presynaptic localisation of the nicotinic acetylcholine receptor ?2 subunit immunoreactivity in rat nigrostriatal dopaminergic neurones. *J Comp Neurol* 439, 235–247. John Wiley & Sons, Ltd.

Jones, S. & Bonci, A. **(2005).** Synaptic plasticity and drug addiction. *Curr Opin Pharmacol* 5, 20–25. Elsevier.

Jordan, B. A. & Devi, L. A. **(1999).** G-protein-coupled receptor heterodimerization modulates receptor function. *Nature* 399, 697–700.

Kaiser, S., Wonnacott, S., Elgoyhen, A. B., Heinemann, S. F. & McIntosh, J. M. **(2000).**

alpha-bungarotoxin-sensitive nicotinic receptors indirectly modulate [(3)H]dopamine release in rat striatal slices via glutamate release. *Mol Pharmacol* 58, 312–8. American Society for Pharmacology and Experimental Therapeutics.

Kakidani, H., Furutani, Y., Takahashi, H., Noda, M., Morimoto, Y., Hirose, T., Asai, M., Inayama, S., Nakanishi, S. & Numa, S. **(1982).** Cloning and sequence analysis of cDNA for porcine β-neo-endorphin/dynorphin precursor. *Nature* 298, 245–249.

Kalamida, D., Poulas, K., Avramopoulou, V., Fostieri, E., Lagoumintzis, G., Lazaridis, K., Sideri, A., Zouridakis, M. & Tzartos, S. J. **(2007).** Muscle and neuronal nicotinic acetylcholine receptors. *FEBS J* 274, 3799–3845.

Kalivas, P. W., Churchill, L. & Klitenick, M. A. **(1993).** GABA and enkephalin projection from the nucleus accumbens and ventral pallidum to the ventral tegmental area. *Neuroscience* 57, 1047–1060. Pergamon.

Kalivas, P. W., Volkow, N. D. & Seamans, J. **(2005).** Unmanageable motivation in addiction: a pathology in prefrontal-accumbens glutamate transmission. *Neuron* 45, 647–50.

Katz, J. L. **(1989).** Interactions of clonidine and naloxone on schedule-controlled behavior in opioid-naive mice. *Psychopharmacology (Berl)* 98, 445–7.

Katz, J. L., Hong, W. C., Hiranita, T. & Su, T.-P. **(2016).** A Role for σRs in Stimulant Self-administration and Addiction. *Behav Pharmacol* 27, 100–115.

Kauer, J. A. & Malenka, R. C. **(2007).** Synaptic plasticity and addiction. *Nat Rev Neurosci* 8, 844–58. Nature Publishing Group.

Kaufling, J., Veinante, P., Pawlowski, S. A., Freund-Mercier, M.-J. & Barrot, M. **(2009).** Afferents to the GABAergic tail of the ventral tegmental area in the rat. *J Comp Neurol* 513, 597–621.

Kawaguchi, Y. **(1993).** Physiological, morphological, and histochemical characterization of three classes of interneurons in rat neostriatum. *J Neurosci* 13, 4908–23. Society for Neuroscience.

Kawashima, K., Fujii, T., Moriwaki, Y., Misawa, H. & Horiguchi, K. **(2015).** Non-neuronal cholinergic system in regulation of immune function with a focus on α7 nAChRs. *Int Immunopharmacol* 29, 127–134.

Kekuda, R., Prasad, P. D., Fei, Y.-J., Leibach, F. H. & Ganapathy, V. **(1996).** Cloning and Functional Expression of the Human Type 1 Sigma Receptor (hSigmaR1). *Biochem Biophys Res Commun* 229, 553–558.

Kendler, K. S. & Prescott, C. A. **(1998).** Cocaine use, abuse and dependence in a population-based sample of female twins. *Br J Psychiatry* 173, 345–50.

Kendler, K. S., Karkowski, L. M., Neale, M. C. & Prescott, C. A. **(2000).** Illicit psychoactive substance use, heavy use, abuse, and dependence in a US population-based sample of male twins. *Arch Gen Psychiatry* 57, 261–9.

Kendler, K. S., Aggen, S. H., Tambs, K. & Reichborn-Kjennerud, T. **(2006).** Illicit psychoactive substance use, abuse and dependence in a population-based sample of Norwegian twins. *Psychol Med* 36, 955–62.

Kenny, P. J., Chartoff, E., Roberto, M., Carlezon, W. A., Markou, A. & Kenny, P. J. **(2009).** NMDA receptors regulate nicotine-enhanced brain reward function and intravenous nicotine self-administration: Role of the ventral tegmental area and central nucleus of the amygdala Markou4. *Neuropsychopharmacology* 34, 266–281. NIH Public Access.

Kenny, P. J. & Markou, A. **(2006).** Nicotine self-administration acutely activates brain reward systems and induces a long-lasting increase in reward sensitivity. *Neuropsychopharmacology* 31, 1203–11.

Kenny, P. J., Paterson, N. E., Boutrel, B., Semenova, S., Harrison, A. A., Gasparini, F., Koob, G. F., Skoubis, P. D. & Markou, A. **(2003).** Metabotropic Glutamate 5 Receptor

Antagonist MPEP Decreased Nicotine and Cocaine Self-Administration but Not Nicotine and Cocaine-Induced Facilitation of Brain Reward Function in Rats. *Ann N Y Acad Sci* 1003, 415–418. John Wiley & Sons, Ltd (10.1111).

Kesner, R. P. & Churchwell, J. C. **(2011).** An analysis of rat prefrontal cortex in mediating executive function. *Neurobiol Learn Mem* 96, 417–431. Academic Press.

Kessler, R. C., Berglund, P., Demler, O., Jin, R., Merikangas, K. R. & Walters, E. E. **(2005).** Lifetime prevalence and age-of-onset distributions of DSM-IV disorders in the National Comorbidity Survey Replication. *Arch Gen Psychiatry* 62, 593–602.

Kieffer, B. L. **(1995).** Recent advances in molecular recognition and signal transduction of active peptides: receptors for opioid peptides. *Cell Mol Neurobiol* 15, 615–35.

Kieffer, B. L. **(1999).** Opioids: first lessons from knockout mice. *Trends Pharmacol Sci* 20, 19–26. Elsevier Current Trends.

Kieffer, B. L. & Gavériaux-Ruff, C. **(2002).** Exploring the opioid system by gene knockout. *Prog Neurobiol* 66, 285–306. Pergamon.

Kieffer, B. L., Befort, K., Gaveriaux-Ruff, C. & Hirth, C. G. **(1992).** The delta-opioid receptor: isolation of a cDNA by expression cloning and pharmacological characterization. *Proc Natl Acad Sci U S A* 89, 12048–52.

Killen, J. D. & Fortmann, S. P. **(1997).** Craving is associated with smoking relapse: Findings from three prospective studies. *Exp Clin Psychopharmacol* 5, 137–142.

Kim, F. J., Kovalyshyn, I., Burgman, M., Neilan, C., Chien, C.-C. & Pasternak, G. W. **(2010).** Sigma 1 receptor modulation of G-protein-coupled receptor signaling: potentiation of opioid transduction independent from receptor binding. *Mol Pharmacol* 77, 695–703. American Society for Pharmacology and Experimental Therapeutics.

Kim, H.-W., Roh, D.-H., Yoon, S.-Y., Seo, H.-S., Kwon, Y.-B., Han, H.-J., Kim, K.-W., Beitz, A. J. & Lee, J.-H. **(2008).** Activation of the spinal sigma-1 receptor enhances NMDA-induced pain via PKC- and PKA-dependent phosphorylation of the NR1 subunit in mice. *Br J Pharmacol* 154, 1125–1134.

Klawonn, A. M. & Malenka, R. C. **(2019).** Nucleus Accumbens Modulation in Reward and Aversion. *Cold Spring Harb Symp Quant Biol* LXXXIII, 037457.

Klink, R., De Kerchove D'exaerde, A., Zoli, M. & Changeux, J.-P. **(2001).** *Molecular and Physiological Diversity of Nicotinic Acetylcholine Receptors in the Midbrain Dopaminergic Nuclei*.

Knackstedt, L. A., LaRowe, S., Mardikian, P., Malcolm, R., Upadhyaya, H., Hedden, S., Markou, A. & Kalivas, P. W. **(2009).** The Role of Cystine-Glutamate Exchange in Nicotine Dependence in Rats and Humans. *Biol Psychiatry* 65, 841. NIH Public Access.

König, M., Zimmer, A. M., Steiner, H., Holmes, P. V, Crawley, J. N., Brownstein, M. J. & Zimmer, A. **(1996).** Pain responses, anxiety and aggression in mice deficient in pre-proenkephalin. *Nature* 383, 535–8.

Koob, G. F. **(2009).** Dynamics of Neuronal Circuits in Addiction: Reward, Antireward, and Emotional Memory. *Pharmacopsychiatry* 42, S32–S41. © Georg Thieme Verlag KG Stuttgart · New York.

Koob, G. F. **(2013).** Addiction is a reward deficit and stress surfeit disorder. *Front psychiatry* 4, 1–18.

Koob, G. F., Buck, C. L., Cohen, A., Edwards, S., Park, P. E., Schlosburg, J. E., Schmeichel, B., Vendruscolo, L. F., Wade, C. L. & other authors. **(2014).** Addiction as a stress surfeit disorder. *Neuropharmacology*.

Koob, G. F. & Le Moal, M. **(2001).** Drug addiction, dysregulation of reward, and allostasis. *Neuropsychopharmacology* 24, 97–129.

Koob, G. F. & Le Moal, M. **(2005).** Plasticity of reward neurocircuitry and the 'dark side' of drug addiction. *Nat Neurosci* 8, 1442–4.

Koob, G. F. & Le Moal, M. **(2008a).** Addiction and the brain antireward system. *Annu Rev Psychol* 59, 29–53.

Koob, G. F. & Le Moal, M. **(2008b).** Review. Neurobiological mechanisms for opponent motivational processes in addiction. *Philos Trans R Soc Lond B Biol Sci* 363, 3113–23.

Koob, G. F., Le Moal, M. & Moal, M. Le. **(1997).** Drug abuse: hedonic homeostatic dysregulation. *Science* 278, 52–8.

Koob, G. F. & Volkow, N. D. **(2016).** Neurobiology of addiction: a neurocircuitry analysis. *The Lancet Psychiatry* 3, 760–773. Elsevier Ltd.

Koós, T. & Tepper, J. M. **(1999).** *Inhibitory control of neostriatal projection neurons by GABAergic interneurons*.

Koós, T. & Tepper, J. M. **(2002).** Dual Cholinergic Control of Fast-Spiking Interneurons in the Neostriatum. *J Neurosci* 22, 529–535.

Kosillo, P., Zhang, Y. F., Threlfell, S. & Cragg, S. J. **(2016).** Cortical Control of Striatal Dopamine Transmission via Striatal Cholinergic Interneurons. *Cereb Cortex* 26, 4160–4169. Oxford University Press.

Kreek, M. J., LaForge, K. S. & Butelman, E. **(2002).** Pharmacotherapy of addictions. *Nat Rev Drug Discov* 1, 710–26. Nature Publishing Group.

Kreek, M. J. & Koob, G. F. **(1998).** Drug dependence: stress and dysregulation of brain reward pathways. *Drug Alcohol Depend* 51, 23–47. Elsevier.

Krishnan-Sarin, S., Rosen, M. I. & O'Malley, S. S. **(1999).** Naloxone challenge in smokers. Preliminary evidence of an opioid component in nicotine dependence. *Arch Gen Psychiatry* 56, 663–8.

Kupchik, Y. M. & Kalivas, P. W. **(2017).** The Direct and Indirect Pathways of the Nucleus Accumbens are not What You Think 42.

Kupchik, Y. M., Brown, R. M., Heinsbroek, J. A., Kay Lobo, M., Schwartz, D. J., Kalivas, P. W. & Neurosci, N. **(2015).** Coding the direct/indirect pathways by D1 and D2 receptors is not valid for accumbens projections HHS Public Access Author manuscript. *Nat Neurosci* 18, 1230–1232.

LaLumiere, R. T. & Kalivas, P. W. **(2008).** Glutamate release in the nucleus accumbens core is necessary for heroin seeking. *J Neurosci* 28, 3170–7. Society for Neuroscience.

Lambe, E. K., Picciotto, M. R. & Aghajanian, G. K. **(2003).** Nicotine Induces Glutamate Release from Thalamocortical Terminals in Prefrontal Cortex. *Neuropsychopharmacology* 28, 216–225.

Lammel, S., Ion, D. I., Roeper, J. & Malenka, R. C. **(2011).** Projection-specific modulation of dopamine neuron synapses by aversive and rewarding stimuli.

Lammel, S., Lim, B. K., Ran, C., Huang, K. W., Betley, M. J., Tye, K., Deisseroth, K. & Malenka, R. C. **(2012).** Input-specific control of reward and aversion in the ventral tegmental area. *Nature* 491, 212–217.

Lammel, S., Hetzel, A., Häckel, O., Jones, I., Liss, B. & Roeper, J. **(2008).** Unique Properties of Mesoprefrontal Neurons within a Dual Mesocorticolimbic Dopamine System. *Neuron* 57, 760–773. Cell Press.

Lança, A. J., Adamson, K. L., Coen, K. M., Chow, B. L. & Corrigall, W. A. **(2000).** The pedunculopontine tegmental nucleus and the role of cholinergic neurons in nicotine self-administration in the rat: a correlative neuroanatomical and behavioral study. *Neuroscience* 96, 735–42.

Langa, F., Codony, X., Tovar, V., Lavado, A., Gimenez, E., Cozar, P., Cantero, M., Dordal, A., Hernandez, E. & other authors. **(2003).** Generation and phenotypic analysis of sigma receptor type I (sigma1) knockout mice. *Eur J Neurosci* 18, 2188–2196. John Wiley & Sons, Ltd (10.1111).

Lavin, A., Nogueira, L., Lapish, C. C., Wightman, R. M., Phillips, P. E. M. & Seamans, J. K. **(2005).** Behavioral/Systems/Cognitive Mesocortical Dopamine Neurons Operate in Distinct Temporal Domains Using Multimodal Signaling.

Law, P.-Y., Wong, Y. H. & Loh, H. H. **(2000).** Molecular Mechanisms and Regulation of Opioid Receptor Signaling. *Annu Rev Pharmacol Toxicol* 40, 389–430. Annual Reviews 4139 El Camino Way, P.O. Box 10139, Palo Alto, CA 94303-0139, USA .

Lê, A. D., Quan, B., Juzytch, W., Fletcher, P. J., Joharchi, N. & Shaham, Y. **(1998).** Reinstatement of alcohol-seeking by priming injections of alcohol and exposure to stress in rats. *Psychopharmacology (Berl)* 135, 169–74.

Lee, A. M., Arreola, A. C., Kimmey, B. A. & Schmidt, H. D. **(2014).** Administration of the nicotinic acetylcholine receptor agonists ABT-089 and ABT-107 attenuates the reinstatement of nicotine-seeking behavior in rats. *Behav Brain Res* 274, 168–75. NIH Public Access.

Lee, J.-H., Lim, Y., Wiederhold, B. K. & Graham, S. J. **(2005).** A Functional Magnetic Resonance Imaging (fMRI) Study of Cue-Induced Smoking Craving in Virtual Environments. *Appl Psychophysiol Biofeedback* 30.

Lee, K.-W., Kim, Y., Kim, A. M., Helmin, K., Nairn, A. C. & Greengard, P. **(2006).** Cocaine-induced dendritic spine formation in D1 and D2 dopamine receptor-containing medium spiny neurons in nucleus accumbens. *Proc Natl Acad Sci U S A* 103, 3399–404.

Lenz, J. D. & Lobo, M. K. **(2013).** Optogenetic insights into striatal function and behavior. *Behav Brain Res* 255, 44–54.

Leslie, F. M., Mojica, C. Y. & Reynaga, D. D. **(2013).** Nicotinic receptors in addiction pathways. *Mol Pharmacol* 83, 753–8. American Society for Pharmacology and Experimental Therapeutics.

Li, C. H. & Chung, D. **(1976).** Isolation and structure of an untriakontapeptide with opiate activity from camel pituitary glands. *Proc Natl Acad Sci U S A* 73, 1145. National Academy of Sciences.

Li, M. D. & Burmeister, M. **(2009).** New insights into the genetics of addiction. *Nat Rev Genet* 10, 225–31. NIH Public Access.

Li, X., Semenova, S., D'Souza, M. S., Stoker, A. K. & Markou, A. **(2014).** Involvement of glutamatergic and GABAergic systems in nicotine dependence: Implications for novel pharmacotherapies for smoking cessation. *Neuropharmacology* 76 Pt B, 554–65. NIH Public Access.

Liechti, M. E., Lhuillier, L., Kaupmann, K. & Markou, A. **(2007).** Metabotropic Glutamate 2/3 Receptors in the Ventral Tegmental Area and the Nucleus Accumbens Shell Are Involved in Behaviors Relating to Nicotine Dependence. *J Neurosci* 27, 9077–9085.

Little, J. P. & Carter, A. G. **(2012).** Subcellular synaptic connectivity of layer 2 pyramidal neurons in the medial prefrontal cortex. *J Neurosci* 32, 12808–19. Society for Neuroscience.

Liu, L., Zhao-Shea, R., Mcintosh, J. M., Gardner, P. D. & Tapper, A. R. **(2012).** Nicotine Persistently Activates Ventral Tegmental Area Dopaminergic Neurons via Nicotinic Acetylcholine Receptors Containing 4 and 6 Subunits.

Liu, X. **(2014).** Effects of blockade of α4β2 and α7 nicotinic acetylcholine receptors on cue-induced reinstatement of nicotine-seeking behaviour in rats. *Int J Neuropsychopharmacol* 17, 105–16. NIH Public Access.

Liu, X. **(2016).** Characterization of Cue-Induced Reinstatement of Nicotine-Seeking Behavior in Smoking Relapse: Use of Animal Models. *Neuropathol Drug Addict Subst Misuse* 237–245. Academic Press.

Liu, X., Palmatier, M. I., Caggiula, A. R., Sved, A. F., Donny, E. C., Gharib, M. & Booth, S. **(2009).** Naltrexone attenuation of conditioned but not primary reinforcement of

nicotine in rats. *Psychopharmacology (Berl)* 202, 589–98.
Liu, X., Caggiula, A. R., Yee, S. K., Nobuta, H., Sved, A. F., Pechnick, R. N. & Poland, R. E. **(2007a).** Mecamylamine attenuates cue-induced reinstatement of nicotine-seeking behavior in rats. *Neuropsychopharmacology* 32, 710–8. NIH Public Access.
Liu, Y., Yu, Y., Shaikh, J., Pouw, B., Daniels, A., Chen, G.-D. & Matsumoto, R. R. **(2007b).** σ Receptors and Drug Abuse. In *Sigma Recept*, pp. 315–336. Boston, MA: Springer US.
Liu, Z., Otsu, Y., Vasuta, C., Nawa, H. & Murphy, T. H. **(2007c).** Action-Potential-Independent GABAergic Tone Mediated by Nicotinic Stimulation of Immature Striatal Miniature Synaptic Transmission. *J Neurophysiol* 98, 581–593. American Physiological Society.
Livak, K. J. & Schmittgen, T. D. **(2001).** Analysis of Relative Gene Expression Data Using Real-Time Quantitative PCR and the 2−ΔΔCT Method. *Methods* 25, 402–408.
Livingstone, P. D. & Wonnacott, S. **(2009).** Nicotinic acetylcholine receptors and the ascending dopamine pathways. *Biochem Pharmacol* 78, 744–755. Elsevier.
Livingstone, P. D., Srinivasan, J., Kew, J. N. C., Dawson, L. A., Gotti, C., Moretti, M., Shoaib, M. & Wonnacott, S. **(2009).** α7 and non-α7 nicotinic acetylcholine receptors modulate dopamine release in vitro and in vivo in the rat prefrontal cortex. *Eur J Neurosci* 29, 539–550.
Lobb, C. J., Wilson, C. J. & Paladini, C. A. **(2010).** A dynamic role for GABA receptors on the firing pattern of midbrain dopaminergic neurons. *J Neurophysiol* 104, 403–13. American Physiological Society.
Lopez-Quintero, C., Pérez De Los Cobos, J., Hasin, D. S., Okuda, M., Wang, S., Grant, B. F. & Blanco, C. **(2011).** Probability and predictors of transition from first use to dependence on nicotine, alcohol, cannabis, and cocaine: Results of the National Epidemiologic Survey on Alcohol and Related Conditions (NESARC) *. *Drug Alcohol Depend* 115, 120–130.
Lord, J. A. H., Waterfield, A. A., Hughes, J. & Kosterlitz, H. W. **(1977).** Endogenous opioid peptides: multiple agonists and receptors. *Nature* 267, 495–9.
Lösel, R. M., Besong, D., Peluso, J. J. & Wehling, M. **(2008).** Progesterone receptor membrane component 1—Many tasks for a versatile protein. *Steroids* 73, 929–934. Elsevier.
Lubbers, B. R., Van Mourik, Y., Schetters, D., Smit, A. B., De Vries, T. J. & Spijker, S. **(2014).** Prefrontal gamma-aminobutyric acid type a receptor insertion controls cue-induced relapse to nicotine seeking. *Biol Psychiatry* 76, 750–758. Elsevier.
Lüscher, C. **(2013).** Cocaine-evoked synaptic plasticity of excitatory transmission in the ventral tegmental area. *Cold Spring Harb Perspect Med* 3, a012013. Cold Spring Harbor Laboratory Press.
Lutz, P.-E. & Kieffer, B. L. **(2013).** Opioid receptors: distinct roles in mood disorders. *Trends Neurosci* 36, 195–206. NIH Public Access.
Maj, J., Rogóz, Z. & Skuza, G. **(1996).** Some behavioral effects of 1,3-di-o-tolylguanidine, opipramol and sertraline, the sigma site ligands. *Pol J Pharmacol* 48, 379–95.
Makram, H., Toledo-Rodriguez, M., Wang, Y., Gupta, A., Silberberg, G. & Wu, C. **(2004).** INTERNEURONS OF THE NEOCORTICAL INHIBITORY SYSTEM. *Nat Rev Neurosci* 5, 793–807.
Maldonado, R. **(2002).** Study of cannabinoid dependence in animals. *Pharmacol Ther* 95, 153–164.
Maldonado, R., Saiardi, A., Valverde, O., Samad, T. A., Roques, B. P. & Borrelli, E. **(1997).** Absence of opiate rewarding effects in mice lacking dopamine D2 receptors. *Nature* 388, 586–589. Nature Publishing Group.
Maldonado, R., Robledo, P., Chover, A. J., Caine, S. B. & Koob, G. F. **(1993).** D1 dopamine

receptors in the nucleus accumbens modulate cocaine self-administration in the rat. *Pharmacol Biochem Behav* 45, 239–42.

Mallet, N., Le Moine, C., Charpier, S. & Gonon, F. **(2005).** Feedforward Inhibition of Projection Neurons by Fast-Spiking GABA Interneurons in the Rat Striatum In Vivo.

Mameli-Engvall, M., Evrard, A., Pons, S., Maskos, U., Svensson, T. H., Changeux, J.-P. & Faure, P. **(2006).** Hierarchical control of dopamine neuron-firing patterns by nicotinic receptors. *Neuron* 50, 911–21.

Mameli, M., Halbout, B., Creton, C., Engblom, D., Parkitna, J. R., Spanagel, R. & Lüscher, C. **(2009).** Cocaine-evoked synaptic plasticity: persistence in the VTA triggers adaptations in the NAc. *Nat Neurosci* 12, 1036–1041. Nature Publishing Group.

Manallack, D. T., Beart, P. M. & Gundlach, A. L. **(1986).** Psychotomimetic σ-opiates and PCP. *Trends Pharmacol Sci* 7, 448–451.

Manglik, A., Kruse, A. C., Kobilka, T. S., Thian, F. S., Mathiesen, J. M., Sunahara, R. K., Pardo, L., Weis, W. I., Kobilka, B. K. & Granier, S. **(2012).** Crystal structure of the μ-opioid receptor bound to a morphinan antagonist. *Nature* 485, 321–326. Nature Publishing Group.

Mansour, A., Khachaturian, H., Lewis, M. E., Akil, H. & Watson, S. J. **(1988).** Anatomy of CNS opioid receptors. *Trends Neurosci* 11, 308–314. Elsevier Current Trends.

Mansour, A., Fox, C. A., Burke, S., Meng, F., Thompson, R. C., Akil, H. & Watson, S. J. **(1994).** Mu, delta, and kappa opioid receptor mRNA expression in the rat CNS: An in situ hybridization study. *J Comp Neurol* 350, 412–438. John Wiley & Sons, Ltd.

Mansvelder, H. D. & Mcgehee, D. S. **(2000).** Long-Term Potentiation of Excitatory Inputs to Brain Reward Areas by Nicotine. *Neuron* 27, 349–357.

Mansvelder, H. D., Keath, J. R. & McGehee, D. S. **(2002).** Synaptic mechanisms underlie nicotine-induced excitability of brain reward areas. *Neuron* 33, 905–19.

Marchi, M., Risso, F., Viola, C., Cavazzani, P. & Raiteri, M. **(2002).** Direct evidence that release-stimulating alpha7* nicotinic cholinergic receptors are localized on human and rat brain glutamatergic axon terminals. *J Neurochem* 80, 1071–1078. John Wiley & Sons, Ltd (10.1111).

Margolis, E. B., Toy, B., Himmels, P., Morales, M. & Fields, H. L. **(2012).** Identification of Rat Ventral Tegmental Area GABAergic Neurons 7, e42365 (L. Groc, Ed.). Public Library of Science.

Markou, A. **(2008).** Review. Neurobiology of nicotine dependence. *Philos Trans R Soc Lond B Biol Sci* 363, 3159–68.

Markou, A., Weiss, F., Gold, L. H., Caine, S. B., Schulteis, G. & Koob, G. F. **(1993).** Animal models of drug craving. *Psychopharmacology (Berl)* 112, 163–82.

Marks, M. J., Rowell, P. P., Cao, J.-Z., Grady, S. R., McCallum, S. E. & Collins, A. C. **(2004).** Subsets of acetylcholine-stimulated 86Rb+ efflux and [125I]-epibatidine binding sites in C57BL/6 mouse brain are differentially affected by chronic nicotine treatment. *Neuropharmacology* 46, 1141–1157.

Marks, M. J., Grady, S. R., Salminen, O., Paley, M. A., Wageman, C. R., Mcintosh, J. M., Whiteaker, P., Wahlen, G. E. & Whiteaker, P. **(2014).** α6β2*-subtype nicotinic acetylcholine receptors are more sensitive than α4β2*-subtype receptors to regulation by chronic nicotine administration. *J Neurochem* 130, 185–198.

Martin-Fardon, R., Maurice, T., Aujla, H., Bowen, W. D. & Weiss, F. **(2007).** Differential Effects of σ1 Receptor Blockade on Self-Administration and Conditioned Reinstatement Motivated by Cocaine vs Natural Reward. *Neuropsychopharmacology* 32, 1967–1973. Nature Publishing Group.

Martin-Fardon, R., Strong, E. M. & Weiss, F. **(2012).** Effect of σ1 receptor antagonism on ethanol and natural reward seeking. *Neuroreport* 23, 809–813.

Martin-García, E., Barbano, M. F., Galeote, L. & Maldonado, R. **(2009).** New operant

model of nicotine-seeking behaviour in mice. *Int J Neuropsychopharmacol* 12, 343–56.

Martin-García, E., Burokas, A., Kostrzewa, E., Gieryk, A., Korostynski, M., Ziolkowska, B., Przewlocka, B., Przewlocki, R. & Maldonado, R. **(2011).** New operant model of reinstatement of food-seeking behavior in mice. *Psychopharmacology (Berl)* 215, 49–70.

Martin-García, E., Robledo, P., Gutiérrez-Cuesta, J. & Maldonado, R. **(2014).** Part II Animal Models in Specific Disease Areas of Drug Discovery. In *Vivo Model Drug Discov*, 1st edn., pp. 167–185. Edited by J. M. Vela, R. Maldonado & M. Hamon. Wiley-VCH Verlag GmbH & Co. KGaA.

Martin, M., Chen, B. T., Hopf, F. W., Bowers, M. S. & Bonci, A. **(2006).** Cocaine self-administration selectively abolishes LTD in the core of the nucleus accumbens. *Nat Neurosci* 9, 868–9.

Martin, W. R., Eades, C. G., Thompson, J. A., Huppler, R. E. & Gilbert, P. E. **(1976).** The effects of morphine- and nalorphine- like drugs in the nondependent and morphine-dependent chronic spinal dog. *J Pharmacol Exp Ther* 197, 517–32.

Martina, M., Turcotte, M.-E. B., Halman, S. & Bergeron, R. **(2007).** The sigma-1 receptor modulates NMDA receptor synaptic transmission and plasticity via SK channels in rat hippocampus. *J Physiol* 578, 143–157.

Martinez, D., Narendran, R., Foltin, R. W., Slifstein, M., Hwang, D.-R., Broft, A., Huang, Y., Cooper, T. B., Fischman, M. W. & other authors. **(2007).** Amphetamine-Induced Dopamine Release: Markedly Blunted in Cocaine Dependence and Predictive of the Choice to Self-Administer Cocaine. *Am J Psychiatry* 164, 622–629.

Marty, M. A., Erwin, V. G., Cornell, K. & Zgombick, J. M. **(1985).** Effects of nicotine on beta-endorphin, alpha MSH, and ACTH secretion by isolated perfused mouse brains and pituitary glands, in vitro. *Pharmacol Biochem Behav* 22, 317–25.

Marubio, L. M., Arroyo-Jimenez, M. del M., Cordero-Erausquin, M., Léna, C., Novère, N. Le, d'Exaerde, A. de K., Huchet, M., Damaj, M. I. & Changeux, J.-P. **(1999).** Reduced antinociception in mice lacking neuronal nicotinic receptor subunits. *Nature* 398, 805–810. Nature Publishing Group.

Mateo, Y., Johnson, K. A., Covey, D. P., Atwood, B. K., Wang, H., Zhang, S., Gildish, I., Cachope, R., Bellocchio, L. & other authors. **(2017).** Endocannabinoids on cortical terminals orchestrate local modulation of dopamine release in the nucleus accumbens. *Neuron* 96, 1112–1126.

Matsui, A., Jarvie, B. C., Robinson, B. G., Hentges, S. T. & Williams, J. T. **(2014).** Separate GABA afferents to dopamine neurons mediate acute action of opioids, development of tolerance, and expression of withdrawal. *Neuron* 82, 1346–56. NIH Public Access.

Matsumoto, R. R. **(2009).** Targeting sigma receptors: novel medication development for drug abuse and addiction. *Expert Rev Clin Pharmacol* 2, 351–8. NIH Public Access.

Matsumoto, R. R., Mccracken, K. A., Pouw, B., Zhang, Y. & Bowen, W. D. **(2002).** Involvement of sigma receptors in the behavioral effects of cocaine: evidence from novel ligands and antisense oligodeoxynucleotides Rae. *Neuropharmacology* 42, 1043–1055. Pergamon.

Matsumoto, R. R., Liu, Y., Lerner, M., Howard, E. W. & Brackett, D. J. **(2003).** σ Receptors: potential medications development target for anti-cocaine agents. *Eur J Pharmacol* 469, 1–12.

Matsumoto, R. R., Li, S.-M., Katz, J. L., Fantegrossi, W. E. & Coop, A. **(2011).** Effects of the selective sigma receptor ligand, 1-(2-phenethyl)piperidine oxalate (AC927), on the behavioral and toxic effects of cocaine. *Drug Alcohol Depend* 118, 40–7. NIH Public Access.

Matsuzaki, M., Honkura, N., Ellis-Davies, G. C. R. & Kasai, H. **(2004).** Structural basis of long-term potentiation in single dendritic spines. *Nature* 429, 761–766.

Matta, S. G., Balfour, D. J., Benowitz, N. L., Boyd, R. T., Buccafusco, J. J., Caggiula, A. R., Craig, C. R., Collins, A. C., Damaj, M. I. & other authors. **(2007).** Guidelines on nicotine dose selection for in vivo research. *Psychopharmacology (Berl)* 190, 269–319. Springer-Verlag.

Matthes, H. W., Maldonado, R., Simonin, F., Valverde, O., Slowe, S., Kitchen, I., Befort, K., Dierich, A., Le Meur, M. & other authors. **(1996).** Loss of morphine-induced analgesia, reward effect and withdrawal symptoms in mice lacking the mu-opioid-receptor gene. *Nature* 383, 819–23.

Maurer, J. J., Sandager-Nielsen, K. & Schmidt, H. D. **(2017).** Attenuation of nicotine taking and seeking in rats by the stoichiometry-selective alpha4beta2 nicotinic acetylcholine receptor positive allosteric modulator NS9283. *Psychopharmacology (Berl)* 234, 475–484. Springer Berlin Heidelberg.

Maurer, S. V & Williams, C. L. **(2017).** The Cholinergic System Modulates Memory and Hippocampal Plasticity via Its Interactions with Non-Neuronal Cells. *Front Immunol* 8, 1489. Frontiers Media SA.

Maurice, T., Casalino, M., Lacroix, M. & Romieu, P. **(2003).** Involvement of the sigma1 receptor in the motivational effects of ethanol in mice. *Pharmacol Biochem Behav* 74, 869–876. Elsevier.

Maurice, T. & Su, T.-P. **(2009).** The pharmacology of sigma-1 receptors. *Pharmacol Ther* 124, 195–206. Elsevier B.V.

Mavlyutov, T. A. & Ruoho, A. E. **(2007).** Ligand-dependent localization and intracellular stability of sigma-1 receptors in CHO-K1 cells. *J Mol Signal* 2, 8. Ubiquity Press.

Mazzo, F., Pistillo, F., Grazioso, G., Clementi, F., Borgese, N., Gotti, C. & Colombo, S. F. **(2013).** Nicotine-modulated subunit stoichiometry affects stability and trafficking of α3β4 nicotinic receptor. *J Neurosci* 33, 12316–28. Society for Neuroscience.

McCann, D. J., Weissman, A. D. & Su, T.-P. **(1994).** Sigma-1 and Sigma-2 sites in rat brain: Comparison of regional, ontogenetic, and subcellular patterns. *Synapse* 17, 182–189. John Wiley & Sons, Ltd.

McCann, D. J. & Su, T. P. **(1990).** Haloperidol-sensitive (+)[3H]SKF-10,047 binding sites (sigma sites) exhibit a unique distribution in rat brain subcellular fractions. *Eur J Pharmacol* 188, 211–8.

McFarland, K., Lapish, C. C. & Kalivas, P. W. **(2003).** Prefrontal glutamate release into the core of the nucleus accumbens mediates cocaine-induced reinstatement of drug-seeking behavior. *J Neurosci* 23, 3531–7. Society for Neuroscience.

Mckay, B. E., Placzek, A. N. & Dani, J. A. **(2007).** Regulation of Synaptic Transmission and Plasticity by Neuronal Nicotinic Acetylcholine Receptors. *Biochem pharmacol* 74, 1120–1133.

McKay, J. R., Merikle, E., Mulvaney, F. D., Weiss, R. V & Koppenhaver, J. M. **(2001).** Factors accounting for cocaine use two years following initiation of continuing care. *Addiction* 96, 213–25.

McLellan, A. T., Lewis, D. C., O'Brien, C. P. & Kleber, H. D. **(2000).** Drug dependence, a chronic medical illness implications for treatment, insurance, and outcomes evaluation. *J Am Med Assoc* 284, 1689–1695.

Mei, J. & Pasternak, G. W. **(2001).** Molecular cloning and pharmacological characterization of the rat sigma1 receptor. *Biochem Pharmacol* 62, 349–55.

Menkel, M., Terry, P., Pontecorvo, M., Katz, J. L. & Witkin, J. M. **(1991).** Selective σ ligands block stimulant effects of cocaine. *Eur J Pharmacol* 201, 251–252. Elsevier.

Meredith, G. E., Baldo, B. A., Andrezjewski, M. E. & Kelley, A. E. **(2008).** The structural basis for mapping behavior onto the striatum and its subdivisions. *Brain Struc*

Funct 213, 17–27.

Merikangas, K. R., Stolar, M., Stevens, D. E., Goulet, J., Preisig, M. A., Fenton, B., Zhang, H., O'Malley, S. S. & Rounsaville, B. J. **(1998).** Familial transmission of substance use disorders. *Arch Gen Psychiatry* 55, 973–9.

Merikangas, K. R., He, J.-P., Burstein, M., Swanson, S. A., Avenevoli, S., Cui, L., Benjet, C., Georgiades, K. & Swendsen, J. **(2010).** Lifetime prevalence of mental disorders in U.S. adolescents: results from the National Comorbidity Survey Replication--Adolescent Supplement (NCS-A). *J Am Acad Child Adolesc Psychiatry* 49, 980–9. NIH Public Access.

Le Merrer, J., Becker, J. A. J., Befort, K. & Kieffer, B. L. **(2009).** Reward processing by the opioid system in the brain. *Physiol Rev* 89, 1379–412. NIH Public Access.

Meunier, J. & Hayashi, T. **(2010).** Sigma-1 Receptors Regulate Bcl-2 Expression by Reactive Oxygen Species-Dependent Transcriptional Regulation of Nuclear Factor □ B. *J Pharmacol Exp Ther* 332, 388–397.

Midanik, L. **(1983).** Familial alcoholism and problem drinking in a national drinking practices survey. *Addict Behav* 8, 133–141. Pergamon.

Millar, N. S. & Gotti, C. **(2009).** Diversity of vertebrate nicotinic acetylcholine receptors. *Neuropharmacology* 56, 237–46.

Millar, N. S. & Harkness, P. C. **(2008, May).** Assembly and trafficking of nicotinic acetylcholine receptors (Review). *Mol Membr Biol*.

Miller, E. K. **(2000).** THE PREFRONTAL CORTEX AND COGNITIVE CONTROL. *Nat Rev Neurosci* 1, 59–65.

Miller, E. K. & Cohen, J. D. **(2001).** An Integrative Theory of Prefrontal Cortex Function. *Annu Rev Neurosci* 24, 167–202. Annual Reviews 4139 El Camino Way, P.O. Box 10139, Palo Alto, CA 94303-0139, USA .

Minami, M. & Satoh, M. **(1995).** Molecular biology of the opioid receptors: structures, functions and distributions. *Neurosci Res* 23, 121–45.

Mollereau, C., Parmentier, M., Mailleux, P., Butour, J.-L., Moisand, C., Chalon, P., Caput, D., Vassart, G. & Meunier, J.-C. **(1994).** ORL1, a novel member of the opioid receptor family. *FEBS Lett* 341, 33–38. John Wiley & Sons, Ltd.

Moorman, D. E., James, M. H., McGlinchey, E. M. & Aston-Jones, G. **(2015).** Differential roles of medial prefrontal subregions in the regulation of drug seeking. *Brain Res* 1628, 130–46. NIH Public Access.

Morel, C., Fattore, L., Pons, S., Hay, Y. A., Marti, F., Lambolez, B., De Biasi, M., Lathrop, M., Fratta, W. & other authors. **(2014).** Nicotine consumption is regulated by a human polymorphism in dopamine neurons. *Mol Psychiatry* 19, 930–936.

Moretti, M., Mugnaini, M., Tessari, M., Zoli, M., Gaimarri, A., Manfredi, I., Pistillo, F., Clementi, F. & Gotti, C. **(2010).** A comparative study of the effects of the intravenous self-administration or subcutaneous minipump infusion of nicotine on the expression of brain neuronal nicotinic receptor subtypes. *Mol Pharmacol* 78, 287–96. American Society for Pharmacology and Experimental Therapeutics.

Mori, T., Yoshizawa, K., Shibasaki, M. & Suzuki, T. **(2012).** Discriminative Stimulus Effects of Hallucinogenic Drugs: a Possible Relation to Reinforcing and Aversive Effects. *J Pharmacol Sci* 120, 70–76.

Mori, T., Rahmadi, M., Yoshizawa, K., Itoh, T., Shibasaki, M. & Suzuki, T. **(2014).** Inhibitory effects of SA4503 on the rewarding effects of abused drugs. *Addict Biol* 19, 362–369. John Wiley & Sons, Ltd (10.1111).

Morin-Surun, M. P., Collin, T., Denavit-Saubié, M., Baulieu, E. E. & Monnet, F. P. **(1999).** Intracellular sigma1 receptor modulates phospholipase C and protein kinase C activities in the brainstem. *Proc Natl Acad Sci U S A* 96, 8196–9. National Academy of Sciences.

Morris, G., Arkadir, D., Nevet, A., Vaadia, E. & Bergman, H. **(2004).** Coincident but Distinct Messages of Midbrain Dopamine and Striatal Tonically Active Neurons. *Neuron* 43, 133–143.

Mugnaini, M., Tessari, M., Tarter, G., Merlo Pich, E., Chiamulera, C. & Bunnemann, B. **(2002).** Upregulation of [3H]methyllycaconitine binding sites following continuous infusion of nicotine, without changes of α7 or α6 subunit mRNA: an autoradiography and *in situ* hybridization study in rat brain. *Eur J Neurosci* 16, 1633–1646. John Wiley & Sons, Ltd (10.1111).

Mukhin, A. G., Kimes, A. S., Chefer, S. I., Matochik, J. A., Contoreggi, C. S., Horti, A. G., Bruce Vaupel, D., Pavlova, O. & Stein, E. A. **(2008).** Greater Nicotinic Acetylcholine Receptor Density in Smokers Than in Nonsmokers: A PET Study with 2-18 F-FA-85380. *J Nucl Med* 49, 1628–1635.

Mulligan, G. J., Wong, J. & Jacks, T. **(1998).** p130 is dispensable in peripheral T lymphocytes: evidence for functional compensation by p107 and pRB. *Mol Cell Biol* 18, 206–20. American Society for Microbiology (ASM).

Mumford, G. K., Evans, S. M., Fleishaker, J. C. & Griffiths, R. R. **(1995).** Alprazolam absorption kinetics affects abuse liability. *Clin Pharmacol Ther* 57, 356–65.

Nägerl, U. V., Eberhorn, N., Cambridge, S. B. & Bonhoeffer, T. **(2004).** Bidirectional activity-dependent morphological plasticity in hippocampal neurons. *Neuron* 44, 759–767.

Nair-Roberts, R. G., Chatelain-Badie, S. D., Benson, E., White-Cooper, H., Bolam, J. P. & Ungless, M. A. **(2008).** Stereological estimates of dopaminergic, GABAergic and glutamatergic neurons in the ventral tegmental area, substantia nigra and retrorubral field in the rat. *Neuroscience* 152, 1024–31. Elsevier.

Nakanishi, S., Inoue, A., Kita, T., Inoue, A., Nakamura, M., Chang, A. C. Y., Cohen, S. N. & Numa, S. **(1979).** Nucleotide sequence of cloned cDNA for bovine corticotropin-β-lipotropin precursor. *Nature* 278, 423–427.

Nashmi, R. & Lester, H. **(2007).** Cell autonomy, receptor autonomy, and thermodynamics in nicotine receptor up-regulation. *Biochem Pharmacol* 74, 1145–54. NIH Public Access.

Natividad, L. A., Buczynski, M. W., Parsons, L. H., Torres, O. V & O'Dell, L. E. **(2012).** Adolescent rats are resistant to adaptations in excitatory and inhibitory mechanisms that modulate mesolimbic dopamine during nicotine withdrawal. *J Neurochem* 123, 578–88. NIH Public Access.

Navarro, G., Moreno, E., Aymerich, M., Marcellino, D., Mccormick, P. J. & Mallol, J. **(2010).** Direct involvement of σ -1 receptors in the dopamine D 1 receptor-mediated effects of cocaine.

Navarro, G., Moreno, E., Bonaventura, J., Brugarolas, M., Farré, D., Aguinaga, D., Mallol, J., Cortés, A., Casadó, V. & other authors. **(2013).** Cocaine inhibits dopamine D2 receptor signaling via sigma-1-D2 receptor heteromers. *PLoS One* 8, e61245.

Neal, C. R., Mansour, A., Reinscheid, R., Nothacker, H. P., Civelli, O., Akil, H. & Watson, S. J. **(1999).** Opioid receptor-like (ORL1) receptor distribution in the rat central nervous system: comparison of ORL1 receptor mRNA expression with (125)I-[(14)Tyr]-orphanin FQ binding. *J Comp Neurol* 412, 563–605.

Nelson, A. B., Bussert, T. G., Kreitzer, A. C. & Seal, R. P. **(2014).** Striatal Cholinergic Neurotransmission Requires VGLUT3 Alexandra. *J Neurosci*.

Nelson, M. E., Kuryatov, A., Choi, C. H., Zhou, Y. & Lindstrom, J. **(2003).** Alternate Stoichiometries of α4β2 Nicotinic Acetylcholine Receptors. *Mol Pharmacol* 63, 332–341. American Society for Pharmacology and Experimental Therapeutics.

Nestler, E. J. **(2005).** Is there a common molecular pathway for addiction? *Nat Neurosci* 8, 1445–1449.

Nestler, E. J. & Hyman, S. E. **(2010).** Animal models of neuropsychiatric disorders. *Nat Neurosci* 13, 1161–9. NIH Public Access.

Nguyen, E. C., McCracken, K. A., Liu, Y., Pouw, B. & Matsumoto, R. R. **(2005).** Involvement of sigma (σ) receptors in the acute actions of methamphetamine: Receptor binding and behavioral studies. *Neuropharmacology* 49, 638–645. Pergamon.

Nguyen, L., Lucke-Wold, B. P., Mookerjee, S., Kaushal, N. & Matsumoto, R. R. **(2017).** Sigma-1 Receptors and Neurodegenerative Diseases: Towards a Hypothesis of Sigma-1 Receptors as Amplifiers of Neurodegeneration and Neuroprotection. In *Adv Exp Med Biol*, pp. 133–152.

Nicolas, L. N., Grutter, T. & Changeux, J.-P. **(2001).** *Models of the extracellular domain of the nicotinic receptors and of agonist-and Ca 2-binding sites*.

Nisell, M., Nomikos, G. G. & Svensson, T. H. **(1994).** Infusion of nicotine in the ventral tegmental area or the nucleus accumbens of the rat differentially affects accumbal dopamine release. *Pharmacol Toxicol* 75, 348–52.

Noda, M., Furutani, Y., Takahashi, H., Toyosato, M., Hirose, T., Inayama, S., Nakanishi, S. & Numa, S. **(1982).** Cloning and sequence analysis of cDNA for bovine adrenal preproenkephalin. *Nature* 295, 202–206.

Norman, A. B., Tabet, M. R., Norman, M. K., Fey, B. K., Tsibulsky, V. L. & Millard, R. W. **(2011).** The affinity of D2-like dopamine receptor antagonists determines the time to maximal effect on cocaine self-administration. *J Pharmacol Exp Ther* 338, 724–8. American Society for Pharmacology and Experimental Therapeutics.

Nutt, D., King, L. A., Saulsbury, W. & Blakemore, C. **(2007).** *Development of a rational scale to assess the harm of drugs of potential misuse*. *Heal Policy www.thelancet.com*.

O'Brien, C. P. **(2003).** Research advances in the understanding and treatment of addiction. *Am J Addict* 12 Suppl 2, S36-47.

O'Connor, E. C., Parker, D., Rollema, H. & Mead, A. N. **(2010).** The α4β2 nicotinic acetylcholine-receptor partial agonist varenicline inhibits both nicotine self-administration following repeated dosing and reinstatement of nicotine seeking in rats. *Psychopharmacology (Berl)* 208, 365–376.

O'Connor, E. C., Chapman, K., Butler, P. & Mead, A. N. **(2011).** The predictive validity of the rat self-administration model for abuse liability. *Neurosci Biobehav Rev* 35, 912–38.

Okamoto, K.-I., Nagai, T., Miyawaki, A. & Hayashi, Y. **(2004).** Rapid and persistent modulation of actin dynamics regulates postsynaptic reorganization underlying bidirectional plasticity. *Nat Neurosci* 7, 1104–12.

Olds, J. & Milner, P. **(1954).** Positive reinforcement produced by electrical stimulation of septal area and other regions of rat brain. *J Comp Physiol Psychol* 47, 419–427.

Olson, G. A., Olson, R. D. & Kastin, A. J. **(1991).** Endogenous opiates: 1990. *Peptides* 12, 1407–32.

Omelchenko, N. & Sesack, S. R. **(2005).** Laterodorsal Tegmental Projections to Identified Cell Populations in the Rat Ventral Tegmental Area. *J Comp Neurol* 483, 217–235.

Omelchenko, N., Bell, R. & Sesack, S. R. **(2009).** Lateral Habenula Projections to the Rat Ventral Tegmental Area: Sparse Synapses Observed Onto Dopamine and GABA Neurons. *Eur J Neurosci* 30, 1239–1250.

Otis, J. M., Namboodiri, V. M. K., Matan, A. M., Voets, E. S., Mohorn, E. P., Kosyk, O., Mchenry, J. A., Robinson, J. E., Resendez, S. L. & other authors. **(2017).** Prefrontal cortex output circuits guide reward seeking through divergent cue encoding HHS Public Access. *Nature* 543, 103–107.

Palacios, G., Muro, A., Vela, J. M., Molina-Holgado, E., Guitart, X., Ovalle, S. & Zamanillo, D. **(2003).** Immunohistochemical localization of the sigma1-receptor in

oligodendrocytes in the rat central nervous system. *Brain Res* 961, 92–9.
Pan, Y. X., Mei, J., Xu, J., Wan, B. L., Zuckerman, A. & Pasternak, G. W. **(1998).** Cloning and characterization of a mouse sigma1 receptor. *J Neurochem* 70, 2279–85.
Papke, R. L. **(2014).** Merging old and new perspectives on nicotinic acetylcholine receptors. *Biochem Pharmacol* 89, 1–11. NIH Public Access.
Pascoli, V., Hiver, A., Van Zessen, R., Loureiro, M., Achargui, R., Harada, M., Flakowski, J. & Lüscher, C. **(2018).** Stochastic synaptic plasticity underlying compulsion in a model of addiction. *Nature* 564, 366–371. Springer US.
Pascual, M. M., Pastor, V. & Bernabeu, R. O. **(2009).** Nicotine-conditioned place preference induced CREB phosphorylation and Fos expression in the adult rat brain. *Psychopharmacology (Berl)* 207, 57–71. Springer-Verlag.
Paterson, N. E., Froestl, W. & Markou, A. **(2005).** Repeated Administration of the GABAB Receptor Agonist CGP44532 Decreased Nicotine Self-Administration, and Acute Administration Decreased Cue-Induced Reinstatement of Nicotine-Seeking in Rats. *Neuropsychopharmacology* 30, 119–128.
Patey, G. & Rossier, J. **(1986).** Discovery, anatomical mapping and biosynthesis of various families of endogenous opioid peptides. *Ann Endocrinol (Paris)* 47, 71–87.
Pati, M. L., Groza, D., Riganti, C., Kopecka, J., Niso, M., Berardi, F., Hager, S., Heffeter, P., Hirai, M. & other authors. **(2017).** Sigma-2 receptor and progesterone receptor membrane component 1 (PGRMC1) are two different proteins: Proofs by fluorescent labeling and binding of sigma-2 receptor ligands to PGRMC1. *Pharmacol Res* 117, 67–74. Academic Press.
Paul, I. a, Basile, A. S., Rojas, E., Youdim, M. B., De Costa, B., Skolnick, P., Pollard, H. B. & Kuijpers, G. a. **(1993).** Sigma receptors modulate nicotinic receptor function in adrenal chromaffin cells. *FASEB J* 7, 1171–8.
Peña, C. J., Bagot, R. C., Labonté, B. & Nestler, E. J. **(2014).** Epigenetic Signaling in Psychiatric Disorders.
Perez, X. A., McIntosh, J. M. & Quik, M. **(2013).** Long-term nicotine treatment down-regulates α6β2* nicotinic receptor expression and function in nucleus accumbens. *J Neurochem* 127, 762–71. NIH Public Access.
Pergadia, M. L., Heath, A. C., Martin, N. G. & Madden, P. A. F. **(2006).** Genetic analyses of DSM-IV nicotine withdrawal in adult twins. *Psychol Med* 36, 963–72.
Perkins, K. A., Gerlach, D., Vender, J., Grobe, J., Meeker, J. & Hutchison, S. **(2001).** Sex differences in the subjective and reinforcing effects of visual and olfactory cigarette smoke stimuli. *Nicotine Tob Res* 3, 141–150. Narnia.
Perry, D. C., Dávila-García, M. I., Stockmeier, C. A., Kellar, K. J., Pezzullo, J. C. & Kellar, K. J. **(2007).** Increased nicotinic receptors in brains from smokers: membrane binding and autoradiography studies. *J Pharmacol Exp Ther* 322, 306–315. American Society for Pharmacology and Experimental Therapeutics.
Perry, D. C., Da´vila, M. I., Da´vila-García, D., Stockmeier, C. A. & Kellar, K. J. **(1999).** *Increased Nicotinic Receptors in Brains from Smokers: Membrane Binding and Autoradiography Studies 1*. *J Pharmacol Exp Ther*.
Pert, C. B. & Snyder, S. H. **(1973).** Opiate receptor: demonstration in nervous tissue. *Science* 179, 1011–4.
Petry, N. M. & O'Brien, C. P. **(2013).** Internet gaming disorder and the DSM-5. *Addiction* 108, 1186–7.
Piazza, P. V. & Deroche-Gamonet, V. **(2013).** A multistep general theory of transition to addiction. *Psychopharmacology (Berl)* 229, 387–413.
Picciotto, M. R. **(2003).** Nicotine as a modulator of behavior: beyond the inverted U. *Trends Pharmacol Sci* 24, 493–499.
Picciotto, M. R., Addy, N. A., Mineur, Y. S. & Brunzell, D. H. **(2008).** It is not 'either/or':

activation and desensitization of nicotinic acetylcholine receptors both contribute to behaviors related to nicotine addiction and mood. *Prog Neurobiol* 84, 329–42.

Piper, M. E., Smith, S. S., Schlam, T. R., Fiore, M. C., Jorenby, D. E., Fraser, D. & Baker, T. B. **(2009).** A Randomized Placebo-Controlled Clinical Trial of 5 Smoking Cessation Pharmacotherapies. *Arch Gen Psychiatry* 66, 1253. American Medical Association.

Pisani, A., Bernardi, G., Ding, J. & Surmeier, D. J. **(2007).** Re-emergence of striatal cholinergic interneurons in movement disorders. *Trends Neurosci* 30, 545–53. Elsevier.

Pistillo, F., Clementi, F., Zoli, M. & Gotti, C. **(2015).** Progress in Neurobiology Nicotinic , glutamatergic and dopaminergic synaptic transmission and plasticity in the mesocorticolimbic system : Focus on nicotine effects. *Prog Neurobiol* 124, 1–27. Elsevier Ltd.

Plaza-Zabala, A., Martín-García, E., De Lecea, L., Maldonado, R. & Berrendero, F. **(2010).** Hypocretins Regulate the Anxiogenic-Like Effects of Nicotine and Induce Reinstatement of Nicotine-Seeking Behavior. *J Neurosci* 30, 2300–2310.

Plaza-Zabala, A., Maldonado, R. & Berrendero, F. **(2012).** The hypocretin/orexin system: implications for drug reward and relapse. *Mol Neurobiol* 45, 424–39.

Plaza-Zabala, A., Flores, Á., Martín-García, E., Saravia, R., Maldonado, R. & Berrendero, F. **(2013).** A role for hypocretin/orexin receptor-1 in cue-induced reinstatement of nicotine-seeking behavior. *Neuropsychopharmacology* 38, 1724–1736.

Pogozheva, I. D., Przydzial, M. J. & Mosberg, H. I. **(2005).** Homology modeling of opioid receptor-ligand complexes using experimental constraints. *AAPS J* 7, E434-48. Springer.

Pontieri, F. E., Tanda, G., Orzi, F. & Di Chiara, G. **(1996).** Effects of nicotine on the nucleus accumbens and similarity to those of addictive drugs. *Nature* 382, 255–7.

Poorthuis, R. B., Bloem, B., Verhoog, M. B. & Mansvelder, H. D. **(2013a).** Development/Plasticity/Repair Layer-Specific Interference with Cholinergic Signaling in the Prefrontal Cortex by Smoking Concentrations of Nicotine.

Poorthuis, R. B., Bloem, B., Schak, B., Wester, J., De Kock, C. P. J. & Mansvelder, H. D. **(2013b).** Layer-Specific Modulation of the Prefrontal Cortex by Nicotinic Acetylcholine Receptors. *Cereb Cortex* 23, 148–161.

Prasad, P. D., Li, H. W., Fei, Y. J., Ganapathy, M. E., Fujita, T., Plumley, L. H., Yang-Feng, T. L., Leibach, F. H. & Ganapathy, V. **(1998).** Exon-intron structure, analysis of promoter region, and chromosomal localization of the human type 1 sigma receptor gene. *J Neurochem* 70, 443–51.

Proulx, E., Piva, M., Tian, M. K., Bailey, C. D. C. & Lambe, E. K. **(2014).** Nicotinic acetylcholine receptors in attention circuitry: the role of layer VI neurons of prefrontal cortex. *Cell Mol Life Sci* 71, 1225–44. Springer.

Przewłocki, R. & Przewłocka, B. **(2001).** Opioids in chronic pain. *Eur J Pharmacol* 429, 79–91. Elsevier.

Puighermanal, E., Marsicano, G., Busquets-Garcia, A., Lutz, B., Maldonado, R. & Ozaita, A. **(2009).** Cannabinoid modulation of hippocampal long-term memory is mediated by mTOR signaling. *Nat Neurosci* 12, 1152–1158. Nature Publishing Group.

Qu, C. L., Huo, F. Q., Huang, F. S. & Tang, J. S. **(2015).** Activation of mu-opioid receptors in the ventrolateral orbital cortex inhibits the GABAergic miniature inhibitory postsynaptic currents in rats. *Neurosci Lett* 592, 64–69. Elsevier Ireland Ltd.

Quadir, S. G., Cottone, P. & Sabino, V. **(2019).** Role of Sigma Receptors in Alcohol Addiction. *Front Pharmacol* 10, 1–7.

Quick, M. W. & Lester, R. A. J. **(2002).** Desensitization of neuronal nicotinic receptors. *J Neurobiol* 53, 457–478. John Wiley & Sons, Ltd.

Quirion, R., Bowen, W. D., Itzhak, Y., Junien, J. L., Musacchio, J. M., Rothman, R. B., Su, T.

P., Tam, S. W. & Taylor, D. P. **(1992).** A proposal for the classification of sigma binding sites. *Trends Pharmacol Sci* 13, 85–6.

Raman, M., Chen, W. & Cobb, M. H. **(2007).** Differential regulation and properties of MAPKs. *Oncogene* 26, 3100–3112. Nature Publishing Group.

Ramirez-Niño, A. M., D'souza, M. S. & Markou, A. **(2013).** N-acetylcysteine decreased nicotine self-administration and cue-induced reinstatement of nicotine seeking in rats: comparison with the effects of N-acetylcysteine on food responding and food seeking. *Psychopharmacology (Berl)* 225, 473–482.

Rapier, C., Lunt, G. G. & Wonnacott, S. **(1990).** Nicotinic Modulation of [3H]Dopamine Release from Striatal Synaptosomes: Pharmacological Characterisation. *J Neurochem* 54, 937–945. John Wiley & Sons, Ltd (10.1111).

Reid, M. S., Ho, L. B. & Berger, S. P. **(1998).** Behavioral and neurochemical components of nicotine sensitization following 15-day pretreatment: studies on contextual conditioning. *Behav Pharmacol* 9, 137–48.

Reid, M. S., Fox, L., Ho, L. B. & Berger, S. P. **(2000).** Nicotine stimulation of extracellular glutamate levels in the nucleus accumbens: Neuropharmacological characterization. *Synapse* 35, 129–136.

Reiss, D., Ceredig, R. A., Secher, T., Boué, J., Barreau, F., Dietrich, G. & Gavériaux-Ruff, C. **(2017).** Mu and delta opioid receptor knockout mice show increased colonic sensitivity. *Eur J Pain* 21, 623–634.

Rhee, S. H., Hewitt, J. K., Young, S. E., Corley, R. P., Crowley, T. J. & Stallings, M. C. **(2003).** Genetic and Environmental Influences on Substance Initiation, Use, and Problem Use in Adolescents. *Arch Gen Psychiatry* 60, 1256.

Rice, M. E. & Cragg, S. J. **(2004).** Nicotine amplifies reward-related dopamine signals in striatum. *Nat Neurosci* 7, 583–584.

Richardson, N. R. & Roberts, D. C. **(1996).** Progressive ratio schedules in drug self-administration studies in rats: a method to evaluate reinforcing efficacy. *J Neurosci Methods* 66, 1–11.

Riga, D., Matos, M. R., Glas, A., Smit, A. B., Spijker, S. & Van den Oever, M. C. **(2014).** Optogenetic dissection of medial prefrontal cortex circuitry. *Front Syst Neurosci* 8, 230. Frontiers Media SA.

Robinson, T. E. & Berridge, K. C. **(2008).** Review. The incentive sensitization theory of addiction: some current issues. *Philos Trans R Soc Lond B Biol Sci* 363, 3137–46.

Rodríguez-Muñoz, M., Sánchez-Blázquez, P., Herrero-Labrador, R., Martínez-Murillo, R., Merlos, M., Vela, J. M. & Garzón, J. **(2015).** The σ1 receptor engages the redox-regulated HINT1 protein to bring opioid analgesia under NMDA receptor negative control. *Antioxid Redox Signal* 22, 799–818.

Roh, D.-H., Kim, H.-W., Yoon, S.-Y., Seo, H.-S., Kwon, Y.-B., Kim, K.-W., Han, H.-J., Beitz, A. J. & Lee, J.-H. **(2008).** Intrathecal administration of sigma-1 receptor agonists facilitates nociception: Involvement of a protein kinase C-dependent pathway. *J Neurosci Res* 86, 3644–3654.

Roh, D.-H., Choi, S.-R., Yoon, S.-Y., Kang, S.-Y., Moon, J.-Y., Kwon, S.-G., Han, H.-J., Beitz, A. J. & Lee, J.-H. **(2011).** Spinal neuronal NOS activation mediates sigma-1 receptor-induced mechanical and thermal hypersensitivity in mice: involvement of PKC-dependent GluN1 phosphorylation. *Br J Pharmacol* 163, 1707–1720.

Rohe, H. J., Ahmed, I. S., Twist, K. E. & Craven, R. J. **(2009).** PGRMC1 (progesterone receptor membrane component 1): a targetable protein with multiple functions in steroid signaling, P450 activation and drug binding. *Pharmacol Ther* 121, 14–9. NIH Public Access.

Romieu, P., Phan, V.-L., Martin-Fardon, R. & Maurice, T. **(2002).** Involvement of the Sigma1 Receptor in Cocaine-induced Conditioned Place Preference Possible

Dependence on Dopamine Uptake Blockade. *Neuropsychopharmacology* 26, 444–455. Nature Publishing Group.

Romieu, P., Martin-Fardon, R. & Maurice, T. **(2000).** Involvement of the σ1 receptor in the cocaine-induced conditioned place preference. *Neuroreport* 11, 2885–2888.

Romieu, P., Martin-Fardon, R., Bowen, W. D. & Maurice, T. **(2003).** Sigma 1 receptor-related neuroactive steroids modulate cocaine-induced reward. *J Neurosci* 23, 3572–6. Society for Neuroscience.

Rose, J. E. **(2006).** Nicotine and nonnicotine factors in cigarette addiction. *Psychopharmacology (Berl)* 184, 274–285. Springer-Verlag.

Rose, J. E., Tashkin, D. P., Ertle, A., Zinser, M. C. & Lafer, R. **(1985).** Sensory blockade of smoking satisfaction. *Pharmacol Biochem Behav* 23, 289–293. Elsevier.

Roset, P. N., Farré, M., de la Torre, R., Mas, M., Menoyo, E., Hernández, C. & Camí, J. **(2001).** Modulation of rate of onset and intensity of drug effects reduces abuse potential in healthy males. *Drug Alcohol Depend* 64, 285–98.

Roth-Deri, I., Green-Sadan, T. & Yadid, G. **(2008).** β-Endorphin and drug-induced reward and reinforcement. *Prog Neurobiol* 86, 1–21. Pergamon.

Rounsaville, B. J., Spitzer, R. L. & Williams, J. B. **(1986).** Proposed changes in DSM-III substance use disorders: description and rationale. *Am J Psychiatry* 143, 463–468.

Rousseau, S. J., Jones, I. W., Pullar, I. A. & Wonnacott, S. **(2005).** Presynaptic α7 and non-α7 nicotinic acetylcholine receptors modulate [3H]d-aspartate release from rat frontal cortex in vitro. *Neuropharmacology* 49, 59–72. Pergamon.

Rubinstein, M., Mogil, J. S., Japón, M., Chan, E. C., Allen, R. G. & Low, M. J. **(1996).** Absence of opioid stress-induced analgesia in mice lacking β-endorphin by site-directed mutagenesis. *Proc Natl Acad Sci U S A* 93, 3995–4000.

Rukstalis, M., Jepson, C., Patterson, F. & Lerman, C. **(2005).** Increases in hyperactive–impulsive symptoms predict relapse among smokers in nicotine replacement therapy. *J Subst Abuse Treat* 28, 297–304. Pergamon.

Russo, S. J., Dietz, D. M., Dumitriu, D., Morrison, J. H., Malenka, R. C. & Nestler, E. J. **(2010, June).** The addicted synapse: Mechanisms of synaptic and structural plasticity in nucleus accumbens. *Trends Neurosci*.

Saal, D., Dong, Y., Bonci, A. & Malenka, R. C. **(2003).** Drugs of abuse and stress trigger a common synaptic adaptation in dopamine neurons. *Neuron* 37, 577–82.

Sabino, V., Cottone, P., Zhao, Y., Steardo, L., Koob, G. F. & Zorrilla, E. P. **(2009a).** Selective reduction of alcohol drinking in Sardinian alcohol-preferring rats by a sigma-1 receptor antagonist. *Psychopharmacology (Berl)* 205, 327–35. NIH Public Access.

Sabino, V., Cottone, P., Zhao, Y., Iyer, M. R., Steardo, L., Steardo, L., Rice, K. C., Conti, B., Koob, G. F. & other authors. **(2009b).** The sigma-receptor antagonist BD-1063 decreases ethanol intake and reinforcement in animal models of excessive drinking. *Neuropsychopharmacology* 34, 1482–93. NIH Public Access.

Sabino, V., Cottone, P., Blasio, A., Iyer, M. R., Steardo, L., Rice, K. C., Conti, B., Koob, G. F. & Zorrilla, E. P. **(2011).** Activation of σ-receptors induces binge-like drinking in Sardinian alcohol-preferring rats. *Neuropsychopharmacology* 36, 1207–18. Nature Publishing Group.

Saddoris, M. P., Sugam, J. A., Cacciapaglia, F. & Carelli, R. M. **(2013).** Rapid dopamine dynamics in the accumbens core and shell: Learning and action. *Front Biosci (Elite Ed)* 5, 273–288.

Salas, R., Sturm, R., Boulter, J. & De Biasi, M. **(2009).** Nicotinic receptors in the habenulo-interpeduncular system are necessary for nicotine withdrawal in mice. *J Neurosci* 29, 3014–8. Society for Neuroscience.

Salkind, N. **(2010).** *Encyclopedia of Research Design*. 2455 Teller Road, Thousand Oaks California 91320 United States : SAGE Publications, Inc.

Salminen, O., Drapeau, J. A., McIntosh, J. M., Collins, A. C., Marks, M. J. & Grady, S. R. **(2007).** Pharmacology of alpha-conotoxin MII-sensitive subtypes of nicotinic acetylcholine receptors isolated by breeding of null mutant mice. *Mol Pharmacol* 71, 1563–71. American Society for Pharmacology and Experimental Therapeutics.

Samovilova, N. N. & Vinogradov, V. A. **(1992).** Subcellular distribution of (+)-[3H]SKF 10,047 binding sites in rat liver. *Eur J Pharmacol* 225, 69–74.

Sánchez-Blázquez, P., Rodríguez-Muñoz, M., Herrero-Labrador, R., Burgueño, J., Zamanillo, D. & Garzón, J. **(2014).** The calcium-sensitive Sigma-1 receptor prevents cannabinoids from provoking glutamate NMDA receptor hypofunction: implications in antinociception and psychotic diseases. *Int J Neuropsychopharmacol* 17, 1943–1955.

Sánchez-Fernández, C., Nieto, F. R., González-Cano, R., Artacho-Cordón, A., Romero, L., Montilla-García, Á., Zamanillo, D., Baeyens, J. M., Entrena, J. M. & Cobos, E. J. **(2013).** Potentiation of morphine-induced mechanical antinociception by σ1 receptor inhibition: Role of peripheral σ1 receptors. *Neuropharmacology* 70, 348–358.

Sanchis-Segura, C. & Spanagel, R. **(2006).** Behavioural assessment of drug reinforcement and addictive features in rodents : an overview. *Addict Biol* 11, 2–38.

Sarter, M., Lustig, C., Howe, W. M., Gritton, H. & Berry, A. S. **(2014).** Deterministic functions of cortical acetylcholine.

Saunders, A., Oldenburg, I. A., Berezovskii, V. K., Johnson, C. A., Kingery, N. D., Elliott, H. L., Xie, T., Gerfen, C. R. & Sabatini, B. L. **(2015).** A direct GABAergic output from the basal ganglia to frontal cortex. *Nature* 521, 85–89.

Schenk, S. **(2002).** Effects of GBR 12909, WIN 35,428 and indatraline on cocaine self-administration and cocaine seeking in rats. *Psychopharmacology (Berl)* 160, 263–270. Springer-Verlag.

Schilström, B., De Villiers, S., Malmerfelt, A., Svensson, T. H. & Nomikos, G. G. **(2000).** Nicotine-induced Fos expression in the nucleus accumbens and the medial prefrontal cortex of the rat: Role of nicotinic and NMDA receptors in the ventral tegmental area. *Synapse* 36, 314–321.

Schilström, B., Rawal, N., Mameli-Engvall, M., Nomikos, G. G. & Svensson, T. H. **(2003).** Dual effects of nicotine on dopamine neurons mediated by different nicotinic receptor subtypes. *Int J Neuropsychopharmacol* 6, 1–11.

Schlam, T. R. & Baker, T. B. **(2013).** Interventions for tobacco smoking. *Annu Rev Clin Psychol* 9, 675–702. NIH Public Access.

Schroeder, J. A., Quick, K. F., Landry, P. M. & Rawls, S. M. **(2011).** Glutamate transporter (GLT-1) activation enhances nicotine antinociception and attenuates nicotine analgesic tolerance. *Neuroreport* 22, 970. NIH Public Access.

Schuckit, M. A. **(2009).** An overview of genetic influences in alcoholism. *J Subst Abuse Treat* 36, S5-14.

Schultz, W. **(2002).** Getting Formal with Dopamine and Reward. *Neuron* 36, 241–263. Cell Press.

Segal, M. **(2005).** Dendritic spines and long-term plasticity. *Nat Rev Neurosci* 6, 277–284.

Self, D. W. & Nestler, E. J. **(1998).** Relapse to drug-seeking: neural and molecular mechanisms. *Drug Alcohol Depend* 51, 49–60.

Sesack, S. R., Deutch, A. Y., Roth, R. H. & Bunney, B. S. **(1989).** Topographical organization of the efferent projections of the medial prefrontal cortex in the rat: An anterograde tract-tracing study withPhaseolus vulgaris leucoagglutinin. *J Comp Neurol* 290, 213–242. John Wiley & Sons, Ltd.

Sesack, S. R. & Grace, A. A. **(2010).** Cortico-Basal Ganglia Reward Network: Microcircuitry. *Neuropsychopharmacol Rev* 35, 27–47.

Sesack, S. R., Carr, D. B., Omelchenko, N. & Pinto, A. **(2003).** Anatomical Substrates for Glutamate-Dopamine Interactions. *Ann N Y Acad Sci* 1003, 36–52. John Wiley & Sons, Ltd (10.1111).

Seth, P., Fei, Y. J., Li, H. W., Huang, W., Leibach, F. H. & Ganapathy, V. **(1998).** Cloning and functional characterization of a sigma receptor from rat brain. *J Neurochem* 70, 922–31.

Seth, P., Leibach, F. H. & Ganapathy, V. **(1997).** Cloning and Structural Analysis of the cDNA and the Gene Encoding the Murine Type 1 Sigma Receptor. *Biochem Biophys Res Commun* 241, 535–540.

Shaham, Y. **(1996).** Effect of stress on opioid-seeking behavior: evidence from studies with rats. *Ann Behav Med* 18, 255–63.

Shaham, Y., Highfield, D., Delfs, J., Leung, S. & Stewart, J. **(2000).** Clonidine blocks stress-induced reinstatement of heroin seeking in rats: an effect independent of locus coeruleus noradrenergic neurons. *Eur J Neurosci* 12, 292–302.

Shaham, Y., Shalev, U., Lu, L., De Wit, H. & Stewart, J. **(2003).** The reinstatement model of drug relapse: history, methodology and major findings. *Psychopharmacology (Berl)* 168, 3–20.

Shalev, U., Grimm, J. W. & Shaham, Y. **(2002).** Neurobiology of relapse to heroin and cocaine seeking: a review. *Pharmacol Rev* 54, 1–42.

Shalev, U., Erb, S. & Shaham, Y. **(2010).** Role of CRF and other neuropeptides in stress-induced reinstatement of drug seeking. *Brain Res* 1314, 15–28.

Sharifi, N., Diehl, N., Yaswen, L., Brennan, M. B. & Hochgeschwender, U. **(2001).** Generation of dynorphin knockout mice. *Mol Brain Res* 86, 70–75.

Sharkey, J., Glen, K. A., Wolfe, S. & Kuhar, M. J. **(1988).** Cocaine binding at σ receptors. *Eur J Pharmacol* 149, 171–174. Elsevier.

Shiffman, S., Hickcox, M., Paty, J. A., Gnys, M., Kassel, J. D. & Richards, T. J. **(1996).** Progression from a smoking lapse to relapse: prediction from abstinence violation effects, nicotine dependence, and lapse characteristics. *J Consult Clin Psychol* 64, 993–1002.

Shim, I., Javaid, J. I., Wirtshafter, D., Jang, S. Y., Shin, K. H., Lee, H. J., Chung, Y. C. & Chun, B. G. **(2001).** Nicotine-induced behavioral sensitization is associated with extracellular dopamine release and expression of c-Fos in the striatum and nucleus accumbens of the rat. *Behav Brain Res* 121, 137–47.

Shippenberg, T. S., Zapata, A. & Chefer, V. I. **(2007).** Dynorphin and the pathophysiology of drug addiction. *Pharmacol Ther* 116, 306–21.

Shoaib, M., Schindler, C. W., Goldberg, S. R. & Pauly, J. R. **(1997).** Behavioural and biochemical adaptations to nicotine in rats: influence of MK801, an NMDA receptor antagonist. *Psychopharmacology (Berl)* 134, 121–30.

Simon, E. J., Hiller, J. M. & Edelman, I. **(1973).** Stereospecific binding of the potent narcotic analgesic (3H) Etorphine to rat-brain homogenate. *Proc Natl Acad Sci U S A* 70, 1947–9.

Simonin, F., Gavériaux-Ruff, C., Befort, K., Matthes, H., Lannes, B., Micheletti, G., Mattéi, M. G., Charron, G., Bloch, B. & Kieffer, B. L. **(1995).** kappa-Opioid receptor in humans: cDNA and genomic cloning, chromosomal assignment, functional expression, pharmacology, and expression pattern in the central nervous system. *Proc Natl Acad Sci U S A* 92, 7006–10. National Academy of Sciences.

Simonin, F., Befort, K., Gaveriaux-Ruff, C., Matthes, H., Nappey, V., Lannes, B., Micheletti, G. & Kieffer, B. L. **(1994).** The human delta-opioid receptor: genomic organization, cDNA cloning, functional expression, and distribution in human brain. *undefined*.

Simonin, F., Valverde, O., Smadja, C., Slowe, S., Kitchen, L., Dierich, A., Le Meur, M., Roques, B. P., Maldonado, R. & Kieffer, B. L. **(1998).** Disruption of the κ-opioid

receptor gene in mice enhances sensitivity to chemical visceral pain, impairs pharmacological actions of the selective κ-agonist U-50,488H and attenuates morphine withdrawal. *EMBO J* 17, 886–897.

Skuza, G. & Rogóz, Z. **(2009).** Antidepressant-like effect of PRE-084, a selective s 1 receptor agonist, in Albino Swiss and C57BL/6J mice. *Pharmacol Reports* 61, 1179–1183.

Soloway, S. B. **(1976).** Naturally occurring insecticides. *Environ Health Perspect* 14, 109–17.

Soria, G., Barbano, M. F., Maldonado, R. & Valverde, O. **(2008).** A reliable method to study cue-, priming-, and stress-induced reinstatement of cocaine self-administration in mice. *Psychopharmacology (Berl)* 199, 593–603.

Soriani, O., le Foll, F., Galas, L., Roman, F., Vaudry, H. & Cazin, L. **(1999a).** The ç-ligand (+)-pentazocine depresses M current and enhances calcium conductances in frog melanotrophs. *Am J Physiol Metab* 277, E73–E80. American Physiological SocietyBethesda, MD .

Soriani, O., Foll, F. Le, Roman, F., Monnet, F. P., Vaudry, H. & Cazin, L. **(1999b).** A-Current Down-Modulated by ç Receptor in Frog Pituitary Melanotrope Cells Through a G Protein-Dependent Pathway. *J Pharmacol Exp Ther* 289.

Spanagel, R., Herz, A. & Shippenberg, T. S. **(1992).** Opposing tonically active endogenous opioid systems modulate the mesolimbic dopaminergic pathway. *Proc Natl Acad Sci U S A* 89, 2046–50. National Academy of Sciences.

Spealman, R. D. & Goldberg, S. R. **(1978).** Drug self-administration by laboratory animals: control by schedules of reinforcement. *Annu Rev Pharmacol Toxicol* 18, 313–39.

Specio, S. E., Wee, S., O'Dell, L. E., Boutrel, B., Zorrilla, E. P. & Koob, G. F. **(2008).** CRF(1) receptor antagonists attenuate escalated cocaine self-administration in rats. *Psychopharmacology (Berl)* 196, 473–82. NIH Public Access.

Spitzer, R. L., Williams, J. B. & Skodol, A. E. **(1980).** DSM-III: the major achievements and an overview. *Am J Psychiatry* 137, 151–164.

Spruce, B. A., Campbell, L. A., McTavish, N., Cooper, M. A., Appleyard, M. V. L., O'Neill, M., Howie, J., Samson, J., Watt, S. & other authors. **(2004).** Small Molecule Antagonists of the σ-1 Receptor Cause Selective Release of the Death Program in Tumor and Self-Reliant Cells and Inhibit Tumor Growth ***in Vitro*** and ***in Vivo*** . *Cancer Res* 64, 4875–4886.

Stahl, S. M. **(2013).** *Stahl's Essential Psychopharmacology Neuroscientific*.

Staley, J. K., Krishnan-Sarin, S., Cosgrove, K. P., Krantzler, E., Frohlich, E., Perry, E., Dubin, J. A., Estok, K., Brenner, E. & other authors. **(2006).** Human Tobacco Smokers in Early Abstinence Have Higher Levels of β2* Nicotinic Acetylcholine Receptors than Nonsmokers. *J Neurosci* 26, 8707. Society for Neuroscience.

Stamatakis, A. M., Jennings, J. H., Ung, R. L., Blair, G. A., Weinberg, R. J., Neve, R. L., Boyce, F., Mattis, J., Ramakrishnan, C. & other authors. **(2013).** A unique population of ventral tegmental area neurons inhibits the lateral habenula to promote reward. *Neuron* 80.

Stefanski, R., Justinova, Z., Hayashi, T., Takebayashi, M., Goldberg, S. & Su, T.-P. **(2004).** Sigma1 receptor upregulation after chronic methamphetamine self-administration in rats: a study with yoked controls. *Psychopharmacology (Berl)* 175, 68–75. Springer-Verlag.

Stein, C. & Lang, L. J. **(2009).** Peripheral mechanisms of opioid analgesia. *Curr Opin Pharmacol* 9, 3–8. Elsevier.

Stolerman, I. P. & Jarvis, M. J. **(1995).** The scientific case that nicotine is addictive. *Psychopharmacology (Berl)* 117, 2–10; discussion 14-20.

Stuber, G. D., Sparta, D. R., Stamatakis, A. M., Van Leeuwen, W. A., Hardjoprajitno, J. E.,

Cho, S., Tye, K. M., Kempadoo, K. A., Zhang, F. & other authors. **(2011).** Excitatory transmission from the amygdala to nucleus accumbens facilitates reward seeking.

Stuber, G. D., Britt, J. P. & Bonci, A. **(2012).** Optogenetic modulation of neural circuits that underlie reward seeking. *Biol Psychiatry* 71, 1061–7. NIH Public Access.

Su, T.-P. & Hayashi, T. **(2003).** Understanding the molecular mechanism of sigma-1 receptors: towards a hypothesis that sigma-1 receptors are intracellular amplifiers for signal transduction. *Curr Med Chem* 10, 2073–80.

Su, T.-P., Hayashi, T., Maurice, T., Buch, S. & Ruoho, A. E. **(2010).** The sigma-1 receptor chaperone as an inter-organelle signaling modulator. *Trends Pharmacol Sci* 31, 557–66. NIH Public Access.

Svingos, A. L., Moriwaki, A., Wang, J. B., Uhl, G. R. & Pickel, V. M. **(1996).** Ultrastructural Immunocytochemical Localization of μ-Opioid Receptors in Rat Nucleus Accumbens: Extrasynaptic Plasmalemmal Distribution and Association with Leu5-Enkephalin. *J Neurosci* 16, 4162–4173. Society for Neuroscience.

Svingos, A. L., Chavkin, C., Colago, E. E. O. & Pickel, V. M. **(2001).** Major coexpression of kappa-opioid receptors and the dopamine transporter in nucleus accumbens axonal profiles. *Synapse* 42, 185–192.

Swanson, L. W. **(1982).** The projections of the ventral tegmental area and adjacent regions: A combined fluorescent retrograde tracer and immunofluorescence study in the rat. *Brain Res Bull* 9, 321–353. Elsevier.

Swendsen, J., Conway, K. P., Degenhardt, L., Dierker, L., Glantz, M., Jin, R., Merikangas, K. R., Sampson, N. & Kessler, R. C. **(2009).** Socio-demographic risk factors for alcohol and drug dependence: the 10-year follow-up of the national comorbidity survey. *Addiction* 104, 1346–55.

Takahashi, S., Miwa, T. & Horikomi, K. **(2000).** Involvement of σ1 receptors in methamphetamine-induced behavioral sensitization in rats. *Neurosci Lett* 289, 21–24. Elsevier.

Taly, A., Corringer, P.-J., Guedin, D., Lestage, P. & Changeux, J.-P. **(2009).** Nicotinic receptors: allosteric transitions and therapeutic targets in the nervous system. *Nat Rev Drug Discov* 8, 733–750.

Tan, K. R., Yvon, C., Turiault, M., Mirzabekov, J. J., Doehner, J., Labouèbe, G., Deisseroth, K., Tye, K. M. & Lüscher, C. **(2012).** GABA Neurons of the VTA Drive Conditioned Place Aversion. *Neuron* 73, 1173–1183.

Tanda, G. & Di Chiara, G. **(1998).** A dopamine-mu1 opioid link in the rat ventral tegmentum shared by palatable food (Fonzies) and non-psychostimulant drugs of abuse. *Eur J Neurosci* 10, 1179–87.

Taverna, S., Ilijic, E. & Surmeier, D. J. **(2008).** Recurrent collateral connections of striatal medium spiny neurons are disrupted in models of Parkinson's disease NIH Public Access. *J Neurosci* 28, 5504–5512.

Taylor, S. B., Lewis, C. R. & Olive, M. F. **(2013).** The neurocircuitry of illicit psychostimulant addiction: acute and chronic effects in humans. *Subst Abuse Rehabil* 4, 29–43. Dove Press.

Taylor, S. R., Badurek, S., Dileone, R. J., Nashmi, R., Minichiello, L. & Picciotto, M. R. **(2014).** GABAergic and Glutamatergic Efferents of the Mouse Ventral Tegmental Area. *J Comp Neurol* 522, 3308–3334.

Tepper, J., Martin, L. & Anderson, D. **(2007).** GABAergic control of substantia nigra dopaminergic neurons. *Prog Brain Res* 160, 189–208. Elsevier.

Tepper, J. M. & Bolam, J. P. **(2004).** Functional diversity and specificity of neostriatal interneurons. *Curr Opin Neurobiol* 14, 685–692.

Terenius, L. **(1973).** Characteristics of the 'receptor' for narcotic analgesics in synaptic plasma membrane fraction from rat brain. *Acta Pharmacol Toxicol (Copenh)* 33,

377–84.

Tessari, M., Pilla, M., Andreoli, M., Hutcheson, D. M. & Heidbreder, C. A. **(2004).** Antagonism at metabotropic glutamate 5 receptors inhibits nicotine- and cocaine-taking behaviours and prevents nicotine-triggered relapse to nicotine-seeking. *Eur J Pharmacol* 499, 121–133.

Thompson, A. A., Liu, W., Chun, E., Katritch, V., Wu, H., Vardy, E., Huang, X.-P., Trapella, C., Guerrini, R. & other authors. **(2012).** Structure of the nociceptin/orphanin FQ receptor in complex with a peptide mimetic. *Nature* 485, 395–9. NIH Public Access.

Thompson, A. C., Zapata, A., Justice, J. B., Vaughan, R. A., Sharpe, L. G. & Shippenberg, T. S. **(2000).** Kappa-opioid receptor activation modifies dopamine uptake in the nucleus accumbens and opposes the effects of cocaine. *J Neurosci* 20, 9333–40. Society for Neuroscience.

Thomsen, M. & Caine, S. B. **(2007).** Intravenous drug self-administration in mice: practical considerations. *Behav Genet* 37, 101–18.

Threlfell, S. & Cragg, S. J. **(2011).** Dopamine signaling in dorsal versus ventral striatum: the dynamic role of cholinergic interneurons. *Front Syst Neurosci* 5.

Threlfell, S., Clements, M. A., Khodai, T., Pienaar, I. S., Exley, R., Wess, J. & Cragg, S. J. **(2010).** Striatal muscarinic receptors promote activity-dependence of dopamine transmission via distinct receptor subtypes on cholinergic interneurons in ventral versus dorsal striatum. *J Neurosci* 30, 3398–3408.

Threlfell, S., Lalic, T., Platt, N. J., Jennings, K. A., Deisseroth, K. & Cragg, S. J. **(2012).** Striatal Dopamine Release Is Triggered by Synchronized Activity in Cholinergic Interneurons. *Neuron* 75, 58–64.

Tiffany, S. T., Carter, B. L. & Singleton, E. G. **(2000).** Challenges in the manipulation, assessment and interpretation of craving relevant variables. *Addiction* 95 Suppl 2, S177-87.

Toll, L., Bruchas, M. R., Calo', G., Cox, B. M. & Zaveri, N. T. **(2016).** Nociceptin/Orphanin FQ Receptor Structure, Signaling, Ligands, Functions, and Interactions with Opioid Systems. *Pharmacol Rev* 68, 419–57. American Society for Pharmacology and Experimental Therapeutics.

Torrecilla, M., Marker, C. L., Cintora, S. C., Stoffel, M., Williams, J. T. & Wickman, K. **(2002).** G-Protein-Gated Potassium Channels Containing Kir3.2 and Kir3.3 Subunits Mediate the Acute Inhibitory Effects of Opioids on Locus Ceruleus Neurons. *J Neurosci* 22, 4328–4334. Society for Neuroscience.

Toth, E., Vizi, E. S. & Lajtha, A. **(1993).** Effect of nicotine on levels of extracellular amino acids in regions of the rat brain in vivo. *Neuropharmacology* 32, 827–32.

Trigo, J. M., Zimmer, A. & Maldonado, R. **(2009).** Nicotine anxiogenic and rewarding effects are decreased in mice lacking beta-endorphin. *Neuropharmacology* 56, 1147–53.

Trigo, J. M., Martin-García, E., Berrendero, F., Robledo, P. & Maldonado, R. **(2010).** The endogenous opioid system: a common substrate in drug addiction. *Drug Alcohol Depend* 108, 183–94.

Tripathi, A., Lucía Prensa, • & Mengual, E. **(2013).** Axonal branching patterns of ventral pallidal neurons in the rat. *Brain Struc Funct* 218, 1133–1157.

Tritsch, N. X. & Sabatini, B. L. **(2012).** Dopaminergic Modulation of Synaptic Transmission in Cortex and Striatum. *Neuron* 76, 33–50. Elsevier Inc.

Tronci, V. & Balfour, D. J. K. **(2011).** The effects of the mGluR5 receptor antagonist 6-methyl-2-(phenylethynyl)-pyridine (MPEP) on the stimulation of dopamine release evoked by nicotine in the rat brain. *Behav Brain Res* 219, 354–357.

Tsai, S.-Y., Hayashi, T., Mori, T. & Su, T.-P. **(2009).** Sigma-1 receptor chaperones and diseases. *Cent Nerv Syst Agents Med Chem* 9, 184–9.

Tsuang, M. T., Lyons, M. J., Eisen, S. A., Goldberg, J., True, W., Lin, N., Meyer, J. M., Toomey, R., Faraone, S. V & Eaves, L. **(1996).** Genetic influences on DSM-III-R drug abuse and dependence: a study of 3,372 twin pairs. *Am J Med Genet* 67, 473–7.

Tuesta, L. M., Fowler, C. D. & Kenny, P. J. **(2011).** Recent advances in understanding nicotinic receptor signaling mechanisms that regulate drug self-administration behavior. *Biochem Pharmacol* 82, 984–95.

Tzschentke, T. M. **(2007).** Measuring reward with the conditioned place preference (CPP) paradigm: update of the last decade. *Addict Biol* 12, 227–462. John Wiley & Sons, Ltd (10.1111).

Ujike, H., Tsuchida, K., Akiyama, K. & Otsuki, S. **(1992).** Supersensitivity of σ receptors after repeated administration of cocaine. *Life Sci* 51, PL31–PL36. Pergamon.

USHHS. **(1990).** *The Health Benefits of Smoking Cessation: A Report of the Surgeon General*. United States. Public Health Service. Office on Smoking and Health.

Uylings, H. B. M., Groenewegen, H. J. & Kolb, B. **(2003).** Do rats have a prefrontal cortex? *Behav Brain Res* 146, 3–17. Elsevier.

Valenza, M., DiLeo, A., Steardo, L., Cottone, P. & Sabino, V. **(2016).** Ethanol-related behaviors in mice lacking the sigma-1 receptor. *Behav Brain Res* 297, 196–203. NIH Public Access.

Vallejo, Y. F., Buisson, B., Bertrand, D. & Green, W. N. **(2005).** Chronic nicotine exposure upregulates nicotinic receptors by a novel mechanism. *J Neurosci* 25, 5563–72.

Vanderschuren, L. J. M. J., Di Ciano, P. & Everitt, B. J. **(2005).** Involvement of the Dorsal Striatum in Cue-Controlled Cocaine Seeking. *J Neurosci* 25, 8665–8670.

Venniro, M., Caprioli, D. & Shaham, Y. **(2015).** *Animal models of drug relapse and craving: from drug priming-induced reinstatement to incubation of craving after voluntary abstinence*. *Neurosci Addict Med From Prev to Rehabil - Methods Interv*, 1st edn. Elsevier B.V.

Vertes, R. P. **(2004).** Differential projections of the infralimbic and prelimbic cortex in the rat. *Synapse* 51, 32–58. John Wiley & Sons, Ltd.

Vertes, R. P. **(2006).** Interactions among the medial prefrontal cortex, hippocampus and midline thalamus in emotional and cognitive processing in the rat. *Neuroscience* 142, 1–20. Pergamon.

Vink, J. M., Willemsen, G. & Boomsma, D. I. **(2005).** Heritability of smoking initiation and nicotine dependence. *Behav Genet* 35, 397–406.

Vlachou, S., Guery, S., Froestl, W., Banerjee, D., Benedict, J., Finn, M. G. & Markou, A. **(2011).** Repeated administration of the GABAB receptor positive modulator BHF177 decreased nicotine self-administration, and acute administration decreased cue-induced reinstatement of nicotine seeking in rats. *Psychopharmacology (Berl)* 215, 117–128.

Volkow, N. D., Wang, G.-J., Fowler, J. S., Logan, J., Gatley, S. J., Hitzemann, R., Chen, A. D., Dewey, S. L. & Pappas, N. **(1997).** Decreased striatal dopaminergic responsiveness in detoxified cocaine-dependent subjects. *Nature* 386, 830–833. Nature Publishing Group.

Volkow, N. D., Fowler, J. S., Wang, G.-J. & Swanson, J. M. **(2004).** Dopamine in drug abuse and addiction: results from imaging studies and treatment implications. *Mol Psychiatry* 9, 557–69.

Volkow, N. D., Fowler, J. S. & Wang, G.-J. **(2003).** The addicted human brain: insights from imaging studies. *J Clin Invest* 111, 1444–51. American Society for Clinical Investigation.

Volkow, N. D., Wang, G.-J., Telang, F., Fowler, J. S., Logan, J., Jayne, M., Ma, Y., Pradhan, K. & Wong, C. **(2007).** Profound decreases in dopamine release in striatum in detoxified alcoholics: possible orbitofrontal involvement. *J Neurosci* 27, 12700–6.

De Vries, T. J. & Schoffelmeer, A. N. M. **(2005).** Cannabinoid CB1 receptors control conditioned drug seeking. *Trends Pharmacol Sci* 26, 420–6.

Walker, D. M. & Nestler, E. J. **(2018).** Neuroepigenetics and addiction. *Handb Clin Neurol* 747–765.

Wallace, T. L. & Bertrand, D. **(2013).** Importance of the nicotinic acetylcholine receptor system in the prefrontal cortex. *Biochem Pharmacol* 85, 1713–1720. Elsevier.

Walters, C. L., Cleck, J. N., Kuo, Y. & Blendy, J. A. **(2005).** Mu-opioid receptor and CREB activation are required for nicotine reward. *Neuron* 46, 933–43.

Wang, F., Chen, H., Steketee, J. D. & Sharp, B. M. **(2007).** Upregulation of Ionotropic Glutamate Receptor Subunits within Specific Mesocorticolimbic Regions during Chronic Nicotine Self-Administration. *Neuropsychopharmacology* 32, 103–109. Nature Publishing Group.

Wang, H. & Sun, X. **(2005).** Desensitized nicotinic receptors in brain. *Brain Res Rev* 48, 420–437.

Wang, J.-C., Kapoor, M. & Goate, A. M. **(2012).** The Genetics of Substance Dependence. *Annu Rev Genomics Hum Genet* 22, 341–261.

Wardle, M. C., Munafò, M. R. & de Wit, H. **(2011).** Effect of social stress during acute nicotine abstinence. *Psychopharmacology (Berl)* 218, 39–48. NIH Public Access.

Warr, O., Takahashi, M. & Attwell, D. **(1999).** Modulation of extracellular glutamate concentration in rat brain slices by cystine-glutamate exchange. *J Physiol* 514 (Pt 3), 783–93. Wiley-Blackwell.

Watabe-Uchida, M., Zhu, L., Ogawa, S. K., Vamanrao, A. & Uchida, N. **(2012).** Whole-Brain Mapping of Direct Inputs to Midbrain Dopamine Neurons. *Neuron* 74, 858–873. Cell Press.

Watson, C., Paxinos, G. & Puelles, L. (Luis). **(2011).** *The mouse nervous system*.

Weibel, R., Reiss, D., Karchewski, L., Gardon, O., Matifas, A., Filliol, D., Becker, J. A. J., Wood, J. N., Kieffer, B. L. & Gaveriaux-Ruff, C. **(2013).** Mu Opioid Receptors on Primary Afferent Nav1.8 Neurons Contribute to Opiate-Induced Analgesia: Insight from Conditional Knockout Mice. *PLoS One* 8.

Weiss, F., Markou, A., Lorang, M. T. & Koob, G. F. **(1992).** Basal extracellular dopamine levels in the nucleus accumbens are decreased during cocaine withdrawal after unlimited-access self-administration. *Brain Res* 593, 314–318. Elsevier.

Wesnes, K. A., Edgar, C. J., Kezic, I., Salih, H. M. & de Boer, P. **(2013).** Effects of nicotine withdrawal on cognition in a clinical trial setting. *Psychopharmacology (Berl)* 229, 133–140. Springer Berlin Heidelberg.

West, R. **(1992).** Nicotine addiction: a re-analysis of the arguments. *Psychopharmacology (Berl)* 108, 408–10; discussion 411-6.

Wewers, M. E., Dhatt, R. K., Snively, T. A. & Tejwani, G. A. **(1999).** The effect of chronic administration of nicotine on antinociception, opioid receptor binding and met-enkelphalin levels in rats. *Brain Res* 822, 107–13.

WHO. **(2002).** *The world health report 2002 - Reducing Risks, Promoting Healthy Life*. World Health Organization.

WHO. **(2017).** *WHO report on the global tobacco epidemic,2017*.

WHO. **(2018).** *Global status report on alcohol and health 2018*.

Wickman, K. & Clapham, D. E. **(1995).** Ion channel regulation by G proteins. *Physiol Rev* 75, 865–85. American Physiological Society Bethesda, MD .

Widiger, T. A. & Smith, G. T. **(2012).** Addiction and nosology. In *APA Addict Syndr handbook, Vol 1 Found Influ expressions Addict*, pp. 49–66. Washington: American Psychological Association.

Wilke, R. A., Mehta, R. P., Lupardus, P. J., Chen, Y., Ruoho, A. E. & Jackson, M. B. **(1999).** Sigma receptor photolabeling and sigma receptor-mediated modulation of

potassium channels in tumor cells. *J Biol Chem* 274, 18387–92. American Society for Biochemistry and Molecular Biology.

Wilson, M. **(1993).** DSM-III and the transformation of American psychiatry: a history. *Am J Psychiatry* 150, 399–410. American Psychiatric Publishing.

Wise, R. A. **(2004).** Dopamine, learning and motivation. *Nat Rev Neurosci* 5, 483–94.

Wise, R. A. & Koob, G. F. **(2014).** The development and maintenance of drug addiction. *Neuropsychopharmacology* 39, 254–62. Nature Publishing Group.

de Wit, H. **(1996).** Priming effects with drugs and other reinforcers. *Exp Clin Psychopharmacol* 4, 5–10.

Witkin, J. M., Terry, P., Menkel, M., Hickey, P., Pontecorvo, M., Ferkany, J. & Katz, J. L. **(1993).** Effects of the selective sigma receptor ligand, 6-[6-(4-hydroxypiperidinyl)hexyloxy]-3-methylflavone (NPC 16377), on behavioral and toxic effects of cocaine. *J Pharmacol Exp Ther* 266.

Wonnacott, S. **(2008).** Gates and filters: unveiling the physiological roles of nicotinic acetylcholine receptors in dopaminergic transmission. *Br J Pharmacol* 153, 2–4.

Wonnacott, S., Drasdo, A., Sanderson, E. & Rowell, P. **(1990).** Presynaptic nicotinic receptors and the modulation of transmitter release. *Ciba Found Symp* 152, 87–101; discussion 102-5.

Wooltorton, J. R. A., Pidoplichko, V. I., Broide, R. S. & Dani, J. A. **(2003).** Differential Desensitization and Distribution of Nicotinic Acetylcholine Receptor Subtypes in Midbrain Dopamine Areas. *J Neurosci* 23, 3176–3185. Society for Neuroscience.

Wu, H., Wacker, D., Mileni, M., Katritch, V., Han, G. W., Vardy, E., Liu, W., Thompson, A. A., Huang, X.-P. & other authors. **(2012).** Structure of the human κ-opioid receptor in complex with JDTic. *Nature* 485, 327–32. NIH Public Access.

Xu, Y.-T., Robson, M. J., Szeszel-Fedorowicz, W., Patel, D., Rooney, R., McCurdy, C. R. & Matsumoto, R. R. **(2012).** CM156, a sigma receptor ligand, reverses cocaine-induced place conditioning and transcriptional responses in the brain. *Pharmacol Biochem Behav* 101, 174–80. NIH Public Access.

Yagasaki, Y., Numakawa, T., Kumamaru, E., Hayashi, T., Su, T.-P. & Kunugi, H. **(2006).** Chronic antidepressants potentiate via sigma-1 receptors the brain-derived neurotrophic factor-induced signaling for glutamate release. *J Biol Chem* 281, 12941–9. American Society for Biochemistry and Molecular Biology.

Yager, L. M., Garcia, A. F., Wunsch, A. M. & Ferguson, S. M. **(2015).** The ins and outs of the striatum: role in drug addiction. *Neuroscience* 301, 529–41. NIH Public Access.

Yamaguchi, T., Sheen, W. & Morales, M. **(2007).** Glutamatergic neurons are present in the rat ventral tegmental area. *Eur J Neurosci* 25, 106–18. NIH Public Access.

Yan, Y. & Nabeshima, T. **(2009).** Mouse model of relapse to the abuse of drugs: procedural considerations and characterizations. *Behav Brain Res* 196, 1–10.

Yang, H., de Jong, J. W., Tak, Y. E., Peck, J., Bateup, H. S. & Lammel, S. **(2018).** Nucleus Accumbens Subnuclei Regulate Motivated Behavior via Direct Inhibition and Disinhibition of VTA Dopamine Subpopulations. *Neuron* 97, 434-449.e4. Elsevier Inc.

Yang, S., Bhardwaj, A., Cheng, J., Alkayed, N. J., Hurn, P. D. & Kirsch, J. R. **(2007).** Sigma Receptor Agonists Provide Neuroprotection In Vitro by Preserving bcl-2. *Anesth Analg* 104, 1179–1184.

Yang, Z.-J., Carter, E. L., Torbey, M. T., Martin, L. J. & Koehler, R. C. **(2010).** Sigma receptor ligand 4-phenyl-1-(4-phenylbutyl)-piperidine modulates neuronal nitric oxide synthase/postsynaptic density-95 coupling mechanisms and protects against neonatal ischemic degeneration of striatal neurons. *Exp Neurol* 221, 166–174.

Yang, Z., Carter, E. L., Torbey, M. T., Martin, L. J. & Raymond, C. **(2011).** NIH Public Access 221, 166–174.

Yau, Y. H. C., Crowley, M. J., Mayes, L. C. & Potenza, M. N. **(2012).** Are Internet use and video-game-playing addictive behaviors? Biological, clinical and public health implications for youths and adults. *Minerva Psichiatr* 53, 153–170.

Yokoo, H., Yamada, S., Yoshida, M., Tanaka, M. & Nishi, S. **(1992).** Attenuation of the inhibitory effect of dynorphin on dopamine release in the rat nucleus accumbens by repeated treatment with methamphetamine. *Eur J Pharmacol* 222, 43–47. Elsevier.

Yoshida, Y., Koide, S., Hirose, N., Takada, K., Tomiyama, K., Koshikawa, N. & Cools, A. . R. **(1999).** Fentanyl increases dopamine release in rat nucleus accumbens: involvement of mesolimbic mu- and delta-2-opioid receptors. *Neuroscience* 92, 1357–65. Pergamon.

Yuste, R. **(2005).** Origin and Classification of Neocortical Interneurons. *Neuron* 48, 524–527.

Zadina, J. E., Hackler, L., Ge, L. J. & Kastin, A. J. **(1997).** A potent and selective endogenous agonist for the mu-opiate receptor. *Nature* 386, 499–502.

Zamanillo, D., Romero, L., Merlos, M. & Vela, J. M. **(2013).** Sigma 1 receptor: A new therapeutic target for pain. *Eur J Pharmacol* 716, 78–93.

Zamponi, G. W. & Snutch, T. P. **(1998).** Modulation of voltage-dependent calcium channels by G proteins. *Curr Opin Neurobiol* 8, 351–356. Elsevier Current Trends.

Van Zessen, R., Phillips, J. L., Budygin, E. A. & Stuber, G. D. **(2012).** Activation of VTA GABA neurons disrupts reward consumption. *Neuron* 73, 1184–1194.

Zhang, H. & Cuevas, J. **(2002).** Sigma Receptors Inhibit High-Voltage–Activated Calcium Channels in Rat Sympathetic and Parasympathetic Neurons. *J Neurophysiol* 87, 2867–2879. American Physiological SocietyBethesda, MD .

Zhang, L., Dong, Y., Doyon, W. M. & Dani, J. A. **(2012).** Withdrawal from chronic nicotine exposure alters dopamine signaling dynamics in the nucleus accumbens. *Biol Psychiatry* 71, 184–91. NIH Public Access.

Zhao-Shea, R., Liu, L., Soll, L. G., Improgo, M. R., Meyers, E. E., Mcintosh, J. M., Grady, S. R., Marks, M. J., Gardner, P. D. & Tapper, A. R. **(2011).** Nicotine-Mediated Activation of Dopaminergic Neurons in Distinct Regions of the Ventral Tegmental Area. *Neuropsychopharmacology* 36, 1021–1032.

Zhao-Shea, R., Liu, L., Pang, X., Gardner, P. D. & Tapper, A. R. **(2013).** Activation of GABAergic neurons in the interpeduncular nucleus triggers physical nicotine withdrawal symptoms. *Curr Biol* 23, 2327–35. NIH Public Access.

Zhou, X., Nonnemaker, J., Sherrill, B., Gilsenan, A. W., Coste, F. & West, R. **(2009).** Attempts to quit smoking and relapse: Factors associated with success or failure from the ATTEMPT cohort study. *Addict Behav* 34, 365–373. Pergamon.

Zhu, Y., Wienecke, C. F. R., Nachtrab, G. & Chen, & X. **(2016).** A thalamic input to the nucleus accumbens mediates opiate dependence. *Nature* 530.

Zoli, M., Pistillo, F. & Gotti, C. **(2015).** Diversity of native nicotinic receptor subtypes in mammalian brain. *Neuropharmacology* 96, 302–311.

van der Zwaluw, C. S. & Engels, R. C. M. E. **(2009).** Gene-environment interactions and alcohol use and dependence: current status and future challenges. *Addiction* 104, 907–914. John Wiley & Sons, Ltd (10.1111).

Zweifel, L. S., Parker, J. G., Lobb, C. J., Rainwater, A., Wall, V. Z., Fadok, J. P., Darvas, M., Kim, M. J., Mizumori, S. J. Y. & other authors. **(2009).** Disruption of NMDAR-dependent burst firing by dopamine neurons provides selective assessment of phasic dopamine-dependent behavior. *Proc Natl Acad Sci U S A* 106, 7281–8. National Academy of Sciences.

Annex

Article 1

Effects of genetic deletion of endogenous opioid system components on the reinstatement of cocaine-seeking behavior in mice.

Gutiérrez-Cuesta J*[1], Burokas A*[1], Mancino S[#1], **Kummer S[#1]**, Martín-Garcia E[1], Maldonado R[1]

Neuropsychopharmacology (2014) 39, 2974–2988

www.neuropsychopharmacology.org

Effects of Genetic Deletion of Endogenous Opioid System Components on the Reinstatement of Cocaine-Seeking Behavior in Mice

Javier Gutiérrez-Cuesta[1,2], Aurelijus Burokas[1,2,4], Samantha Mancino[1,3], Sami Kummer[1,3], Elena Martín-García[1] and Rafael Maldonado*[,1]

[1]*Departament de Ciències Experimentals i de la Salut, Universitat Pompeu Fabra, Barcelona, Spain*

The repeated cycles of cessation of consumption and relapse remain the major clinical concern in treating drug addiction. The endogenous opioid system is a crucial component of the reward circuit that participates in the adaptive changes leading to relapse in the addictive processes. We have used genetically modified mice to evaluate the involvement of μ-opioid receptor (MOR) and δ-opioid receptor (DOR) and their main endogenous ligands, the enkephalins derived from proenkephalin (PENK) and prodynorphin (PDYN), in the reinstatement of cocaine-seeking behavior. Constitutive knockout mice of MOR, DOR, PENK, and PDYN, and their wild-type littermates were trained to self-administer cocaine or to seek for palatable food, followed by a period of extinction and finally tested on a cue-induced reinstatement of seeking behavior. The four lines of knockout mice acquired operant cocaine self-administration behavior, although DOR and PENK knockout mice showed less motivation for cocaine than wild-type littermates. Moreover, cue-induced relapse was significantly decreased in MOR and DOR knockout mice. In contrast, PDYN knockout mice showed a slower extinction and increased relapse than wild-type littermates. C-Fos expression analysis revealed differential activation in brain areas related with memory and reward in these knockout mice. No differences were found in any of the four genotypes in operant responding to obtain palatable food, indicating that the changes revealed in knockout mice were not due to unspecific deficit in operant performance. Our results indicate that MOR, DOR, and PDYN have a differential role in cue-induced reinstatement of cocaine-seeking behavior.
Neuropsychopharmacology (2014) **39,** 2974–2988; doi:10.1038/npp.2014.149; published online 23 July 2014

INTRODUCTION

Addiction is a chronic brain disease characterized by the compulsive use of drugs in spite of their adverse consequences, loss of control over drug taking, and relapse even after long periods of abstinence according to the 'Diagnostic and Statistical Manual of Mental Disorders (5th edition; DSM-5; American Psychiatric Association, 2013), the most widely accepted nomenclature used by clinicians and researchers for the classification of mental disorders. The repeated cycles of relapse after cessation of consumption remain the major clinical concern in the treatment of drug addiction (Miller and Gold, 1994; Weiss, 2010). In our laboratory, we have recently validated novel models of reinstatement of drug and food-seeking behavior (Martin-Garcia *et al*, 2011; Soria *et al*, 2008) in mice that allow to study the neurobiological mechanisms of relapse through the use of genetically modified mice.

Complex adaptive changes within the brain reward circuits occurring during the addictive processes are responsible of drug relapse. Several neurotransmitters, including the endogenous opioid system are involved in these changes (Bodnar, 2008; Volkow *et al*, 2009). Chronic exposure to the different prototypical drugs of abuse, including opioids, alcohol, nicotine, psychostimulants, and cannabinoids has been reported to produce significant alterations within the endogenous opioid system, which seem to have an important role in the development of the addictive process (Trigo *et al*, 2010). The endogenous opioid system is integrated by different families of endogenous opioid peptides, and three different opioid receptors, μ (MOR), δ (DOR), and κ (KOR), widely distributed in the central nervous system and peripheral tissues. The activation of these opioid receptors leads to different intracellular responses that produce an inhibition of neuronal activity and a reduction of neurotransmitter release (Law *et al*, 2000).

Three families of endogenous peptides derived from either proopiomelanocortin (POMC), proenkephalin (PENK), or prodynorphin (PDYN) generate several final

*Correspondence: Professor R Maldonado, Laboratory of Neuropharmacology, Pompeu Fabra University, Dr Aiguader 88, Parc de Recerca Biomèdica de Barcelona, Barcelona 08003, Spain. Tel: +1 34 93 3160824, Fax: +1 34 93 3160901,
E-mail: rafael.maldonado@upf.edu
[2]These authors contributed equally to this work.
[3]These authors contributed equally to this work.
[4]Present address: Laboratory of Neurogastroenterology, Alimentary Pharmabiotic Centre, University College Cork, Cork, Ireland.
Received 12 December 2013; revised 30 May 2014; accepted 10 June 2014; accepted article preview online 19 June 2014

active peptides including β-endorphin, met- and leu-enkephalin, dynorphins, and neo-endorphins, respectively, that exhibit different affinities for each opioid receptor (Kieffer and Gaveriaux-Ruff, 2002). The opioid peptides derived from PENK represent the main endogenous ligands that activate MOR and DOR in multiple brain areas, although endogenous enkephalins also derive from PDYN (Kieffer and Gaveriaux-Ruff 2002). These receptors have an important role in regulating mood and reward, and are key components in the control of drug reinforcing effects leading to addictive behavior. Multiple studies have suggested an important role for opioid receptors and their endogenous ligands in cocaine addiction (Charbogne *et al*, 2014). Administration of MOR antagonists attenuates cocaine-induced conditioned place preference and reduces cocaine self-administration and reinstatement in rats (Soderman and Unterwald, 2008; Tang *et al*, 2005; Ward *et al*, 2003), and cocaine reinforcement was reduced in MOR knockout mice (Mathon *et al*, 2005), suggesting the involvement of MOR in cocaine addiction. DOR antagonists can increase or decrease cocaine self-administration in rats depending on the brain area microinjected (Ward *et al*, 2003). The role of endogenous opioid peptides derived from PENK in cocaine responses is still unknown, although these peptides participate in the reinforcing effects of other drugs of abuse (Berrendero *et al*, 2005; Marinelli *et al*, 2005). Several opioid peptides have opposite roles in the control of behavioral responses such as dynorphins and Leu-enkephalin derived from PDYN (Butelman *et al*, 2012), and their specific involvement in cocaine reinforcement remains unclaryfied.

Both drug and food reward has in common the involvement of similar neurochemical pathways within the mesolimbic system (Lutter and Nestler, 2009). Indeed, the endogenous opioid system also has an important role in the mechanisms underlying the behavioral responses directed to obtain food (Kelley, 2004; Shippenberg *et al*, 2007). In agreement, pharmacological agonism or antagonism of MOR and DOR increased or decreased, respectively, food intake (Bodnar, 2004; Zhang *et al*, 1998).

The aim of this study is to investigate the participation of the two main opioid receptors involved in drug reinforcing effects, MOR and DOR, and enkephalins derived from PENK and PDYN that represent their main endogenous ligands, in the reinstatement of cocaine-seeking behavior by using knockout mice deficient in these four components of the endogenous opioid system and their wild-type littermates. We have also evaluated the impact of the deletion of the components of the opioid system on cue-induced reinstatement using c-Fos expression as a marker of neuronal activity in brain areas involved in addiction. The use of knockout mice is an essential tool for understanding the role of the opioid system in drug reinforcement and relapse and complement the information previously obtained on pharmacological studies (Lutz and Kieffer, 2013).

MATERIALS AND METHODS

Animals

Homozygous knockout mice deficient in MOR, DOR, PENK and PDYN on a C57BL/6J background and their respective wild-type littermates were used (Matthes *et al*, 1996; Filliol *et al*, 2000; König *et al*, 1996; Galeote *et al*, 2009). Previous studies have shown that the genetic ablation of a specific opioid receptor did not result in major changes in other opioid receptor sites (Kieffer and Gaveriaux-Ruff, 2002). Mice were housed individually in controlled laboratory conditions with the temperature maintained at 21 ± 1 °C and humidity at 55 ± 10%. Mice were tested during the first hours of the dark phase of a reversed light/dark cycle (lights off at 08:00 h and on at 20:00 h). Food and water were available *ad libitum* in mice used in the cocaine experiment. For operant behavior maintained by food, mice were food deprived (85% of the initial weight) and water was available *ad libitum*. Animal procedures were conducted in strict accordance with the guidelines of the European Communities Directive 86/609/EEC regulating animal research and were approved by the local ethical committee (CEEA-PRBB).

Cocaine Self-Administration Apparatus

Cocaine self-administration training was performed in operant chambers (Model ENV-307A-CT, Med Associates, Georgia, VT, USA) equipped with two holes, one randomly selected as the active hole and the other as the inactive (see Supplementary Information).

Surgery

Mice were anaesthetized with a ketamine/xylazine mixture (20 ml/kg of body weight) and then implanted with indwelling i.v. silastic catheters as previously described (Soria *et al*, 2005) (see Supplementary Information). The success rate for maintaining patency of the catheter (mean duration of 13 days) until the end of the cocaine self-administration training was 88%.

Drugs

Cocaine hydrochloride was obtained from Ministerio de Sanidad y Consumo (Spain) and dissolved in sterile 0.9% physiological saline. Ketamine hydrochloride (100 mg/kg) (Imalgène 1000; Rhône Mérieux, Lyon, France) and xylazine hydrochloride (20 mg/kg) (Sigma, Madrid, Spain) were mixed and dissolved in ethanol (5%) and distilled water (95%). This anesthetic mixture was administered intraperitoneally in an injection volume of 20 ml/kg of body weight. Thiopental sodium (5 mg/ml) (Braun Medical S.A, Barcelona, Spain) was dissolved in distilled water and delivered by infusion of 0.1 ml through the i.v. catheter.

Food-Maintained Operant Behavior Apparatus

Operant responding maintained by food was performed in mouse operant chambers (Model ENV-307A-CT, Med Associates, Georgia, VT, USA) equipped with two retractable levers, one randomly selected as the active lever and the other as the inactive (see Supplementary Information).

Experimental Design

A first group of mice ($n = 101$) was trained for cocaine self-administration experiments, during 2-h daily sessions

to acquire operant responding maintained by cocaine (0.5 mg/kg/infusion, i.v.) under fixed ratio 1 (FR1) (5 consecutive days) and FR3 (7 consecutive days). The criteria for acquisition of operant responding were achieved when mice maintained a stable responding with less than 20% deviation from the mean of the total number of infusions earned in three consecutive sessions, with at least 75% responding on the reinforced nose-poke, and a minimum of 10 reinforcements per session (Martin-Garcia *et al*, 2011; Soria *et al*, 2008). After the 12 FR sessions, animals were tested in a progressive ratio (PR) schedule where the response requirement to earn infusions escalated according to the following series: 1–2–3–5–12–18–27–40–60–90–135–200–300–450–675–1000. The maximum duration of the PR session was 4 h or until mice did not respond on any hole within 1 h, and was performed only once. After PR session, the thiopental test was applied and only mice that showed patency of catheter were moved to the extinction and relapse phases. The first extinction session occurred 48 h after the thiopental tests to avoid any possible influence of thiopental residual effects.

During the extinction phase, the experimental conditions were similar to the acquisition sessions except that cocaine was not available and the cue light was not presented after active responding. Mice were given 2 h daily extinction sessions, during 15 consecutive days until the criteria for extinction was achieved ie, during three consecutive sessions, mice responded on the active lever less than 30% of the responses reached in the three last acquisition days, and made less than 15 active responses per session. After extinction, mice were tested for reinstatement. Cues-induced reinstatement was conducted under the same conditions used in the acquisition phase except that cocaine was not delivered. Each response on the active manipulandum in this phase led to the presentation of the cue light for 2 s. The reinstatement criterion was achieved when responding in the nose-poke doubled with respect to extinction responding.

For food-maintained operant behavior experiments, a second group of mice ($n=63$) was trained during 1 h for 10 consecutive days to lever press for highly caloric and banana-flavored food pellets (14% protein, 60% fat, 26% carbohydrate, with a caloric value of 5.32 kcal/g) (Bio-Serv, Frenchtown, NJ, USA) paired with the presentation of a cue light on a FR1 schedule followed by 10 sessions under FR5, using the same criteria for the acquisition of operant behavior previously described. After the 20 FR sessions, animals were trained in one single PR schedule session where the response requirement to earn pellets escalated according to the following series: 1–5–12–21–33–51–75–90–120–155–180–225–260–300–350–410–465–540–630–730–850–1000–1200–1500–1800–2100–2400–2700–3000–3400–3800–4200–4600–5000–5500. The maximum duration of the PR session was 5 h or until mice did not respond on any lever within 1 h. This second group of mice was food deprived during the whole experiment at 85% of their *ad libitum* initial weight adjusted for growth.

Immunohistochemistry Studies

See Supplementary Information for tissue preparation, immunofluorescence and c-Fos quantification.

Statistical Analysis

Analysis of the data obtained during the acquisition and extinction phase was conducted using two-way ANOVA with manipulandum (active/inactive) as within-subjects factor and genotype as between-subjects factor. *Post hoc* analysis (Newman–Keuls) was performed when required. Progressive ratio, day of extinction, cues-induced reinstatement, and immunohistochemistry results were compared using one-way ANOVA.

All results are expressed as mean ± SEM. Differences were considered significant at $p<0.05$. The statistical analysis was performed using the Statistical Package for Social Science program SPSS 19.0 (SPSS, Chicago, USA).

RESULTS

Acquisition and Maintenance of Cocaine Self-Administration

MOR knockout mice ($n=11$) and wild-type littermates ($n=13$) were trained to self-administer cocaine under FR1 (5 days), and FR3 (7 days) schedule of reinforcement. Two-way ANOVA revealed significant main effects of hole during the training period indicating a continuous operant responding for cocaine and discrimination between holes. Significant effects of genotype on day 2, 3 and 4, and a significant interaction between genotype and hole were revealed on day 3 (Table 1A). Subsequent *post hoc* analysis (Newman–Keuls) showed significant differences between genotypes on day 3 ($p<0.05$) (Figure 1a). The acquisition criteria were achieved by 90% of the MOR knockout mice and 77% of wild-type littermates. No significant difference was revealed between the breaking point achieved by MOR knockout and wild-type littermates in the PR session [$F_{(1,22)}=0.652$; NS] (Figure 1e).

For DOR knockout ($n=14$) and wild-type littermates ($n=10$), two-way ANOVA revealed significant main effects of hole during the training period, indicating a continuous operant responding for cocaine and discrimination between holes. No main genotype effects but significant interactions between genotype and hole on days 8, 9, 10, and 11 were revealed (Table 1A). Subsequent *post hoc* analysis (Newman–Keuls) showed significant differences between genotypes on day 8 ($p<0.01$), 9 ($p<0.05$) and 11 ($p<0.05$) (Figure 1b). The acquisition criteria were achieved by 93% of the DOR knockout mice and 100% of wild-type littermates. One-way ANOVA showed a significant decrease of the breaking point achieved by DOR knockout mice when compared with wild-type littermates [$F_{(1,23)}=5.673$; $p<0.05$] (Figure 1f).

For PENK knockout ($n=14$) and wild-type littermates ($n=14$), two-way ANOVA revealed a significant effect of hole during the whole training period, indicating a continuous operant responding for cocaine and discrimination between holes. Significant effects of genotype on day 1, 2, 11, and 12, and a significant interaction between genotype and hole on day 4, 11 and 12 were revealed (Table 1A). Subsequent *post hoc* analysis (Newman–Keuls) showed significant differences between genotypes on day 4 ($p<0.05$), 11 ($p<0.05$) and 12 ($p<0.05$) (Figure 1c). The acquisition criteria were achieved by 76% of the PENK

Table 1A *Two-Way* ANOVA of the Operant Responses During the Acquisition Phase

	Dependent variables	Two-way ANOVA															
		Cocaine self-administration								Food-maintained operant behaviour							
		MOR		DOR		PENK		PDYN		MOR		DOR		PENK		PDYN	
		F(1.44)	Sig.	F(1.46)	Sig.	F(1.52)	Sig.	F(1.46)	Sig.	F(1.28)	Sig.	F(1.28)	Sig.	F(1.28)	Sig.	F(1.26)	Sig.
Genotype	Day 1	1.55	NS	1.92	NS	5.97	p<.05	2.30	NS	2.57	NS	.07	NS	.00	NS	.19	NS
	Day 2	5.17	p<.05	.05	NS	4.17	p<.05	1.56	NS	.06	NS	.12	NS	.93	NS	.35	NS
	Day 3	5.7	p<.05	.00	NS	1.93	NS	.00	NS	1.32	NS	.96	NS	1.23	NS	.19	NS
	Day 4	5.5	p<.05	.2	NS	3.95	NS	.18	NS	.01	NS	.27	NS	.17	NS	.01	NS
	Day 5	3.5	NS	.1	NS	1.88	NS	.20	NS	.86	NS	.81	NS	.00	NS	.05	NS
	Day 6	.72	NS	.93	NS	.5	NS	.17	NS	.15	NS	.18	NS	.00	NS	.2	NS
	Day 7	.32	NS	.79	NS	.53	NS	.37	NS	.86	NS	.01	NS	.0	NS	4.82	NS
	Day 8	.29	NS	2.91	NS	1.10	NS	.0	NS	.16	NS	.18	NS	.04	NS	.01	NS
	Day 9	.31	NS	1.94	NS	2.96	NS	.00	NS	1.00	NS	2.53	NS	.10	NS	9.7	p<.01
	Day 10	.05	NS	.45	NS	3.00	NS	.0	NS	.98	NS	.72	NS	.16	NS	5.88	p<.05
	Day 11	.3	NS	1.57	NS	4.23	p<.05	.0	NS	.00	NS	2.29	NS	.27	NS	2.29	NS
	Day 12	.01	NS	.05	NS	5.28	p<.05	.07	NS	0.00	NS	3.91	NS	.19	NS	.25	NS
	Day 13									1.16	NS	2.28	NS	.4	NS	.22	NS
	Day 14									.35	NS	.28	NS	.34	NS	.64	NS
	Day 15									.60	NS	.24	NS	.0	NS	.84	NS
	Day 16									.02	NS	.59	NS	.05	NS	.37	NS
	Day 17									.33	NS	.31	NS	.6	NS	.12	NS
	Day 18									.23	NS	.52	NS	.80	NS	.64	NS
	Day 19									.53	NS	.72	NS	.29	NS	.7	NS
	Day 20									.01	NS	.58	NS	1.2	NS	.08	NS
Hole / lever	Day 1	1.66	NS	7.21	p<.05	7.94	p<.01	.37	NS	8.7	p<.01	11.95	p<.0	2.5	NS	.13	NS
	Day 2	0.51	p<.01	10.59	p<.01	7.38	p<.01	4.91	p<.05	13.45	p<.00	38.28	p<.001	8.82	p<.01	7.10	p<.05
	Day 3	2.36	p<.01	2.21	NS	5.46	p<.05	9.19	p<.01	41.68	p<.00	54.36	p<.001	41.59	p<.001	31.30	p<.001
	Day 4	9.71	p<.001	10.55	p<.01	19.50	p<.001	16.87	p<.001	49.77	p<.00	55.55	p<.001	43.95	p<.001	49.40	p<.001
	Day 5	25.82	p<.001	8.36	p<.01	11.15	p<.01	13.73	p<.01	107.46	p<.00	104.11	p<.001	41.31	p<.001	63.60	p<.001
	Day 6	9.19	p<.001	4.93	p<.001	29.72	p<.001	17.75	p<.001	35.79	p<.00	2.6.37	p<.001	41.08	p<.001	106.30	p<.001
	Day 7	21.32	p<.001	34.00	p<.001	36.61	p<.001	25.08	p<.001	83.16	p<.00	359.66	p<.001	70.01	p<.001	146.85	p<.001
	Day 8	27.24	p<.001	73.53	p<.001	45.4	p<.001	24.51	p<.001	48.17	p<.00	157.71	p<.001	39.97	p<.001	106.70	p<.001
	Day 9	39.77	p<.001	107.6	p<.001	64.22	p<.001	28.69	p<.001	65.6	p<.00	170.91	p<.001	77.28	p<.001	227.70	p<.001
	Day 10	41.03	p<.001	37.13	p<.001	75.22	p<.001	34.35	p<.001	64.0	p<.00	301.18	p<.001	36.81	p<.001	3.0.00	p<.001
	Day 11	67.00	p<.001	49.36	p<.001	170.44	p<.001	35.94	p<.001	54.55	p<.00	175.64	p<.001	48.78	p<.001	174.50	p<.001
	Day 12	74.35	p<.001	37.87	p<.001	108.45	p<.001	32.39	p<.001	45.35	p<.00	135.39	p<.001	64.97	p<.001	247.10	p<.001
	Day 13									83.27	p<.00	249.98	p<.001	44.83	p<.001	170.00	p<.001

Table 1A (Continued)

	Dependent variables	Two-way ANOVA																	
		Cocaine self-administration								Food-maintained operant behaviour									
		MOR		DOR		PENK		PDYN		MOR		DOR		PENK		PDYN			
		F(1.44)	Sig.	F(1.46)	Sig.	F(1.52)	Sig.	F(1.46)	Sig.	F(1.28)	Sig.	F(1.28)	Sig.	F(1.28)	Sig.	F(1.26)	Sig.		
	Day 4									97.59	$p<.001$	325.17	$p<.001$	63.06	$p<.001$	127.20	$p<.001$		
	Day 5									79.42	$p<.001$	182.57	$p<.001$	53.33	$p<.001$	81.20	$p<.001$		
	Day 6									83.50	$p<.001$	146.48	$p<.001$	40.37	$p<.001$	107.60	$p<.001$		
	Day 7									99.72	$p<.001$	134.11	$p<.001$	45.75	$p<.001$	120.30	$p<.001$		
	Day 8									108.65	$p<.001$	137.28	$p<.001$	52.95	$p<.001$	86.20	$p<.001$		
	Day 9									104.72	$p<.001$	209.91	$p<.001$	58.54	$p<.001$	78.80	$p<.001$		
	Day 20									135.97	$p<.001$	249.66	$p<.001$	55.56	$p<.001$	171.20	$p<.001$		
Genotype * Hole / lever	Day 1	.23	NS	.03	NS	2.64	NS	.19	NS	3.13	NS	.01	NS	.58	NS	.22	NS		
	Day 2	3.6	NS	1.05	NS	1.02	NS	.14	NS	.10	NS	.12	NS	1.37	NS	.10	NS		
	Day 3	5.39	$p<.05$	.50	NS	2.49	NS	.54	NS	1.11	NS	.14	NS	.90	NS	.41	NS		
	Day 4	1.67	NS	.25	NS	4.63	$p<.05$	.89	NS	.22	NS	.9	NS	2.11	NS	6.76	$p<.05$		
	Day 5	.41	NS	.54	NS	2.38	NS	.28	NS	.31	NS	.10	NS	3.86	NS	5.22	$p<.05$		
	Day 6	.71	NS	3.24	NS	.71	NS	.93	NS	.27	NS	.27	NS	.01	NS	1.18	NS		
	Day 7	.43	NS	3.5	NS	.63	NS	.26	NS	.00	NS	.47	NS	.07	NS	.27	NS		
	Day 8	.00	NS	11.38	$p<.01$	1.51	NS	.00	NS	.27	NS	2.32	NS	1.86	NS	.08	NS		
	Day 9	.52	NS	8.84	$p<.01$	3.52	NS	.06	NS	1.00	NS	3.23	NS	1.16	NS	.00	NS		
	Day 10	.06	NS	4.94	$p<.05$	2.32	NS	.06	NS	5.95	$p<.05$	.53	NS	.07	NS	2.46	NS		
	Day 11	.02	NS	6.96	$p<.05$	5.49	$p<.05$	.14	NS	.22	NS	.86	NS	.58	NS	3.01	NS		
	Day 12	.18	NS	2.86	NS	5.56	$p<.05$	.39	NS	.19	NS	.71	NS	.11	NS	.13	NS		
	Day 13									2.53	NS	1.2	NS	.58	NS	2.22	NS		
	Day 14									1.08	NS	.83	NS	.10	NS	.00	NS		
	Day 15									.18	NS	.24	NS	.00	NS	.11	NS		
	Day 16									.00	NS	.28	NS	.03	NS	2.12	NS		
	Day 17									.03	NS	.14	NS	.21	NS	.32	NS		
	Day 18									.00	NS	.15	NS	.48	NS	.62	NS		
	Day 19									.43	NS	.49	NS	.20	NS	.14	NS		
	Day 20									.00	NS	.16	NS	.88	NS	.55	NS		

Table 1B Two-Way ANOVA of the Operant Responses During the Extinction Phase

	Dependent variables	Two-way ANOVA							
		Extinction							
		MOR		DOR		PENK		PDYN	
		F(1.38)	Sig.	F(1.32)	Sig.	F(1.40)	Sig.	F(1.36)	Sig.
Genotype	Day 1	.47	NS	.01	NS	.49	NS	6.54	$p<0.05$
	Day 2	.04	NS	.00	NS	.01	NS	8.11	$p<0.05$
	Day 3	.01	NS	.54	NS	.06	NS	3.94	NS
	Day 4	.52	NS	.73	NS	.13	NS	8.49	$p<0.01$
	Day 5	.01	NS	.30	NS	6.47	$p<0.05$	1.73	NS
	Day 6	3.33	NS	.47	NS	.01	NS	11.97	$p<0.01$
	Day 7	5.79	$p<0.05$	.08	NS	.92	NS	3.17	NS
	Day 8	3.43	NS	.04	NS	.11	NS	.95	NS
	Day 9	2.57	NS	.21	NS	.79	NS	3.31	NS
	Day 10	5.85	$p<0.05$	2.13	NS	.98	NS	5.73	$p<0.05$
	Day 11	3.96	NS	.08	NS	2.08	NS	12.11	$p<0.01$
	Day 12	.33	NS	1.75	NS	.66	NS	6.86	$p<0.05$
	Day 13	1.76	NS	3.11	NS	.18	NS	2.94	NS
	Day 14	1.76	NS	.71	NS	.00	NS	.14	NS
	Day 15	4.21	$p<0.05$	1.39	NS	.14	NS	1.10	NS
Hole	Day 1	37.84	$p<0.001$	33.34	$p<0.001$	154.23	$p<0.001$	59.82	$p<0.001$
	Day 2	26.69	$p<0.001$	14.23	$p<0.01$	112.36	$p<0.001$	32.37	$p<0.001$
	Day 3	24.65	$p<0.001$	7.61	$p<0.01$	95.73	$p<0.001$	27.62	$p<0.001$
	Day 4	34.55	$p<0.001$	4.52	$p<0.05$	84.69	$p<0.001$	21.87	$p<0.001$
	Day 5	34.27	$p<0.001$	26.34	$p<0.001$	60.60	$p<0.001$	37.38	$p<0.001$
	Day 6	16.40	$p<0.001$	17.05	$p<0.001$	53.00	$p<0.001$	54.52	$p<0.001$
	Day 7	20.08	$p<0.001$	6.12	$p<0.05$	48.03	$p<0.001$	54.62	$p<0.001$
	Day 8	11.35	$p<0.01$	14.22	$p<0.01$	35.49	$p<0.001$	22.76	$p<0.001$
	Day 9	10.78	$p<0.01$	11.49	$p<0.01$	46.10	$p<0.001$	30.39	$p<0.001$
	Day 10	21.1	$p<0.001$	13.99	$p<0.01$	50.17	$p<0.001$	27.27	$p<0.001$
	Day 11	16.4	$p<0.001$	10.84	$p<0.01$	28.30	$p<0.001$	32.26	$p<0.001$
	Day 12	29.16	$p<0.001$	8.94	$p<0.01$	15.66	$p<0.001$	26.02	$p<0.001$
	Day 13	10.95	$p<0.01$	4.06	NS	33.83	$p<0.001$	35.23	$p<0.001$
	Day 14	6.94	$p<0.05$	7.34	$p<0.05$	31.23	$p<0.001$	12.70	$p<0.01$
	Day 15	8.65	$p<0.01$	3.26	NS	25.51	$p<0.001$	24.46	$p<0.001$
Genotype*	Day 1	.78	NS	2.46	NS	1.93	NS	5.61	$p<0.05$
Hole	Day 2	.65	NS	1.79	NS	1.90	NS	7.80	$p<0.01$
	Day 3	.66	NS	.09	NS	1.84	NS	8.84	$p<0.01$
	Day 4	.92	NS	2.05	NS	2.95	NS	5.24	$p<0.05$
	Day 5	.2	NS	7.76	$p<0.01$	.09	NS	2.69	NS
	Day 6	.23	NS	4.05	NS	.51	NS	8.66	$p<0.01$
	Day 7	.14	NS	2.14	NS	.01	NS	8.52	$p<0.01$
	Day 8	.00	NS	3.81	NS	.67	NS	5.86	$p<0.05$
	Day 9	.45	NS	2.68	NS	.04	NS	4.09	NS
	Day 10	.51	NS	4.94	$p<0.05$	.07	NS	5.29	$p<0.05$
	Day 11	.03	NS	4.1	NS	.85	NS	4.66	$p<0.05$
	Day 12	.05	NS	.14	NS	2.02	NS	7.61	$p<0.01$
	Day 13	.49	NS	.05	NS	1.23	NS	2.48	NS
	Day 14	.00	NS	2.18	NS	1.16	NS	.46	NS
	Day 15	.12	NS	.21	NS	.94	NS	.81	NS

knockout mice and 100% of wild-type littermates. One-way ANOVA showed a significant decrease of the breaking point achieved by PENK knockout mice when compared with wild-type littermates [$F_{(1,26)} = 7.123$; $p < 0.05$] (Figure 1g).

For PDYN knockout ($n = 14$) and wild-type littermates ($n = 11$), two-way ANOVA revealed significant main effects of hole during the whole training period, indicating a continuous operant responding for cocaine and discrimination between holes. Two-way ANOVA did not reveal main effects of genotype nor interaction between genotype and hole through the entire acquisition phase (Table 1A; Figure 1d). All PDYN KO mice and wild-type littermates achieved the acquisition criteria in the last experimental sequence. One-way ANOVA showed no significant differences in the breaking point achieved by PDYN knockout mice and wild-type littermates [$F_{(1,23)} = 0.213$; NS] (Figure 1h).

Extinction and Cues-Induced Reinstatement of Cocaine-Seeking Behavior

The extinction criteria were achieved by all mice. Two-way ANOVA revealed significant main effects in hole during the whole extinction phase in the four experiments (Table 1B).

In MOR experiment, two-way ANOVA showed significant effects of genotypes on day 7, 10, and 15 without interaction between genotype and hole (Table 1B; Figure 2a). One-way ANOVA did not reveal significant differences in the time required to achieve the extinction criteria [$F_{(1,19)} = 0.012$; NS] (Figure 2e). After 15 daily sessions of extinction, one-way ANOVA demonstrated a significant decrease in cues-induced reinstatement of cocaine-seeking behavior in MOR knockout mice compared with wild-type littermates [$F_{(1,19)} = 5.255$; $p < 0.05$] (Figure 2i).

In DOR experiment, no significant main effects of genotype were obtained (two-way ANOVA), although a significant interaction between genotype and hole was revealed on day 5 and 10 (Table 1B). Subsequent *post hoc* analysis (Newman–Keuls) showed significant differences between genotypes on day 5 ($p < 0.05$) and 10 ($p < 0.001$) (Figure 2b). One-way ANOVA did not reveal significant differences in the time required to achieve the extinction criteria [$F_{(1,21)} = 1.492$; NS] (Figure 2f). After extinction, one-way ANOVA showed a significant decrease in cues-induced reinstatement in cocaine-seeking behavior in knockout mice compared with wild-type littermates [$F_{(1,21)} = 17.581$; $p < 0.001$] (Figure 2j).

In PENK experiment, two-way ANOVA revealed significant main effects of genotype on day 5 without significant interaction between genotype and hole (Table 1B; Figure 2c). One-way ANOVA did not show significant differences in the time required to achieve extinction [$F_{(1,23)} = 0.172$; NS] (Figure 2g) nor in cues-induced reinstatement [$F_{(1,23)} = 0.55$; NS] (Figure 2k).

In PDYN experiment, two-way ANOVA revealed significant main effects of genotype on day 1, 2, 4, 6, 10, 11, and 12, as well as a significant interaction between genotype and hole on day 1, 2, 3, 4, 6, 7, 8, 10, 11, and 12 (Table 1B). *Post hoc* analysis (Newman–Keuls) showed significant differences between genotypes on day 1 ($p < 0.01$), 2 ($p < 0.001$), 3 ($p < 0.01$), 4 ($p < 0.001$), 6 ($p < 0.01$), 7 ($p < 0.01$), 8 ($p < 0.05$), 10 ($p < 0.01$) and 12 ($p < 0.001$) (Figure 2d). One-way ANOVA revealed a significant increase in the time required to achieve extinction [$F_{(1,18)} = 10.618$; $p < 0.01$] (Figure 2h) and cues-induced reinstatement of cocaine-seeking behavior in PDYN knockout mice compared with wild-type littermates [$F_{(1,18)} = 12.892$; $p < 0.01$] (Figure 2l).

C-Fos Expression

Fos protein levels were evaluated in brain areas involved in drug operant reinstatement (striatum, nucleus accumbens core, amygdala, prelimbic cortex, and CA1, CA2, CA3 regions of the hippocampus) in different knockout mice and wild-type littermates after the cues-induced reinstatement session. One-way ANOVA showed significant decreases in c-Fos levels in MOR knockout mice compared with wild-type littermates in CA1 [$F_{(1,11)} = 9.48$; $p < 0.05$], CA2 [$F_{(1,11)} = 7.60$; $p < 0.05$] and CA3 [$F_{(1,11)} = 5.42$; $p < 0.05$] regions of the hippocampus. No significant differences were observed in other brain areas (Figures 3a and 4).

One-way ANOVA showed a significant decrease in c-Fos levels in DOR knockout mice compared with wild-type littermates in the striatum [$F_{(1,11)} = 6.04$; $p < 0.05$] and CA1 region of the hippocampus [$F_{(1,11)} = 57.24$; $p < 0.001$]. No significant differences were revealed in other brain areas (Figures 3b and 4). Significant decreases in c-Fos levels in PENK knockout mice compared with wild-type littermates were shown in the striatum [$F_{(1,11)} = 13.12$; $p < 0.01$], amygdala [$F_{(1,11)} = 7.53$; $p < 0.05$], CA2 [$F_{(1,11)} = 10.45$; $p < 0.01$] and CA3 [$F_{(1,11)} = 37.46$; $p < 0.001$] region of the hippocampus, without significant differences in other brain areas (Figures 3c and 4).

One-way ANOVA showed a significant increase in c-Fos levels in PDYN knockout mice compared with wild-type littermates in the striatum [$F_{(1,16)} = 4.51$; $p < 0.05$], nucleus accumbens core [$F_{(1,16)} = 5{,}12$; $p < 0.05$] and CA2 region of the hippocampus [$F_{(1,16)} = 5{,}42$; $p < 0.05$]. No significant differences were revealed in other brain areas (Figures 3d and 4).

Acquisition and Maintenance of Operant Conditioning Maintained by Food

MOR knockout ($n = 8$) and wild-type littermates ($n = 8$) mice were trained to acquire an operant responding

Figure 1 Operant behavior to obtain cocaine in MOR, DOR, PENK, and PDYN knockout mice. Mean number of nose-pokes in the active and inactive hole during the acquisition training in fixed ratio 1 (FR1) and FR3 schedule of reinforcement to obtain cocaine (0.5 mg/kg/infusion) (a) MOR knockout mice ($n = 11$) and wild-type littermates ($n = 13$). (b) DOR knockout mice ($n = 14$) and wild-type littermates ($n = 10$). (c) PENK knockout mice ($n = 14$) and wild-type littermates ($n = 14$). (d) PDYN knockout mice ($n = 14$) and wild-type littermates ($n = 11$). (e) Breaking point achieved in the progressive ratio session in MOR knockout mice and wild-type littermates. (f) Breaking point in DOR knockout mice and wild-type littermates. (g) Breaking point in PENK knockout mice and wild-type littermates. (h) Breaking point in PDYN knockout mice and wild-type littermates. Data are expressed as mean ± SEM. $^{*}p < 0.05$, $^{**}p < 0.01$ *vs* knockout group (Newman–Keuls test (acquisition) or one-way ANOVA (progressive ratio)).

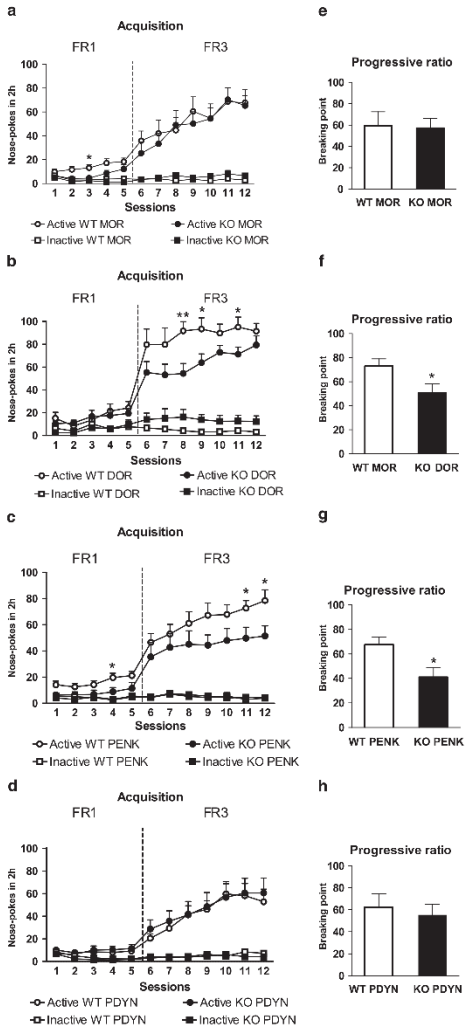
a
Acquisition
FR1
FR3
Nose-pokes in 2h
Sessions
Active WT MOR
Active KO MOR
Inactive WT MOR
Inactive KO MOR
e
Progressive ratio
Breaking point
WT MOR
KO MOR
b
Acquisition
FR1
FR3
Nose-pokes in 2h
Sessions
Active WT DOR
Active KO DOR
Inactive WT DOR
Inactive KO DOR
f
Progressive ratio
Breaking point
WT MOR
KO DOR
c
Acquisition
FR1
FR3
Nose-pokes in 2h
Sessions
Active WT PENK
Active KO PENK
Inactive WT PENK
Inactive KO PENK
g
Progressive ratio
Breaking point
WT PENK
KO PENK
d
Acquisition
FR1
FR3
Nose-pokes in 2h
Sessions
Active WT PDYN
Active KO PDYN
Inactive WT PDYN
Inactive KO PDYN
h
Progressive ratio
Breaking point
WT PDYN
KO PDYN

maintained by high palatable food pellets under FR1 (10 days), and FR5 (10 days) schedule. Two-way ANOVA revealed significant main effects of lever during the whole training period indicating a continuous operant responding for food pellets and discrimination between levers. No significant effects of genotype were revealed (Tables 1A and B). The mean number of active lever presses during the 3 days when the acquisition criteria were achieved was 216.17 ± 11.96 in MOR knockout group and 226.83 ± 21.08 in wild-type littermates (number of inactive lever presses 13.67 ± 3.63 and 16.25 ± 4.43, respectively). The breaking point achieved by MOR knockout mice in the PR session was 248.13 ± 33.57 and 213.13 ± 20.72 in wild-type littermates [$F_{(1,14)} = 0.787$; NS] (data not shown).

In DOR knockout ($n = 8$) and wild-type littermates ($n = 8$), two-way ANOVA revealed significant main effects of lever during the whole training period, indicating a continuous operant responding for food pellets and discrimination between levers. No significant effects of genotype were revealed (Table 1A). The mean number of active lever presses during the 3 days when the acquisition criteria were achieved was 333.5 ± 33.21 in DOR knockout group and 364.13 ± 42.73 in wild-type littermates (number of inactive lever presses 12.42 ± 3.25 and 19.75 ± 6.17, respectively). The breaking point achieved by DOR knockout mice in the PR session was 305 ± 21.46 and 426.88 ± 63.21 in wild-type littermates [$F_{(1,14)} = 3.333$; NS] (data not shown).

In PENK knockout mice ($n = 8$) and wild-type littermates ($n = 8$), two-way ANOVA revealed significant main effects of lever during the whole training period indicating a continuous operant responding for food pellets and discrimination between levers. No significant effects of genotype were revealed (Table 1A). The mean number of active lever presses during the 3 days when the acquisition criteria were achieved was 249.88 ± 43.62 in PENK knockout group and 304.25 ± 39.87 in wild-type littermates (number of inactive lever presses 19.25 ± 5.32 and 24.25 ± 3.97, respectively). The breaking point achieved by PENK knockout mice in the PR session was 237.5 ± 33.74 and 275 ± 37.86 in wild-type littermates [$F_{(1,14)} = 0.547$; NS] (data not shown).

In PDYN knockout mice ($n = 5$) and wild-type littermates ($n = 10$), two-way ANOVA revealed significant main effects of lever during the whole training period indicating a continuous operant responding for food pellets and discrimination between levers. Significant effects of genotype were revealed only on day 9 and 10 (Tables 1A and B). The mean number of active lever presses during the 3 days when the acquisition criteria were achieved was 324.87 ± 37.38 in PDYN knockout group and 334.6 ± 23.63 in wild-type littermates (number of inactive lever presses 16.2 ± 7.22 and 36.63 ± 7.9, respectively). The breaking point achieved by PDYN knockout mice in the PR session was 248 ± 27.14 and 251.5 ± 23.66 in wild-type littermates [$F_{(1,13)} = 0.008$; NS] (data not shown).

DISCUSSION

The present study shows the specific involvement of four components of the endogenous opioid system in the acquisition and relapse of cocaine self-administration in mice. We have used a reliable operant model of reinstatement validated in our laboratory (Martin-Garcia *et al*, 2011; Soria *et al*, 2008) to demonstrate that the constitutive deletion of MOR, DOR, PENK, and PDYN differentially modifies the acquisition and reinstatement of cocaine-seeking behavior, but has no significant consequences in a similar operant training for palatable food. Indeed, a similar performance in operant responding maintained by food was obtained in all knockout mice and wild-type littermates under our experimental conditions, which ruled out a potential learning impairment for operant training in these four lines of knockout mice. This experimental control was mandatory considering that MOR knockout mice displayed learning impairment in the radial-maze task (Jamot *et al*, 2003) and DOR knockout mice showed impaired place conditioning (Le Merrer *et al*, 2011). These spatial memory impairments have no consequences in the performance of an operant training to obtain a rewarding stimulus, such as palatable food.

Previous studies have reported that selective MOR antagonists attenuate cocaine-conditioned place preference (Schroeder *et al*, 2007) and self-administration in rats (Ward *et al*, 2003), while the deletion of MOR in knockout mice reduced oral ethanol self-administration and intravenous cocaine self-administration (Becker *et al*, 2002; Mathon *et al*, 2005). In our experimental conditions, no major differences in the acquisition of cocaine self-administration were revealed in MOR knockout mice, as only a single significant reduction of active nose-poking was observed on day 3, and no differences in cocaine motivation was shown in the PR. This discrepancy could be due to differences in experimental protocol used in terms of cocaine dose, and time of conditioning sessions, as the previous study only found significant differences at high cocaine doses in shorter session times. Our results reveal

Figure 2 Operant behavior in extinction phase, the day of extinction and cues-induced reinstatement of cocaine-seeking behavior in MOR, DOR, PENK, and PDYN knockout mice. Mean number of nose-pokes in the active and inactive hole during the extinction training. (a) MOR knockout mice ($n = 10$) and wild-type littermates ($n = 11$). (b) DOR knockout mice ($n = 13$) and wild-type littermates ($n = 9$). (c) PENK knockout mice ($n = 11$) and wild-type littermates ($n = 14$). (d) PDYN knockout mice ($n = 9$) and wild-type littermates ($n = 11$). (e) Time in days necessary to accomplish extinction criteria in MOR KO mice ($n = 10$) and wild type littermates ($n = 11$). (f) DOR KO mice ($n = 13$) and wild type littermates ($n = 9$). (g) PENK KO mice ($n = 11$) and wild-type littermates ($n = 14$). (h) PDYN KO ($n = 9$) mice and wild-type littermates ($n = 11$). (i) Cues-induced reinstatement of cocaine-seeking behavior shown as normalized nose pokes in the active hole in MOR KO mice ($n = 10$) and wild-type littermates ($n = 11$). (j) DOR KO mice ($n = 13$) and wild-type littermates ($n = 9$). (k) PENK KO mice ($n = 11$) and wild-type littermates ($n = 14$). (l) PDYN KO mice ($n = 9$) and wild-type littermates ($n = 11$). Data are expressed as mean ± SI M. *$p < 0.05$, **$p < 0.01$, ***$p < 0.001$ *vs* KO group; (Newman–Keuls test (extinction) or one-way ANOVA (day of extinction and cues-induced reinstatement)).

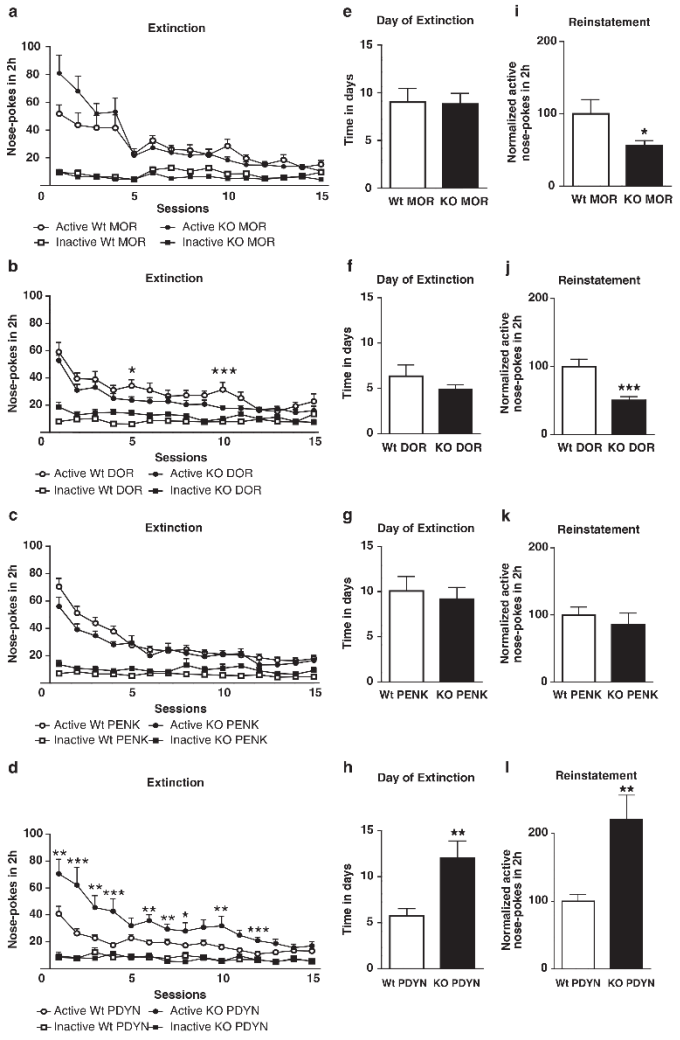
a
Extinction
Nose-pokes in 2h
Sessions
Active Wt MOR
Active KO MOR
Inactive Wt MOR
Inactive KO MOR
e
Day of Extinction
Time in days
Wt MOR KO MOR
i
Reinstatement
Normalized active nose-pokes in 2h
Wt MOR KO MOR
b
Extinction
Nose-pokes in 2h
Sessions
Active Wt DOR
Active KO DOR
Inactive Wt DOR
Inactive KO DOR
f
Day of Extinction
Time in days
Wt DOR KO DOR
j
Reinstatement
Normalized active nose-pokes in 2h
Wt DOR KO DOR
c
Extinction
Nose-pokes in 2h
Sessions
Active Wt PENK
Active KO PENK
Inactive Wt PENK
Inactive KO PENK
g
Day of Extinction
Time in days
Wt PENK KO PENK
k
Reinstatement
Normalized active nose-pokes in 2h
Wt PENK KO PENK
d
Extinction
Nose-pokes in 2h
Sessions
Active Wt PDYN
Active KO PDYN
Inactive Wt PDYN
Inactive KO PDYN
h
Day of Extinction
Time in days
Wt PDYN KO PDYN
l
Reinstatement
Normalized active nose-pokes in 2h
Wt PDYN KO PDYN

that MOR is involved in cocaine relapse, as reinstatement of cocaine-seeking behavior was attenuated in MOR knockout mice. In agreement, pharmacological studies have shown that MOR antagonists reduced cocaine relapse in rats (Tang *et al*, 2005). Furthermore, the non-selective opioid antagonist naltrexone reduced cue-induced cocaine-seeking behavior (Burattini *et al*, 2008), and had no effects on cocaine priming-induced reinstatement in rats (Comer *et al*, 1993), although repeated naltrexone treatment suppressed this priming-induced reinstatement (Gerrits *et al*, 2005). Accordingly, microinjection of selective MOR agonists into the nucleus accumbens reinstated cocaine-seeking behavior in rats (Simmons and Self, 2009). Interestingly, the number of positive c-Fos-immunostained cells was lower in MOR knockout mice after cue-induced cocaine reinstatement than in wild-type mice in CA1, CA2 and CA3 regions of the hippocampus. This result reflects a decreased neuronal activation in this brain structure closely involved in memory processing after the exposure to the cocaine-associated cues when the activity of MOR is absent. These behavioral and neurochemical results suggest that MOR is involved in cocaine reinstatement by modifying the neuronal activity in brain areas involved in memory.

Cocaine self-administration was significantly attenuated in DOR knockout mice when trained in FR3, but not in FR1, suggesting that the response is impaired only when the effort required to obtain the reward is enhanced. Other studies showed that DOR knockout mice acquired morphine self-administration similarly to wild-type mice (Le Merrer *et al*, 2011), although these mutants showed a decreased operant responding when trained to obtain high doses of intravenous nicotine (Berrendero *et al*, 2012). In agreement, with our acquisition data, the breaking point achieved by DOR knockout mice was significantly lower than wild-type littermates during the PR session. In contrast, DOR knockout were reported to achieve a similar breaking point for morphine than wild-type mice under a PR schedule (Le Merrer *et al*, 2011). The reinstatement of cocaine-seeking behavior was also significantly reduced in DOR knockout mice. In agreement, pharmacological studies have suggested the participation of DOR in particular brain areas in cocaine-reinforcing effects (Le Merrer *et al*, 2009), and microinjection of selective DOR agonists in the nucleus accumbens reinstated cocaine-seeking behavior in rats (Simmons and Self, 2009). Furthermore, the enhancement of positive c-Fos-immunostained cells induced by cocaine reinstatement was attenuated in DOR knockout mice in the striatum, and the CA1 region of the hippocampus. These results revealed a decreased neuronal activation in these brain structures involved in motor and motivation control, and memory processing after the exposure to cocaine-associated cues in the absence of DOR activity. Our findings suggest that DOR modulates the motivation to obtain cocaine and cocaine reinstatement by modifying neuronal activity in brain areas involved in motor, motivation, and memory processing.

Cocaine self-administration was attenuated in PENK knockout mice, mainly when animals were trained in FR3. In agreement, the breaking point achieved by PENK knockout mice was also reduced during the PR session suggesting that opioid peptides derived from PENK have an important role in cocaine-reinforcing properties. PENK has been postulated to mediate the reinforcing effects of other drugs of abuse (Berrendero *et al*, 2005; Marinelli *et al*, 2005; Shoblock and Maidment, 2007), and changes in PENK gene expression have been revealed after long-term cocaine self-administration (Crespo *et al*, 2001). In contrast, cue-induced reinstatement of cocaine-seeking behavior was not modified in PENK knockout mice, which suggests that other opioid peptides different from those derived from PENK must be involved in the reinstatement of cocaine-seeking behavior. However, the number of positive c-Fos-immunostained cells was decreased in PENK knockout in the striatum, amygdala, CA2, and CA3 regions of the hippocampus after cue-induced reinstatement. Therefore, the absence of PENK decreases neuron activation in several brain structures during cue-induced reinstatement session, although these changes were not associated with a significant modification of cues-induced reinstatement of cocaine-seeking behavior.

The acquisition of cocaine self-administration and the motivation to obtain cocaine in the PR schedule were not modified in PDYN knockout mice. However, PDYN knockouts showed slower extinction and increased cues-induced reinstatement of cocaine-seeking behavior when compared with wild-type littermates, the opposite result to that obtained in MOR and DOR knockout mice on cocaine reinstatement. Opioids derived from PDYN include the MOR and DOR agonist leu-enkephalin as well as other opioid peptides with preferential KOR agonist properties, such as dynorphins (Kieffer and Gaveriaux-Ruff 2002). Considering the opposite role on the control of the rewarding pathways of KOR with regards to MOR and DOR (Trigo *et al*, 2010), and the opposite responses on cocaine reinstatement of our lines of knockout mice, we can postulate that the enhanced reinstatement of cocaine seeking revealed in PDYN knockout mice would be related to opioid peptides acting on KOR, such as dynorphins. In agreement, the DYN/KOR system appears to participate in the aversive effects related to cocaine exposure. Thus, KOR reduces the effects of stress on the reinstatement of cocaine-seeking behavior in mice (McLaughlin *et al*, 2006) and rats (Beardsley *et al*, 2005). Furthermore, repeated cocaine administration increases levels of dynorphins and prePDYN mRNA in animals and humans (Trifilieff and Martinez, 2013). In support of our hypothesis, c-fos mapping reveals an opposite result to other lines of opioid knockout in PDYN knockouts after cocaine reinstatement. Indeed, the number of positive c-Fos-immunostained cells induced by cocaine reinstatement was enhanced in PDYN knockout mice in the striatum, the core of nucleus accumbens and CA2 region of the hippocampus, revealing an increased neuronal activation in these brain structures related to motor, motivation, and memory processing. The findings suggest that PDYN modulates cocaine reinstatement by modifying neuronal activity in these brain areas.

Our behavioral and neurochemical results suggest that DOR and PENK are involved in the motivation to obtain cocaine, and the absence of these opioid components reduces cocaine self-administration mainly when the effort to obtain the reward is increased. Moreover, cocaine reinstatement is reduced in MOR and DOR knockout mice, whereas it is not modified in the absence of PENK and

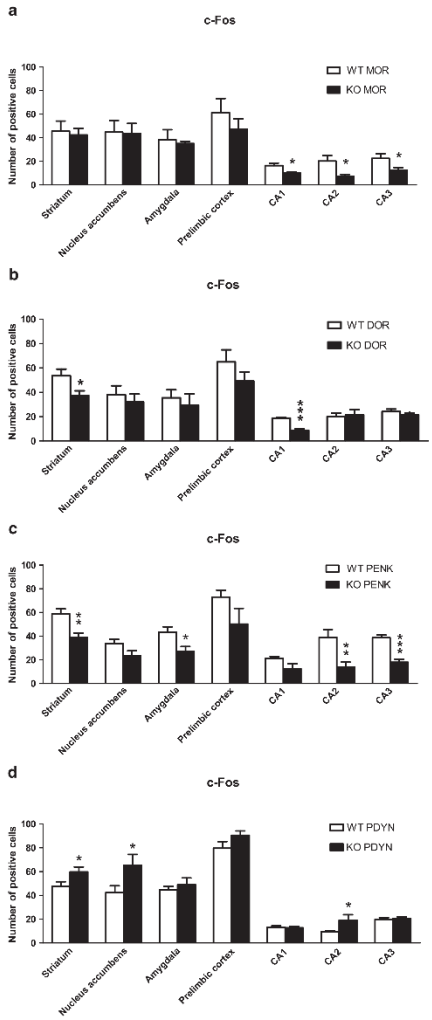

Figure 3 Levels of c-Fos expression in different brain areas after cues-induced reinstatement of cocaine-seeking behavior in MOR, DOR, PENK, and PDYN knockout mice. Number of positive immunostained cells in the striatum, nucleus accumbens core, amygdala, prelimbic cortex, CA1 of the hippocampus, CA2 of the hippocampus, and CA3 of the hippocampus. (a) MOR knockout mice ($n=7$) and wild-type littermates ($n=6$). (b) DOR knockout mice ($n=7$) and wild-type littermates ($n=6$). (c) PENK knockout mice ($n=7$) and wild-type littermates ($n=6$). (d) PDYN knockout mice ($n=8$) and wild-type littermates ($n=10$). Data are expressed as mean ± SEM. $^{*}p<0.05$, $^{**}p<0.01$, $^{***}p<0.001$ *vs* wild-type (one-way ANOVA).

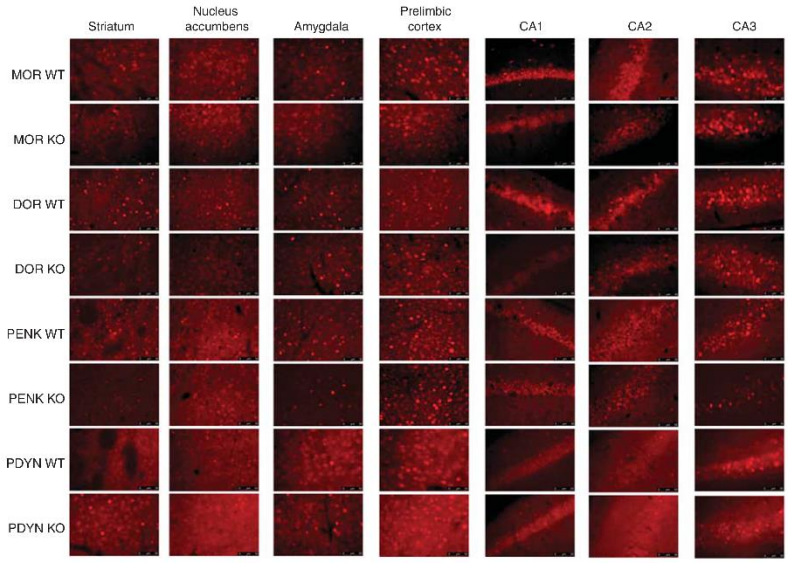

Figure 4 Representative images of c-Fos immunoreactivity in different brain areas after cues-induced reinstatement of cocaine-seeking behavior in MOR, DOR, PENK, and PDYN knockout mice. Striatum, nucleus accumbens core, amygdala, prelimbic cortex, CA1 of the hippocampus, CA2 of the hippocampus, and CA3 of the hippocampus.

results increased in the absence of PDYN. Therefore, the reduced cocaine reinstatement revealed in MOR and DOR was not mediated by the main endogenous ligand of these receptors, enkephalins, as the deletion of the two precursors of these endogenous opioid peptides, PENK and PDYN, did not mimic this behavioral response. In agreement, we have previously demonstrated that another MOR and DOR endogenous ligand, β-endorphin, has a crucial role in the rewarding properties of other drugs of abuse such as nicotine (Trigo *et al*, 2009).

The genetic deletion of MOR, DOR, PENK, and PDYN did not modify the acquisition and motivation to maintain operant responding to obtain palatable food in deprived mice. In agreement, opioid receptor antagonists did not significantly modify food-seeking behavior (Abdoullaye *et al*, 2010) nor preference for high-caloric food in rats (Dela Cruz *et al*, 2012). However, the enhancement of opioid activity by administration of opioid agonists increased preferentially high-caloric food intake (Taha, 2010). In addition, rats with chronic access to highly palatable food increased their mRNA expression of POMC in the medial prefrontal cortex (Blasio *et al*, 2013). Taken together, these results suggest that the absence of the basal tone of MOR, DOR, PENK, and PDYN did not modify food-seeking behavior in agreement with previous pharmacological studies, whereas opioid system activation promotes this behavior.

In conclusion, our results suggest that opioid peptides derived from PENK acting on DOR have an important role in cocaine-reinforcing properties. MOR and DOR, and endogenous opioid peptides different from enkephalins are crucial for cue-induced reinstatement of cocaine-seeking behavior by modulating neuronal activation of brain areas involved in the control of motor, motivation, and memory processes. Opioid peptides derived from PDYN have an opposite role to MOR and DOR in the control of cocaine reinstatement. The elucidation of these neurobiological mechanisms involved in cocaine-reinforcing effects and relapse opens new possibilities for developing new therapeutic strategies targeting the endogenous opioid system.

FUNDING AND DISCLOSURE

The authors declare no conflict of interest.

ACKNOWLEDGEMENTS

This work was supported by the DG Research of the European Commission (PHECOMP, no. LHSM-CT-2007-037669,

the Spanish 'Instituto de Salud Carlos III' (RTA, no. RD06/001/001), the Spanish 'Ministerio de Ciencia e Innovación' (no. SAF2007-64062, no. SAF2011-29864), the Catalan Government (SGR2009-00131), the ICREA Foundation (ICREA Academia-2008). JG-C was supported by a 'Juan de la Cierva' post-doctoral fellowship from the Spanish 'Ministerio de Ciencia e Innovación', A.B. and S.M. were supported by a FI predoctoral fellowships of the Catalan Government, and E. M-G. was supported by a 'Sara Borrell' post-doctoral fellowship from the Spanish 'Instituto de Salud Carlos III'. Partial support from FEDER funds is also acknowledged. We thank Alberto Allica Abellan for invaluable technical assistance.

Author Contributions

J. G-C., A.B., S.M., S.K., and E. M-G. conducted the behavioral studies and participated in the interpretation and manuscript writing. R.M. participated in the experimental design, interpretation and manuscript writing and funded the project.

REFERENCES

Abdoullaye D, Acevedo I, Adebayo AA, Behrmann-Godel J, Benjamin RC, Bock DG *et al* (2010). Permanent Genetic Resources added to Molecular Ecology Resources Database 1 August 2009-30 September 2009. *Mol Ecol Res* **10**: 232–236.

American Psychiatric Association (2013). *Diagnostic and Statistical Manual of Mental Disorders* (5th edition DSM-5) and proposed draft revisions (DSM-V). American Psychiatric Press: Washington, DC.

Beardsley PM, Howard JL, Shelton KL, Carroll FI (2005). Differential effects of the novel kappa opioid receptor antagonist, JDTic, on reinstatement of cocaine-seeking induced by footshock stressors vs cocaine primes and its antidepressant-like effects in rats. *Psychopharmacology* **183**: 118–126.

Becker A, Grecksch G, Kraus J, Loh HH, Schroeder H, Hollt V (2002). Rewarding effects of ethanol and cocaine in mu opioid receptor-deficient mice. *Naunyn Schmiedebergs Arch Pharmacol* **365**: 296–302.

Berrendero F, Mendizabal V, Robledo P, Galeote L, Bilkei-Gorzo A, Zimmer A *et al* (2005). Nicotine-induced antinociception, rewarding effects, and physical dependence are decreased in mice lacking the preproenkephalin gene. *J Neurosci* **25**: 1103–1112.

Berrendero F, Plaza-Zabala A, Galeote L, Flores A, Bura SA, Kieffer BL *et al* (2012). Influence of delta-opioid receptors in the behavioral effects of nicotine. *Neuropsychopharmacology* **37**: 2332–2344.

Blasio A, Steardo L, Sabino V, Cottone P (2013). Opioid system in the medial prefrontal cortex mediates binge-like eating. *Addict Biol*; doi:10.1111/adb.12033 (e-pub ahead of print).

Bodnar RJ (2004). Endogenous opioids and feeding behavior: a 30-year historical perspective. *Peptides* **25**: 697–725.

Bodnar RJ (2008). Endogenous opiates and behavior: 2007. *Peptides* **29**: 2292–2375.

Burattini C, Burbassi S, Aicardi G, Cervo L (2008). Effects of naltrexone on cocaine- and sucrose-seeking behavior in response to associated stimuli in rats. *Int J Neuropsychopharmacol* **11**: 103–109.

Butelman ER, Yuferov V, Kreek MJ (2012). Kappa-opioid receptor/dynorphin system: genetic and pharmacotherapeutic implications for addiction. *Trends Neurosci* **35**: 587–596.

Charbogne P, Kieffer BL, Befort K (2014). 15 years of genetic approaches *in vivo* for addiction research: opioid receptor and peptide gene knockout in mouse models of drug abuse. *Neuropharmacology* **76**: 204–217.

Comer SD, Lac ST, Curtis LK, Carroll ME (1993). Effects of buprenorphine and naltrexone on reinstatement of cocaine-reinforced responding in rats. *J Pharmacol Exp Ther* **267**: 1470–1477.

Crespo JA, Manzanares J, Oliva JM, Corchero J, Palomo T, Ambrosio E (2001). Extinction of cocaine self-administration produces a differential time-related regulation of proenkephalin gene expression in rat brain. *Neuropsychopharmacology* **25**: 185–194.

Dela Cruz JA, Bae VS, Icaza-Cukali D, Sampson C, Bamshad D, Samra A *et al* (2012). Critical role of NMDA but not opioid receptors in the acquisition of fat-conditioned flavor preferences in rats. *Neurobiol Learn Mem* **98**: 341–347.

Filliol D, Ghozland S, Chluba J, Martin M, Matthes HW, Simonin F *et al* (2000). Mice deficient for delta- and mu-opioid receptors exhibit opposing alterations of emotional responses. *Nat Genet* **25**: 195–200.

Galeote L, Berrendero F, Bura SA, Zimmer A, Maldonado R (2009). Prodynorphin gene disruption increases the sensitivity to nicotine self-administration in mice. *Int J Neuropsychopharmacol* **12**: 615–625.

Gerrits MA, Kuzmin AV, van Ree JM (2005). Reinstatement of cocaine-seeking behavior in rats is attenuated following repeated treatment with the opioid receptor antagonist naltrexone. *Eur Neuropsychopharmacol* **15**: 297–303.

Jamot L, Matthes HW, Simonin F, Kieffer BL, Roder JC (2003). Differential involvement of the mu and kappa opioid receptors in spatial learning. *Genes Brain Behav* **2**: 80–92.

Kelley AE (2004). Memory and addiction: shared neural circuitry and molecular mechanisms. *Neuron* **44**: 161–179.

Kieffer BL, Gaveriaux-Ruff C (2002). Exploring the opioid system by gene knockout. *Prog Neurobiol* **66**: 285–306.

König M, Zimmer AM, Steiner H, Holmes PV, Crawley JN, Brownstein MJ *et al* (1996). Pain responses, anxiety and aggression in mice deficient in pre-proenkephalin. *Nature* **383**: 535–538.

Law PY, Wong YH, Loh HH (2000). Molecular mechanisms and regulation of opioid receptor signaling. *Annu Rev Pharmacol Toxicol* **40**: 389–430.

Le Merrer J, Becker JA, Befort K, Kieffer BL (2009). Reward processing by the opioid system in the brain. *Physiol Rev* **89**: 1379–1412.

Le Merrer J, Plaza-Zabala A, Del Boca C, Matifas A, Maldonado R, Kieffer BL (2011). Deletion of the delta opioid receptor gene impairs place conditioning but preserves morphine reinforcement. *Biol Psychiatry* **69**: 700–703.

Lutter M, Nestler EJ (2009). Homeostatic and hedonic signals interact in the regulation of food intake. *J Nutr* **139**: 629–632.

Lutz PE, Kieffer BL (2013). The multiple facets of opioid receptor function: implications for addiction. *Curr Opin Neurobiol* **23**: 473–479.

Marinelli PW, Bai L, Quirion R, Gianoulakis C (2005). A microdialysis profile of Met-enkephalin release in the rat nucleus accumbens following alcohol administration. *Alcohol Clin Exp Res* **29**: 1821–1828.

Martin-Garcia E, Burokas A, Kostrzewa E, Gieryk A, Korostynski M, Ziolkowska B *et al* (2011). New operant model of reinstatement of food-seeking behavior in mice. *Psychopharmacology* **215**: 49–70.

Mathon DS, Lesscher HM, Gerrits MA, Kamal A, Pintar JE, Schuller AG *et al* (2005). Increased gabaergic input to ventral tegmental area dopaminergic neurons associated with decreased cocaine reinforcement in mu-opioid receptor knockout mice. *Neuroscience* **130**: 359–367.

Matthes HW, Maldonado R, Simonin F, Valverde O, Slowe S, Kitchen I *et al* (1996). Loss of morphine-induced analgesia, reward effect and withdrawal symptoms in mice lacking the mu-opioid-receptor gene. *Nature* **383**: 819–823.

McLaughlin JP, Land BB, Li S, Pintar JE, Chavkin C (2006). Prior activation of kappa opioid receptors by U50,488 mimics repeated forced swim stress to potentiate cocaine place preference conditioning. *Neuropsychopharmacology* **31**: 787–794.

Miller NS, Gold MS (1994). Dissociation of 'conscious desire' (craving) from and relapse in alcohol and cocaine dependence. *Ann Clin Psychiatry* **6**: 99–106.

Schroeder JA, Hummel M, Simpson AD, Sheikh R, Soderman AR, Unterwald EM (2007). A role for mu opioid receptors in cocaine-induced activity, sensitization, and reward in the rat. *Psychopharmacology* **195**: 265–272.

Shippenberg TS, Zapata A, Chefer VI (2007). Dynorphin and the pathophysiology of drug addiction. *Pharmacol Ther* **116**: 306–321.

Shoblock JR, Maidment NT (2007). Enkephalin release promotes homeostatic increases in constitutively active mu opioid receptors during morphine withdrawal. *Neuroscience* **149**: 642–649.

Simmons D, Self DW (2009). Role of mu- and delta-opioid receptors in the nucleus accumbens in cocaine-seeking behavior. *Neuropsychopharmacology* **34**: 1946–1957.

Soderman AR, Unterwald EM (2008). Cocaine reward and hyperactivity in the rat: sites of mu opioid receptor modulation. *Neuroscience* **154**: 1506–1516.

Soria G, Barbano MF, Maldonado R, Valverde O (2008). A reliable method to study cue-, priming-, and stress-induced reinstatement of cocaine self-administration in mice. *Psychopharmacology* **199**: 593–603.

Soria G, Mendizabal V, Tourino C, Robledo P, Ledent C, Parmentier M *et al* (2005). Lack of CB1 cannabinoid receptor impairs cocaine self-administration. *Neuropsychopharmacology* **30**: 1670–1680.

Taha SA (2010). Preference or fat? Revisiting opioid effects on food intake. *Physiol Behav* **100**: 429–437.

Tang XC, McFarland K, Cagle S, Kalivas PW (2005). Cocaine-induced reinstatement requires endogenous stimulation of mu-opioid receptors in the ventral pallidum. *J Neurosci* **25**: 4512–4520.

Trifilieff P, Martinez D (2013). Kappa-opioid receptor signaling in the striatum as a potential modulator of dopamine transmission in cocaine dependence. *Front Psychiatry* **4**: 44.

Trigo JM, Martin-Garcia E, Berrendero F, Robledo P, Maldonado R (2010). The endogenous opioid system: a common substrate in drug addiction. *Drug Alcohol Depend* **108**: 183–194.

Trigo JM, Zimmer A, Maldonado R (2009). Nicotine anxiogenic and rewarding effects are decreased in mice lacking beta-endorphin. *Neuropharmacology* **56**: 1147–1153.

Volkow ND, Fowler JS, Wang GJ, Baler R, Telang F (2009). Imaging dopamine's role in drug abuse and addiction. *Neuropharmacology* **56 Suppl 1**: 3–8.

Ward SJ, Martin TJ, Roberts DC (2003). Beta-funaltrexamine affects cocaine self-administration in rats responding on a progressive ratio schedule of reinforcement. *Pharmacol Biochem Behav* **75**: 301–307.

Weiss F (2010). Advances in animal models of relapse for addiction research. In: Kuhn CM and Koob GF (eds). *Advances in the Neuroscience of Addiction*. 2nd edn, Boca Raton (FL): London.

Zhang M, Gosnell BA, Kelley AE (1998). Intake of high-fat food is selectively enhanced by mu opioid receptor stimulation within the nucleus accumbens. *J Pharmacol Exp Ther* **285**: 908–914.

Supplementary Information accompanies the paper on the Neuropsychopharmacology website (http://www.nature.com/npp)

Article 2

Sigma-1 receptor modulates neuroinflammation associated with mechanical hypersensitivity and opioid tolerance in a mouse model of osteoarthritis pain.

Carcolé M[1], Kummer S[#1], Gonçalves L[3], Zamanillo D[2], Dickenson AH[3], Fernández-Pastor B[2], Cabañero D[1], Maldonado R[1]

Received: 5 April 2019 | Revised: 6 July 2019 | Accepted: 9 July 2019
DOI: 10.1111/bph.14794

RESEARCH PAPER

Sigma-1 receptor modulates neuroinflammation associated with mechanical hypersensitivity and opioid tolerance in a mouse model of osteoarthritis pain

Mireia Carcolé[1] | Sami Kummer[1] | Leonor Gonçalves[3] | Daniel Zamanillo[2] | Manuel Merlos[2] | Anthony H. Dickenson[3] | Begoña Fernández-Pastor[2] | David Cabañero[1] | Rafael Maldonado[1]

[1]Neuropharmacology Lab, Department of Experimental and Health Sciences, University Pompeu Fabra, Barcelona, Spain
[2]Drug Discovery and Preclinical Development, Laboratories Esteve, Barcelona Science Park, Barcelona, Spain
[3]Department of Neuroscience, Physiology and Pharmacology, University College London, London, UK

Correspondence
Rafael Maldonado López, Neuropharmacology Lab, Department of Experimental and Health Sciences, University Pompeu Fabra, c/Dr. Aiguader 88, 08003 Barcelona, Spain.
Email: rafael.maldonado@upf.edu

Funding information
Agència de Gestió d'Ajuts Universitaris i de Recerca, Grant/Award Number: ICREA Academia Award 2015; AGAUR, Grant/Award Numbers: #2014-DI-040 and #SGR2017-669; Spanish Instituto de Salud Carlos III, Grant/Award Number: #RD16/0017/0020; Seventh Framework Programme, Grant/Award Number: #2013-602891

Background and Purpose: Osteoarthritic pain is a chronic disabling condition lacking effective treatment. Continuous use of opioid drugs during osteoarthritic pain induces tolerance and may result in dose escalation and abuse. Sigma-1 (σ1) receptors, a chaperone expressed in key areas for pain control, modulates μ-opioid receptor activity and represents a promising target to tackle these problems. The present study investigates the efficacy of the σ1 receptor antagonist E-52862 to inhibit pain sensitization, morphine tolerance, and associated electrophysiological and molecular changes in a murine model of osteoarthritic pain.

Experimental Approach: Mice received an intra-knee injection of monoiodoacetate followed by 14-day treatment with E-52862, morphine, or vehicle, and mechanical sensitivity was assessed before and after the daily doses.

Key Results: Monoiodoacetate-injected mice developed persistent mechanical hypersensitivity, which was dose-dependently inhibited by E-52862. Mechanical thresholds assessed before the daily E-52862 dose showed gradual recovery, reaching complete restoration by the end of the treatment. When repeated treatment started 15 days after knee injury, E-52862 produced enhanced short-term analgesia, but recovery to baseline threshold was slower. Both a σ1 receptor agonist and a μ receptor antagonist blocked the analgesic effects of E-52862. An acute, sub-effective dose of E-52862 restored morphine analgesia in opioid-tolerant mice. Moreover, E-52862 abolished spinal sensitization in osteoarthritic mice and inhibited pain-related molecular changes.

Conclusion and Implications: These findings show dual effects of σ1 receptor antagonism alleviating both short- and long-lasting antinociception during chronic osteoarthritis pain. They identify E-52862 as a promising pharmacological agent to treat chronic pain and avoid opioid tolerance.

Abbreviation: BDNF, brain-derived neurotrophic factor; DRG, dorsal root ganglia; MIA, monoiodoacetate; NPY, neuropeptide Y; WDR, wide dynamic range; σ1 receptor, sigma-1 receptor

David Cabañero and Rafael Maldonado contributed equally.

1 | INTRODUCTION

Osteoarthritis is the most frequent chronic musculoskeletal pain condition (Breivik, Collett, Ventafridda, Cohen, & Gallacher, 2006), characterized by progressive destruction of articular cartilage (Sutton et al., 2009; Zhang, Ren, & Dubner, 2013). Pain is the major symptom of osteoarthritis and the reason for presentation of patients to clinical services. However, available therapeutic approaches do not control the progression of the disease and do not provide satisfactory analgesia (Wieland, Michaelis, Kirschbaum, & Rudolphi, 2005). Opioids are potent analgesics widely used for severe pain management. However, prolonged administration has been associated with tolerance, abuse liability, and hyperalgesia (Vowles et al., 2015). Long-term opioid prescriptions increased importantly over the last decade, mainly in the United States, becoming a public health problem with devastating consequences including overdose-related deaths (Lyden & Binswanger, 2019). Therefore, there is an urgent need to develop safer therapeutic alternatives for chronic pain.

The **sigma-1 (σ1) receptor** is a ligand-regulated chaperone located mainly in the endoplasmic reticulum (Alonso et al., 2000). It has been proposed as an amplifier of signal transduction cascades that modulate a variety of receptors and ion channels (Su, Hayashi, Maurice, Buch, & Ruoho, 2010; Zamanillo, Romero, Merlos, & Vela, 2013). The σ1 receptors are expressed in areas of the nervous system crucial for pain transmission such as the dorsal root ganglia (DRG), dorsal horn, and periaqueductal grey (Alonso et al., 2000; Bangaru et al., 2013). Behavioural studies showed their involvement in models of neuropathic and inflammatory pain (Romero, Merlos, & Vela, 2016).

Osteoarthritis involves inflammatory and neuropathic pain mechanisms (Ivanavicius et al., 2007; Wylde, Hewlett, Learmonth, & Dieppe, 2011) at distinct points of the disease (Arendt-Nielsen et al., 2010), but the role of σ1 receptors in these different stages has not been yet investigated. Moreover, functional interactions have been reported between σ1 receptors and **μ-opioid receptors** (Kim et al., 2010). Indeed, σ1 receptor antagonists enhance opioid-induced analgesia in rodent models of acute nociception and inflammation (Chien & Pasternak, 1995; Montilla-García et al., 2019; Vidal-Torres et al., 2013) and did not potentiate opioid-induced side effects such as tolerance or physical dependence (Vidal-Torres et al., 2013), which could represent an important advantage for long-term opioid treatment. However, it is not known if σ1 receptors modulate opioid analgesia and tolerance during osteoarthritis chronic pain. Interestingly, σ1 receptors are up-regulated and redistributed from the endoplasmic reticulum to other subcellular locations under cellular stress (Hayashi & Su, 2007; Zamanillo et al., 2013), which is associated to chronic pain and morphine tolerance (Inceoglu et al., 2015; Liu et al., 2018). Hence, characterizing the role of σ1 receptors in osteoarthritic pain and opioid tolerance could provide insights into improving the available therapeutic strategies.

This study investigated the role of σ1 receptors in the monoiodoacetate (MIA) mouse model of osteoarthritic pain and its participation on opioid tolerance. We assessed the antinociceptive effects of acute and chronic treatment with the σ1 receptor antagonist E-52862 (also named S1RA [Romero et al., 2012] and MR309 [Castany, Gris, Vela, Verdú, & Boadas-Vaello, 2018]) and evaluated its effects in vivo on spinal electrophysiological recordings performed in animals with osteoarthritic pain. Involvement of **μ opioid receptors** in the analgesic effects of E-52862 and its participation on morphine tolerance were also investigated. Pain and morphine-associated biochemical alterations were also investigated in spinal cord and DRG of mice with osteoarthritic pain.

What is already known

- σ1 receptor antagonists modulate μ-opioid receptor activity and acutely alleviate inflammatory and neuropathic pain.

What this study adds

- Repeated E-52862 promotes gradual normalization of mechanical sensitivity inhibiting neuroinflammation, critical for osteoarthritic pain.
- E-52862 antinociception involves μ-opioid receptors and reverses morphine tolerance during chronic osteoarthritic pain.

What is the clinical significance

- E-52862 could dampen deleterious side effects of opioid and be an alternative for long-term treatments.
- E-52862 provides acute and long-lasting pain-relieving effects during osteoarthritic pain.

2 | METHODS

2.1 | Animals

All experimental procedures and animal husbandry were conducted following the ARRIVE guidelines and according to the ethical principles of the International Association for the Study of Pain (IASP) for the evaluation of pain in conscious animals (Zimmermann, 1986) and the European Parliament and the Council Directive (2010/63/EU) and were approved by the Animal Care and Use Committees of the PRBB and *Departament de Territori I Habitatge* of Generalitat de Catalunya. Animal studies are reported in compliance with the ARRIVE guidelines (Kilkenny, Browne, Cuthill, Emerson, & Altman, 2010) and with the recommendations made by the *British Journal of Pharmacology*.

Swiss albino male mice (Charles River, Lyon, France) 8 to 12 weeks old were used in all the experiments. Mice weighed 22 to 24 g at the beginning of the experiments and were housed in groups of 3–4 with free access to water and food. Housing conditions were maintained at 21 ± 1°C and 55 ± 10% relative humidity in a controlled light/dark cycle (light on between 8:00 a.m. and 8:00 p.m.). All experiments were performed under blinded conditions.

2.2 | Intra-articular injection of MIA

Osteoarthritic pain was induced in mice briefly anaesthetized with isoflurane (2% v/v) vaporized in oxygen. The knee joint was shaved and flexed at a 90° angle and 10 µl of MIA (10 mg·ml^{-1}, Sigma-Aldrich, UK) dissolved in sterile saline (NaCl 0.9%) were injected into the joint space with a 30-gauge needle, as previously described (Negrete, García Gutiérrez, Manzanares, & Maldonado, 2017). Sham mice received the same volume of sterile saline.

2.3 | Nociceptive behaviour

Hypersensitivity to punctate stimuli (which will be referred as mechanical allodynia) was used as outcome measure of osteoarthritic pain by measuring the hind paw withdrawal response to von Frey filaments stimulation (Chaplan, Bach, Pogrel, Chung, & Yaksh, 1994). Briefly, animals were placed in Plexiglas cylinders (20 cm high, 9 cm diameter) positioned on a grid surface through which calibrated von Frey filaments (North Coast Medical, USA) were applied following the up-down paradigm as previously reported (Chaplan et al., 1994). The 0.4-g filament was used first, and the strength of the next filament was decreased or increased according to the response following this sequence 0.07, 0.16, 0.4, 0.6, 1, 2 g. The 2-g filament was used as a cut-off. The mechanical threshold (in grams) was then calculated by the up-down Excel program (Dixon, 1965). Animals were habituated for 1 hr before testing to allow an appropriate behavioural immobility. Clear paw withdrawal, shaking, or licking was considered as a nociceptive response. Both ipsilateral and contralateral hind paws were tested. Only ipsilateral responses are shown since contralateral sides showed no significant alteration of the mechanical thresholds. The percentage of inhibition of mechanical nociception for the dose–response curves was calculated based on the hypersensitivity before the drug administration (0%) and the maximal possible mechanical thresholds (100%).

2.4 | Drug preparation

The selective σ1 receptor antagonist E-52862 (4-(2-[5-methyl-1-(naphthalen-2-yl)-1H-pyrazol-3-yloxy]ethyl) morpholine) and the µ receptor agonist morphine were dissolved in an aqueous solution (0.5% hydroxypropylmethyl cellulose, HPMC) and were administered by the i.p. route at a volume of 10 ml·kg^{-1} 30 min before behavioural testing. For spinal electrophysiological recordings, the doses of E-52862 were selected based on previous studies showing antinociceptive effects after intrathecal administration (Vidal-Torres et al., 2014). The σ1 receptor agonist PRE-084 ([2-(4-morpholinethyl)1-phenylcyclohexanecarboxylate]) and naloxone hydrochloride were diluted in physiological saline (0.9% sodium chloride) and were administered s.c. at a volume of 5 ml·kg^{-1}, 5 min before E-52862.

2.5 | In vivo spinal cord electrophysiology

In vivo electrophysiology was performed 13–17 days following MIA/sham injection. Animals were anaesthetized with 3.5% v/v isoflurane delivered in 3:2 ratio of nitrous oxide and oxygen and were maintained on 1.5% v/v for the whole duration of the experiment (approximately 5–7 hr), core body temperature was regulated with a homeothermic blanket, and respiratory rate was visually monitored. Mice were secured in a stereotaxic frame and a laminectomy was performed exposing L3-L5 of the spinal cord. Extracellular recordings were performed using 127-µm-diameter parylene-coated tungsten electrodes. Single wide dynamic range (WDR) neurons receiving inputs from the hind paw were isolated in the ipsilateral dorsal horn, and the receptive field was then stimulated using a wide range of stimuli: brush, von Frey filaments (0.16, 0.4, 0.6, 1, 2, 4, 6, 8, 15, 26, 60 g), static pressure (pinch), and heat (48°C) applied over a period of 10 s per stimulus. Stimuli were applied starting with the stimulus of lowest intensity in the following order: brush, von Frey, pressure, and heat; 1–2 WDR cells were isolated from each animal, and the average response was calculated. A sample size of six to eight animals per group was obtained except for the sham group where only four animals could be recorded due to casualties during the process of neuron isolation, where animals are maintained under anaesthesia for long periods of time.

Baseline recordings were made with 15-µl vehicle (0.9% saline) applied to the dorsal part of the spinal cord. After obtaining three to four baseline responses (with 5 min between each set of trials, data were averaged to obtain control values), the vehicle was removed and 90 and 180 µg E-52862 diluted in saline were applied to the spinal cord in a volume of 15 µl. Firing frequency was recorded 10 and 30 min after application of the drug. All mice were terminally anaesthetized with isoflurane after the experiment. Data were captured and analysed using a CED 1401 interface coupled to a computer running Spike 2 software.

2.6 | Tissue isolation

Mice were killed by cervical dislocation 1 or 15 days after sham or induction of osteoarthritis. The dorsal lumbar region of the spinal cord and L3-L5 DRG ipsilateral to the side of the knee injection were rapidly isolated. Tissues were fresh frozen and stored at −80°C until use.

2.7 | Immunoblot analysis

The antibody-related procedures used comply with the recommendations made by the *British Journal of Pharmacology* (Alexander et al., 2018). Frozen tissues were processed to obtain the total solubilized fraction, as previously described (Ozaita, Puighermanal, & Maldonado, 2007). Briefly, tissues were homogenized (Dounce homogenizer) in 30 volumes of lysis buffer (50 mmol·L^{-1} Tris–HCl pH 7.4, 150 mmol·L^{-1} NaCl, 10% glycerol, 1 mmol·L^{-1} EDTA, 1 µg·ml^{-1} aprotinin, 1 µg·ml^{-1} leupeptin, 1 µg·ml^{-1} pepstatin, 1 mmol·L^{-1} sodium fluoride, 5 mmol·L^{-1} sodium pyrophosphate, and 40 mmol·L^{-1} β-glycerolphosphate) with

1% Triton X-100. After 10 min of incubation at 4°C, samples were centrifuged at 16,000 *g* for 30 min to remove insoluble debris. Protein contents in the supernatants were determined by DC-micro plate assay following manufacturer's instructions. Blots containing equal amounts of protein samples were probed for different primary antibodies: anti-Iba1 (1:500), anti-GluA2 (1:2,000), anti-phosphoGluN1 (1:500), anti- GluN1 (1:2,000), anti-phospho GluN2B (1:500), anti-GluN2B (1:1,000), anti-$mGlu_5$ (1:2,000), and anti-GAPDH (1:10,000), and anti-actin (1:10,000). Bound primary antibodies were detected using HRP-conjugated antibodies to rabbit (1:2,000) or mouse antibodies (1:2000) and visualized by enhanced chemiluminescence detection (Clarity Western ECL Substrate). When necessary, Immobilon-P membranes were stripped in buffer containing 62.5-mM Tris pH 6.5, 2% SDS (v/v), and 0.1-M β-mercaptoethanol for 30 min at 37°C, followed by extensive washing in 100-mM NaCl, 10-mM Tris, and 0.1% Tween 20 (pH 7.4) before re-blocking and re-probing. The optical density of the relevant immunoreactive bands was quantified after acquisition on a ChemiDoc MP Imaging System controlled by Image Lab Touch Software. For quantitative purposes, the optical density values of phospho-specific antibodies were normalized to the detection of non-phospho antibodies in the same sample, and GAPDH or actin was used as the housekeeping control. Data were expressed as a fold change of the control sham-vehicle group.

2.8 | Gene expression analysis by real-time PCR

Total RNA was isolated from frozen (−80°C) spinal cords and DRG with TRIzol reagent plus RNA purification kit and subsequently retrotranscribed to cDNA with the High-capacity cDNA reverse transcription kit. Gene expression of neuropeptide Y (NPY), brain-derived neurotrophic factor (BDNF), TNF-α, and IL-1β in both tissues obtained 1 and 15 days after MIA injection was assessed by real-time PCR. Quantitative analysis of gene expression was measured with TaqMan Gene Expression assays "Mm01410146_m1" for NPY, "Mm01334043_m1" for BDNF, "Mm00443258_m1" for TNF-α, and "Mm00434228_m1" for IL-1β as a double-stranded DNA-specific fluorescent dye and performed on the ABI Prism 7900 HT. HPRT was used as housekeeping gene, detected with TaqMan gene expression assay "Mm00446968_m1." Data for each target gene were normalized to HPRT, and the fold change in target gene mRNA abundance was determined by the $2^{(-Ct)}$ method (Livak & Schmittgen, 2001).

2.9 | Data and statistical analysis

The data and statistical analysis comply with the recommendations of the *British Journal of Pharmacology* on experimental design and analysis in pharmacology (Curtis et al., 2018). Sample size was based on previous behavioural studies with similar number of factors under the same experimental conditions that achieved statistically significant results (Gris, Merlos, Vela, Zamanillo, & Portillo-Salido, 2014; Negrete et al., 2017). Mice were randomly assigned to each surgery and/or treatment group, generating groups with similar initial number of animals for each experiment. The minor variations in the final number among the groups in each experiment are due to the loss of one to two animals during the whole experimental sequence mainly as a result of surgical procedures and subsequent consequences. Animals showing behavioural abnormalities after surgical procedures were killed following the ethical committee criteria. Animal casualties during the electrophysiological recordings were higher, and a group of four mice was obtained, which was not subjected to statistical analysis. Outliers were not excluded, and the declared group size is the number of independent values. A three-way repeated measure ANOVA with "surgery" as between factor and "day" and "pre versus post" as within-subject factors was used to analyse von Frey data during chronic treatment. To analyse the differences between early and late treatments and pre and post values, the slopes of the regression lines were calculated for each animal and the average slope for each group. Afterwards, a two-way ANOVA was used with "early and late" as between factor and "pre and post" as within-subject factor. For von Frey assessment on Day 14 before and after acute treatments, a two-way repeated measures ANOVA was used, with "treatment" as between-subjects factor and "pre versus post" as within-subject factor. For dose–response curves, an *F* test was used to compare the non-linear regression fittings. Electrophysiological data were analysed with an *F* test to compare non-linear regressions and a two-way repeated measure ANOVA ("surgery" as between-subject factor and "stimulus" as within-subject factor). A two-way ANOVA ("surgery" and "treatment") was used to analyse data from molecular studies. In all comparisons, Fisher least significant difference (LSD) post hoc analysis was applied when appropriate (significant interaction between factors). STATISTICA 6.0 software was used. The differences were considered statistically significant when the *P* value was below .05.

2.10 | Materials

The selective σ1 receptor antagonist E-52862 (4-(2-[5-methyl-1-(naphthalen-2-yl)-1H-pyrazol-3-yloxy]ethyl) morpholine) and the σ1 receptor agonist PRE-084 ([2-(4-morpholinethyl)1-phenylcyclohexanecarboxylate]) were developed and supplied by Laboratories Esteve (Barcelona, Spain). The μ receptor agonist morphine hydrochloride was obtained from the General Directorate of Pharmacy and Drugs, Spanish Ministry of Health (Madrid, Spain), and the μ receptor antagonist naloxone hydrochloride was purchased from Sigma-Aldrich (Saint Louis, United States). HPMC was obtained from Sigma-Aldrich (Saint Louis, United States). For the electrophysiological study, parylene-coated tungsten electrodes from A-M Systems (Sequim, United States) and Spike 2 software from Cambridge Electronic Design (Cambridge, United Kingdom, RRID:SCR_000903) were used. DC-micro plate assay was purchase from Bio-Rad (Hercules, United States), and Immobilon-P membranes from Merck Millipore (Burlington, United States; Cat# IPVH09120). In the molecular studies, the following antibodies were used: anti-Iba1 (Wako Pure Chemical

Industries, Osaka, Japan; Cat# 016-20001, RRID:AB_839506), anti-GluR2 (Merck Millipore; Cat# AB1768, RRID:AB_2313802), anti-phosphoNR1 (Cell Signalling, Danvers, United States; Cat# 3381, RRID:AB_2294781), anti-NR1 (Novus Biologicals, Centennial, United States; Cat# NB300-118, RRID:AB_10002447), anti-phosphoNR2B (Sigma-Aldrich, Saint Louis, United States; Cat# M2442, RRID: AB_262150), anti-NR2B (Merck Millipore; Cat# AB1557P, RRID: AB_90772), anti-mGluR5 (Merck Millipore; Cat# AB5675, RRID: AB_2295173), anti-GAPDH (Santa Cruz Technologies, Dallas, United States; Cat# sc-32233, RRID:AB_627679), anti-Actin (Sigma-Aldrich, Saint Louis, United States; Cat# A5441, RRID:AB_476744), anti-rabbit (Cell signalling; Cat# 7074, RRID:AB_2099233) and anti-mouse (Santa Cruz Technologies; Cat# sc-2005, RRID:AB_631736). The optical density of the relevant immunoreactive bands was visualized using Clarity Western ECL Substrate (Cat# 1705061) and the ChemiDoc MP Imaging System from Bio-Rad. For the gene expression analysis by real-time PCR, the following reagents were used: TRIzol reagent plus RNA purification kit from Ambion (Waltham, United States; Cat#

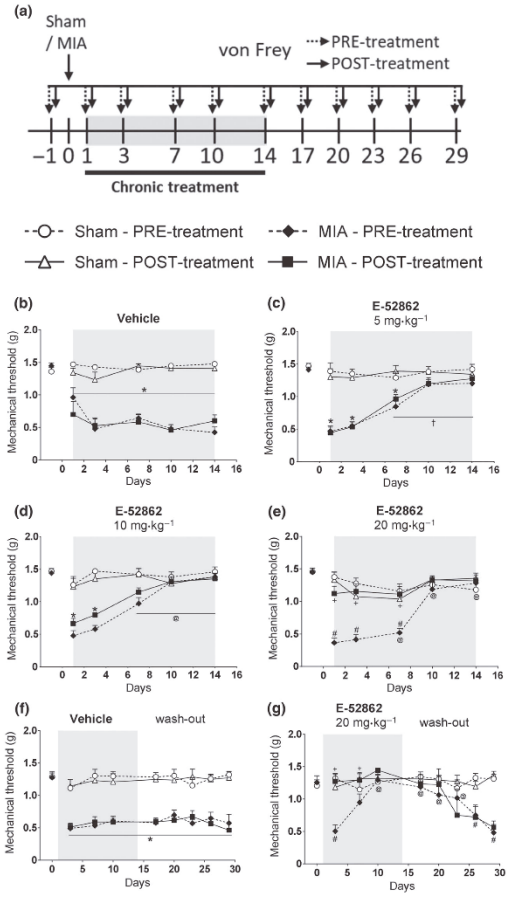

FIGURE 1 The σ1 receptor antagonist E-52862 produces both acute anti-allodynia and a gradual normalization of mechanical thresholds in a model of osteoarthritic pain. (a) Mice received an intra-knee injection of MIA or saline and were treated with vehicle (0.5% HMPC) or E-52862 (5, 10, or 20 mg·kg^{-1}) twice a day from Day 1 to Day 14. Mechanical allodynia was assessed with the von Frey test before (PRE) and 30 min after (POST) the first daily dose, under basal conditions and 1, 3, 7, 10, 14, and 17, 20, 23, 26, and 29 days after the intra-articular injection. (b) MIA-injected mice treated with vehicle showed a persistent decrease on mechanical thresholds. (c–e) E-52862 produced acute dose-dependent antiallodynic effects (POST values) and a gradual recovery of mechanical thresholds observed before the daily doses (PRE values). (f) MIA-induced reduction of mechanical thresholds persisted up to 29 days in vehicle-treated mice. (g) The sustained recovery induced by chronic E-52862 was maintained for 9 days after interrupting the repeated treatment. The von Frey pressure (g) required to elicit the paw withdrawal is expressed as mean ± SEM. The number of animals is as follows (first value represents sham groups and second value represents MIA groups): (b) 8, 8; (c) 8, 8; (d) 8, 8; (e) 8, 10; (f) 8, 16; and (g) 8, 8. *P<.05, significant difference between MIA and sham; † P<.05, significant difference between MIA-PRE and MIA-PRE at Day 1; #P<.05, significant difference between MIA-PRE and Sham-PRE; + P<.05, significant difference between MIA-PRE and MIA-POST; three-way repeated measures ANOVA plus Fisher least significant difference test. MIA, monoiodoacetate

AM1924), and high-capacity cDNA reverse transcription kit (Cat# 4368814), TaqMan Gene Expression assays, and ABI Prism 7900 HT from Applied Biosystems (Waltham, United States). The statistical analysis was performed with the STATISTICA 6.0 software was used (StatSoft, Inc., Tulsa, United States, RRID:SCR_014213).

2.11 | Nomenclature of targets and ligands

Key protein targets and ligands in this article are hyperlinked to corresponding entries in http://www.guidetopharmacology.org, the common portal for data from the IUPHAR/BPS Guide to PHARMACOLOGY (Harding et al., 2018), and are permanently archived in the Concise Guide to PHARMACOLOGY 2017/18 (Alexander, Christopoulos, et al., 2017; Alexander, Kelly et al., 2017; Alexander, Peters et al., 2017).

3 | RESULTS

3.1 | The σ1 receptor antagonist E-52862 produces acute antinociception and a gradual normalization of mechanical sensitivity during osteoarthritic pain

To assess the therapeutic potential of E-52862 in pain due to chronic osteoarthritis, we evaluated its effects on mechanical allodynia in mice subjected to joint pain induced by MIA. Mice received vehicle or different i.p. E-52862 doses (5–10–20 mg·kg^{-1}) twice a day during 14 days, starting the first day after MIA or sham injection. Mechanical thresholds were measured before (PRE values) and 30 min after (POST) the first daily administration (Figure 1a). Baseline mechanical thresholds were similar in all groups, and sham animals did not show nociceptive changes during the experiment, regardless of the treatment (Figure 1b,g). Intra-knee injection of MIA led to a marked decrease of withdrawal thresholds to mechanical stimuli when compared with sham. Mechanical allodynia was shown from the first day after MIA until the end of the experiment in vehicle-treated mice (Figure 1b,f). Acute E-52862 doses of 5 and 10 mg·kg^{-1} were sub-effective, whereas 20 mg·kg^{-1} clearly alleviated MIA-induced hypersensitivity, demonstrating dose-dependent analgesic effects of E-52862 after single administration (POST values compared with PRE values at Day 1; Figure 1c,e). Interestingly, E-52862 also induced a gradual recovery of the mechanical thresholds measured before its daily administration. This recovery was significant after the seventh day of treatment for all doses tested (Figure 1c,e). Hence, the sustained recovery of mechanical thresholds was independent of the E-52862 doses tested.

To evaluate the persistence of E-52862-induced antiallodynic effects, we continued the evaluation of mechanical thresholds after ending the repeated treatment (wash-out period; Figure 1f,g). Mice previously treated with vehicle or E-52862 (20 mg·kg^{-1}, 14 days) were evaluated for 15 additional days after ending the treatment. The reduction of mechanical allodynia induced by the 14-day treatment was maintained for 9 days after interrupting E-52862 administration (Figure 1g). Therefore, the blockade of σ1 receptors had sustained antiallodynic effects that lasted for several days after treatment discontinuation.

3.2 | The analgesic efficacy of acute or repeated treatments with E-52862 depends on the stage of the osteoarthritic pain sensitization

Treatment with the σ1 receptor antagonist showed acute and long-lasting efficacy inhibiting osteoarthritic pain at stages in which inflammatory and neuroplastic changes may have not been fully developed. Thus, we wanted to assess its analgesic efficacy once these changes were already present. We compared the efficacy of acute and chronic E-52862 treatments starting 1 (Early) or 15 (Late) days after MIA injection (Figure 2a). MIA-injected mice showed similar decrease of mechanical thresholds 1 and 15 days after MIA (Figures 1b and 2b). We observed a significant shift to the left of the dose–response curve of E-52862 measured 15 days after MIA injection, when compared with the curve assessed on Day 1 (Figure 2c). This was reflected in lower median effective dose (ED_{50}) of the σ1 receptor antagonist 15 days after MIA (ED_{50} = 7.024 mg·kg^{-1}) than on Day 1 (ED_{50} = 14.10 mg·kg^{-1}). Thus, the dose needed to induce pain relief on Day 15 was half of the dose required on Day 1.

Comparison between early and late repeated treatments with E-52862 (5 and 10 mg·kg^{-1}) revealed that the time period in which the σ1 receptor antagonist was applied had a significant effect on the gradual recovery of mechanical thresholds. MIA-induced sensitization was stable in vehicle-treated mice up to 28 days after intra-knee injection (Figure 2b). Mice receiving the late chronic E-52862 treatment also showed the sustained restoration of mechanical sensitivity observed in the previous treatment schedule (Figure 2d,f), but this improvement was slower compared to the treatment starting at Day 1, as reflected on reduced slopes of the time-course curves of mechanical allodynia (Figure 2e,g). Therefore, late repeated treatments with E-52862 required a longer duration of treatment to restore mechanical thresholds than that for early treatments, even if single administrations at late time points showed higher acute antinociceptive effects.

3.3 | Spinal administration of the σ1 receptor antagonist reduces evoked firing frequency of spinal neurons from mice with osteoarthritic pain

To distinguish whether E-52862 could modulate central sensitization in the spinal cord of mice with osteoarthritic pain (Harvey & Dickenson, 2009), in vivo electrophysiological recordings were performed in WDR neurons of lamina V of the dorsal horn. These neurons respond to mechanical and thermal stimuli, including punctate stimulation, dynamic brush, static pressure, and heat (Figure 3a). In this exploratory experiment, evoked responses to punctate mechanical stimuli were facilitated in osteoarthritic mice (Figure 3b). However, firing frequency evoked by the other stimuli was similar in MIA and sham

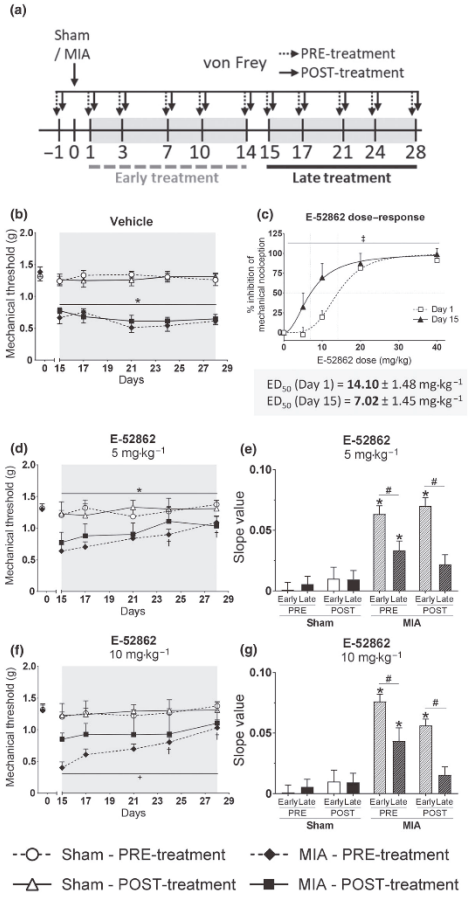

FIGURE 2 Acute and repeated E-52862 treatments starting 1 or 15 days after MIA injection differ in their analgesic efficacy. (a) The analgesic effects of acute and chronic E-52862 (5 or 10 mg·kg^{-1}, twice a day during 14 days) were compared between treatments starting 1 (early) or 15 (late) days after the injection of MIA. (b) MIA-induced sensitization was stable in vehicle-treated mice from Day 15 to Day 28 after intra-knee injection. (c) Lower doses were needed to induce acute relief of mechanical hypersensitivity 15 days than 1 day after the intra-knee injection of MIA. Mice receiving chronic late treatments with E-52862 5 mg·kg^{-1} (d) and 10 mg·kg^{-1} (f) also showed a recovery of the mechanical thresholds. (e,g) The restoration of mechanical sensitivity was slower in the late than in the early treatment protocol, as reflected on reduced slopes of the time-course curves of mechanical allodynia. Data are expressed as mean ± SEM. The number of animals is the following (first value represents Day 1 or sham groups and second value represents Day 15 or MIA groups): (b) 9, 8; (c) 10, 8; and (d) 8, 8; (f) 8, 8. For panels (b) and (d–g), *P<.05, significant difference between MIA and Sham; †P<.05, significant difference between MIA and MIA at Day 1; + for MIA-PRE versus MIA-POST (three-way repeated measures ANOVA plus Fisher least significant difference test). For panel (c), ‡P<.05, significant difference between Day 1 and Day 15 (F test of non-linear regression). ED_{50}, median effective dose; MIA, monoiodoacetate

animals (Figure 3c). Application of 90 μg of E-52862 to the exposed dorsal horn of mice with osteoarthritis significantly reduced firing frequency in response to mechanical and thermal stimuli 30 min after administration (Figure 3d,e). Application of 180 μg induced earlier inhibitory effects that were evident 10 and 30 min after E-52862 (Figure 3f,g), indicating dose-dependent drug effects. Hence, MIA induced central sensitization characterized by increased firing frequency of spinal WDR neurons that was normalized by the pharmacological blockade of σ1 receptors. This effect is associated with the short-term antiallodynic effects of E-52862 observed in mice with osteoarthritic pain.

3.4 | σ1 receptors and μ receptors show reciprocal modulation in chronic osteoarthritic pain

The σ1 receptors have been shown to modulate opioid tolerance during acute nociception (Chien & Pasternak, 1995; Mei & Pasternak,

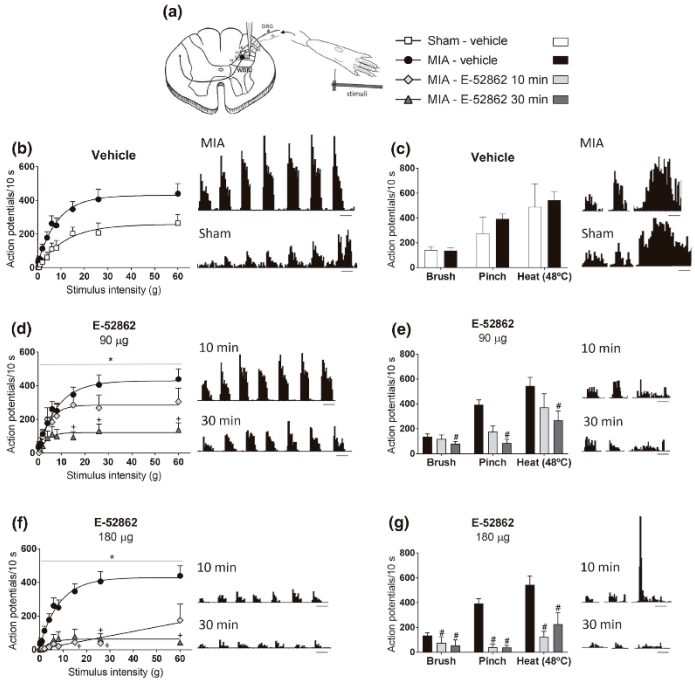

FIGURE 3 E-52862 reduces osteoarthritic pain-facilitated firing frequency of WDR spinal neurons. (a) Extracellular recordings were assessed from ipsilateral WDR neurons in the lamina 5 of the dorsal horn. The receptive field in the hind paw was stimulated using von Frey filaments, dynamic brush, static pressure (pinch), and heat (48°C). (b) MIA injection facilitated the evoked responses to punctate mechanical stimuli. (c) Firing frequency evoked by brush, pinch, or heat was similar in MIA and sham-injected animals. (d,e) 90 µg of E-52862 significantly reduced the evoked responses to mechanical and thermal stimuli 30 min after intrathecal application in mice with osteoarthritis pain. (f,g) Application of 180 µg of E-52862 inhibited the firing frequency in response to stimulation of the hind paw 10 and 30 min after administration. Stimuli were applied for 10 s, and responses are presented as mean ± SEM. Histogram traces for single unit responses of WDR neurons representative for each group are presented. The number of animals is the following: sham-vehicle = 4; MIA-vehicle = 8; and MIA-E-52862 (10 and 30 min) = 6. Panels (d) and (f): $^{*}P<.05$, significant difference between MIA-E-52862 (10 and 30 min) and MIA-vehicle (F test of non-linear regression) and $+P<.05$, significant difference between MIA-E-52862 and MIA-vehicle (two-way repeated-measures ANOVA plus Fisher least significant difference test). Panels (e) and (g): # $P<.05$, significant difference between MIA-E-52862 and MIA-vehicle (two-way repeated-measures ANOVA plus Fisher least significant difference test). MIA, monoiodoacetate

2002), but this effect has not been investigated under chronic pain conditions. To address this question, we induced opioid tolerance in mice with osteoarthritic pain using a chronic treatment with 2.5 mg·kg^{-1} morphine administered twice a day for 14 days. Afterwards, mice received acute morphine (2.5 mg·kg^{-1}), E-52862 (5–20 mg·kg^{-1}), or combinations of both, and mechanical sensitivity was assessed (Figure 4a). Osteoarthritic mice developed tolerance to the antinociceptive effects of morphine, revealed by the absence of an opioid response at the end of the repeated treatment (Figure 4b,d). This tolerance persisted for at least 9 days, as morphine antinociception was still absent 17, 20, and 23 days after MIA (Figure 4b). In this context, a single sub-effective dose of E-52862 (5 mg·kg^{-1}), combined with morphine, restored opioid analgesia (Days 17 and 23, Figure 4c). This restorative effect was not observed when morphine was administered alone 3 days after the first morphine-E-52862 combination, suggesting that may be a transient effect (Day

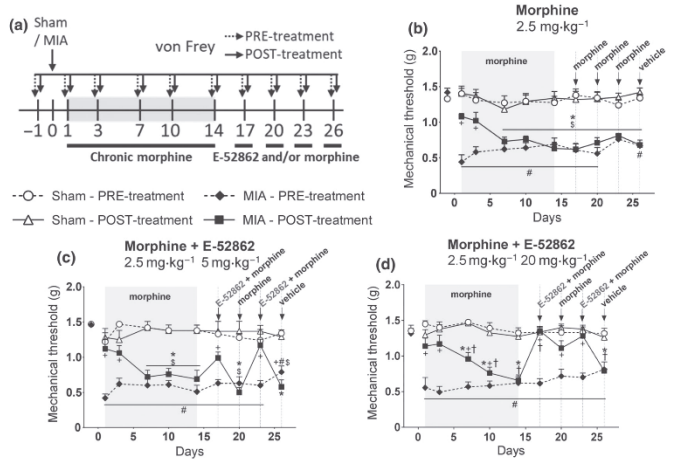

FIGURE 4 A single administration of the σ1 receptor antagonist restores morphine analgesia in opioid-tolerant mice. (a) After a 14-day treatment with morphine (2.5 mg·kg^{-1}, twice a day during 14 days), mice received acute administrations of morphine (2.5 mg·kg^{-1}), E-52862 (5–20 mg·kg^{-1}), or combinations of both drugs. (b–d) Mice repeatedly treated with the opioid developed analgesic tolerance. (b) The antinociceptive effect of morphine was not recovered for at least 9 days after the end of the repeated treatment. Single sub-effective (5 mg·kg^{-1}) (c) and effective doses (20 mg·kg^{-1}) (d) of E-52862 combined with morphine produced a restoration of opioid analgesia in morphine-tolerant mice. Mechanical thresholds expressed as mean ± SEM. The number of animals is the following (first value represents sham groups and second value represents MIA groups): (b) 8, 8; (c) 8, 8; and (d) 8, 10. *P<.05, significant difference between MIA-POST and Sham-POST; #P<.05, significant difference between MIA-PRE and Sham-PRE; +P<.05, significant difference between MIA-PRE and MIA-POST; †P<.05, significant difference between MIA-POST and MIA-POST at Day 1 (three-way repeated-measures ANOVA plus Fisher least significant difference test). MIA, monoiodoacetate

20; Figure 4c). To assess the effect of higher doses of the σ1 receptor antagonist, we co-administered E-52862 20 mg·kg^{-1} with morphine. As expected, this combination produced complete restoration of mechanosensitivity to baseline levels (Days 17 and 23, Figure 4d). Interestingly, this dose induced a long-lasting recovery, revealed by increased mechanical thresholds when morphine was given alone 3 days after the first morphine-E-52862 combination (Day 20, Figure 4d). This was not a residual effect of the earlier E-52862 dose, because the mechanical sensitivity assessed before the administration of morphine showed regular nociceptive sensitization (Figure 4d). Therefore, these results suggest that σ1 receptors participate in morphine tolerance during chronic osteoarthritic pain and its antagonism can restore opioid analgesia.

The σ1 receptor antagonist showed efficacy increasing the antinociceptive effect of morphine. However, it is not known whether μ receptors contribute to the analgesic effects of σ1 receptor ligands. Thus, we evaluated the involvement of σ1 receptors and μ receptors on the analgesic efficacy of E-52862. Mice with osteoarthritic pain were treated with vehicle or E-52862 for 13 days and on Day 14 received acute doses of E-52862 (20 mg·kg^{-1}), naloxone (1 mg·kg^{-1}), the σ1 receptor agonist PRE-084 (32 mg·kg^{-1}), or combinations of these drugs (Figure 5a). MIA-injected mice receiving vehicle showed reduced mechanical thresholds before drug administration (PRE values; Figure 5b). Acute injection of E-52862 decreased mechanical allodynia, whereas acute naloxone or PRE-084 did not induce significant responses. As expected, PRE-084 reduced the acute antiallodynic effect of the σ1 receptor antagonist (Figure 5b). Interestingly, co-administration of E-52862 with naloxone revealed a trend towards reduced analgesic effects of the σ1 receptor antagonist (Figure 5b), suggesting μ receptors also contribute to these acute responses. We also investigated whether μ receptors participate in the sustained recovery of mechanical thresholds induced by repeated E-52862 (PRE values; Figure 5c). In these conditions, both naloxone and PRE-084 injections decreased the mechanical thresholds (Figure 5c). Hence, the results indicate that the effects of E-52862 were selective for the σ1 receptors and a possible participation of μ receptors on the acute and sustained effects of E-52862 was noted.

An additional experiment was conducted to assess whether chronic stimulation of μ receptors could in turn modulate E-52862-induced antinociception. Different E-52862 doses were administered to mice with osteoarthritic pain after chronic morphine or vehicle (Figure 5a,d). Interestingly, we observed a significant shift to the right

of the E-52862 dose–response curve when the drug was administered to morphine-tolerant mice. The σ1 receptor antagonist produced higher antinociceptive effects when mice were not exposed to morphine (ED_{50} = 7.028 mg·kg^{-1}) than when mice were chronically treated with the opioid (ED_{50} = 17.77 mg·kg^{-1}). Thus, the antinociceptive effect of E-52862 was 2.5 times lower when μ receptors were desensitized after repeated morphine. Hence, the results suggest bidirectional modulation of σ1 receptors and μ receptors during chronic osteoarthritic pain.

3.5 | Molecular changes associated with chronic osteoarthritic pain are reversed by repeated treatment with the σ1 receptor antagonist E-52862

The σ1 receptor antagonist induced acute and long-lasting analgesic effects in mice with osteoarthritis pain, in contrast with morphine, which was devoid of antinociceptive effects after 14-day repeated administration. To compare the effects of these drugs at the molecular level, expression of markers associated with chronic pain was assessed in DRG and spinal cord samples of sham- or MIA-injected mice treated with vehicle, morphine, or E-52862 (Figure 6). One day after MIA, BDNF and NPY were over-expressed in the DRG (Figure 6b,c). This over-expression was reduced by acute morphine administration, but not by acute E-52862 (Figure 6b,c). This suggests peripheral effects of acute morphine treatments at early time points of the intra-knee injury. At spinal level, MIA-injected mice also showed early over-expression of TNF-α (Figure 6d), whereas IL-1β and NPY were unchanged (Figure 6e,f). No effect of the treatments was observed on these spinal markers at this early time point (Figure 6d,f).

After the 14-day treatment with vehicle, BDNF and TNF-α were still increased in osteoarthritic mice (Figure 6b,d), whereas NPY levels in the DRG showed a marked over-expression (Figure 6c). At this time point, spinal IL-1β and NPY levels were also enhanced (Figure 6e,f). Thus, additional molecular changes were established at later stages of osteoarthritic pain. Continuous blockade of σ1 receptors normalized the over-expression of all these markers (Figure 6b,f), whereas chronic morphine further increased BDNF, IL-1β, and spinal NPY expression (Figure 6b,e,f). Thus, the σ1 receptor antagonist disrupted the expression of pain signalling-related molecules after chronic treatment, whereas repeated morphine promoted the expression of neuroinflammatory mediators.

To further investigate the neuroinflammatory mechanisms underlying the long-term effects of E-52862 and morphine, we also analysed protein levels of the macrophage and microglial marker Iba-1 in DRG and spinal cord (Figure 7a). We did not observe significant differences in DRG (Figure 7b). In contrast, increased spinal Iba-1 levels were detected in osteoarthritic mice and after repeated morphine (Figure 7c). Interestingly, E-52862 reversed the enhancement of Iba-1 expression associated with osteoarthritic pain, suggesting a role for σ1 receptors in modulating glial reactivity. As microgliosis is

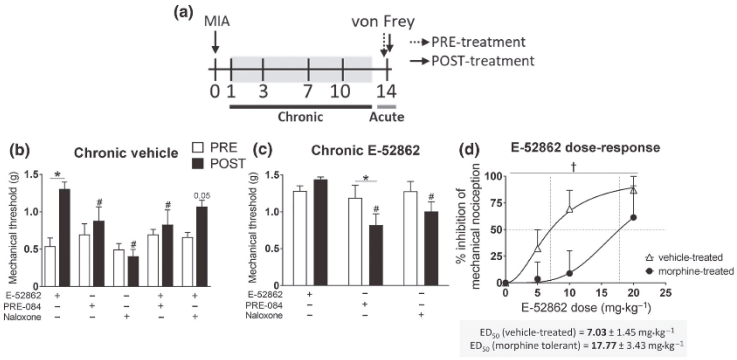

FIGURE 5 Participation of μ receptors in the antiallodynic effect of E-52862. (a) Osteoarthritic mice were treated with vehicle (0.5% HPMC), E-52862 (20 mg·kg^{-1}), or morphine (2.5 mg·kg^{-1}, twice a day during 14 days). In the last day of treatment, mice received acute doses of E-52862 (5–20 mg·kg^{-1}), PRE-084 (32 mg·kg^{-1}), naloxone (1 mg·kg^{-1}), or combinations of these drugs. (b) Acute E-52862 (20 mg·kg^{-1}) showed reduced anti-allodynic effect when co-administered with PRE-084 and a trend towards a decreased antinociception when given together with naloxone. (c) Once mechanical allodynia was normalized after chronic E-52862, acute administration of PRE-084 and naloxone induced reduction of the mechanical thresholds. (d) E-52862 administered to morphine-tolerant mice showed reduced antinociceptive effects. Data are expressed as mean ± SEM. The number of animals is the following: (b) 6 per group; (c) 6 per group; (d) 8 for vehicle-treated, 6 for morphine-treated. For panels (b) and (c): *P<.05, significant difference between PRE and POST; # P<.05, significant difference from E-52862 POST (two-way repeated measures ANOVA plus Fisher least significant difference test). For panel (d): † P<.05, significant difference between vehicle-treated and morphine-treated (F test of non-linear regression). MIA, monoiodoacetate. †

associated with glutamate excitotoxicity on neurons (Takeuchi, 2013), we decided to explore the spinal levels of glutamate receptors. We observed that chronic morphine significantly increased the levels of GluA2 AMPA receptor subunit (Figure 7d), whereas MIA enhanced phosphorylation of the NMDA receptor subunits GluN1 and GluN2B and the expression of metabotropic glutamate $mGlu_5$ receptor (Figure 7e,g). While the increases in phospho-GluN1 and phospho-GluN2B were independent of the treatment, the results showed that over-expression of $mGlu_5$ receptors was completely reversed by E-52862 (Figure 7g), revealing a novel effect of σ1 receptor antagonism in modulating glutamatergic signalling.

Overall, acute administration of morphine decreased expression of peripheral nociceptive markers, but chronic administration aggravated the pain-related molecular changes. On the contrary, E-52862 did not affect the expression of these markers after acute administration, but repeated treatment abolished central and peripheral long-term alterations associated with chronic osteoarthritic pain.

4 | DISCUSSION

This work reveals that the selective σ1 receptor antagonist E-52862 has short- and long-term analgesic effects and reverses morphine tolerance in mice subjected to a model of chronic osteoarthritic pain. Our findings indicate dose-dependent, short-term antinociception observed 30 min after E-52862 and sustained recovery of the mechanical thresholds when the drug was repeatedly given. Importantly, electrophysiological recordings revealed that E-52862 inhibited central sensitization of spinal WDR neurons in osteoarthritic mice. These effects partly involved μ receptors and σ1 receptor antagonism reversed morphine tolerance during osteoarthritic pain, demnstrating a crosstalk between σ1 receptors and the opioid system. Biochemical assays identified common alterations of neuroinflammatory markers and glutamatergic signalling associated with chronic pain and repeated opioid exposure, both specifically inhibited by E-52862.

Acute E-52862 induced short-term inhibition of MIA-induced hypersensitivity, confirming the analgesic efficacy of the σ1 receptor antagonist observed in different pain models (Romero et al., 2016). E-52862 or vehicle treatments did not induce significant changes in mechanical sensitivity of sham mice, although minor variations associated with the intra-knee saline injections were occasionally observed. Thus, normal mechanosensitivity remains intact following σ1 receptor antagonism. In agreement, it was proposed that σ1 receptors do not have a primary role in physiological conditions (Su et al., 2010; Zamanillo et al., 2013). The repeated treatment with E-52862 also produced a gradual recovery of sensitivity, which was observed with all the doses tested and maintained after interrupting the treatment. Previous studies in mice investigated acute antinociceptive effects of E-52862 (González-Cano, Merlos, Baeyens, & Cendán, 2013; Gris et al., 2014; Romero et al., 2012) and its effects during chronic administration without testing mechanical allodynia before the daily dose of the compound (Bura, Guegan, Zamanillo, Vela, & Maldonado, 2013; Romero et al., 2012). Our work shows long-lasting restorative effects of the σ1 receptor antagonist, suggesting an additional benefit for long-term chronic pain treatments.

E-52862 showed different efficacy depending on the stage of the osteoarthritic pain sensitization. It was proposed that the initial mechanical hyperalgesia in osteoarthritis is caused by inflammatory processes, while later stages involve neuropathic mechanisms (Thakur, Rahman, Hobbs, Dickenson, & Bennett, 2012). In agreement, rat models showed an increase of the nerve injury marker ATF-3 in the DRG between 8 and 14 days after MIA (Ivanavicius et al., 2007; Orita et al., 2011), and our mice increased expression of neuroinflammatory markers 15 days after intra-knee injury. The doses of E-52862 needed to exert acute antiallodynic effect 15 days after MIA were lower than on 1 day post-injection. Thus, acute effects of E-52862 were more prominent once the neuropathic component of osteoarthritic pain was established. Such intra-model differences agree with previous results showing higher efficacy of E-52862 after neuropathic injuries than during inflammatory pain (Gris et al., 2014; Romero et al., 2012). The long-lasting alleviation of pain required longer exposure to the σ1 receptor antagonist when persistent neuroinflammatory changes were present, although E-52862 was still able to restore normal sensitivity. Thus, the σ1 receptor antagonist showed higher short-term analgesic efficacy when pain had become chronic, while preserving its long-term effects on chronic pain sensitization.

In vivo electrophysiological recordings showed facilitation of the firing frequency of spinal WDR neurons after MIA, revealing central sensitization in mice with osteoarthritic pain. Our result in CD1 mice agrees with previous work using C57Bl/6 mice, which revealed similar MIA-induced responses to mechanical stimuli (Harvey & Dickenson, 2009). Furthermore, the lack of increased firing in response to thermal stimuli is in agreement with previous behavioural studies showing that MIA-injected mice do not exhibit consistent heat hyperalgesia (La Porta, Bura, Aracil-Fernández, Manzanares, & Maldonado, 2013). Interestingly, we found that intrathecal application of E-52862 reduced these MIA-facilitated responses. This is in line with previous ex vivo electrophysiological studies showing that E-52862 inhibited wind-up responses elicited after repeated nociceptor stimulation (Romero et al., 2012). In agreement, spinal cords of σ1 receptor knockout mice exhibited reduced wind-up responses compared to wild-type mice (de la Puente et al., 2009). Therefore, our experiments demonstrate that spinal central sensitization associated with osteoarthritis pain in live animals was reversed by the σ1 receptor antagonist.

It has been suggested that σ1 receptor agonists induce phosphorylation of μ receptors, a process involved in opioid tolerance (Rodríguez-Muñoz et al., 2015; Rodríguez-Muñoz, Cortés-Montero, Pozo-Rodrigálvarez, Sánchez-Blázquez, & Garzón-Niño, 2015). We found modulation, by σ1 receptors, of opioid analgesia during chronic osteoarthritic pain, showing that a single sub-effective dose of E-52862 co-administered with morphine restored opioid antinociception. Earlier preclinical research had shown this modulatory role in the absence of chronic pain, using σ1 receptor knockout mice and σ1 receptor antagonists (Chien & Pasternak, 1994; Sánchez-Fernández et al., 2013; Sánchez-Fernández et al., 2014). Moreover, E-52862 demonstrated efficacy restoring morphine analgesia in

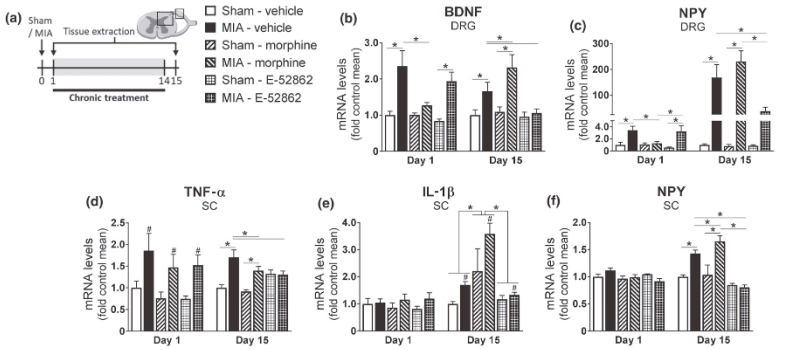

FIGURE 6 Repeated E-52862 reduces the expression of neuroinflammatory mediators associated with osteoarthritis pain and chronic morphine administration. (a) Spinal cord and DRG were extracted 1 or 15 days after sham or MIA injection from mice treated with vehicle (0.5% HPMC), morphine (2.5 $mg \cdot kg^{-1}$), or E-52862 (20 $mg \cdot kg^{-1}$). The first day after the intra-knee injection, MIA induced over-expression of BDNF (b) and NPY (c) in the DRG, which were reduced by the acute administration of morphine. In the spinal cord, MIA-injected mice showed increased levels of TNF-α (d), whereas IL-1β (e) and NPY (f) were not altered; 15 days after MIA or sham injection, BDNF (b) and NPY (c) in the DRG, and spinal TNF-α (d), IL-1β (e), and NPY (f) were increased in osteoarthritic mice and normalized by E-52862 chronic treatment. Morphine treatment further increased expression of BDNF (b), IL-1β (e), and spinal NPY (f). Data are expressed as mean ± SEM. The number of animals is the following: Day 1 = 5 per group; Day 15 = 6 per group. #$P<.05$, main effect, significant difference between MIA and sham, *$P<.05$, significantly different as indicated; two-way ANOVA followed by Fisher least significant difference test for each time point. BDNF, brain-derived neurotrophic factor; DRG, dorsal root ganglia; MIA, monoiodoacetate; NPY, neuropeptide Y; SC, spinal cord

tolerant animals with acute nociceptive and inflammatory pain (Montilla-García et al., 2019; Rodríguez-Muñoz, Sánchez-Blázquez, et al., 2015; Vidal-Torres et al., 2013). Surprisingly, there were no previous studies assessing the role of σ1 receptors in modulation of opioid analgesia under conditions of chronic pain. Our data suggest that σ1 receptor antagonists could be efficient not only alleviating pain by themselves but also restoring opioid analgesia in tolerant individuals. Taking into account that opioid tolerance drives dose escalation and abuse, and E-52862 did not produce tolerance development during this long-term treatment and it is void of reinforcing effects in animals without pain (Bura et al., 2013), the σ1 receptor antagonist could represent a valuable alternative for chronic pain treatment. Considering the lifespan of mice (2.5 years) and humans (80 years), the length of the treatment used in this study could be compared to the duration of chronic pain treatments that produce adverse events in patients.

We observed inhibition of the acute and sustained effects of E-52862 after administration of the σ1 receptor agonist PRE-084. Previous studies using pharmacological and genetic approaches demonstrated that acute analgesic effects of E-52862 are selectively mediated by σ1 receptors (Gris et al., 2014; Sánchez-Fernández et al., 2014). Our work also showed that long-term restoration of mechanical thresholds is also σ1 receptor-dependent. Interestingly, naloxone also diminished the acute and sustained antinociceptive effects of E-52862 revealing opioid participation. In addition, morphine-tolerant mice showed decreased E-52862 efficacy. antagonism of σ1 receptors facilitates σ1 receptor- μ receptor binding and protects μ receptors from phosphorylation, thus preserving their activity. Such phosphorylation is enhanced after persistent stimulation of μ receptors (Rodríguez-Muñoz, Cortés-Montero, et al., 2015, Rodríguez-Muñoz, Sánchez-Blázquez, et al., 2015). As both naloxone and μ receptor desensitization after chronic morphine decreased the antinociceptive effects of E-52862, it can be concluded that part of the analgesic effects of the σ1 receptor antagonist rely on the enhancement of endogenous μ receptor activity.

We investigated pain-related molecular alterations involved in morphine and E-52862 analgesia during osteoarthritis. One day after MIA, BDNF and NPY over-expression was observed in the DRG and TNF-α expression increased in the spinal cord. Previous studies reported similar changes after nerve injuries, including immediate increases in BDNF and TNF-α expression that persisted for long-term periods (Ohtori, Takahashi, Moriya, & Myers, 2004; Uchida, Matsushita, & Ueda, 2013). Several researchers also showed prominent NPY up-regulation in nerve-injured primary afferents (Benoliel, Eliav, & Iadarola, 2001; Son et al., 2007). This synthesis de novo could represent an adaptive response to nociceptive sensitization (Munglani et al., 1995). While acute morphine inhibited pain-related over-expression of BDNF and NPY, a single E-52862 administration did not provoke such effects, suggesting that its acute effects do not rely on these molecules.

Later stages of osteoarthritic pain involved pronounced increases of IL-1β and NPY levels in spinal cord or DRG, accompanied by enhancement of microglial marker Iba1. In addition, the enhanced

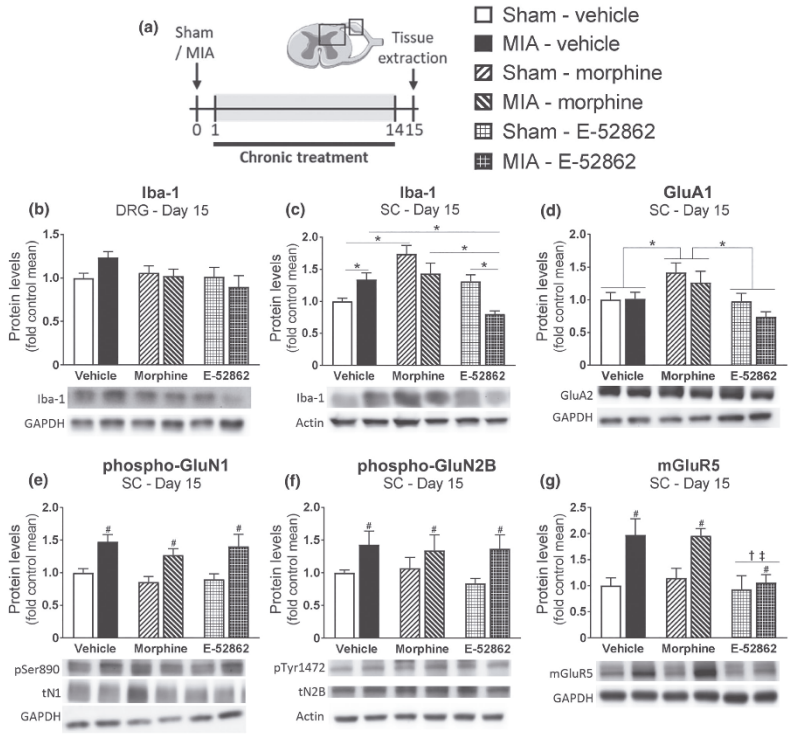

FIGURE 7 Repeated treatment with E-52862 decreases pain-induced microgliosis and mGluR5 up-regulation. (a) Fifteen days after sham or MIA injection, spinal cord, and DRG were extracted from vehicle- (0.5% HPMC), morphine- (2.5 mg·kg^{-1}), or E-52862- (20 mg·kg^{-1}) treated mice. (b) Protein levels of Iba-1 showed no significant differences in the DRG. (c) At spinal level, Iba-1 was increased after MIA or chronic morphine and reduced by E-52862. (d) Morphine induced an up-regulation of GluA2 AMPA receptor subunit. Phosphorylation levels of GluN1 (e) and GluN2B subunits (f) of the NMDA receptor were increased after MIA injection regardless of the treatment received. (g) MIA injection significantly increased the protein levels of $mGlu_5$, which were reduced after E-52862. GAPDH or actin was used as a housekeeping control. Data are expressed as mean ± SEM. The number of animals is 6 per group. #P <.05, significant difference between MIA and sham; †P <.05, significant difference between E-52862 and vehicle; ‡P <.05, significant difference between E-52862 and morphine; *P <.05, significantly different as indicated; two-way ANOVA followed by Fisher least significant difference test: MIA, monoiodoacetate; SC, spinal cord; DRG, dorsal root ganglia; pSer890, phosphorylation of Ser^{890} of the N1 subunit of the NMDA receptor; tN1, total N1 subunit; pTyr1472, phosphorylation of Tyr^{1472} of the N2B subunit of the NMDA receptor; tN2B, total N2B subunit

levels of BDNF and TNF-α were maintained in DRG and spinal cord respectively. Thus, the intra-knee injury induced persistent changes in neuroinflammatory mediators possibly contributing to the osteoarthritic phenotype. These pain-related changes were reported to increase glutamate release and stimulate the glutamatergic system (Takeuchi, 2013; Vaz, Lérias, Parreira, Diógenes, & Sebastião, 2015). In agreement, osteoarthritic mice showed over-expression of $mGlu_5$ receptors, which is associated with increased glutamate levels in the nervous system (Wang, Wang, Zhong, Li, & Cong, 2012). As previously described, chronic morphine further increased neuroinflammation and glutamatergic signalling (Cabañero et al., 2013; Johnston et al., 2004), characterized by exacerbated BDNF, IL-1β, spinal microgliosis, and

AMPA receptor expression. Interestingly, increased BDNF/TrkB signalling contributes to chronic pain by eliciting microglial reactivity and glutamate release (Zhou et al., 2011). At the same time, IL-1β and TNF-α are mainly released by activated microglia, which also liberate BDNF after chronic morphine (Takayama & Ueda, 2005). Thus, repeated morphine contributed to an overall increase of spinal neuroinflammation. In sharp contrast, chronic E-52862 normalized the expression of BDNF and proinflammatory cytokines. These findings agree with previous studies revealing potentiation of BDNF effects after over-expression of σ1 receptors (Yagasaki et al., 2006) or chronic σ1 receptor activation (Kikuchi-Utsumi & Nakaki, 2008). Likewise, recent experiments showed normalization of TNF-α and IL-1β expression in spinal cord-injured σ1 receptor knockout mice (Castany et al., 2018). E-52862 also reduced MIA-induced microgliosis, consistent with the effects of the σ1 receptor antagonist BD1047 attenuating spinal microgliosis in a model of bone cancer pain (Zhu et al., 2015) and with the high levels of σ1 receptors reported in microglia (Gekker et al., 2006). Interestingly, E-52862 was effective in preventing the increased microglial density induced by MIA in supraspinal structures (Carcolé et al., 2019). In addition, over-expression of $mGlu_5$ receptors was completely abolished by E-52862. Hence, contrary to chronic morphine, repeated treatment with the σ1 receptor antagonist normalized the expression of neuroinflammatory mediators and glutamate receptors involved in chronic osteoarthritic pain.

In summary, the present study shows a dual effect of the σ1 receptor antagonist E-52862 alleviating pain in our model of osteoarthritis. On the one hand, the σ1 receptor antagonist reduced acute mechanical allodynia, involving inhibition of spinal sensitization without modification of pain-related molecular alterations. On the other hand, repeated E-52862 exposure induced gradual recovery of the mechanical thresholds in osteoarthritic mice without inducing tolerance. This effect was associated with inhibition of biochemical changes related to osteoarthritic pain and opioid tolerance. Such alterations involve neuroinflammatory mediators, microglial reactivity and glutamatergic signalling, which could constitute a common pathway by which the σ1 receptor antagonist provided relief of chronic pain and restoration of opioid analgesia in tolerant individuals. Hence, the σ1 receptor antagonist could dampen deleterious side effects of opioid prescription drugs, which has reached now dramatic consequences in the United States (Lyden & Binswanger, 2019), and represents a promising alternative to opioids in chronic pain conditions requiring long-term treatment with analgesics.

ACKNOWLEDGEMENTS

We acknowledge the financial support of the European Commission (Seventh Framework Programme, NeuroPain #2013-602891), the Catalan Government (AGAUR, #SGR2017-669), the Spanish Instituto de Salud Carlos III (RTA, #RD16/0017/0020), and AGAUR (ICREA Academia Award 2015). M.C. is the recipient of an Industrial Doctorate contract from the Catalan Government and Laboratorios Esteve (AGAUR, #2014-DI-040). Partial support from FEDER funds is also acknowledged.

AUTHOR CONTRIBUTIONS

All authors listed above have contributed sufficiently to be included as authors. M.C. conducted the behavioural, electrophysiological, and molecular experiments and wrote the manuscript. S.K. conducted the molecular studies. L.G. supervised all the electrophysiological experiments. D.Z. and M.M. participated in the experimental design. A.H.D. provided the electrophysiological equipment. B.F-P. supervised the project and participated in the experimental design. D.C. conceptualized and supervised the project, participated in the experimental design, and wrote the manuscript. R.M. conceptualized, supervised, and funded the project, participated in the experimental design, and wrote the manuscript. All the authors have revised the work critically for important intellectual content and approved the final version to be published.

CONFLICT OF INTEREST

The authors declare no conflicts of interest.

DECLARATION OF TRANSPARENCY AND SCIENTIFIC RIGOUR

This Declaration acknowledges that this paper adheres to the principles for transparent reporting and scientific rigour of preclinical research as stated in the *BJP* guidelines for Design & Analysis, Immunoblotting and Immunochemistry, and Animal Experimentation, and as recommended by funding agencies, publishers and other organisations engaged with supporting research.

ORCID

Rafael Maldonado https://orcid.org/0000-0002-4359-8773

REFERENCES

Alexander, S. P., Christopoulos, A., Davenport, A. P., Kelly, E., Marrion, N. V., Peters, J. A., … CGTP Collaborators (2017). The Concise Guide to PHARMACOLOGY 2017/18: G protein-coupled receptors. *British Journal of Pharmacology*, *174*, S17–S129. https://doi.org/10.1111/bph.13878

Alexander, S. P., Kelly, E., Marrion, N. V., Peters, J. A., Faccenda, E., Harding, S. D., … CGTP Collaborators (2017). The concise guide to PHARMACOLOGY 2017/18: Other proteins. *British Journal of Pharmacology*, *174*, S1–S16. https://doi.org/10.1111/bph.13882

Alexander, S. P. H., Peters, J. A., Kelly, E., Marrion, N. V., Faccenda, E., Harding, S. D., … CGTP Collaborators (2017). The Concise Guide to PHARMACOLOGY 2017/18: Ligand-gated ion channels. *British Journal of Pharmacology*, *174*, S130–S159. https://doi.org/10.1111/bph.13879

Alexander, S. P. H., Roberts, R. E., Broughton, B. R. S., Sobey, C. G., George, C. H., Stanford, S. C., … Ahluwalia, A. (2018). Goals and practicalities of immunoblotting and immunohistochemistry: A guide for submission to the British Journal of Pharmacology. *British Journal of Pharmacology*, *175*, 407–411. https://doi.org/10.1111/bph.14112

Alonso, G., Phan, V., Guillemain, I., Saunier, M., Legrand, A., Anoal, M., & Maurice, T. (2000). Immunocytochemical localization of the sigma(1) receptor in the adult rat central nervous system. *Neuroscience*, *97*, 155–170. https://doi.org/10.1016/S0306-4522(00)00014-2

Arendt-Nielsen, L., Nie, H., Laursen, M. B., Laursen, B. S., Madeleine, P., Simonsen, O. H., & Graven-Nielsen, T. (2010). Sensitization in patients with painful knee osteoarthritis. *Pain*, *149*, 573–581. https://doi.org/10.1016/j.pain.2010.04.003

Bangaru, M. L., Weihrauch, D., Tang, Q.-B., Zoga, V., Hogan, Q., & Wu, H. (2013). Sigma-1 receptor expression in sensory neurons and the effect of painful peripheral nerve injury. *Molecular Pain*, *9*, 47.

Benoliel, R., Eliav, E., & Iadarola, M. J. (2001). Neuropeptide Y in trigeminal ganglion following chronic constriction injury of the rat infraorbital nerve: is there correlation to somatosensory parameters? *Pain*, *91*, 111–121. https://doi.org/10.1016/S0304-3959(00)00417-6

Breivik, H., Collett, B., Ventafridda, V., Cohen, R., & Gallacher, D. (2006). Survey of chronic pain in Europe: Prevalence, impact on daily life, and treatment. *European Journal of Pain*, *10*, 287–287. https://doi.org/10.1016/j.ejpain.2005.06.009

Bura, A. S., Guegan, T., Zamanillo, D., Vela, J. M., & Maldonado, R. (2013). Operant self-administration of a sigma ligand improves nociceptive and emotional manifestations of neuropathic pain. *European Journal of Pain*, *17*, 832–843. https://doi.org/10.1002/j.1532-2149.2012.00251.x

Cabañero, D., Baker, A., Zhou, S., Hargett, G. L., Irie, T., Xia, Y., … Morón, J. A. (2013). Pain after discontinuation of morphine treatment is associated with synaptic increase of GluA4-containing AMPAR in the dorsal horn of the spinal cord. *Neuropsychopharmacology*, *38*, 1472–1484. https://doi.org/10.1038/npp.2013.46

Carcolé, M., Zamanillo, D., Merlos, M., Fernández-Pastor, B., Cabañero, D., & Maldonado, R. (2019). Blockade of the sigma-1 receptor relieves cognitive and emotional impairments associated to chronic osteoarthritis pain. *Frontiers in Pharmacology*, *10*. https://doi.org/10.3389/fphar.2019.00468

Castany, S., Gris, G., Vela, J. M., Verdú, E., & Boadas-Vaello, P. (2018). Critical role of sigma-1 receptors in central neuropathic pain-related behaviours after mild spinal cord injury in mice. *Scientific Reports*, *8*, 3873. https://doi.org/10.1038/s41598-018-22217-9

Chaplan, S. R., Bach, F. W., Pogrel, J. W., Chung, J. M., & Yaksh, T. L. (1994). Quantitative assessment of tactile allodynia in the rat paw. *Journal of Neuroscience Methods*, *53*, 55–63. https://doi.org/10.1016/0165-0270(94)90144-9

Chien, C. C., & Pasternak, G. W. (1994). Selective antagonism of opioid analgesia by sigma system. *The Journal of Pharmacology and Experimental Therapeutics*, *271*, 1583–1590.

Chien, C. C., & Pasternak, G. W. (1995). Sigma antagonists potentiate opioid analgesia in rats. *Neuroscience Letters*, *190*, 137–139. https://doi.org/10.1016/0304-3940(95)11504-P

Curtis, M. J., Alexander, S., Cirino, G., Docherty, J. R., George, C. H., Giembycz, M. A., … Ahluwalia, A. (2018). Experimental design and analysis and their reporting II: Updated and simplified guidance for authors and peer reviewers. *British Journal of Pharmacology*, *175*, 987–993. https://doi.org/10.1111/bph.14153

de la Puente, B., Nadal, X., Portillo-Salido, E., Sánchez-Arroyos, R., Ovalle, S., Palacios, G., … Vela, J. M. (2009). Sigma-1 receptors regulate activity-induced spinal sensitization and neuropathic pain after peripheral nerve injury. *Pain*, *145*, 294–303.

Dixon, W. J. (1965). The up-and-down method for small samples. *Journal of the American Statistical Association*, *60*, 967–978. https://doi.org/10.1080/01621459.1965.10480843

Gekker, G., Hu, S., Sheng, W. S., Rock, R. B., Lokensgard, J. R., & Peterson, P. K. (2006). Cocaine-induced HIV-1 expression in microglia involves sigma-1 receptors and transforming growth factor-β1. *International Immunopharmacology*, *6*, 1029–1033. https://doi.org/10.1016/j.intimp.2005.12.005

González-Cano, R., Merlos, M., Baeyens, J. M., & Cendán, C. M. (2013). σ1 Receptors are involved in the visceral pain induced by intracolonic administration of capsaicin in mice. *Anesthesiology*, *118*, 691–700. https://doi.org/10.1097/ALN.0b013e318280a60a

Gris, G., Merlos, M., Vela, J. M., Zamanillo, D., & Portillo-Salido, E. (2014). S1RA, a selective sigma-1 receptor antagonist, inhibits inflammatory pain in the carrageenan and complete Freund's adjuvant models in mice. *Behavioural Pharmacology*, *25*, 226–235. https://doi.org/10.1097/FBP.0000000000000038

Harding, S. D., Sharman, J. L., Faccenda, E., Southan, C., Pawson, A. J., Ireland, S., … NC-IUPHAR (2018). The IUPHAR/BPS Guide to PHARMACOLOGY in 2018: Updates and expansion to encompass the new guide to IMMUNOPHARMACOLOGY. *Nucleic Acids Research*, *46*, D1091–D1106. https://doi.org/10.1093/nar/gkx1121

Harvey, V. L., & Dickenson, A. H. (2009). Behavioural and electrophysiological characterisation of experimentally induced osteoarthritis and neuropathy in C57Bl/6 mice. *Molecular Pain*, *5*, 18.

Hayashi, T., & Su, T.-P. (2007). Sigma-1 receptor chaperones at the ER-mitochondrion interface regulate Ca^{2+} signaling and cell survival. *Cell*, *131*, 596–610. https://doi.org/10.1016/j.cell.2007.08.036

Inceoglu, B., Bettaieb, A., Trindade da Silva, C. A., Lee, K. S. S., Haj, F. G., & Hammock, B. D. (2015). Endoplasmic reticulum stress in the peripheral nervous system is a significant driver of neuropathic pain. *Proceedings of the National Academy of Sciences*, *112*, 9082–9087. https://doi.org/10.1073/pnas.1510137112

Ivanavicius, S. P., Ball, A. D., Heapy, C. G., Westwood, F. R., Murray, F., & Read, S. J. (2007). Structural pathology in a rodent model of osteoarthritis is associated with neuropathic pain: Increased expression of ATF-3 and pharmacological characterisation. *Pain*, *128*, 272–282. https://doi.org/10.1016/j.pain.2006.12.022

Johnston, I. N., Milligan, E. D., Wieseler-Frank, J., Frank, M. G., Zapata, V., Campisi, J., … Watkins, L. R. (2004). A role for proinflammatory cytokines and fractalkine in analgesia, tolerance, and subsequent pain facilitation induced by chronic intrathecal morphine. *The Journal of Neuroscience*, *24*, 7353–7365. https://doi.org/10.1523/JNEUROSCI.1850-04.2004

Kilkenny, C., Browne, W., Cuthill, I. C., Emerson, M., & Altman, D. G. (2010). Animal research: Reporting *in vivo* experiments: The ARRIVE guidelines. *British Journal of Pharmacology*, *160*, 1577–1579.

Kikuchi-Utsumi, K., & Nakaki, T. (2008). Chronic treatment with a selective ligand for the sigma-1 receptor chaperone, SA4503, up-regulates BDNF protein levels in the rat hippocampus. *Neuroscience Letters*, *440*, 19–22. https://doi.org/10.1016/j.neulet.2008.05.055

Kim, F. J., Kovalyshyn, I., Burgman, M., Neilan, C., Chien, C.-C., & Pasternak, G. W. (2010). σ_1 Receptor modulation of G-protein-coupled receptor signaling: Potentiation of opioid transduction independent from receptor binding. *Molecular Pharmacology*, *77*, 695–703. https://doi.org/10.1124/mol.109.057083

La Porta, C., Bura, S. A., Aracil-Fernández, A., Manzanares, J., & Maldonado, R. (2013). Role of CB1 and CB2 cannabinoid receptors in the development of joint pain induced by monosodium iodoacetate. *Pain*, *154*, 160–174. https://doi.org/10.1016/j.pain.2012.10.009

Liu, D., Zhou, Y., Peng, Y., Su, P., Li, Z., Xu, Q., … Gao, F. (2018). Endoplasmic reticulum stress in spinal cord contributes to the development of morphine tolerance. *Frontiers in Molecular Neuroscience*, *11*, 72. https://doi.org/10.3389/fnmol.2018.00072

Livak, K. J., & Schmittgen, T. D. (2001). Analysis of relative gene expression data using real-time quantitative PCR and the 2−ΔΔCT Method. *Methods*, *25*, 402–408. https://doi.org/10.1006/meth.2001.1262

Lyden, J., & Binswanger, I. A. (2019). The United States opioid epidemic. *Seminars in Perinatology*, *43*, 123–131. https://doi.org/10.1053/j.semperi.2019.01.001

Mei, J., & Pasternak, G. W. (2002). Sigma1 receptor modulation of opioid analgesia in the mouse. *The Journal of Pharmacology and Experimental Therapeutics*, *300*, 1070–1074. https://doi.org/10.1124/jpet.300.3.1070

Montilla-García, Á., Tejada, M. Á., Ruiz-Cantero, M. C., Bravo-Caparrós, I., Yeste, S., Zamanillo, D., & Cobos, E. J. (2019). Modulation by sigma-1 receptor of morphine analgesia and tolerance: Nociceptive pain, tactile allodynia and grip strength deficits during joint inflammation. *Frontiers in Pharmacology*, *10*, 136. https://doi.org/10.3389/fphar.2019.00136

Munglani, R., Bond, A., Smith, G. D., Harrison, S. M., Elliot, P. J., Birch, P. J., & Hunt, S. P. (1995). Changes in neuronal markers in a mononeuropathic rat model relationship between neuropeptide Y, pre-emptive drug treatment and long-term mechanical hyperalgesia. *Pain*, *63*, 21–31. https://doi.org/10.1016/0304-3959(95)00013-I

Negrete, R., García Gutiérrez, M. S., Manzanares, J., & Maldonado, R. (2017). Involvement of the dynorphin/KOR system on the nociceptive, emotional and cognitive manifestations of joint pain in mice. *Neuropharmacology*, *116*, 315–327. https://doi.org/10.1016/j.neuropharm.2016.08.026

Ohtori, S., Takahashi, K., Moriya, H., & Myers, R. R. (2004). TNF-α and TNF-α receptor type 1 upregulation in glia and neurons after peripheral nerve injury: studies in murine DRG and spinal cord. *Spine (Phila pa 1976)*, *29*, 1082–1088.

Orita, S., Ishikawa, T., Miyagi, M., Ochiai, N., Inoue, G., Eguchi, Y., … Ohtori, S. (2011). Pain-related sensory innervation in monoiodoacetate-induced osteoarthritis in rat knees that gradually develops neuronal injury in addition to inflammatory pain. *BMC Musculoskeletal Disorders*, *12*, 134. https://doi.org/10.1186/1471-2474-12-134

Ozaita, A., Puighermanal, E., & Maldonado, R. (2007). Regulation of PI3K/Akt/GSK-3 pathway by cannabinoids in the brain. *Journal of Neurochemistry*, *102*, 1105–1114. https://doi.org/10.1111/j.1471-4159.2007.04642.x

Rodríguez-Muñoz, M., Cortés-Montero, E., Pozo-Rodrigálvarez, A., Sánchez-Blázquez, P., & Garzón-Niño, J. (2015). The ON:OFF switch, σ1R-HINT1 protein, controls GPCR-NMDA receptor cross-regulation: implications in neurological disorders. *Oncotarget*, *6*, 35458–35477. https://doi.org/10.18632/oncotarget.6064

Rodríguez-Muñoz, M., Sánchez-Blázquez, P., Herrero-Labrador, R., Martínez-Murillo, R., Merlos, M., Vela, J. M., & Garzón, J. (2015). The σ1 receptor engages the redox-regulated HINT1 protein to bring opioid analgesia under NMDA receptor negative control. *Antioxidants & Redox Signaling*, *22*, 799–818. https://doi.org/10.1089/ars.2014.5993

Romero, L., Merlos, M., & Vela, J. M. (2016). Antinociception by sigma-1 receptor antagonists: Central and peripheral effects. *Advances in Pharmacology (San Diego, Calif.)*, *75*, 179–215.

Romero, L., Zamanillo, D., Nadal, X., Sánchez-Arroyos, R., Rivera-Arconada, I., Dordal, A., … Vela, J. M. (2012). Pharmacological properties of S1RA, a new sigma-1 receptor antagonist that inhibits neuropathic pain and activity-induced spinal sensitization. *British Journal of Pharmacology*, *166*, 2289–2306. https://doi.org/10.1111/j.1476-5381.2012.01942.x

Sánchez-Fernández, C., Montilla-García, A., Gonzalez-Cano, R., Nieto, F. R., Romero, L., Artacho-Cordon, A., … Cobos, E. J. (2014). Modulation of peripheral μ-opioid analgesia by σ1 receptors. *The Journal of Pharmacology and Experimental Therapeutics*, *348*, 32–45.

Sánchez-Fernández, C., Nieto, F. R., González-Cano, R., Artacho-Cordón, A., Romero, L., Montilla-García, Á., … Cobos, E. J. (2013). Potentiation of morphine-induced mechanical antinociception by σ1 receptor inhibition: Role of peripheral σ1 receptors. *Neuropharmacology*, *70*, 348–358. https://doi.org/10.1016/j.neuropharm.2013.03.002

Son, S.-J., Lee, K.-M., Jeon, S.-M., Park, E.-S., Park, K.-M., & Cho, H.-J. (2007). Activation of transcription factor c-jun in dorsal root ganglia induces VIP and NPY upregulation and contributes to the pathogenesis of neuropathic pain. *Experimental Neurology*, *204*, 467–472. https://doi.org/10.1016/j.expneurol.2006.09.020

Su, T.-P., Hayashi, T., Maurice, T., Buch, S., & Ruoho, A. E. (2010). The sigma-1 receptor chaperone as an inter-organelle signaling modulator. *Trends in Pharmacological Sciences*, *31*, 557–566. https://doi.org/10.1016/j.tips.2010.08.007

Sutton, S., Clutterbuck, A., Harris, P., Gent, T., Freeman, S., Foster, N., … Mobasheri, A. (2009). The contribution of the synovium, synovial derived inflammatory cytokines and neuropeptides to the pathogenesis of osteoarthritis. *Veterinary Journal*, *179*, 10–24. https://doi.org/10.1016/j.tvjl.2007.08.013

Takayama, N., & Ueda, H. (2005). Morphine-induced chemotaxis and brain-derived neurotrophic factor expression in microglia. *The Journal of Neuroscience*, *25*, 430–435. https://doi.org/10.1523/JNEUROSCI.3170-04.2005

Takeuchi, H. (2013). Microglia and glutamate. *Advances in Neuroimmune Biology*, *4*(2), 77–83.

Thakur, M., Rahman, W., Hobbs, C., Dickenson, A. H., & Bennett, D. L. H. (2012). Characterisation of a peripheral neuropathic component of the rat monoiodoacetate model of osteoarthritis. *PLoS ONE*, *7*, e33730. https://doi.org/10.1371/journal.pone.0033730

Uchida, H., Matsushita, Y., & Ueda, H. (2013). Epigenetic regulation of BDNF expression in the primary sensory neurons after peripheral nerve injury: Implications in the development of neuropathic pain. *Neuroscience*, *240*, 147–154. https://doi.org/10.1016/j.neuroscience.2013.02.053

Vaz, S. H., Lérias, S. R., Parreira, S., Diógenes, M. J., & Sebastião, A. M. (2015). Adenosine A_{2A} receptor activation is determinant for BDNF actions upon GABA and glutamate release from rat hippocampal synaptosomes. *Purinergic Signal*, *11*, 607–612. https://doi.org/10.1007/s11302-015-9476-1

Vidal-Torres, A., de la Puente, B., Rocasalbas, M., Touriño, C., Bura, S. A., Fernández-Pastor, B., … Vela, J. M. (2013). Sigma-1 receptor antagonism as opioid adjuvant strategy: Enhancement of opioid antinociception without increasing adverse effects. *European Journal of Pharmacology*, *711*, 63–72. https://doi.org/10.1016/j.ejphar.2013.04.018

Vidal-Torres, A., Fernández-Pastor, B., Carceller, A., Vela, J. M., Merlos, M., & Zamanillo, D. (2014). Effects of the selective sigma-1 receptor antagonist S1RA on formalin-induced pain behavior and neurotransmitter release in the spinal cord in rats. *Journal of Neurochemistry*, *129*, 484–494. https://doi.org/10.1111/jnc.12648

Vowles, K. E., McEntee, M. L., Julnes, P. S., Frohe, T., Ney, J. P., & van der Goes, D. N. (2015). Rates of opioid misuse, abuse, and addiction in chronic pain: A systematic review and data synthesis. *Pain*, *156*, 569–576. https://doi.org/10.1097/01.j.pain.0000460357.01998.f1

Wang, J.-W., Wang, H.-D., Zhong, W.-Z., Li, N., & Cong, Z.-X. (2012). Expression and cell distribution of metabotropic glutamate receptor 5 in the rat cortex following traumatic brain injury. *Brain Research*, *1464*, 73–81. https://doi.org/10.1016/j.brainres.2012.05.014

Wieland, H. A., Michaelis, M., Kirschbaum, B. J., & Rudolphi, K. A. (2005). Osteoarthritis—An untreatable disease? *Nature Reviews. Drug Discovery*, *4*, 331–344. https://doi.org/10.1038/nrd1693

Wylde, V., Hewlett, S., Learmonth, I. D., & Dieppe, P. (2011). Persistent pain after joint replacement: Prevalence, sensory qualities, and postoperative determinants. *Pain*, *152*, 566–572. https://doi.org/10.1016/j.pain.2010.11.023

Yagasaki, Y., Numakawa, T., Kumamaru, E., Hayashi, T., Su, T.-P., & Kunugi, H. (2006). Chronic antidepressants potentiate via sigma-1 receptors the brain-derived neurotrophic factor-induced signaling for glutamate release. *The Journal of Biological Chemistry*, *281*, 12941–12949. https://doi.org/10.1074/jbc.M508157200

Zamanillo, D., Romero, L., Merlos, M., & Vela, J. M. (2013). Sigma 1 receptor: A new therapeutic target for pain. *European Journal of Pharmacology*, *716*, 78–93. https://doi.org/10.1016/j.ejphar.2013.01.068

Zhang, R.-X., Ren, K., & Dubner, R. (2013). Osteoarthritis pain mechanisms: Basic studies in animal models. *Osteoarthritis and Cartilage*, *21*, 1308–1315. https://doi.org/10.1016/j.joca.2013.06.013

Zhou, L.-J., Yang, T., Wei, X., Liu, Y., Xin, W.-J., Chen, Y., … Liu, X. G. (2011). Brain-derived neurotrophic factor contributes to spinal long-term potentiation and mechanical hypersensitivity by activation of spinal microglia in rat. *Brain, Behavior, and Immunity*, *25*, 322–334. https://doi.org/10.1016/j.bbi.2010.09.025

Zhu, S., Wang, C., Han, Y., Song, C., Hu, X., & Liu, Y. (2015). Sigma-1 receptor antagonist BD1047 reduces mechanical allodynia in a rat model of bone cancer pain through the inhibition of spinal NR1 phosphorylation and microglia activation. *Mediators of Inflammation*, *2015*, 1–11.

Zimmermann, M. (1986). Ethical considerations in relation to pain in animal experimentation. *Acta Physiologica Scandinavica. Supplementum*, *554*, 221–233.

How to cite this article: Carcolé M, Kummer S, Gonçalves L, et al. Sigma-1 receptor modulates neuroinflammation associated with mechanical hypersensitivity and opioid tolerance in a mouse model of osteoarthritis pain. *Br J Pharmacol*. 2019;1–17. https://doi.org/10.1111/bph.14794